A GIS-BASED STRUCTURAL ANALYSIS OF THE BUSHVELD COMPLEX AND SURROUNDING AREAS

by

RENEé M. GREYVENSTEYN

Submitted in partial fulfillment of the requirements for the degree

MAGISTER SCIENTIAE

in the Faculty of Natural and Agricultural Sciences
University of Pretoria

PRETORIA

February 2001

ABSTRACT

GIS (Geographic Information Systems) techniques were successfully applied as a tool in structural analysis of the Bushveld Complex and surrounding areas. An existing digital geological database, BOSGIS, was used as basis of this study. A GIS structural database, based on a literature study, was created using the program ArcView 3.2 GIS. In addition, the program was customized to calculate the orientations of the structural lines (faults, folds, dykes and lineaments) in BOSGIS, and to represent these orientations by rose diagrams. Also, by using ArcView's analytical capabilities, ages or structural domains were assigned to these structures.

Stress analysis was done in order to obtain an understanding of the stress fields influencing the formation and subsequent deformation of the Bushveld Complex and surrounding areas. Five main geological time periods are considered: pre-Transvaal, post-Transvaal/pre-Bushveld, post-Bushveld/pre-Waterberg, post-Waterberg/pre-Karoo, Pilanesberg and post-Karoo. Based on the structural information gained from the literature study the directions of the possible stresses responsible for producing these structures, are derived.

The study found that structures, such as dykes, lineaments, faults and folds, in and around the Bushveld Complex reflect a definite NE and NW structural trend. It is also evident that NE and NW stress directions were constantly reutilized, and during the structural history of the area the identities of the principal stress directions alternated between the NE and NW orientations. The only variation to this occurs during post-Waterberg times, when prominent NS stress directions prevailed. However, during post-Karoo times the characteristical NE and NW directions reoccurred. The derived stress fields are consistent with constant reactivation of the Thabazimbi-Murchison-Lineament (TML). Left-lateral, right-lateral, thrust and normal movements are known to have occurred at various times along the TML during the history of the Bushveld Complex and surrounding areas.

SAMEVATTING

GIS (Geografiese Inligting Stelsels) tegnieke was met sukses toegepas in 'n strukturele analise van die Bosveldompleks. 'n Bestaande digitale geologiese databasis, BOSGIS, was gebruik as basis gedurende die studie. Met behulp van die program ArcView 3.2 GIS wass 'n GIS strukturele databasis ontwerp gebaseer op 'n literatuurstudie. Daarby was die program aangepas om die orientasies van strukturele lyne (verskuiwings, plooie, gange en lineamente) in BOSGIS te bereken. ArcView se analitiese vermoëns was gebruik om ouderdomme en strukturele gebiedens toe te ken aan die strukture.

Spannings analise was gedoen om insig te verkry in die spanningsvelde wat die formasie en daaropvolgende deformasie van die Bosveldkompleks en die omliggende areas beïnvloed het. Vyf hoof geologiese tydperke was oorweeg: voor-Transvaal, na-Transvaal/voor-Bosveld, na-Bosveld/voor-Waterberg, Pilanesberg, na-Waterberg/voor-Karoo. Die orientasies van die moontlike spannings wat verantwoordelik was vir die vorming van die strukture was afgelei uit inligting verwerf uit die literatuurstudie.

Die studie het bevind dat strukture soos gange, lineamente, verskuiwings en plooie in en om die Bosveldkompleks en omliggende gebiede 'n defnitiewe NW en NO strukturele neiging toon. Dit is ook opsigtelik dat NW en NO spanningsrigtings gedurig herbenut was, en dat gedurende die strukturele geskiedenis van die area die identiteite van die hoofspanningsrigtings gewissel het tussen NO en NW. Die enigste afwyking hiervan kom voor tydens die na-Waterberg tydperk, toe prominente NS spanningsrigtings geheers het. Die afgeleide spanningsvelde was konsekwent met voortdurende heraktifeering van dieThabazimbi-Murchison-Lineament (TML). Links-laterale, regs-laterale, op en normaal beweging het plaasgevind langs die TML gedurende verskillende tye in die geskiedenis van die Bosveldkompleks en omliggende gebiede.

TABLE OF CONTENTS

LIST OF FIGURES

LIST OF TABLES

1. INTRODUCTION

1.1 Location of the study area

The 2050 Ma (Harmer and Von Grunewaldt, 1991) Bushveld Complex of South Africa is the world's largest layered igneous complex extending over 66 000 km^2. The Complex is host to several economically important ore deposits such as chromium, vanadium and platinum-group elements (Von Grunewaldt and Harmer, 1993). The study area encompasses the whole of the Bushveld Complex and surrounding areas, stretching from longitude 25.6° E in the west to 31°E in the east, and from latitude -26.25°S in the south up to –23°S in the north (Figure 1.1).

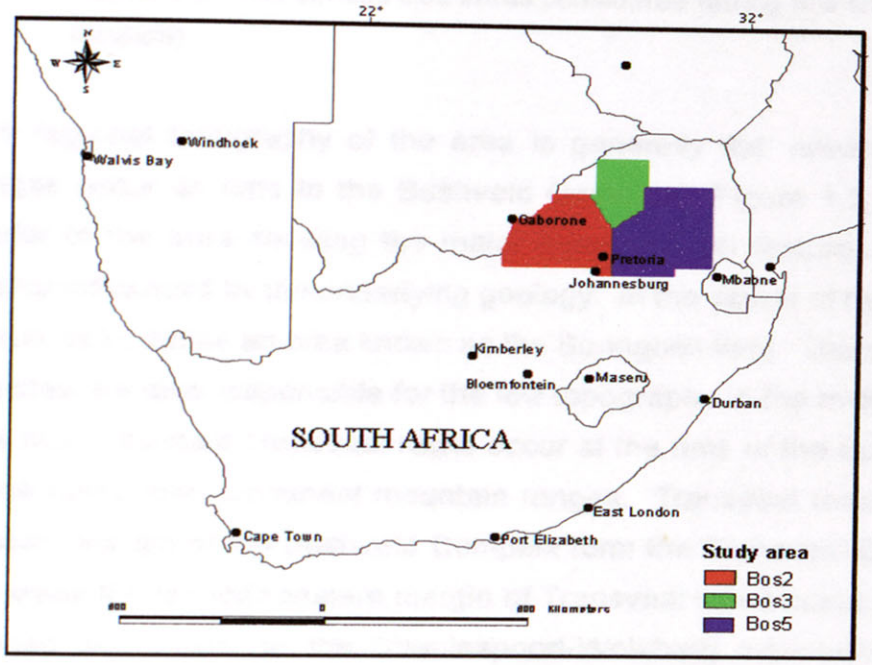

Figure 1.1. Location of the study area.

The study area was divided into three smaller regions based on the outcrop distribution of the Bushveld Complex. These areas include the western (Bos2), northern (Bos3) and eastern (Bos5) Bushveld Complex (Figure 1.2).

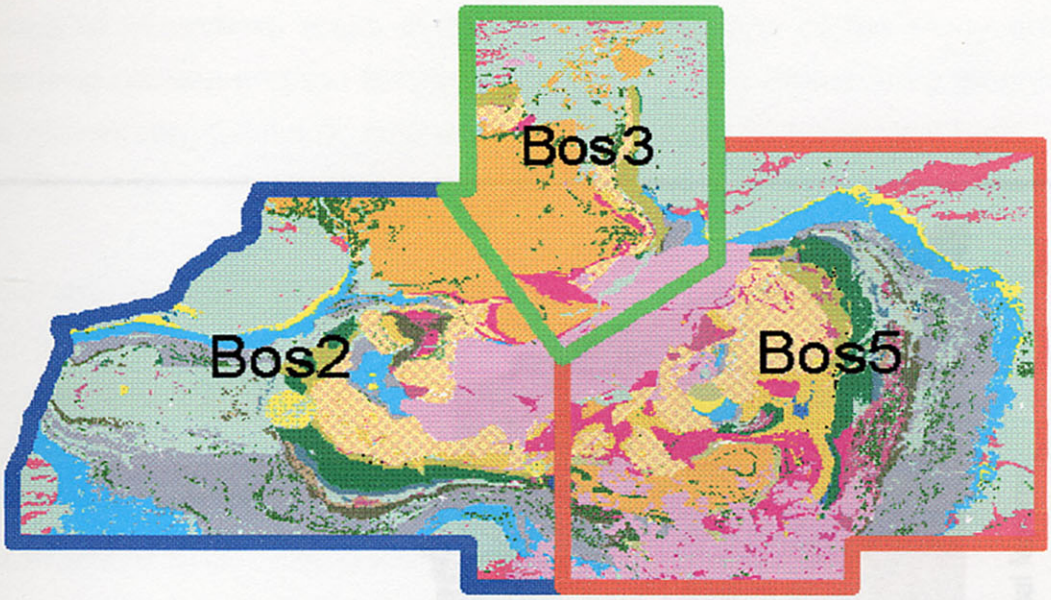

Figure 1.2. The various Bos areas considered during this study. (See Figure 1.1 for location)

The regional topography of the area is generally flat, however various mountain ranges occur as rims to the Bushveld Complex. Figure 1.3 is a digital elevation model of the area showing the major topographical features. The topography is mainly influenced by the underlying geology. In the center of the study area flat-lying Karoo rocks define an area known as the Springbok flats. The surrounding Bushveld granites are also responsible for the low topography in the middle of the study area. The more resistant Transvaal rocks occur at the rims of the Bushveld Complex and these rocks form prominent mountain ranges. Transvaal rocks exposed along the eastern margin of the Bushveld Complex form the Transvaal-Drakensberg plateau. Whereas the far northeastern margin of Transvaal rocks occur in a conspicuous NE striking belt known as the Chuniespoort-Wolkberg mountains. The northwestern exposure of Transvaal rocks form the Dwarsberg mountains, and the far southwestern margin defines the Tshwenyana-Enzelberg mountains. Along the southern margin of the Bushveld Complex, the Magaliesberg mountains form a prominent ridge, stretching from Rustenburg to Pretoria. Various isolated occurrences of Transvaal rocks in the Bushveld Complex depict hilly areas such as the Rooiberg fragment. The northern part of the study area is known as the Waterberg plateau, due to flat-lying Waterberg rocks. The southern margin of the plateau is delineated by the Waterberg mountains. This mountain range strikes ENE from Thabazimbi to Naboomspruit. However, just to the south it is locally known as the Swaershoek mountains.

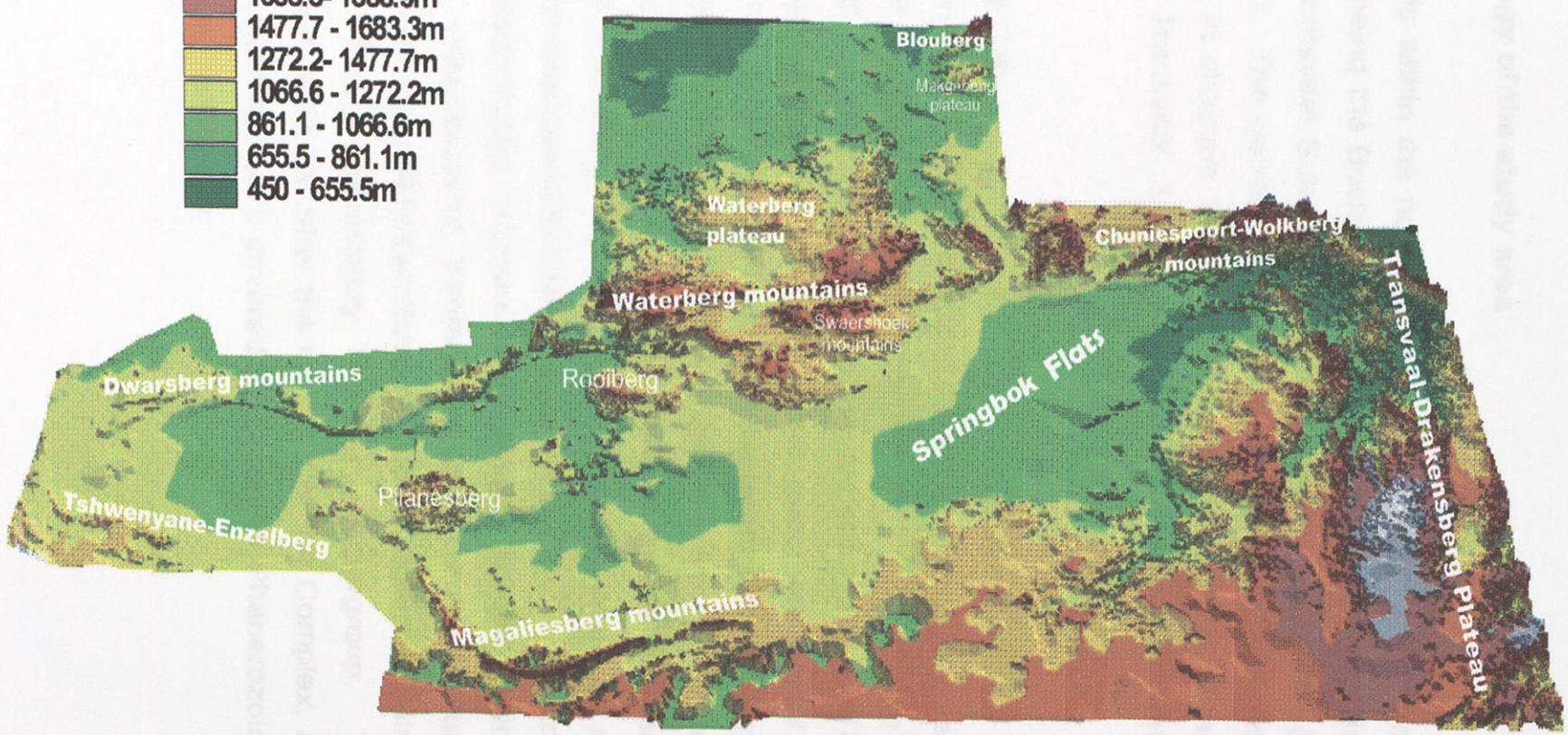

Figure 1.3. Digital elevation map of the study area showing the main topographical features

Outcrops of Waterberg rocks in the far northern parts of the study area, form the Makgabeng plateau and the Blouberg mountains. The Pilanesberg mountains, related to the Pilanesberg Complex, outline a striking circular topographical high.

1.2 General Geology of the study area

The study area falls within the northern part of the Kaapvaal Craton, with the main geological feature being the Bushveld Complex (Figure 1.4). The Bushveld Complex intruded into the Transvaal Supergroup at approximately 2050 Ma (Harmer and Von Gruenewaldt, 1991). The geology of the area, as well as the regional geology, are discussed in detail in chapters 3 and 4. Only a brief outline of the geology of the Kaapvaal Craton, Transvaal Supergroup and Bushveld Complex will serve as introduction.

1.2.1 The Kaapvaal Craton

The Kaapvaal Craton of South Africa is one of the world's best examples of an Archaean continental fragment. It covers an area of approximately 1.2×10^6 km^2 and formed and stabilized between 3.7 and 2.7 Ma years ago (de Wit et al., 1992). The boundaries of the Craton have been well defined using, structural, geochronological and geophysical data (Corner et al., 1990). The Lebombo monocline defines the eastern boundary, Mid-Proterozoic orogenic belts (Namaqua-Natal Mobile Belt) form the western and southern boundaries, while the northern limit is generally taken to be the Southern Marginal Zone of the Limpopo Belt (Thomas et al., 1993). The Craton comprises mainly Archaean granitoid terranes with interleaved remnants of greenstone belts. In addition several late Archaean volcano-sedimentary sequences developed on the Craton, such as the Pongola, Dominion, Witwatersrand, Ventersdorp, and Transvaal Supergroups. The Craton furthermore hosts the well known Bushveld Complex layered intrusion which was emplaced into the volcano-sedimentary Transvaal Supergroup. The Proterozoic Waterberg Group developed just after the intrusion of the Complex, and finally these Precambrian rock sequences were covered in places by Phanerozoic sediments and volcanics of the Karoo Supergroup.

Geological Map of the Study Area

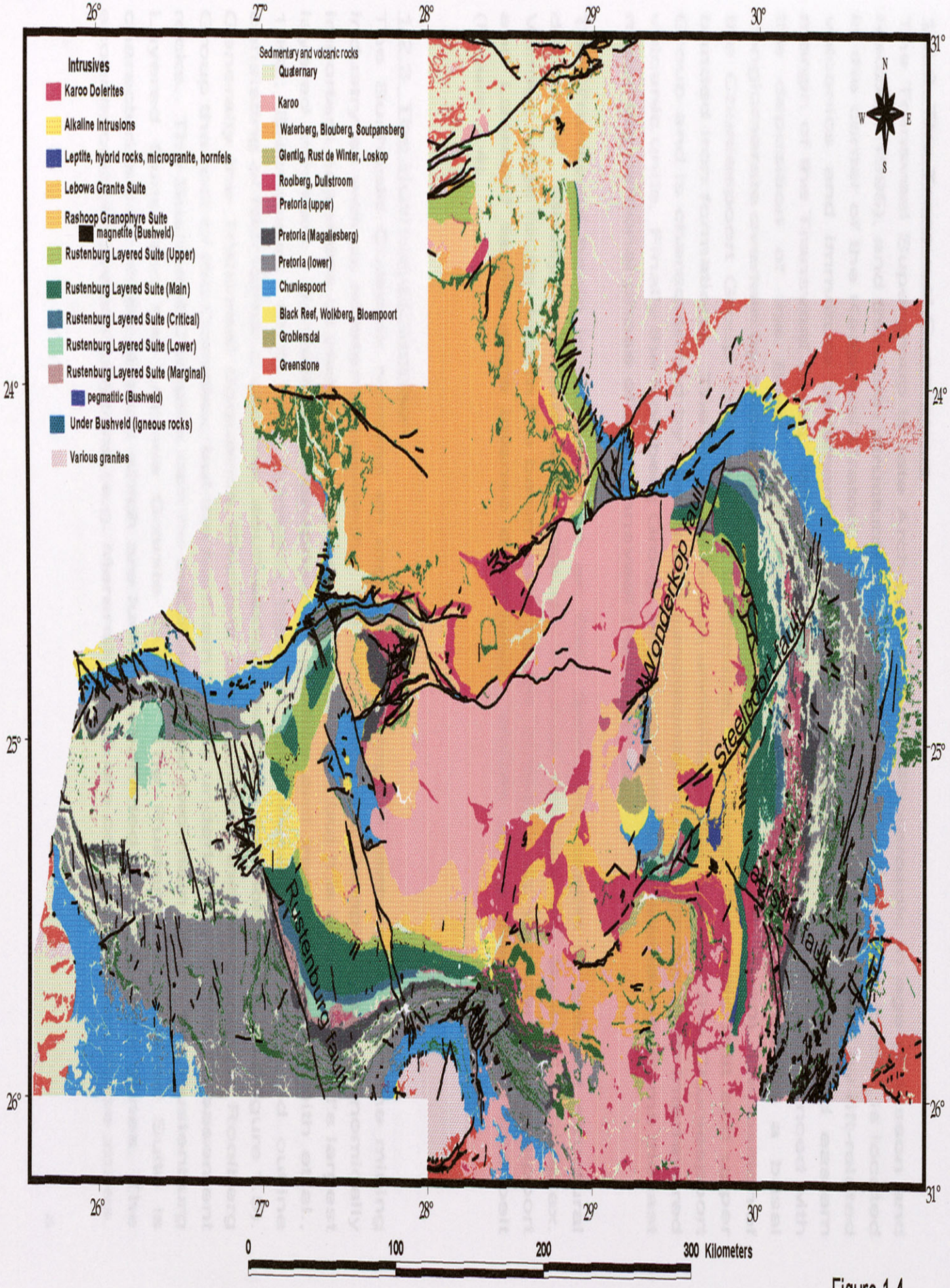

Figure 1.4

1.2.2 The Transvaal Supergroup

The Transvaal Supergroup is late Archaean to early-Proterozoic in age (Eriksson and Reczko, 1995), and the main structural basin, known as the Transvaal basin, is located in the center of the Kaapvaal Craton. Proto-basinal rocks, characterized by rift-related volcanics and immature sediments, are preserved along the northern and eastern margin of the Transvaal basin. Widespread Transvaal sedimentation commenced with the deposition of the Black Reef Formation which is characterized by a basal conglomerate overlain by feldspathic quartzite and shale (S.A.C.S., 1980). Deposition of the Chuniespoort Group followed and it consists of a lower dolomitic unit and upper banded iron formations. The Pretoria Group unconformably overlies the Chuniespoort Group and is characterized by alternating sandstones and mudrocks, with interlayered volcanic units. Finally the Rooiberg Group, which consists of felsitic lavas, forms the last major depositional phase of the Transvaal Supergroup.

The Transvaal basin is elongated in an ENE direction parallel to ancient structural directions. Mostly the Transvaal strata dip inwards, towards the Bushveld Complex. Various large faults deform the basin such as the, Rustenburg, Wonderkop, Steelpoort and Laersdrif faults, while intense deformation occurs along the Mhlapitsi fold belt (Figure 1.4).

1.2.3 The Bushveld Complex

The Bushveld Complex remains an important geological feature for both the mining industry as well as academic research. Not only does the Complex hold economically important quantities of platinum, chrome and vanadium, but it is also the world's largest layered intrusion. According to geophysical studies and investigations (Smith et al., 1962; Biesheuvel, 1970) the Complex has an approximate clover-shaped outline consisting of four lobes: a western, southeastern, eastern and northern lobe (Figure 1.5). Generally the Transvaal Sequence (Pretoria Group) forms the floor and the Rooiberg Group the roof of the Complex, but the northern lobe is underlain by Archaean basement rocks. The Bushveld Complex can be subdivided into two main units: the Rustenburg Layered Suite and the Lebowa Granite Suite. The Rustenburg Layered Suite is characterized by mafic phases which are further subdivided into five major zones. The economically important horizons (e.g. Merensky reef) are contained within these zones.

The Lebowa Granite Suite is slightly younger and marks the acid phase of the layered intrusion.

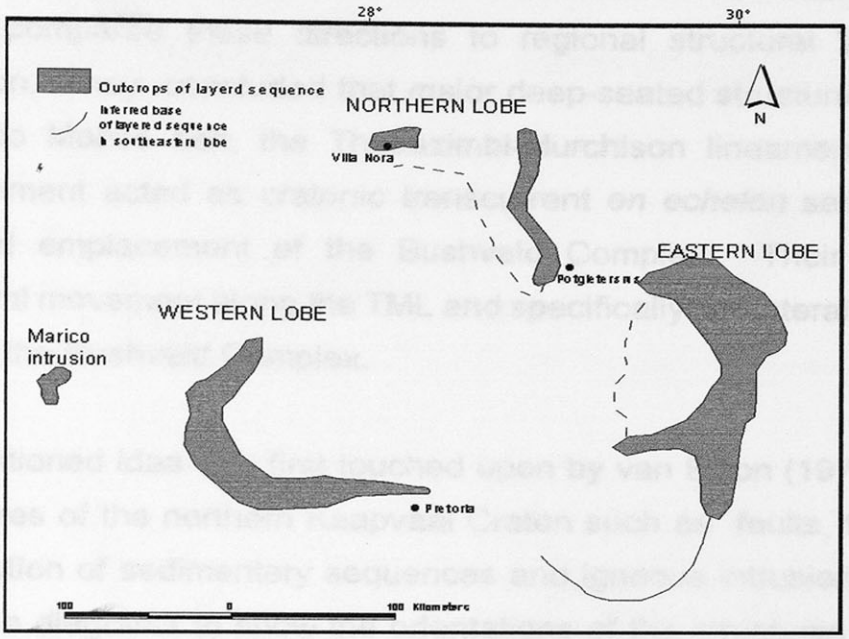

Figure 1.5. The clover shape outline of the Bushveld Complex, (after Tankard et al., 1982.)

Isolated occurrences of deformed Transvaal rocks occur within the Bushveld Complex, they are known as Transvaal Inliers. It is believed (Hartzer, 1995) that earlier tectonic activity caused interference folding in the Transvaal rocks and that Bushveld magmas solidified around these domes. However, some domes are interpreted as diapirs (Sharpe and Chadwick, 1982). Overall the dips of the layered sequences in each lobe are gently (10° to 25°) towards the center except for the northern lobe where dips of up to 60° occur. These dips are generally the same as those in the Transvaal Supergroup and it is proposed by Harmer and Von Gruenewaldt (1991), that this reflects thermal collapse after the emplacement of the Complex.

1.3 Previous research

The Bushveld complex and its tectonic setting has been the subject of much research in the past. Opinions vary greatly from a regional compressional setting (Sharpe and Snyman, 1980; Harmer & von Gruenewaldt, 1991; Uken & Watkeys 1997b) to tensional

environments (Van Biljon, 1976). The main theories which consider the orientations of structures are outlined below:

Du Plessis and Walraven (1990) examined the orientations of structures in the Bushveld Complex and compared these directions to regional structural lineaments of the Kaapvaal Craton. They concluded that major deep-seated structural lineaments such as the Limpopo Mobile belt, the Thabazimbi-Murchison lineament (TML), and the Barberton lineament acted as cratonic transcurrent *en echelon* sets, influencing the distribution and emplacement of the Bushveld Complex. Their model promotes continuing lateral movement along the TML and specifically left-lateral movement during the intrusion of the Bushveld Complex.

The above mentioned idea was first touched upon by van Biljon (1976). He examined structural features of the northern Kaapvaal Craton such as faults, folds, lineaments, and the distribution of sedimentary sequences and igneous intrusions. In addition he constructed rose diagrams to show the orientations of the structures in various areas, (Figure 1.6). Van Biljon (1976) attributes the intrusion of the Bushveld Complex to an active spreading center in which major lineaments acted as large transcurrent faults.

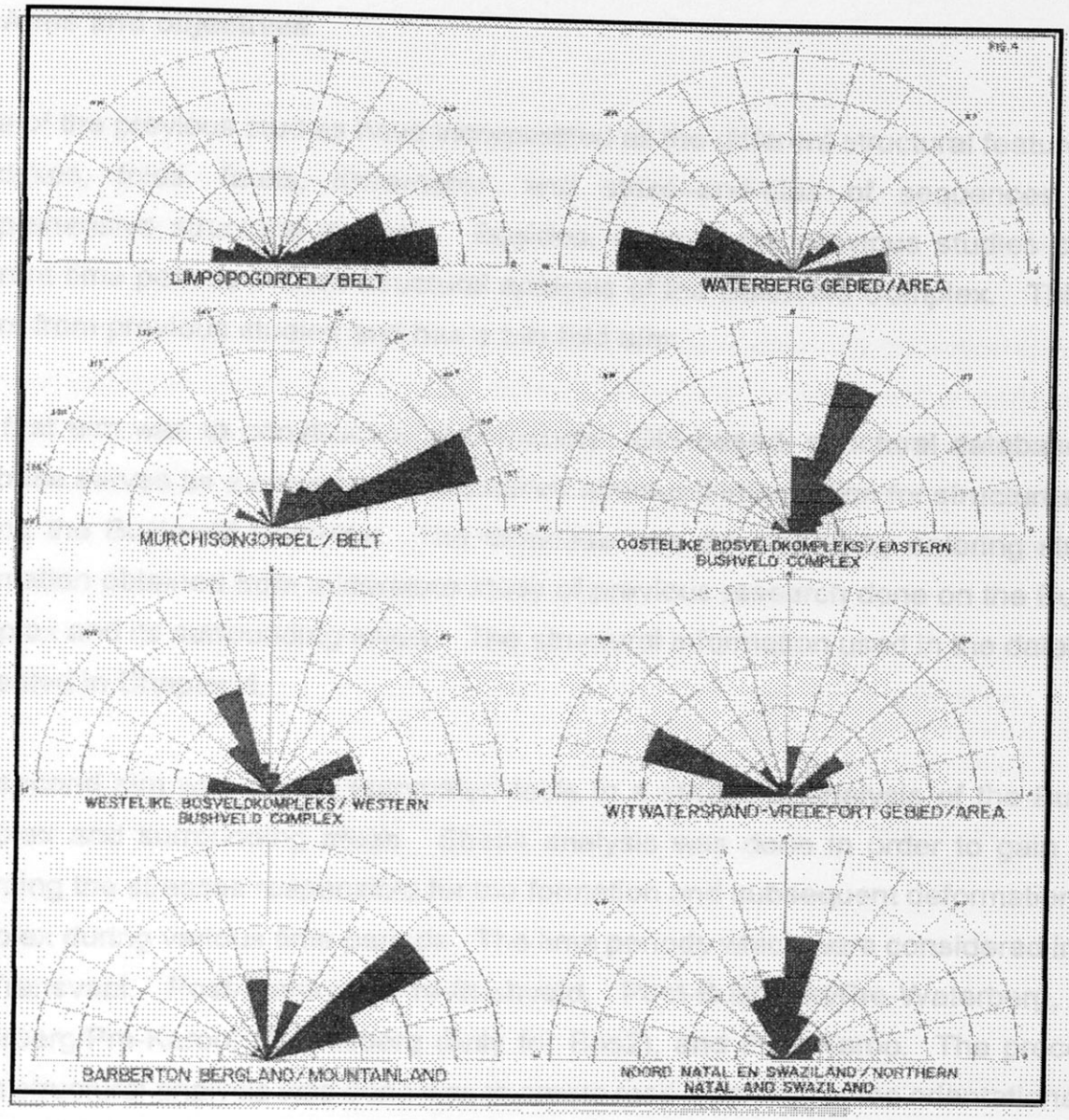

Figure 1.6 Rose diagrams of fault directions (after van Biljon, 1976)

A study done by Lee and Sharpe (1986) on the structural setting of the Bushveld Complex, aided by LANDSAT imagery, are at variance with the above mentioned theories. They concluded that no evidence is present for deep-seated crustal fractures which influenced the location and form of the Bushveld Complex. They based their findings on the fact that no pervasive lineaments are visible with landsat imagery.

1.4 Aims and objectives

None of the previous studies have incorporated all the different structural features such as dykes, folds, faults, lineaments, and strike–and-dips of sequences into a comprehensive structural analysis. Besides, none of the previous studies consider different time periods in their structural analysis of the Bushveld Complex. This study differs from previous studies and has a two fold aim:

The first aim was to construct a 'user-friendly', GIS-based, structural database. The database serves as a compilation of detailed structural information for structures in and around the Bushveld Complex. The database was developed by entering structural information obtained from a literature study of previous research done on the Bushveld Complex and its surrounding areas. The structural information used in the database is presented in Chapter 4.

The second aim was to use automated tools in a structural analysis of the Bushveld Complex and surrounding areas. Stress analysis was done in order to gain insight regarding the stresses responsible for the formation and subsequent deformation of the Complex during various time periods. The time periods which were considered include; Pre-Transvaal, Post-Transvaal/Pre-Bushveld, Post-Bushveld/Pre-Waterberg, Post-Waterberg/Pre-Karoo, Pilanesberg (only for Bos2), and Post-Karoo. The process by which structural analysis was done was to create rose diagrams of the orientations of the various structures using ArcView 3.2 GIS. Stress directions were interpreted from the rose diagrams, and attempts were made to related these stress directions to tectonic processes affecting the Kaapvaal Craton. In addition, stereographical plots of strike-and-dip data of the Bushveld Complex and surrounding areas were analysed to assist with structural analyses.

By incorporating the structural information gained from the literature study together with structural analyses of rose diagrams and stereographical plots, a clear understanding of the stresses responsible for the formation and subsequent deformation of the Bushveld Complex and surrounding areas should be possible.

1.5 Methodology

GIS (Geographic Information Systems) techniques have been used successfully in a number of fields (wild life studies, agriculture, telecommunications, etc.) This study aims to test the suitability of GIS as a tool in structural analysis, because it allows for the input, storing, manipulation and output of vast amounts of data. By definition GIS makes use of geographic data, which through manipulation and analysis, will provide answers to questions based on the data. Similarly, during this study, structural data were used as input in creating a database, and through manipulation, mostly by creating rose diagrams, a structural analysis of the Bushveld Complex and surrounding areas was done. The GIS process is illustrated by the following diagram:

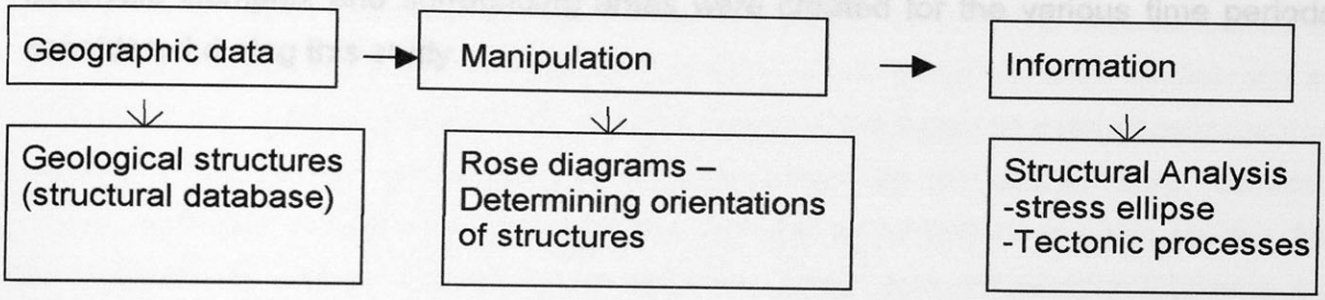

The basic methods employed during this study were two fold:

Firstly, a detailed literature study was done, to gather structural information relating to the Bushveld Complex and surrounding areas. Detailed research done by Jansen (1982), Du Plessis (1991); Potgieter (1992); Hartzer (1987, 1994); and Bumby (1997, 2000), as well as various review articles and books (Tankard et al., 1982; Thomas et al., 1993; Mc Court 1995; Brandl and de Wit, 1997; Visser 1998) provided much of the information. The structural database was mainly developed for all faults and folds occurring in the Bushveld Complex area. Information for faults include; name of the fault, fault type, displacement style, age, reactivation age as well as any references pertaining to the fault. Folds information include; name for the fold, fold type, axial plane dip, fold axis plunge, age, and references pertaining to the fold. The structural information was coded to allow for easy data retrieval, and can also be easily updated. The coded fields can be linked with appropriate look-up tables which provide the descriptions for the codes.

Secondly, by using GIS techniques, the orientations of structural lines were determined, as well as ages of faults and folds based on cross-cutting relationships. ArcView 3.2 GIS was customized to represent the orientations of these lines with rose diagrams representing different time periods. Structural lines such as dykes and lineaments were grouped into structural domains and rose diagrams were created for the various domains. Stress directions were interpreted from these rose diagrams based on the type of structure using Anderson's theory (1951) of faulting and dyke formation. Strike-and-dip data of the Bushveld Complex and surrounding areas were used to create stereographic plots using Spheristat 2. By using all the structural information gained from the literature study together with information from structural analyses of rose diagrams and stereographic plots, geo-chronological tables of the tectonic history of the Bushveld Complex and surrounding areas were created for the various time periods considered during this study.

2. EXPERIMENTAL METHODS – GEOGRAPHIC INFORMATION SYSTEMS

2.1 Geographic Information Systems

Geographic Information Systems (GIS) are automated tools which are used in the input, storing, manipulation, analysis, and reporting of spatial data. The ideas originated in the 1960's but at first the applications were limited. Today GIS is applied to a wide variety of business and organizations and the applications are almost endless. However, the use of GIS applications within geological discipline, are primarily used as map creation software, and the true value of a Geographic Information System is under-utilized. GIS can be especially useful in geology because, instead of working with conventional printed geological maps, the user can now analyze, explore and visualize spatial data as separate coverages. GIS also allows for the storing of attributes of a map coverage and therefore, queries and calculations can be performed on the spatial data. DeMers' (1997) definition of GIS describes well the application of GIS during this study. He defines GIS as follows; "In the broadest terms, Geographic Information Systems are tools that allow for the processing of spatial data into information, generally information tied explicitly to, and used to make decisions about, some portion of the earth". The GIS *'tools'* (software) that were used during this study is ArcView 3.2. The *'spatial data'* are BOSGIS (see 2.2), and the *'decisions'* that were made, involve the interpretation of the structural history of the Bushveld Complex (see Chapter 6).

2.1.1 The Software – ArcView 3.2 GIS

Many different GIS software packages are available on the market. ArcView 3.2 GIS, created by Environmental Systems Research Institute (ESRI), was the main GIS software program used during this study. The foundation of ArcView is it's ability to manage spatial data. Spatial data is geographic data that stores the geometric location of particular features, along with attribute information describing what these features represent. ArcView organizes its spatial data into projects, and each project consists of various documents:

- **Views** – A view consists of a logical group of related point, line or polygon features known as layers or themes which cover more or less the same geographical area. These themes are stored as shape files (*.shp), which is a simple non-topological format for storing the geometric location and attribute information of geographic features.
- **Tables** – An ArcView table references the tabular data source it represents, but doesn't contain the tabular data itself. Tabular data can be stored in dBASE, INFO (an ArcInfo data file format), and ASCII delimited text files.
- **Charts** – Charts are also fully integrated into ArcView's geographic environment, and allows for the graphical display of tabular and chart representations of the attributes of geographic data.
- **Layouts** – Layouts assemble all the components of a project to produce high quality printable maps. A direct live link exist between the layout and the data it represents.
- **Scripts** – Avenue, the object-orientated programming language of ArcView allows for the customization of ArcView by changing the graphical user interface, by directing ArcView to perform a specific task or manipulating tabular data. ArcView scripts (*.ave files) are macros written in Avenue. Various scripts are included with ArcView and additional scripts can be obtained from the ESRI homepage (www.esri.com).

ArcView has many analytical capabilities a few of which are mentioned here.

1. Adjacency analysis – 'Theme on theme' selections can be performed between any feature themes displayed in a view. For example: all the points that completely fall within a selected region of a polygon theme can be selected or, all the lines that intersect a specific point theme can be chosen.
2. Proximity analysis - 'In distance of' operations can also be performed between any feature themes displayed in a view. For example all the points that lie within a distance of 3 km from a selected point theme can be chosen.
3. Queries – When themes need to meet specific requirements queries can be performed on the theme. For example: all the lines with a length greater than 100 m need to be selected. Arc View's query builder allows complex queries to be executed using logical operators such as 'and', 'or', '≤', '=' and the like statements.

4. Calculations – Mathematical calculations can be performed on number fields in the attribute table of a theme. ArcView allows for a range of mathematical operations such as square root, trigonometric functions, logs, etc.

ArcView contains many extensions which have the potential to be very useful to geological problems. These extensions include, Spatial Analyst, 3D Analyst and various other image processing tools. None of these extensions were employed during this study.

2.1.2. Other non-GIS software

Other non-GIS software, used in conjunction with ArcView, include Spheristat 2. Spheristat allows for the entering of structural field measurements (either axial/non-directed or polar/vector) in tabular form and plotting them in a variety of ways: on a stereonet (Schmidt equal area or Wulff equal angle), on a map, or rose diagram. Each plotting method offers one or more analytical tools to extract more information from the data (Stesky, 1998).

2.2 BOSGIS

BOSGIS is a computerized geological database of the Bushveld Complex. The database was created by the Department of Earth Sciences, University of Pretoria in collaboration with the Council for Geoscience. The basis for BOSGIS is a generalized digital geological database, comprising the Pietersburg (2328), Tzaneen (2330), Thabazimbi (2426), Nylstroom (2428), Pelgrimsrus (2430), Mafikeng (2524), Rustenburg (2526), Pretoria (2528), Barberton (2530), and East Rand (2628), 1:250 000 map sheets. Other data include cadastral, contour, topographical and geochemical data of the Bushveld Complex and surrounding areas. A manual for the use of BOSGIS was compiled by Brynard (1996) as an internal report to the Department of Earth Sciences, University of Pretoria. Since the database serves as foundation for this study, a brief description of the nature of the various components of BOSGIS follows:

2.2.1 Geological data

Geological data are subdivided into polygon (gst), point (gsp), and line (gsr & gdb) data.

- *Polygon* – This includes the geological boundaries of the Bushveld Complex and surrounding areas. The geological map of the Bushveld Complex and surrounding areas was divided into six subdivisions, namely Bos1 to Bos6 (Figure 2.1). These maps include the stratigraphical subdivisions of the Bushveld Complex as present on the 1:250 000 geological maps as well as a simplified version of the formations younger and older than the Bushveld Complex (Figure 1.4). Only three of these map areas contain rocks of the Bushveld Complex. They are Bos2 (western Bushveld Complex), Bos3 (northern Bushveld Complex), and Bos5 (eastern Bushveld Complex). The lithostratigraphic units of these maps are identified by a unique numeric key (code) defined by the 'newclass' field in the theme's attribute tables. This descriptive data or attributes allow logical selections to be made at Formation, Group or Supergroup level for sedimentary units, and Suite or Complex level for igneous rocks.

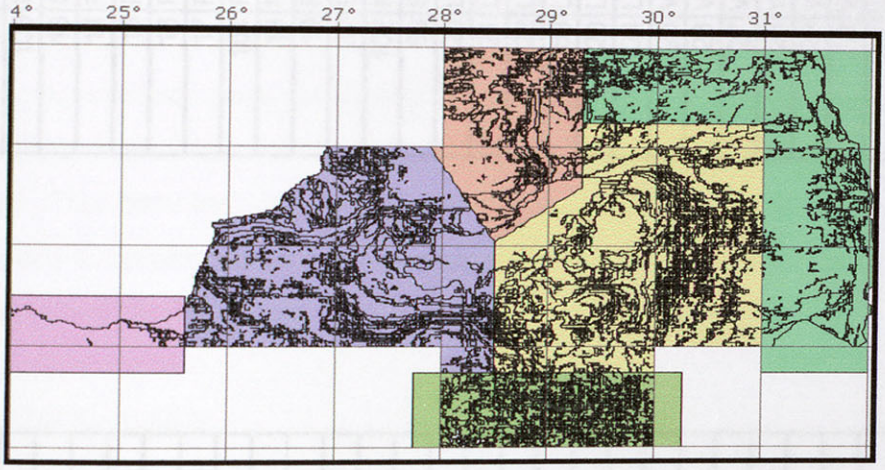

Figure 2.1: The various component maps of the BOSGIS database

- *Point* data (gsp) contain all the point features found on the 1:250 000 geological maps comprising the Bushveld Complex area. This includes most importantly strike and dip values recorded in dip-dip direction format. Other points include mines, trigonometric points, diatremes, mineral deposits etc. (Table 2.1). The 'lin' field in the theme's attribute table reflects the key to the various point features.

Table 2.1. Point features in BOSGIS.

LIN	Description
10	Horizontal bed
69	Strike of vertical bedding
12	Strike and dip of bed (facing unknown)
21	Strike of anticlinal axis
197	Strike of antiformal axis
24	Strike of overturned anticline
27	Strike of inverted anticlinal axial plane
22	Strike of synclinal axis
198	Strike of synformal axis
25	Strike of overturned syncline
26	Strike of inverted synclinal axial plane
23	Strike of monoclinal axis
29	Strike of vertical axial plane
11	Strike and dip of bed
13	Strike and dip of overturned bed
9	Volcanic pipe, basic
8	Volcanic pipe, alkaline
6	Kimberlite pipe
5	Kimberlite pipe (suboutcrop)
113	Diatreme
4	Magnetite pipe
184	Mine in production
185	Mine in disuse
55	alluvial workings
56	Alluvial workings in disuse
114	Mineral occurrence/deposit
53	Gravity base station
54	Gravity observation point

Table 2.2. Line features in BOSGIS

LIN	Description
10	Fault, observed
11	Fault, observed, normal
12	Fault, observed reverse
100	Fault, observed, high angle reverse
13	Fault, observed thrust
14	Fault, observed, slip
15	Fault, inferred/concealed
16	Fault, inferred, normal
17	Fault, inferred, reverse
101	Fault, inferred, high angle reverse
18	Fault, inferred, thrust
19	Fault, inferred, slip
82	Breccia fault
102	Mylonitization
69	Shear zone
20	Linear feature, undifferentiated
21	Linear feature, possible dyke
22	Linear feature, aeromagnetic
68	Linear feature, magnetic anomaly, surface survey
23	Linear feature, satellite imagery
24	Linear feature, aeromag. & sat. imagery
25	Vein, undifferentiated
26	Vein, quartz
27	Vein, iron-rich
28	Vein, aplite
29	Vein pegmatite
30	Vein, granophyre
31	Vein, breccia
32	Joint
33	Fold axis, undifferentiated
34	Anticlinal axis
35	Synclinal axis
36	Antiformal axis
37	Synformal axis
103	Structural form line

- *Line* data (gdb = dykes and beds), and (gsr = structural lines) contain various structural lines found on the 1:250 000 geological maps. Each gdb folder contains a unique 'dat' file which provides a key for the type of dyke represented on the map. The 'key' field of the 'dat' file can be joined with the 'key' field of the attribute table of the theme to enable logical selection of the dykes. For example distinction can be made between dolerite, diabase, and syenite dykes. Structural lines (gsr), include data such as faults, folds and linear features (Table 2.2). The 'lin' field in the theme's attribute tables provide a key for the type of line represented on the map.

2.2.2 Cadastral data.

The cadastral data were provided by the Department of Land Affairs. The data include the provincial-, magistrate-, and farm boundaries of portions of Mphumalanga (etvl), Gauteng (gaut), the Northern Province (ntvl), and the Northwestern Province (nwes) which encompasses the Bushveld Complex area. It is recommended that the data should not be used at a scale larger than 1:500 000 (Brynard, 1996).

2.2.3 Topographical data

The topographical data were originally obtained from the Department of Land Affairs and converted from the National Exchange format (NES) by Brynard (1996) into Arc/Info format. The data include all general topographical and man-made features found in the Bushveld Complex area, for example, tunnels, railways, dams, channels, buildings, mines, power lines, urban areas, etc.

2.2.4 Contour data

The data include a line theme of 100 m contour intervals, and at some places, 50 m intervals for the Bushveld Complex and surrounding areas, as shown in Figure 2.2.

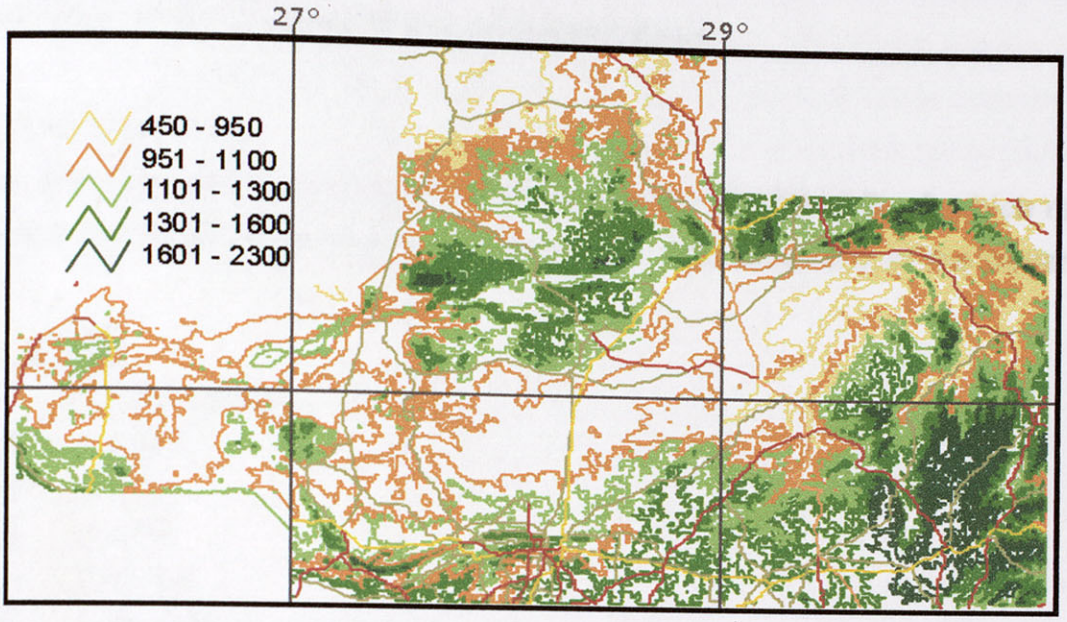

Figure 2.2 100 m topographic contour intervals of BOSGIS

2.2.5 Geochemical data

Geochemical data include a geochemical database created by Brynard (1996). Chemical analyses from theses, publications, and other sources were digitized and compiled into a database. The database currently contains 1 700 georeferenced chemical analyses of mostly main and trace elements of rocks comprising the Bushveld Complex.

2.3 GIS Methods and Techniques

During this study GIS methods and techniques were applied on a revised version of BOSGIS. The new database was modified from the existing BOSGIS. A few modifications had to be made in order for the database to function correctly during execution of the various GIS techniques. In addition the revised BOSGIS was organized in such a way to serve as a proper structural database. Firstly the file structure, project structure and modifications to the revised BOSGIS are discussed. Secondly the structural database creation process is outlined and then finally the GIS methods and techniques are explained.

2.3.1 Revised BOSGIS

An explanation of the creation of this database follows.

2.3.1.1 File structure

The files are organized into three main folders, Bos2, Bos3 and Bos5 which reflect the components of BOSGIS as explained previously. The hierarchy of the folders are as follows:

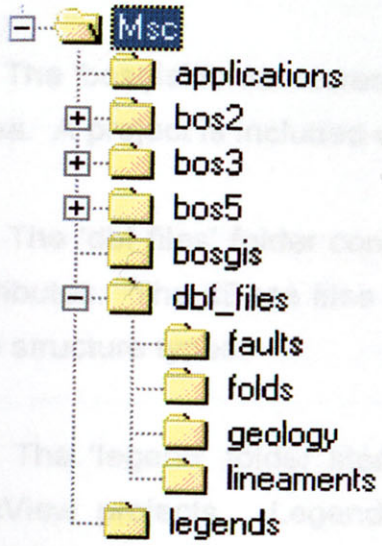

1. The 'Applications' folder contains all the avenue scripts and other programs used to customize the ArcView projects. All scripts are included in Appendix 1.

2. Bos2, Bos3, and Bos5 folders store all the projects and structural data which were created for the structural analyses. Each of these folders contains the following sub-folders, as well as five ArcView project files:

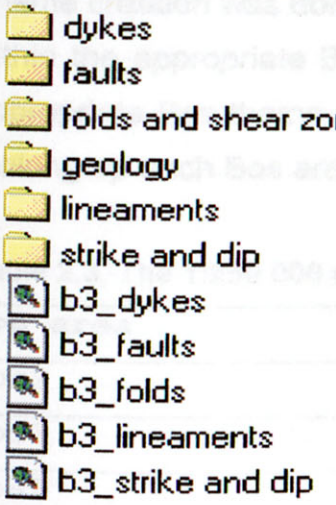

The project files organize and compile the different types of structural data which were considered in the structural analyses, and will be described in more detail later. The sub-folders store the data which are used by each project. The Dykes, Faults, Folds and Shear zones, and Lineaments sub-folders each contain 'gen file' folders which store the generate and output files used to create rose diagrams, which will be explained later. The Geology folder has a sub-folder named, 'age layers' storing the various age layers. The strike and dip folder has a sub-folder named 'spheristat files' which stores the spheristat data.

3. The 'bosgis' folder stores data which encompass the whole of the Bushveld Complex area. A project is included which compiles and presents the various BOSGIS data.

4. The 'dbf files' folder contains all the dBase files used for explanation of a theme's attributes. The dBase files are organized under the appropriate sub-folders reflecting the structure types.

5. The 'legend' folder stores all the legends which were applied to themes of the ArcView projects. Legends were created based on specific attribute information contained in a theme.

2.3.1.2 Theme creation

The Bos2, Bos3 and Bos5 geology themes already existed but new dykes, faults, folds, and lineament themes for these areas had to be created from the existing BOSGIS data. Theme creation was done by merging the respective gsp, gsr and gdb themes which lie within the appropriate Bos area. These themes were clipped to the exact size of the appropriate Bos theme size. The following table shows the gsp, gsr and gdb themes making up each Bos area:

Table 2.3. The 1:250 000 map sheet numbers used in creation of the respective Bos areas.

Bos area	gsp, gsr and gdb themes
Bos2	2426 2428 2524 2526 2528 2628
Bos3	2428 2328
Bos5	2328 2330 2428 2430 2528 2530 2628

The strike and dip themes were generated by selecting the points from the gsp theme with Lin field values of 10, 11, 12, 13, and 69 (Table 2.1). The faults, folds and lineament themes were created by selecting Lin field values (Table 2.2) from the gsr themes as shown in the following table:

Table 2.4 The lin field values selected from BOSGIS for the creation of the respective themes.

Theme	Lin field values
Faults	10, 11,12,13,14,15,16,17,18,19,82,100
Folds and shear zones	33,34,35,36,37,69
Lineaments	20,21,22,23,24,68

The dyke themes were more cumbersome to create since no uniform field existed which described the different types of dykes. Each gdb file contains its own attribute file which were joined with the gdb theme. These joins were performed before merging the gdb files and then only the diabase, dolerite and syenite dykes were selected and converted into the respective dyke themes.

2.3.1.3 Project Structures

All the projects of the various Bos areas consist of the same structure. A detailed description of the organization of the projects follows:

- **Fault projects** – Each fault project consists of four *Views* namely, Fault Map, Age Map, Rose diagram Map1 and Rose diagram Map2. The Fault Map view is the geological map of the area with the Fault theme displaying the various types of faults present in the area. The Age Map view displays the fault related themes according to the ages of the faults. The Rose diagram Map view displays an outline of the geology of the area as well as the various age fault themes used in the creation of the rose diagrams. The *Table* documents include all the fault related dBase files which can be joined with the feature attribute table to provide descriptive data. Three map *layouts* were created for each fault project. The layouts include a general geological map made from the Fault Map view, as well as layouts of the two Rose diagram maps. Four Avenue *scripts* are included in the Fault projects which were used for rose diagram production.

- **Dyke projects** – These projects consist of two *Views*, a Dyke Map view and a Rose diagram Map view. *Table* documents included a domain dBase table which explains the domains used in the rose diagrams. Two *layouts* were made of the general dyke map and rose diagram map.
- **Lineament projects** - The structure of the lineament projects is the same as the dyke projects.
- **Folds projects** – These projects consist of three *views*, a general geological map, Age Map view and a Rose diagram view. *Tables* include all the dBase files explaining the codes for the folds attribute table. Two *layouts* were made of the general geological map and the rose diagram map view.
- **Strike and dip projects** – These projects consist of two *Views*, a Strike and Dip Map and a Spheristat Map. *Table* documents include a dBase file for explaining the domains in the attribute field. The number of *layouts* varied according to the amount of stereonet plots.

2.3.1.4 Changes to the existing BOSGIS database

Stratigraphy

- A new lithostratigraphic attribute file was created which accurately portrays the stratigraphy of the Bushveld Complex and surrounding areas. Table 2.5 and Table 2.6 show the difference between the two stratigraphic tables. The MEMBER field was discarded since it is redundant, as only generalized distinction is being made between the various formations. Furthermore, changes were made, such as the division of the Pretoria Group into an Upper, Magaliesberg, and Lower formations. Also newclass 13 was changed to Wolkberg/Black Reef formations and Newclass 24, labeled Soutpansberg was useless, see Chapter 3.

Table 2.5. Lithostratigraphic attributes of BOSGIS

USER ID	SUPERGROUP	GROUP	FORMATION	MEMBER	NEW CLASS
1	Bushveld Complex	Rashoop Granophyre Suite			1
2	Bushveld Complex	Lebowa Granite Suite			2
3	Bushveld Complex	Rustenburg Layered Suite	Upper Zone		3
4	Bushveld Complex	Rustenburg Layered Suite	Main Zone		4
5	Bushveld Complex	Rustenburg Layered Suite	Critical Zone		5
6	Bushveld Complex	Rustenburg Layered Suite	Lower Zone		6
7	Bushveld Complex	Rustenburg Layered Suite	Marginal Zone		7
8		Glentig, Rust de Winter, Loskop			8
9		Rooiberg, Dullstroom			9
10	Transvaal	Pretoria	Rayton	Houtenbek	10
10	Transvaal	Pretoria		Steenkampsberg	10
10	Transvaal	Pretoria		Nederhorst	10
10	Transvaal	Pretoria		Lakenvlei	10
10	Transvaal	Pretoria		Vermont	10
10	Transvaal	Pretoria		Makekaan	10
10	Transvaal	Pretoria		Smelterskop	10
10	Transvaal	Pretoria		Leeuwpoort	10
10	Transvaal	Pretoria		Rayton	10
11	Transvaal	Pretoria		Dwaalheuwel	11
11	Transvaal	Pretoria		Boshoek	11
11	Transvaal	Pretoria		Rooihoogte	11
11	Transvaal	Pretoria		Silverton	11
11	Transvaal	Pretoria		Daspoort	11
11	Transvaal	Pretoria		Strubenkop	11
11	Transvaal	Pretoria		Hekpoort	11
12		Chuniespoort	Duitschland, Penge, Malmani	Frisco	12
12		Chuniespoort	Duitschland, Penge, Malmani	Eccles	12
12		Chuniespoort	Lyttleton, Oaktree, Black Reef	Monte Christo	12
13		Groblersdal	Dennilton		13
14		Groblersdal	Dennilton		14
15	Transvaal	Pretoria		Magaliesberg	15
16	Karoo	Karoo Dolerites			16
20		Archaean Rocks			20
21	Karoo	Karoo			21
22		Waterberg			22
23		Quaternary			23
24		Soutpansberg			24
25		Intrusions			25
26		Pilanesberg, Spitskop etc.			26
27		Various Granites			27
28		Hybrid rocks			28
29		Dunites			29
30	Bushveld Complex	Under Bushveld			30
31	Bushveld Complex	Magnetite			31

Table 2.6 Revised lithostratigraphic attributes for the BOSGIS database

SUPERGROUP	GROUP	NEWCLASS
Bushveld Complex	Rashoop Granophyre Suite	1
Bushveld Complex	Lebowa Granite Suite	2
Bushveld Complex	Rustenburg Layered Suite (Upper)	3
Bushveld Complex	Rustenburg Layered Suite (Main)	4
Bushveld Complex	Rustenburg Layered Suite (Critical)	5
Bushveld Complex	Rustenburg Layered Suite (Lower)	6
Bushveld Complex	Rustenburg Layered Suite (Marginal)	7
Transvaal	Glentig, Rust de Winter, Loskop	8
Transvaal	Rooiberg, Dullstroom	9
Transvaal	Pretoria (upper)	10
Transvaal	Pretoria (lower)	11
Transvaal	Chuniespoort	12
Transvaal	Wolkberg	13
Transvaal	Groblersdal	14
Transvaal	Pretoria (Magaliesberg)	15
Karoo	Karoo Dolerites	16
Archaean Rocks	Archaean Rocks	20
Karoo	Karoo	21
Waterberg	Waterberg, Blouberg	22
Quaternary	Quaternary	23
Soutpansberg	Soutpansberg	24
Intrusions	Intrusions (diabase)	25
Pilanesberg	Alkaline Intrusions	26
Precambrian granites	Various Granites	27
Post-Transvaal	Leptite, Hybrid rocks	28
Bushveld Complex	Pegmatitic	29
Bushveld Complex	Under Bushveld igneous rocks	30
Bushveld Complex	Magnetite	31
Bushveld Complex	Rashoop	32
Dam		100

Legends:

- The original BOSGIS geology legend was appropriately changed to a revised legend which reflects the changes of the revised lithostratigraphic attribute table. Other legends which were created include a lineament, fault-type, folds, and a strike-and-dip legend. These legends were based on attribute values obtained from the BOSGIS database, and provided symbols to discern between the various objects. However, the strike-and-dip themes needed an additional field, which was used to rotate the dip symbol. ArcView uses a cartesian orientation system and not a geographic one where north is at 0°. The Azimuth field was

therefore not appropriate to use as rotation field for dip symbols. A new field was created, Dip_Rot, and these values were obtained from a simple calculation expression: [360 – [Azimuth]].

Addition of new data

- Fold themes were expanded by digitizing folds documented in the literature. Digitized structures include: folds of the Mhlapitsi fold belt as mapped by Potgieter (1992), Hartzer's (1992) folds in the Transvaal Inliers, a few folds around the Pilanesberg Complex, and minor folding in the far Western Transvaal basin as mapped by Vermaak (1970). In addition, folds along the southern margin of the Waterberg basin (Jansen, 1982), and estimated folds around the Johannesburg dome recorded by Gibson et al. (1999) were included.

Dykes

- The original dyke theme from the BOSGIS database contained a few discrepancies. These discrepancies, however, were carried over from the original data capturing during the production of the 1:250 000 geological maps. Firstly, since the geological maps were compiled by different people, inconsistencies exist between the dykes and their compositions as recorded from one map to another (Figure 2.3). However, no automated solution could be employed to resolve this problem, and the different compositions were simply ignored.

  Secondly, many of the dykes present in the Bos5 area have a very sinuous nature, as illustrated by Figure 2.3. Dykes are known to be more or less vertical planar features, and therefore it's surface intersection should be fairly straight. It is therefore unlikely that these 'sinuous dykes' are representative of real dykes, but is thought to rather be a reflection of sills intersecting the surface. It was therefore decided to exclude these 'sinuous dykes' from the Bos5 project.

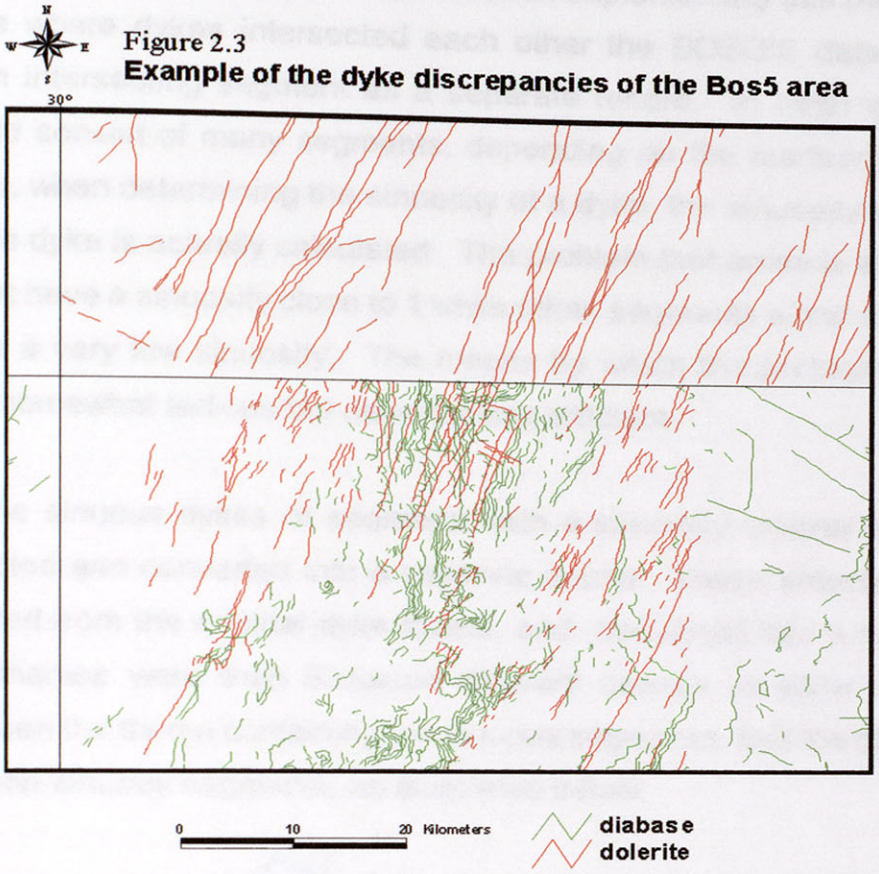

Figure 2.3
Example of the dyke discrepancies of the Bos5 area

The method by which this was done is based on calculating the sinuosity of all the dykes. Sinuosity is the straight line length divided by the total length of the dyke, thus perfectly straight dykes would have a sinuosity of one. In this study all the dykes with a sinuosity smaller than 0.824 were deleted. The total length of the dykes were determined by a simple ArcView calculation command, [Shape].returnLength. However, calculating the straight line length was somewhat more involved. Firstly an ArcView system script was executed which calculated the beginning and end X/Y coordinates of every dyke record. Pythagoras's theorem was then used to calculate the straight line length, as illustrated below:

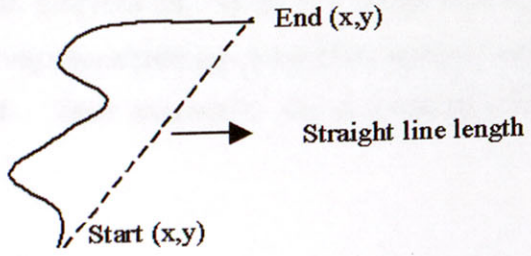

However, a few problems occurred when implementing this method. For each case where dykes intersected each other the BOSGIS database registered each intersecting segment as a separate record. In other words, one dyke would consist of many segments, depending on the number of intersections. Thus, when determining the sinuosity of a dyke, the sinuosity of each segment of the dyke is actually calculated. The problem that arose is that one segment might have a sinuosity close to 1 while other segments of the same dyke would have a very low sinuosity. The means by which the problem was overcome was somewhat tedious but nevertheless efficient.

All the sinuous dykes or segments with a sinuosity smaller than 0.824 were selected and converted into a separate theme. These selected records were deleted from the original dyke theme, and converted into a new theme. The two themes were then allocated different colours to allow easy distinction between the theme containing the sinuous segments, and the theme containing the non-sinuous segments, as illustrated below.

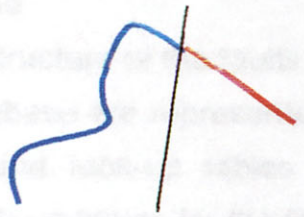

The non-sinuous dyke theme was then manually checked for every case where a sinuous dyke was broken up into segments of which one dyke consists of straight and sinuous segments. These straight segments were then deleted from the non-sinuous theme. This non-sinuous dyke theme was lastly converted to a new theme.

Faults

- At every intersection of one fault line with another, the fault line was split into various segments, as in the case of the dykes. Therefore, instead of one fault being represented by a single record, each segment of the fault was an individual record. This posed to be a problem for later queries performed on the fault

themes. Therefore, all the segments pertaining to a single fault were selected and unioned so that each fault was represented by a single record.

2.3.2 Database design

After changes were made to the original BOSGIS, the structural database was developed. The database was created for all the fault and fold themes of each of the Bos areas considered during this study. Structural data were obtained from a literature study which is described in detail in Chapter 4. However, creating the database from this information was not straightforward, since different opinions and theories regarding the age, type, displacement style etc. of the same structures exist. These differences are not all reflected in the database since attribute fields contain single entries. However, a complete reference list of all the references pertaining to a particular structure form part of the database which covers all the previous research done on a structure.

2.3.2.1 Faults database

Figure 2.4 shows the structure of the faults database with its associated look-up tables. All the data in the database are represented by codes. The codes allow for easy data retrieval or queries, and look-up tables can easily be joined with the database. Examples of all the look-up tables for the faults database of Bos2, 3 and 5 are included in Appendix 1. The following fields make up the fault database:

- *Id* – Each fault was allocated a unique ID.
- *Name* – Fault names were entered where possible. If no names were found in the literature a name would be assigned either, reflecting the geological structure, for example the Pilanesberg Complex, or the geographic area, such as the Dwarsberg Mountains.
- *Type1* – This field reflects the first type of faulting proposed for the fault, for example normal, thrust etc. If the type is unknown the original code from the BOSGIS database was used, such as 'fault observed' or 'fault inferred'.
- *Type2* – If a fault was reactivated at some stage, the reactivation type is recorded in this field. If no reactivation is known for the fault, the code would stay the same as in the Type1 field.

- *Displ1* – This field records the displacement style of Fault type1, for example normal, thrust etc.
- *Displ2* – This field records the displacement style of Fault type2.
- *Comp_Age* – The ages of the faults selected by ArcView are recorded in this field. The method by which this was done is explained below.
- *Age1* – The values of this field are a combination of the Comp_Age values and ages of the faults obtained from the literature, with literature ages given priority.
- *Age2* – This field reflects the known reactivation ages of the faults. If no reactivation is known, the value would be the same as Age1.
- *Length* – The lengths of the faults are given in meters and were calculated in a projected view, using Transverse Mercator projection, and a simple calculation formula: [Shape].returnLength.
- *Ref1, Ref2, etc.* – All the known references found during the literature study pertaining to a structure are reflected by these fields. To allow for easy querying and sorting each field contain only one entry. Therefore, the number of 'Ref' fields reflect the number of references.

Figure 2.4 Entities relationship diagram for the faults database.

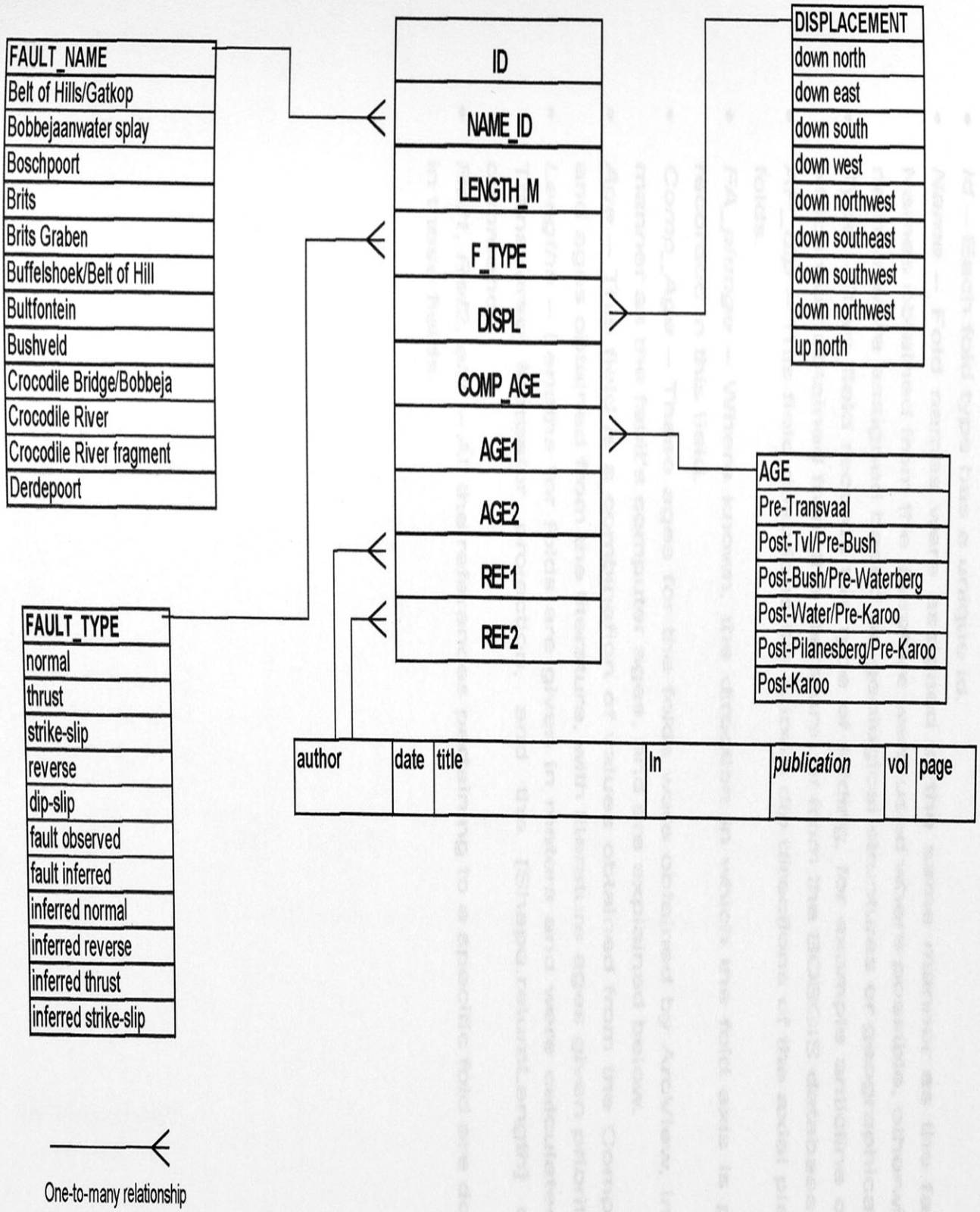

2.3.2.2 Folds database

The folds database follows the same general structure as the faults database (Figure 2.5). Codes are used to describe the various attributes and look-up tables were created which store the explanations of these codes (see Appendix 2). The folds database consists of the following fields:

- *Id* – Each fold type has a unique id.
- *Name* – Fold names were assigned in the same manner as the fault names. Names obtained from the literature were used where possible, otherwise general names were assigned based on geological structures or geographical area.
- *Type* – This field records the type of folding, for example anticline or syncline, which was obtained from the literature, or from the BOSGIS database.
- *AP_dip* – This field describes the known dip directions of the axial planes of the folds.
- *FA_plunge* – Where known, the direction in which the fold axis is plunging is recorded in this field.
- *Comp_Age* – These ages for the folds were obtained by ArcView, in the same manner as the fault's computer ages, and are explained below.
- *Age* – This field is a combination of values obtained from the Comp_Age field and ages obtained from the literature, with literature ages given priority.
- *Lengths* – Lengths for folds are given in meters and were calculated by using Transverse Mercator projection, and the [Shape.returnLength] calculation command.
- *Ref1, Ref2, etc.* – All the references pertaining to a specific fold are documented in these fields.

Figure 2.5 Entities relationship diagram for the folds database.

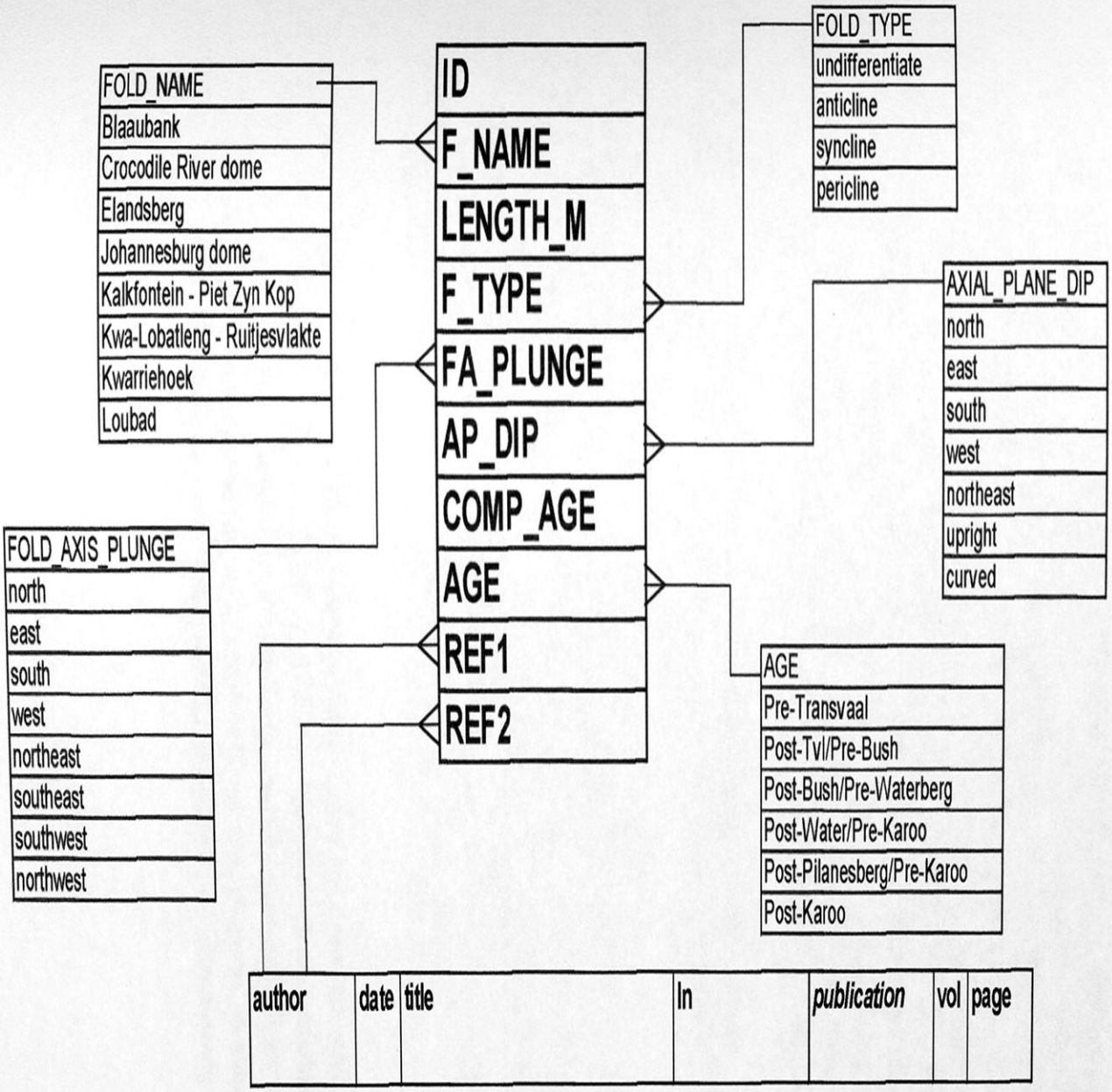

One-to-many relationship

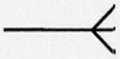

Method of determining 'Comp_Age' for faults and folds

This method involves an automated technique which assigns a maximum age for a fault based on cross-cutting relationships. These are the steps which were followed:

Firstly 'age layers' were created. Age layers are polygon themes representing the various rocks which were present during the five different geological time periods, namely; Pre-Transvaal (500), Post-Transvaal/Pre-Bushveld (400), Post-Bushveld/Pre-Waterberg (300), Post-Waterberg/Pre-Karoo (200) and Post-Karoo (100). Age layers for the Bos2 area differ in that an age of Post-Pilanesberg/Pre-Karoo (150) was added. Age layers were created by building queries based on the newclass field of the geology themes. The query selects all the lithostratigraphic units which fall within the above mentioned time period. The selected polygons were converted into a new shape file and age codes were used as names. Table 2.7 shows the Newclass values which were considered when creating each of the age layers for the Bos maps.

Table 2.7 Newclass values used for creation of age layers.

Age layer	Newclass field values	Age code
Pre-Transvaal	20, 27	500
Post-Transvaal/ Pre-Bushveld	'Age layer 500' + 8,9,10,11,12,13,14,15	400
Post-Bushveld/ Pre-Waterberg	'Age layer 400' + 1,2,3,4,5,6,7,30,31,28,29,25	300
Post-Waterberg/ Pre-Karoo	'Age layer 300' + 1,2,3,4,5,6,7,30,31,28,29,25,22	200
Pilanesberg	'Age layer 200' + 1,2,3,4,5,6,7,30,31,28,29,26,25,22	150
Post-Karoo	Select all records	100

To determine the computer ages of the faults, ArcView's 'Select by Theme' function was used. All the faults 'that completely lie within' each of the respective age layer themes, were selected and given an age code similar to the age layer theme. The 'select by theme' function, will not operate correctly if all the polygons of each age layer had not been unioned.

2.3.2.3 Attribute tables of the other themes

No new structural data were entered for the dykes, lineaments and strike and dip themes. However, the attribute tables of the other themes were cleared of redundant fields to only contain the following attributes:

ID	LENGTH	LIN	L_DOM
1	0.040075	24	1
2	0.025833	24	1
3	0.099680	24	1
4	0.040064	24	1
5	0.028411	24	1
6	0.078712	24	1
7	0.047851	24	1
8	0.046829	24	1

Each structure received a unique key as reflected by the ID field. Secondly, line lengths were calculated for all the dykes and lineaments, whereas the LIN field was carried over from BOSGIS. Lastly, the domain field (L_DOM) represents structural domains which were determined for each theme. Domains were chosen based on preferred orientations of the structures and no specific method was used in determining the extent of a structural domain. Therefore, domains vary between themes. Legends were created to represent each of the various domains of the respective Bos areas.

2.3.3 Rose diagram production

The creation of rose diagrams is not one of ArcView's primary functions and therefore the software had to be customized to achieve this aim. The steps followed in rose diagram production are explained below:

1. Three Avenue scripts (Appendix 2) are necessary for the execution of the rose diagram process. The first script (*newshape2gen.ave)* exports a shape file to a generate format file. The generate file is a comma delimited text file, and contains an ID number, and x and y coordinates of the beginning and ending of each segment of a line as captured in Arc/Info. This script was modified from the original ArcView system script. The modification to this script changed the exporting format of the gen file, so that, instead of giving one ID for each record which was exported, every segment of a record received an ID.

The function of the second script (calclino.ave) is to activate an external application program (Brynard, pers. comm. 2000). This C++ program (linears.exe) determines the orientation and calculates the length of each segment of a record from the 'gen file' (Brynard, pers. comm. 2000). This new data are exported as a text file with an '*.out ' extension.

The final script (rose.ave) creates rose diagrams from the data stored in a '*.out file'. This script was obtained from the ESRI home page. Rose diagrams can be drawn based on the number of segments or according to the cumulate length of the segments i.e. weighted histograms. All the rose diagrams in this study are based on the cumulative lengths of the segments since it is a statistically more accurate representation of the orientation of the data.

2. The second step was to customize the interface of ArcView by creating buttons and tools to execute each of the scripts. The figure below shows the three customized buttons and tools. The creation of rose diagrams are done by simply clicking consecutively on the three rose diagram icons.

The diamond icon executes the 'newshape2gen' script, the run icon will execute the 'calclino' script and the rose diagram icon executes the 'rose' script. Rose diagrams are drawn as graphics in a view.

3. Rose diagrams were created for all the Fault, Dyke, Folds and Lineament projects. The Rose diagrams for the fault projects were created based on the geological time periods which were considered during this study. However, since some faults experienced reactivation, two sets of rose diagrams, Age1 and Age2 rose diagram sets were made. Rose diagrams of the Fold themes were also based on their ages. Rose diagrams for Dyke and Lineament themes were based on structural domains which were described earlier.

4. Lastly, layouts were made of the Rose Diagram Views on which stress directions were interpreted (Chapter 6).

2.3.4 Production of Stereonet plots

Strike and Dip projects were developed of the different Bushveld Complex areas in order to create stereographic plots of the BOSGIS data. Stereonet plots were produced using the program Spheristat 2, and these plots were included as graphics in the projects layouts. The following steps outline the stereonet production:

- A Spheristat map view was created for each strike and dip project. These views contain an outline theme of the geology, as well as strike and dip locations indicated as points or with other symbols.
- Structural domains were chosen based on the outcrop distribution of these points. For example: ArcView's 'select by theme' function was utilized to select all the strike-and-dip points contained within the Transvaal rocks, or Waterberg rocks. The strike-and dip symbols of the Transvaal rocks were further grouped into domains according to different areas. Domains were represented by displaying the points as different colours and symbols on the maps.
- Each structural domain was converted to a separate theme. These themes' attribute tables (dBase files) were converted to formatted text (.txt) files using Excel, to be imported into Spheristat.
- Stereonet plots were created of the poles to bedding. Similar symbols and colours where assigned to the stereonet plots as were used in the Spheristat map views. Plots were saved as windows meta files (.wmf).
- The '.wmf' files were imported as graphics into the ArcView project's layout.
- In addition, Spheristat's analytical capabilities such as contouring and principal direction analyses, were utilized to evaluate individual stereonet plots.

3. STRATIGRAPHY

The study area contains rocks representing different stages in the tectonic evolution of the Kaapvaal Craton from late Archaean to present times. However, this study only considers a simplified stratigraphical subdivision (Table 3.1) for all the sequences except those of the Bushveld Complex, as is present in BOSGIS. The simplified stratigraphical divisions do not affect the purpose of the study, which is a regional structural analysis. In this chapter the subdivisions of BOSGIS are compared to that of the geological map of South Africa (Keyser, 1997). A brief description of the lithology of each subdivision is also given. For a detailed description and discussion of the stratigraphy and lithology of the Bushveld Complex and its surrounding areas, the reader is referred to S.A.C.S.(1980).

3.1 Archaean Rocks

The 'Archaean Rocks' subdivision is a collective term for all the greenstone- type rocks, of Swazian age, occurring in the study area. These greenstone belts represent ancient volcano-sedimentary packages which underwent greenschist metamorphism. Three greenstone belts can be distinguished in the study area, namely the Pietersburg, Murchison and a portion of the Barberton greenstone belt. In this study no distinction is made between the various formations of the greenstone belts, and all the belts are represented as one undifferentiated unit. Table 3.2 provides an outline of the simplified stratigraphy used in the study versus the detailed lithological subdivisions according to Keyser (1997).

Table 3.1 Stratigraphic subdivisions considered during this study

Erathem	Supergroup	Group	Formation	Intrusives		
Cenozoic			Alluvium, sand, calcrete			
Mesozoic	KAROO			Karoo dolerites		
Palaeozoic	KAROO					
Mogolian				Alkaline Intrusions, Pilanesberg etc.		
		WATERBERG		Diabase Intrusions?		
Vaalian					Micro granite, Hornfels, Leptite, Hybrid rocks	
				BUSHVELD COMPLEX	LEBOWA GRANITE SUITE (with pegmatite zones)	
					RASHOOP GRANOHYRE	
					RUSTENBURG LAYERED SUITE	Upper Zone (with magnetite bands)
						Main Zone (with pegmatite zones)
						Critical Zone
						Lower Zone
						Marginal Zone
						'Under Bushveld'
				Diabase Intrusions?		
	TRANSVAAL		Loskop, Rust de Winter, Glentig			
		ROOIBERG				
		PRETORIA	upper Pretoria			
			Magaliesberg			
			lower Pretoria			
		CHUNIESPOORT				
Randian		WOLKBERG/ Black Reef				
		GROBLERSDAL				
				Various Granites		
Swazian	Archaean rocks					

Table 3.2 Stratigraphic subdivisions of Swazian-age greenstone belts:

a) According to Keyser (1997)

Erathem	Sequences					
Swazian	Pietersburg	Giyani	Gravelotte	Rubbervale	Barberton	Moodies
				Mac Kop, Weigel & La France		Fig Tree
				Leydsdorp		
				Mulati		Onverwacht

b) This study

Swazian	Archaean Rocks

3.2 Various Precambrian Granites

A large continuous stretch of Precambrian granitic rocks are exposed in the eastern portion of the study area. This area is characterized by individual massive granite plutons as well as intensely deformed gneissic and mylonitic zones. Different ages and modes of emplacement have been determined for the various granites, and compositional differences are well recorded (S.A.C.S., 1980, Keyser, 1997). Some granites pre-date the formation of greenstone belts, whereas some are intrusive into the greenstone belts. However, in this study all the granites are considered as an undifferentiated unit. In addition, 'Various Precambrian Granites' do not only include the granitic rocks of the eastern region, but also the rocks of the Makoppa dome, Johannesburg dome, and the Dennilton dome. Table 3.3 shows the compositional and age distinctions made by Keyser (1997) versus the simplified divisions of this study.

Table 3.3 Stratigraphic subdivisions of Precambrian Granites

a) According to Keyser (1997)

Erathem	Intrusive rocks		
Randian	Unnamed biotite granite		
	Mashishimale Suite	Granites: Maranda, Moletsi, Mpageni, Palmietfontein, Shirindi, Smitskraal, Turfloof, Utrecht	Granites: Baderoukwe, Pompey, Willie, Lekkersmaak, Lunsklip, Uitloop
	Granites: Hugomond, Jerome, Matlala, Matok, Mosita, Meinhardskraal		
		Unnamed Ultrabasic rocks	Harmony Granite, Cunning Moor Tonalite
		Sailsbury Kop Granite	
		Rooiwater Complex	
Swazian	Houtrivier Gneiss, Vaalfontein Gneiss	Unnamed potassic granite and gneiss	Modipe Complex
		Nelspruit Suite	Makhutswi Gneiss
	Halfway House Granite		Unnamed trondhjemitic and tonalitic gneiss
		Goudplaats Gneiss	Kaap Valley Tonalite

b) This study

Randian	Various Granites

3.3 Transvaal Supergroup

A complete succession of the Transvaal Supergroup is present in the study area. The Transvaal rocks generally act as the floor and roof of the Bushveld Complex. Furthermore, isolated occurrences of Transvaal rocks, known as Transvaal Inliers, are found within the Bushveld Complex (Hartzer, 1987). The Transvaal Supergroup can broadly be subdivided, from base to top, into the Wolkberg, Chuniespoort, Pretoria, and lastly the Rooiberg Group. Detailed studies done on the Transvaal Sequence have established well defined lithological subdivisions (S.A.C.S. 1980). The proto-basinal rocks of the Wolkberg Group are characterized by rift-related volcanics and immature sediments (Eriksson and Reczko, 1995). Widespread Transvaal deposition commenced with the Black Reef formation consisting of a basal dolomitic unit and upper banded iron formations (S.A.C.S., 1980). The Pretoria Group unconformably overlies the Chuniespoort Group and is characterized by alternating sandstones and mudrocks, with interlayered volcanic units (Eriksson and Reczko, 1995). Finally, the Rooiberg Group consisting of felsic lavas occur at the top of the sequence. Table 3.4 provides the detailed subdivisions of the Transvaal Supergroup as depicted by the geological map of South Africa (Keyser, 1997) versus the generalized subdivisions used in this study.

3.4 The Bushveld Complex

Extensive work has been done in the past on the stratigraphic subdivisions and lithology of the Bushveld Complex, and the reader is referred to S.A.C.S. (1980) for a detailed description. The major subdivisions, from bottom to top, include the Rustenburg Layered Suite, Rashoop Granophyre Suite and the Lebowa Granite Suite. The Rustenburg Layered suite can further be subdivided into five zones namely, from base to top, the Marginal Zone, Lower Zone, Critical Zone, Main Zone, and Upper Zone. The Marginal Zone consists of fine-grained plagioclase-orthopyroxene cumulates (Vermaak, 1976; Teigler 1990; Eales et al., 1993) and the Lower Zone is characterized by orthopyroxenites and harzburgites (Von Grunewaldt and Harmer, 1993). The Critical Zone contains the economically important Merensky reef and UG1 and UG2 layers, and is marked by a lower feldspathic pyroxenite, followed by norite and anorthosite (Visser, 1998, Von Grunewaldt & Harmer, 1993). The Main Zone marks the presence of gabbronorite and anorthosite, with the absence of chromite and olivine. Lastly, the Upper Zone is characterized by numerous magnetite layers (Visser, 1998). The Rashoop Granophyre suite consists primarily of granophyre, granophyric granite, granophyre porphyry and pseudogranophyre (Visser, 1998). The thick Lebowa Granite Suite consists mostly of coarse to medium grained granites. The BOSGIS data base reflect most of these stratigraphical subdivisions of the Bushveld Complex (Table 3.5).

Table 3.4 Stratigraphical subdivisions of the Transvaal Supergroup.

a) According to Keyser (1997)

Erathem	Supergroup	Group	Formation
Vaalian	TRANSVAAL		Loskop, Rust de Winter, Glentig
		ROOIBERG	Selons River
			Schrikkloof
			Kwaggasnek
			Damwal
			Dullstroom
			Rinkhalskop
			Smelterskop
		PRETORIA	Houtenbek
			Salie Sloot
			Leeuwpoort
			Steenkampsberg
			Cyferfontein/Riffontein
			Nederhorst
			Kwarriehoek
			Lakenvalei
			Vermont
			Rayton
			Magaliesberg
			Silverton
			Daspoort
			Strubenkop
			Dwaalheuwel
			Hekpoort & Boshoek
			Timeball Hill & Rooihoogte
		CHUNIESPOORT	Duitschland
			Penge
			Malmani
			Black Reef
Randian		WOLKBERG/ BUFFELSFONTEIN/Bloempoort/ Wachteenbeetje	

b) This study

Erathem	Supergroup	Group	Formation
Vaalian	TRANSVAAL		Loskop, Rust de Winter, Glentig
		ROOIBERG	
		PRETORIA	upper Pretoria
			Magaliesberg
			lower Pretoria
		CHUNIESPOORT	
Randian		WOLKBERG/ Black Reef	
		GROBLERSDAL	

Table 3.5 The stratigraphical subdivisions of the Bushveld Complex.

a) According to Keyser (1997)

Vaalian	BUSHVELD COMPLEX	LEBOWA GRANITE SUITE		
		RUSTENBURG LAYERED SUITE	Upper Zone	Roossenekal Subsuite, Bierkraal Magnetite Gabbro, Molendraai Magnetite Gabbro (Magnetite)
			Main Zone	Dsjate Subsuite, Pyramid Gabbro-Norite & Grasvally, Norite-Anorthosite (Plat Reef)
			Critical Zone	Dwars River Subsuite, Schilpadnest Subsuite (chromite) (Merensky Reef)
			Lower Zone	Croydon Subsuite & Shelter Norite, Vlakfontein Subsuite & Kolobeng Norite, Zoetveld Subsuite (chromitite)
		RASHOOP GRANOPHYRE SUITE/ Unnamed granodiorite		

b) This study

Vaalian	BUSHVELD COMPLEX	LEBOWA GRANITE SUITE (with pegmatite zones)	
		RASHOOP GRANOPHYRE SUITE/ 'Under Bushveld'	
		RUSTENBURG LAYERED SUITE	Upper Zone (with magnetite bands)
			Main Zone (with pegmatite zones)
			Critical Zone
			Lower Zone
			Marginal Zone

3.5 Diabase Intrusions

It is well known (Cawthorn et al., 1981) that the diabase intrusions occurring in the Bushveld Complex and surrounding areas are of distinctly different ages and compositions. They vary from pre-, syn-, and post-Bushveld in age to post-Waterberg in age. On the 1:000 000 geological map of South Africa (Keyser, 1997), diabase intrusions occurring in and around the Bushveld Complex are indicated to be pre/post or syn-Bushveld in age whereas the diabase intrusions occurring in the Waterberg Group are believed to be post-Waterberg in age. Since the BOSGIS database makes no distinction between the various ages, all the diabase intrusions are regarded to be of the same age.

3.6 The Waterberg Group

Two major Waterberg basins occur in the study area, the Middelburg-Cullinan basin in the south and the main Waterberg basin in the northwestern part of the study area. Good stratigraphic correlation exists between various formations of these two basins. The Waterberg Group can broadly be divided into a lower, middle and upper sequence and consists of brownish-red sandstone, conglomerate, grit, tuff, lava and yellowish to white sandstone (Snyman, 1996). However, in the study area, the Waterberg Group is represented as an undifferentiated sequence. Table 3.6 shows the subdivisions as present on the published geological map (Keyser, 1997), versus the undifferentiated sequence of the study area.

Table 3.6 Stratigraphical subdivisions of the Waterberg Group

a) According to Keyser (19997)

Erathem	Group	Sub-Group	Formation
Mokolian	WATERBERG	Kransberg	Vaalwater
			Cleremont
			Sandriviersberg & Mogalakwena
		Matlabas	Aasvoëlkop & Makgabeng
			Skilppadkop & Setlaole
		Nylstroom	Alma
			Swaershoek
			Wilger River
			Blouberg

b) This study

Erathem	Mokolian	WATERBERG GROUP	

Alkaline and carbonatite complexes are distributed throughout the study area. They include the Pienaarsrivier, Pilanesberg, Spitskop, Kruidfontein, Nooitgedacht, Tweerivier, and Ystervark (previously Goudini) Complexes. All these complexes are of late Mokolian in age and are considered to have an emplacement age between 1430 and 1200 Ma (Visser, 1998). In this study, however, no distinction is being made between the various complexes and they are merely treated as 'Alkaline Intrusions'. Figure 3.1 shows the locations of the individual complexes in the study area.

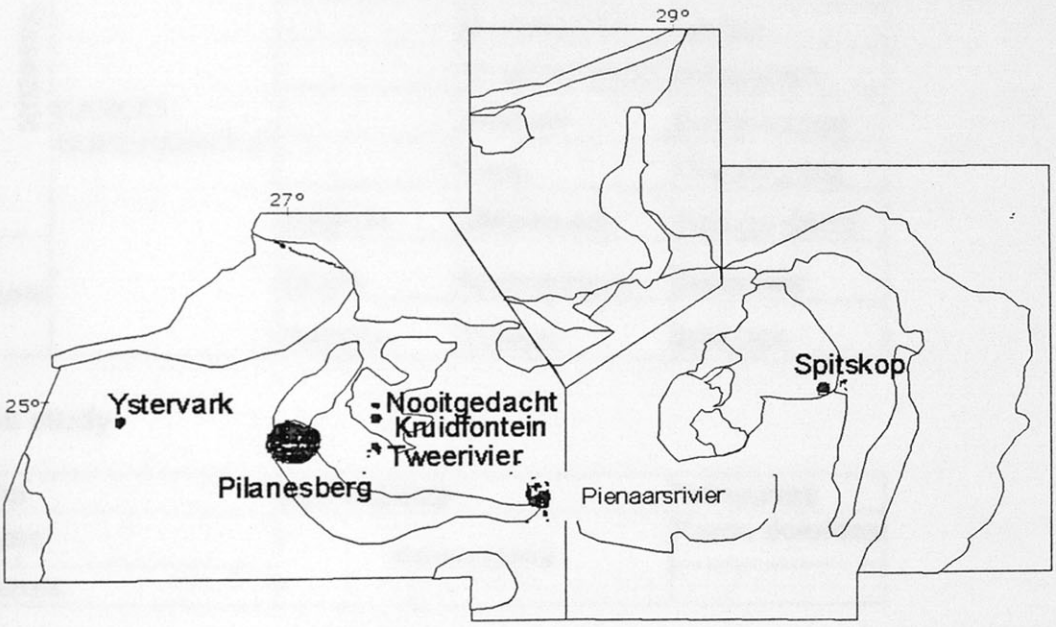

Figure 3.1 The distribution of alkaline complexes in the study area.

3.8 Karoo Supergroup

The Karoo Supergroup is broadly characterized by glacial deposits, deltaic successions, aeolian deposits and flood basalts. Rocks of the Karoo Supergroup occur in several regions in the study area and the stratigraphy vary within these respective regions (Keyser, 1997). In the center of the study area, just north of Pretoria, the Karoo rocks underlie an area known as the Springbok Flats. In this area the Karoo rocks occur in a basin with an east-north-easterly axis which represents one of the smaller preserved basins of the main Karoo basin. In addition, some patches of Karoo rocks are found to the south of the Springbok Flats, mainly in the Witbank-Middelburg region. The second region includes scattered occurrences of Karoo rocks in the north of the study area, along the Palala shear zone. These rocks do not correlate with the Karoo rocks found in the Springbok Flats and Middelburg-Witbank area. Lastly, in the North West Province minor outcrops of Karoo rocks occur which again do not correlate with the Karoo rocks occurring in some of the other regions. This study considers the Karoo rock as an

undifferentiated sequence, irrespective of the region in which these rocks occur. However, dolerites which intruded during Karoo times (Keyser, 1997) are presented as a separate unit . Table 3.7 shows the classification of the Karoo Sequence according to the various regions versus undifferentiated Karoo rocks found in the study area.

Table 3.7 The stratigraphical subdivision of the Karoo Supergroup

a) According to Keyser (1997)

Erathem	Supergroup	Springbok Flats area	Northern Province	Northwestern Province
Mesozoic	KAROO SUPERGROUP	Letaba	Letaba	
		Clarens	Clarens	
			Bosbokpoort	Lisbon
			Klopperfontein	Greenwich
			Solitude	Eendragtpan
			Fripp	Grootegeluk
		Irrigasie	Mikambeni	Goedgedacht
Paleozoic		ECCA	Madzaringwe	Swartrant
		DWYKA	Tshidzi	DWYKA

b) This study

Erathem	Supergroup	Intrusives
Mesozoic	Karoo rocks	Karoo dolerites
Palaeozoic		

4. REGIONAL TECTONIC AND STRUCTURAL SETTING OF THE BUSHVELD COMPLEX

The structural history of the Bushveld Complex directly relates to tectonic processes affecting the Kaapvaal Craton. It is therefore essential to understand these processes and how the regional structures of the Craton influenced the formation and subsequent deformation of the Bushveld Complex. The first part of the chapter deals with the regional tectonic and structural framework of the Kaapvaal Craton. A brief overview is given of all the major structural features found on the Craton, their origin and structural characteristics are discussed. The second part of the chapter focuses on the tectonic setting and structural characteristics of the Bushveld Complex. Only a broad overview is given of the tectonic and structural setting of the Bushveld Complex while a more detailed discussion of the specific structures follow in the next chapter.

4.1 TECTONIC AND STRUCTURAL FRAMEWORK OF THE KAAPVAAL CRATON

The Kaapvaal Craton represents an Archaean continental fragment of a once much larger continent (de Wit et al., 1988; Groenewald et al., 1991). The Kaapvaal Craton's boundaries are somewhat obscured by younger sediments but are reasonably well established (McCourt, 1995) (Figure 4.1). To the north it is bounded by the Limpopo Belt which represents a collisional zone between the Zimbabwe Craton and the Kaapvaal Craton. The eastern boundary is the north-south trending Lebombo monocline which was formed as a response to the break-up of Gondwana around 150 Ma. In the west and south the Kaapvaal Craton is delineated by the Natal-Namaqua belt. This belt mainly represents an accretionary tectonic event during Kibaran (1.2 Ga) times. The formation of the Kaapvaal Craton can be divided into two main periods (de Wit et al., 1992; de Wit and Hart, 1993). The first period is characterized by the formation of the mid-Archaean Kaapvaal Shield (Figure 4.1), during which major periods of intraoceanic tectonics were active between 3.64 and 3.08 Ga. This period marks the development of granitoid-greenstone terrains, and ended with a major pulse of accretionary tectonics around 3.2 Ga (Brandl and de Wit, 1997). The second period is characterized by intra-cratonic tectonics as well as continental-edge processes between 3.1 and 2.65 Ga (Brandl and de Wit, 1997). Major basin development on the Craton as well as

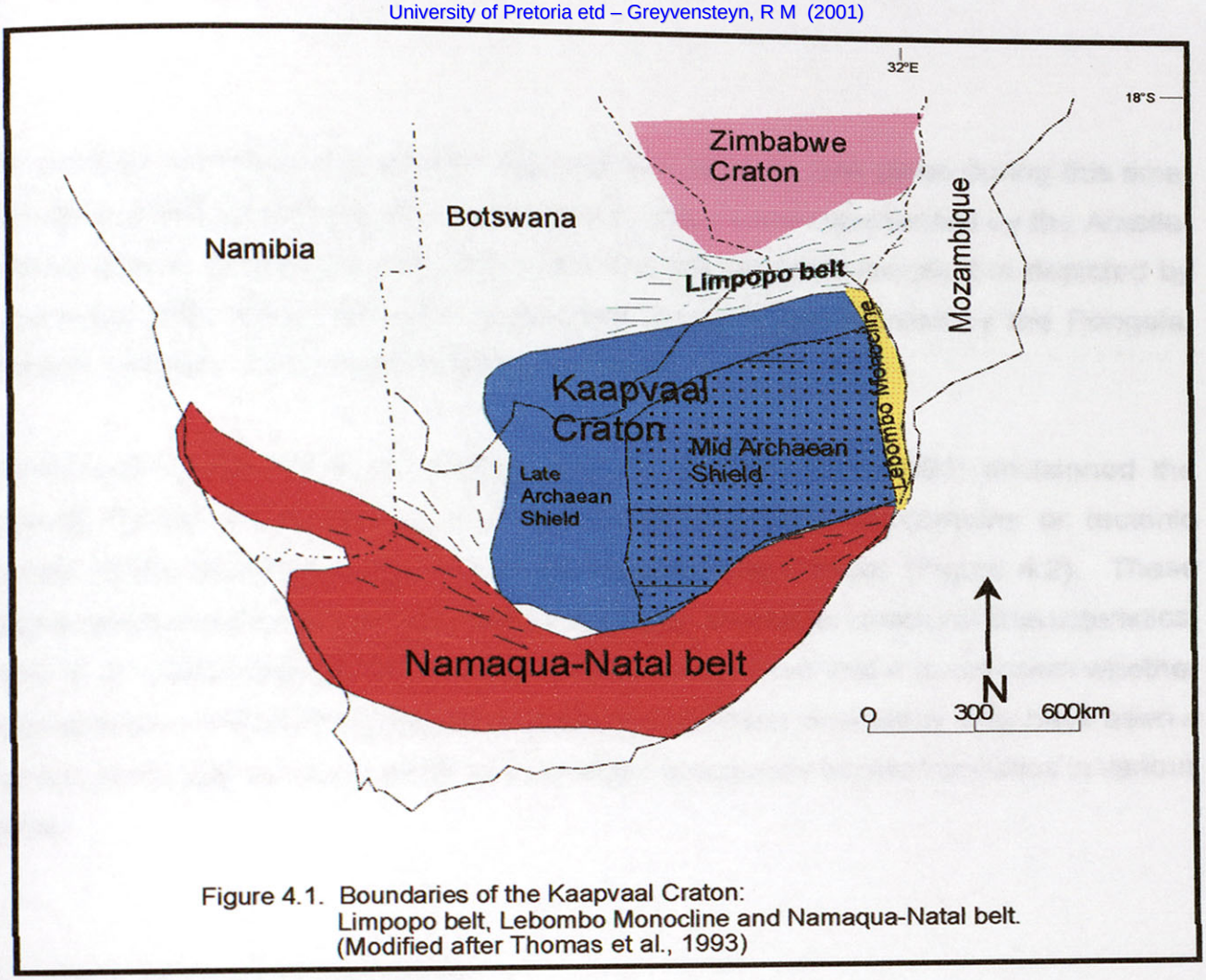

Figure 4.1. Boundaries of the Kaapvaal Craton: Limpopo belt, Lebombo Monocline and Namaqua-Natal belt. (Modified after Thomas et al., 1993)

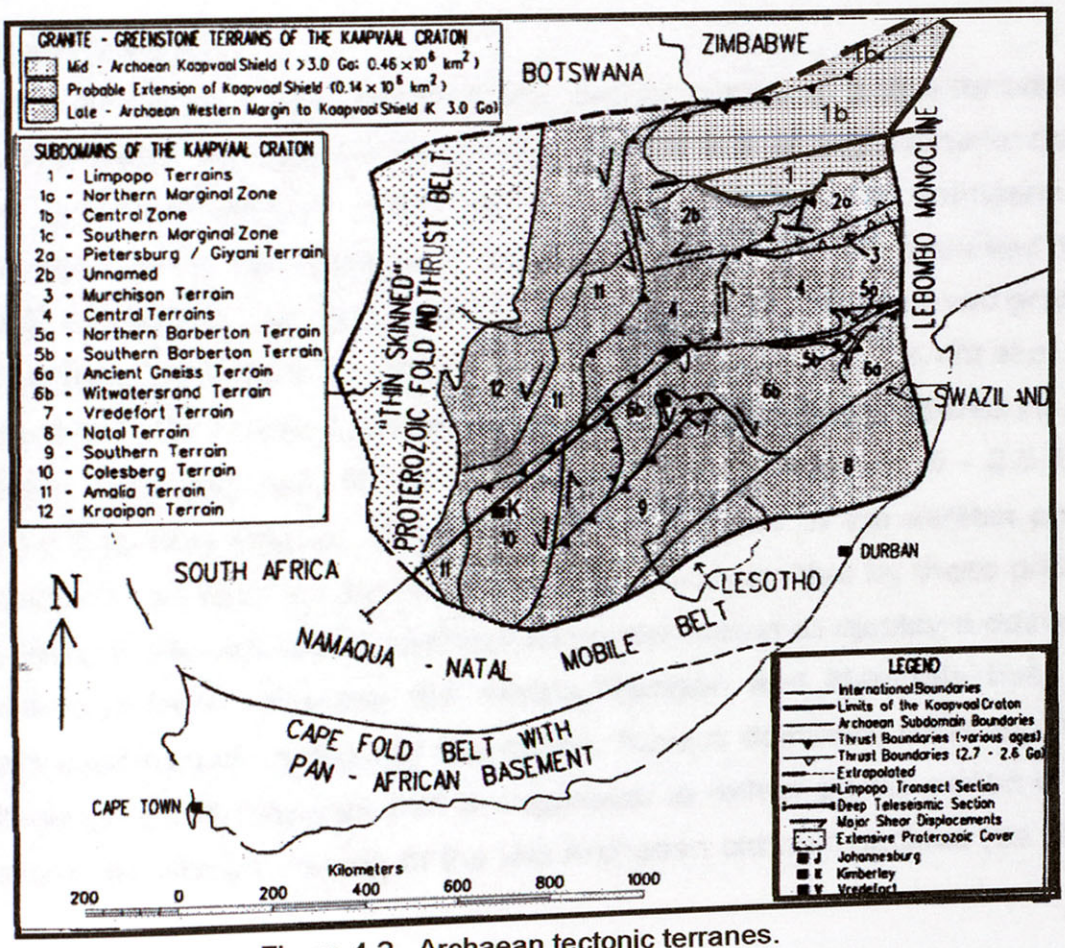

Figure 4.2. Archaean tectonic terranes. (After de Wit et al., 1992)

continental growth along the western and northern margins took place during this time. Continental growth processes along the western margin are represented by the Amalia-Kraaipan granite-greenstone belt, whereas along the northern margin it is depicted by the Limpopo belt. Basin formation during this period is represented by the Pongola, Dominion, Witwatersrand, and Ventersdorp basins.

Authors such as de Wit et al. (1992a) and de Wit and Hart (1993) envisioned the Kaapvaal Craton as consisting of a number of Archaean subdomains or tectonic terranes, which accreted along large ENE trending shear zones (Figure 4.2). These domains are defined based on age, lithostratigraphy as well as structural characteristics. de Wit et al. (1992) and de Wit and Hart (1993) pointed out that it is unknown whether these terranes are allochthonous with respect to each other or whether they have been a coherent geological province which has undergone separate tectonic activities in various regions.

4.1.1 Early Archaean architecture

4.1.1.1 Greenstone belts.

The Archaean greenstone belts represent the earliest period of craton formation. The volcano-sedimentary packages are believed to be the result of "intra-oceanic obduction of hydrated Archaean oceanic crust" (de Wit et al., 1992). The formation of the greenstone belts, along with extensive granitoid emplacement, represented the first continental lithosphere (de Wit et al., 1992). The oldest and best preserved greenstone belt is the Barberton belt which formed between 3.7 and 3.2 Ga ago (de Wit et al., 1992). Other greenstone belts include in the north, the Giyani/Sutherland, Pietersburg (2.8Ga) and Murchison (3.09 Ga) belt, in the west the Amalia-Kraaipan (2.95 - 2.5 Ga) and Marydale (3.0 Ga) belts (Visser, 1998), (Figure 4.3). Some of the earliest prominent structural trends to be seen on the Kaapvaal Craton are depicted by these greenstone belts. The belts in the central and northern Kaapvaal Craton all display a dominant NE to ENE structural trend, whereas the Amalia-Kraaipan and Marydale belts on the western and southwestern margin of the craton, have a dominant NNW to NS trend. The NS trending Amalia-Kraaipan belt is suggested to reflect a later period of terrane accretion along the western margin of the Mid Archaean cratonic nucleus (de Wit et al.,

1992). All the greenstone belts have characteristic internal deformation such as steeply dipping schistosities, folding, thrusting, and in some places transcurrent faulting. These internal structural directions generally follow the same regional trends as exhibited by the individual belts.

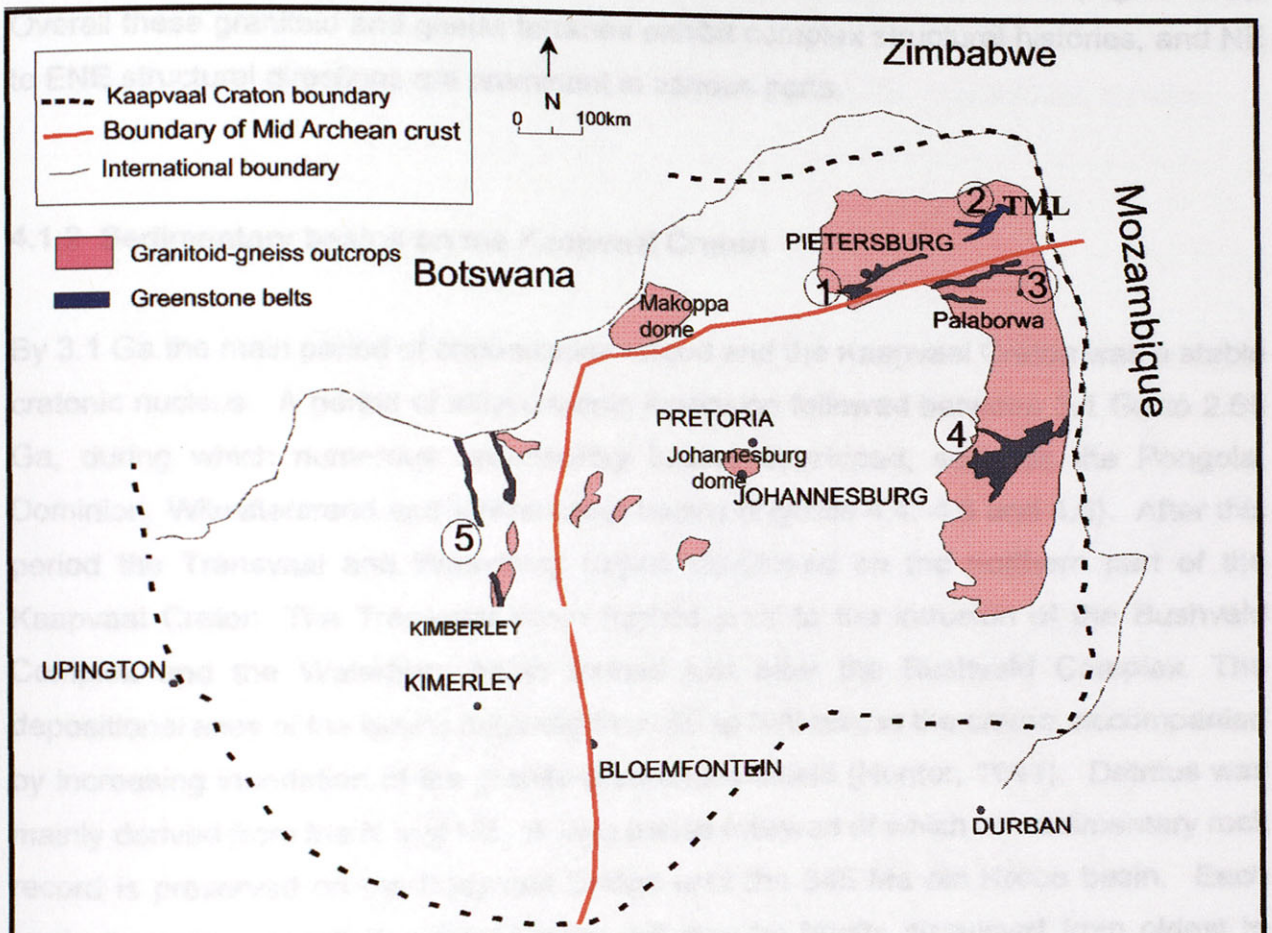

Figure 4.3. Distribution of the granitoid-gneiss terranes and major greenstone belts on the Kaapvaal Craton.
1. Pietersburg, 2. Sutherland, 3. Murchison, 4. Barberton, 5. Amalia-Kraaipan belts.

4.1.1.2 Granitoid terranes

The extensive granitoid terranes with subordinate gneisses exposed in the eastern and northeastern part of the Craton are suggested to represent the early Archaean basement of the Kaapvaal Craton (Tankard et al., 1982). This episode of granitoid emplacement together with greenstone development characterize the first period in the evolutionary history of continental crust and craton formation. Two different opinions exist regarding the formation of these granitoid terranes. Some authors believe that the granitoid terranes developed before the formation of the greenstone belts whereas some authors

believe they are intrusive into the greenstone belts (Hunter, 1981). De Wit and Roering (1990) have suggested that the gneisses of the northern Kaapvaal Craton are significantly younger than those of the southern Kaapvaal Craton, with the Thabazimbi-Murchison-Lineament (TML) forming the boundary between the two (Figure 4.3). Overall these granitoid and gneiss terranes exhibit complex structural histories, and NE to ENE structural directions are prominent in various parts.

4.1.2 Sedimentary basins on the Kaapvaal Craton

By 3.1 Ga the main period of cratonization ended and the Kaapvaal Craton was a stable cratonic nucleus. A period of intra-cratonic extension followed between 3.1 Ga to 2.65 Ga, during which numerous sedimentary basins developed, such as the Pongola, Dominion, Witwatersrand and Ventersdorp basins (Figures 4.4. 4.5 and 4.6). After this period the Transvaal and Waterberg basins developed on the northern part of the Kaapvaal Craton. The Transvaal basin formed prior to the intrusion of the Bushveld Complex and the Waterberg basin formed just after the Bushveld Complex. The depositional axes of the basins migrated from SE to NW across the craton, accompanied by increasing inundation of the granite-greenstone shield (Hunter, 1981). Detritus was mainly derived from the N and NE. A long period followed of which no sedimentary rock record is preserved on the Kaapvaal Craton until the 345 Ma old Karoo basin. Each basin occurring on the Kaapvaal Craton will now be briefly discussed from oldest to youngest.

4.1.2.1 Pongola basin.

The Pongola sediments and volcanics are mainly preserved along the southeastern margin of the Kaapvaal Craton. The Pongola basin is estimated to have formed around 3.1 – 2.9 Ga ago (Tankard et al., 1982), and is interpreted to have been an epicontinental basin which was open to the southeast. The structures of the Pongola Supergroup have been complicated by early northwest-directed thrusting, followed by NS dextral and NW-SE sinistral shearing (Gold, 1983). It has been suggested by Matthews (1990) that the Pongola basin might have been deformed in a region which

was part of a major transform boundary located at the southern margin of the Kaapvaal Craton. The main structural trend is depicted by the NW-SE orientated, and southeast plunging Amsterdam Syncline in the northern part of the Pongola Supergroup (Figure 4.4). The 2.87 Ga layered Usushwana Complex intruded along the flanks of the Amsterdam syncline and is aligned in the same direction. In addition a large open syncline which plunges to the SE is situated to the south of the Amsterdam syncline.

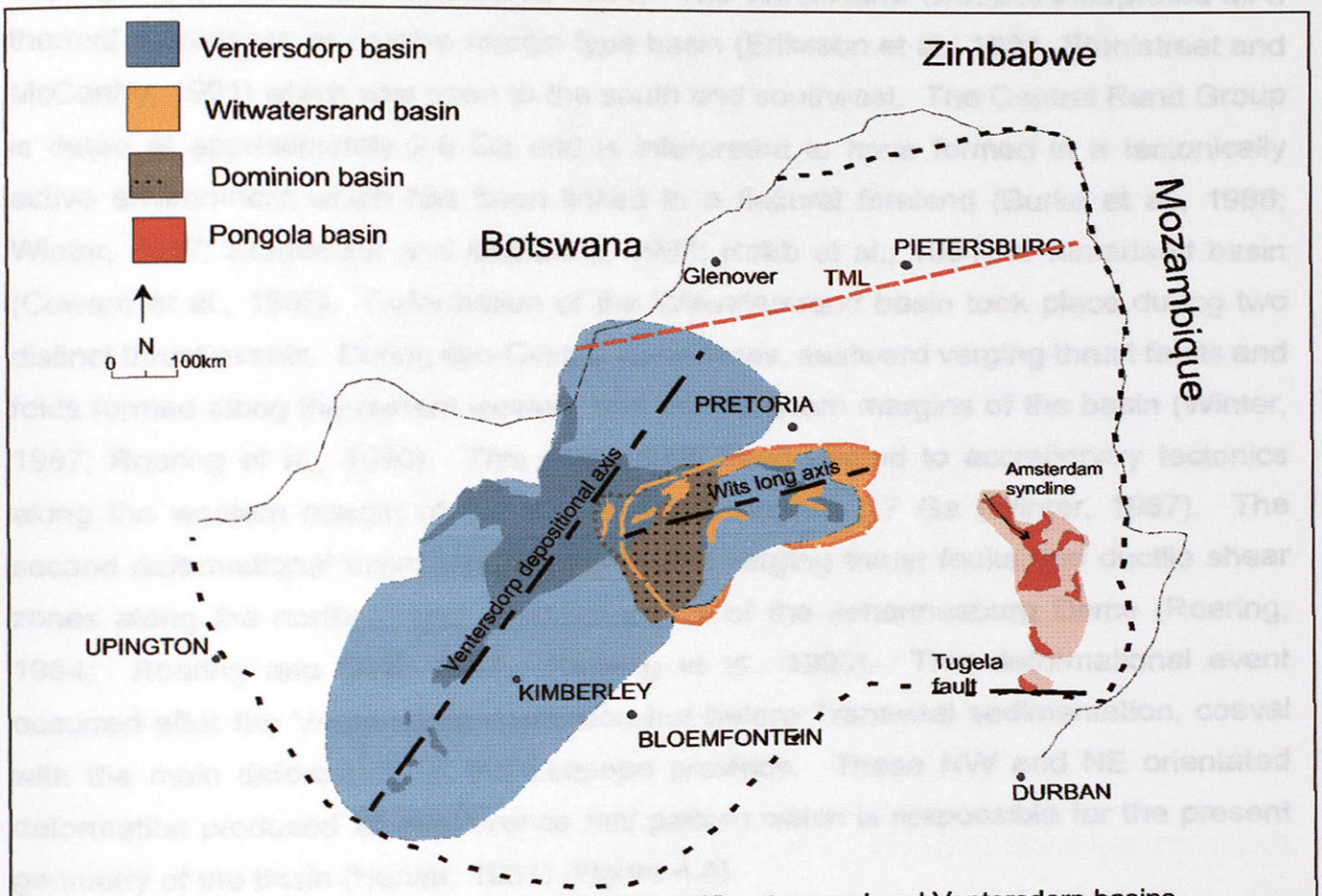

Figure 4.4 The distribution of the Pongola, Dominion, Witwatersrand and Ventersdorp basins. Lighter colours reflect inferred original outcrops, (after Tankard et al., 1982)

4.1.2.2 Dominion basin.

The Dominion Group situated in the center of the Kaapvaal Craton consists mainly of volcanics with minor sediments and has been dated between 3.09 - 3.07 Ga (Armstrong et al., 1990). The sediments are believed to have accumulated in an Andean-type back-arc basin (Burke et al., 1985) or in a failed rift basin (Bickle and Eriksson, 1982; Tankard et al., 1982). The basin is elongated with a NE-SW direction (Figure 4.4). The prominent structural features include northward verging ductile thrusting and folding (Van der Merwe, 1994).

4.1.2.3 Witwatersrand basin

The Witwatersrand basin is elongated in an ENE-WSW direction, and is divided into the older West Rand Group and a younger Central Rand Group (S.A.C.S., 1980). The West Rand Group is dated at approximately 3.0 Ga and is correlated with the Pongola Supergroup (Beukes and Cairncross, 1991). The West Rand Group is interpreted as a thermal subsidence or passive margin type basin (Eriksson et al., 1981, Stanistreet and McCarthy, 1991) which was open to the south and southeast. The Central Rand Group is dated at approximately 2.8 Ga and is interpreted to have formed in a tectonically active environment which has been linked to a flexural foreland (Burke et al., 1986; Winter, 1987; Stanistreet and McCarthy, 1991; Robb et al., 1991) or hinterland basin (Coward et al., 1995). Deformation of the Witwatersrand basin took place during two distinct thrust events. During syn-Central Rand times, eastward verging thrust faults and folds formed along the current western and northwestern margins of the basin (Winter, 1987; Roering et al., 1990). This might have been related to accretionary tectonics along the western margin of the central shield around 2.7 Ga (Winter, 1987). The second deformational event includes northward verging thrust faults and ductile shear zones along the northern and southern edges of the Johannesburg Dome (Roering, 1984; Roering and Smit, 1987; Roering et al., 1990). This deformational event occurred after the Ventersdorp deposition but before Transvaal sedimentation, coeval with the main deformation in the Limpopo province. These NW and NE orientated deformation produced an interference fold pattern which is responsible for the present geometry of the basin (Hunter, 1981) (Figure 4.4).

4.1.2.4 Ventersdorp basin

The Ventersdorp basin formed during a period of large scale crustal extension in the central Kaapvaal Craton. The basin is believed to have developed in a rift setting where extensional faults exploited the earlier formed NE-SW orientated thrust faults of the Witwatersrand basin. Subsequently, the Ventersdorp sediments were deposited in large NE-SW orientated grabens (Figure 4.4). The Ventersdorp basin is dated at approximately 2714 Ma for the base (Klipriviersberg Group) and 2709 Ma for the Platberg Group (Armstrong et al., 1991). The extrusion of the Ventersdorp lavas might

have been a response to orogenic activity along the northern margin of the Kaapvaal Craton in the Limpopo Belt (Burke et al., 1985). Button (1981) described the Ventersdorp basin as being gently deformed.

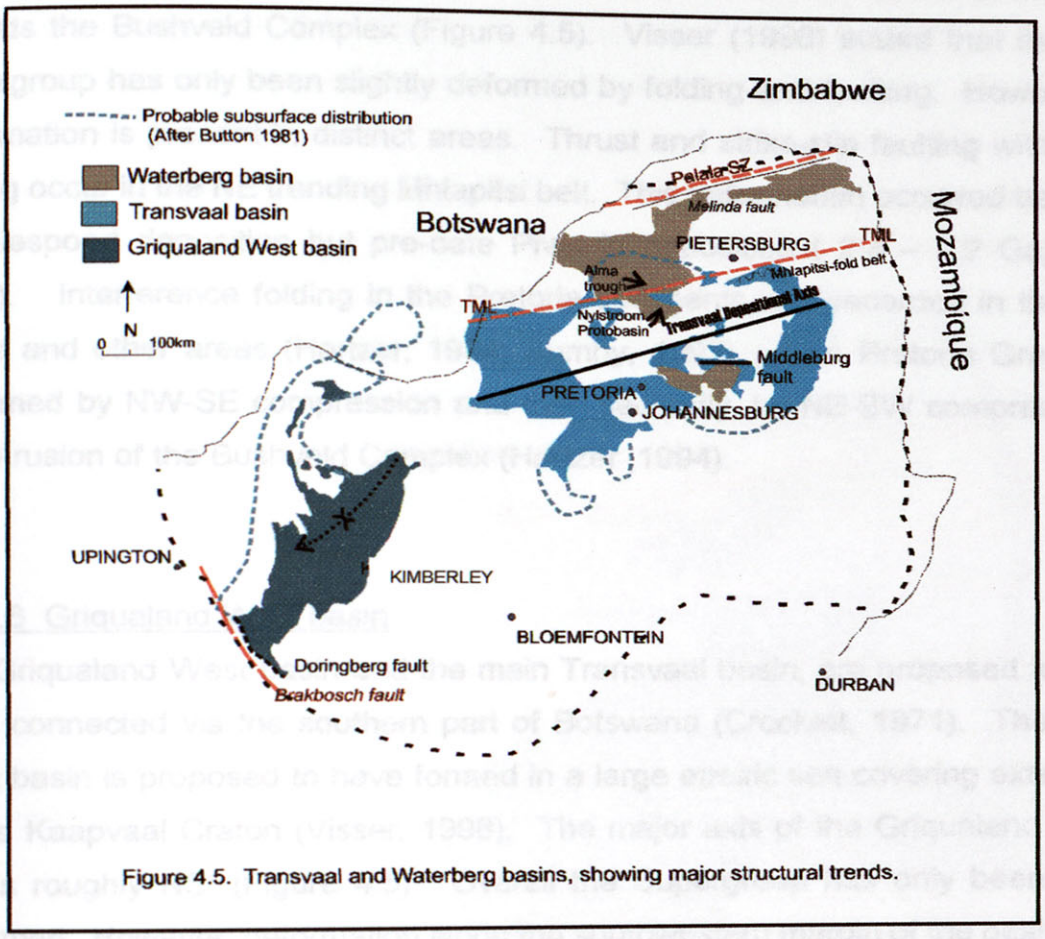

Figure 4.5. Transvaal and Waterberg basins, showing major structural trends.

4.1.2.5 Transvaal basin

The Transvaal basin is an important sedimentary basin influencing the structural setting of the Bushveld Complex since it acts as the floor and roof to the Complex. The Transvaal basin can be subdivided into three distinct depositional periods. The proto basin represented by the Wolkberg Group is dated at approximately 2600Ma (Eriksson et al., 1996) . The basin is believed to be rift related, with the Thabazimbi-Murchison fault zone at its northern margin strongly influencing deposition (Eriksson et al., 1996). Protobasinal rocks, characterized by rift-related volcanic rocks and immature sediments, are preserved along the northern and eastern margin of the Transvaal basin. The chemical sediments of the Chuniespoort Group followed which represents a thermal subsidence basin dated at approximately 2550 Ma (Clendenin, 1989). The sedimentation of the Pretoria Group commenced in an extensional tectonic setting,

either within half-grabens, controlled by the TML (Eriksson et al., 1991), or the beginning of a continental rift (Schreiber et al., 1992). The main depositional axis of the Transvaal basin trends roughly ENE, and generally strata dip towards the center of the basin and towards the Bushveld Complex (Figure 4.5). Visser (1998) stated that the Transvaal Supergroup has only been slightly deformed by folding and faulting. However, intense deformation is present in distinct areas. Thrust and strike-slip faulting with associated folding occur in the NE trending Mhlapitsi belt. This deformation occurred between post-Chuniespoort deposition but pre-date Pretoria deposition (2.4 – 2.2 Ga) (Potgieter, 1992). Interference folding in the Pretoria sediments was recorded in the Transvaal inliers and other areas (Hartzer, 1994; Bumby, 1997). The Pretoria Group was first deformed by NW-SE compression and then secondly, by NE-SW compression before the intrusion of the Bushveld Complex (Hartzer ,1994).

4.1.2.6 Griqualand West basin

The Griqualand West basin and the main Transvaal basin, are proposed to have once been connected via the southern part of Botswana (Crockett, 1971). The Griqualand West basin is proposed to have formed in a large epeiric sea covering extensive areas of the Kaapvaal Craton (Visser, 1998). The major axis of the Griqualand West Basin trends roughly NS, (Figure 4.5). Overall the Supergroup has only been moderately deformed. However, deformation along the southwestern margin of the basin is believed to be in response to deformation during the Kheis orogeny at 2.0 Ga (Visser, 1998). Other structures include a large gentle syncline which trends SW, situated in the center of the basin. Fold orientations include NW-SE, NE-SW and NS (Visser, 1998), and faulting follows NNE, NW and some NS orientations.

4.1.2.7 Waterberg basin

The Waterberg basin formed in a half graben setting with the Thabazimbi-Murchison fault zone forming the southern boundary (Callaghan et al., 1991) The 1.8 Ga Waterberg basin came into being during a period where tensional conditions existed on the Kaapvaal Craton due to cooling of the crust after the intrusion of the Bushveld Complex (Jansen, 1982). The Nylstroom protobasin developed to the south of the Thabazimbi-Murchison fault while a deep trough, known as the Alma trough, developed

on the northern side of the Thabazimbi-Murchison fault zone (Figure 4.5). ENE to EW trending structures, such as thrust faults and folds, dominate the southern margin of the main Waterberg basin. A southward extension of the Steelpoort fault forms the northwestern margin of the Middelburg-Cullinan basin. Characteristic structures of the Cullinan Middelburg basin also include ENE to EW orientated faults and folds (van der Neut and van der Merwe, 2000).

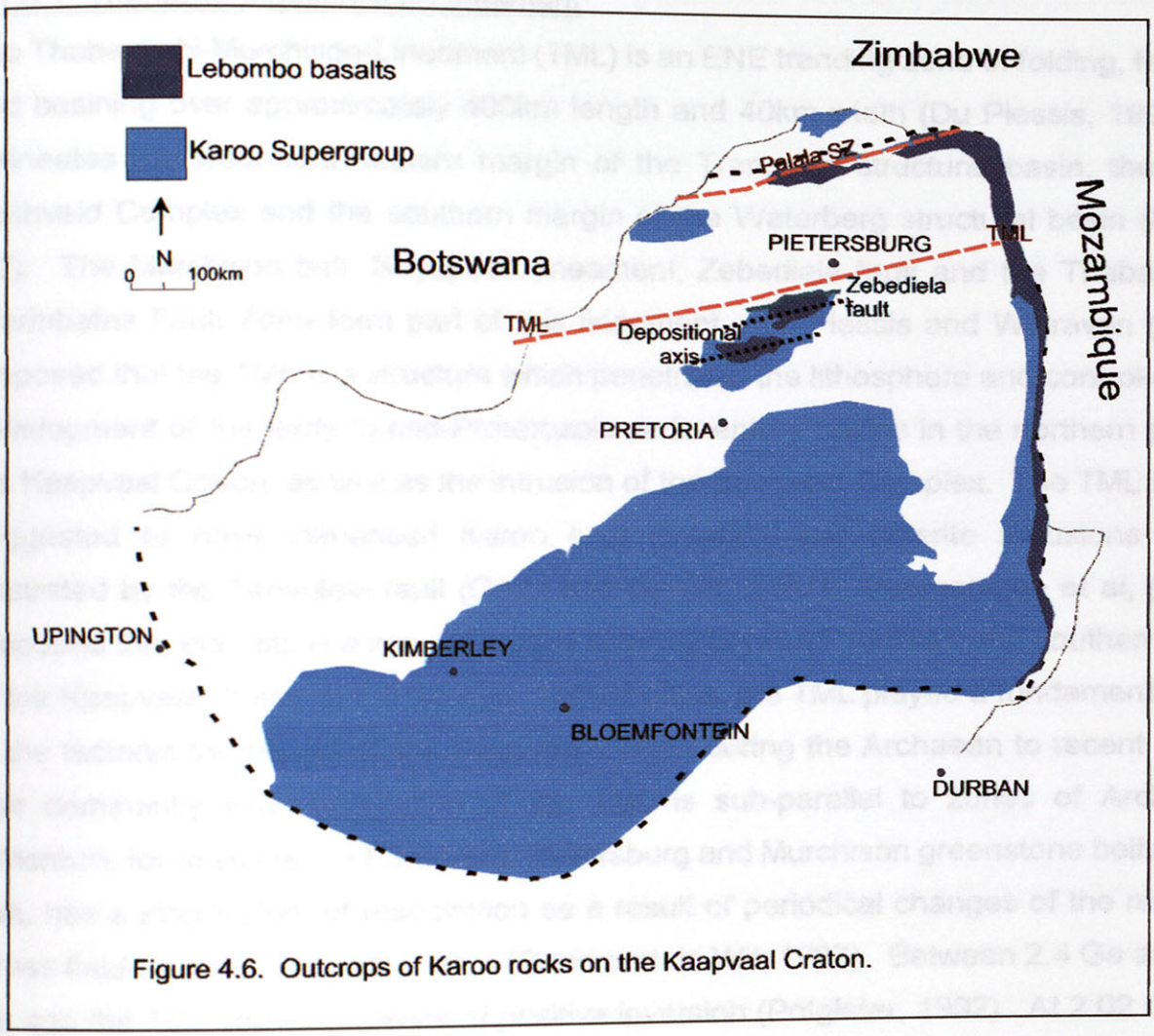

Figure 4.6. Outcrops of Karoo rocks on the Kaapvaal Craton.

4.1.2.8 Karoo basin

The main Karoo basin is interpreted to be a foreland basin of roughly 345 Ma old covering a large portion of southern Africa (Cole, 1992). Located in the center of the Bushveld Complex is what is known to be a preserved remnant of the main Karoo basin. Here the Karoo rocks occur in a basin with an ENE trending axis, roughly parallel to that of the Bushveld Complex and Transvaal basin (Figure 4.6). The basin is bounded on the northwest side by the roughly NE striking Zebediela fault. Karoo rocks also occur in

the northern part of the Kaapvaal Craton against the Palala shear zone and the Central Zone of the Limpopo mobile belt (Figure 4.6).

4.1.3 Major Structural lineaments on the Kaapvaal Craton

4.1.3.1 Thabazimbi-Murchison-Lineament

The Thabazimbi-Murchison-Lineament (TML) is an ENE trending zone of folding, faulting and basining over approximately 400km length and 40km width (Du Plessis, 1991). It delineates the west-northwestern margin of the Transvaal structural basin, the main Bushveld Complex and the southern margin of the Waterberg structural basin (Figure 4.7). The Murchison belt, Strydpoort lineament, Zebediela fault and the Thabazimbi-Warmbaths Fault Zone form part of this lineament. Du Plessis and Walraven (1990) proposed that the TML is a structure which penetrated the lithosphere and controlled the development of the early to mid-Proterozoic sedimentary basins in the northern part of the Kaapvaal Craton, as well as the intrusion of the Bushveld Complex. The TML is also suggested to have influenced Karoo sedimentation and dolerite intrusions as is illustrated by the Zebediela fault (Good and de Wit, 1997). Vearncombe et al, (1992) proposed that the TML is a zone of crustal suturing between northern and southern parts of the Kaapvaal Craton at 2.8 Ga ago. Nonetheless, the TML played a fundamental role in the tectonic framework of the Kaapvaal Craton during the Archaean to recent times. The dominantly ENE orientation of the TML is sub-parallel to zones of Archaean tectonism, for example the Barberton, Pietersburg and Murchison greenstone belts. The TML has a long history of reactivation as a result of periodical changes of the regional stress fields on the Kaapvaal Craton (Good and de Wit, 1997). Between 2.4 Ga and 2.2 Ga ago the TML shows evidence of positive inversion (Potgieter, 1992). At 2.02 Ga the TML was reactivated during the intrusion of the Bushveld Complex as left-lateral strike-slip faults (Du Plessis and Walraven, 1990). The final reactivation was normal movement in post-Karoo times, along structures such as the Zebediela Fault (Good and de Wit, 1997).

4.1.3.2 Limpopo Mobile Belt

The Limpopo Belt is a major ENE trending orogenic belt which represents a suture zone between the Zimbabwe Craton to the north and the Kaapvaal Craton in the south.

These two cratons are believed to have collided at around 2.65Ga ago involving oblique collision, with the Kaapvaal Craton moving northwestwards (Roering et al., 1992). However, many authors are of the opinion that the two cratons collided by NS directed collision (Coward and Fairhead, 1980; Light, 1982, Van Reenen et al., 1988). Also, it has been recently proposed (Barton et al., 1994; Holzer et al., 1998) that the collision may be as young as early Proterozoic, the time of the 2.0 Ga tectonothermal event (Van Breemen and Dodson, 1972). This tectonothermal event could, however, be related to the intrusion of the Bushveld Complex. Three zones can be recognized in the belt based on their distinct geological characteristics (van Reenen et al., 1992). They include the Southern Marginal Zone, the Central Zone and the Northern Marginal Zone (Figure 4.8). Detailed work on the lithological character of each zone has been done by authors such as van Reenen et al. (1992). The boundary between the Southern Marginal Zone and the Kaapvaal Craton is a northward-dipping shear zone. The boundary between the Southern Marginal Zone and the central zone is marked by the Palala shear zone, a left-lateral strike-slip fault zone, which was active after the intrusion of the Bushveld Complex (Brandl and Reimold, 1990). While the Northern Marginal Zone and the Central Zone are separated by the Tuli-Sabi shear zone, a gently-dipping dextral strike-slip fault (McCourt and Vearncombe, 1987). The boundary between the Northern Marginal Zone and the Zimbabwe Craton is marked by a southward-dipping thrust fault, (Figure 4.8).

4.1.3.3 Other proposed lineaments

Trompsburg-Great Dyke lineament

It has been noted that layered mafic intrusives, such as the Great Dyke of Zimbabwe, the Losberg Complex, the northern lobe of the Bushveld Complex and the Trompsburg intrusive Complex all lie along a NS trending lineament (Hall, 1932). All these layered intrusives have similar geochemistries and they become progressively younger towards the south. The Great Dyke of Zimbabwe is dated at around 2.5 Ga, and the Losberg Complex at 2.04 Ga. The Bushveld Complex has an age around 2.05 Ga and the Trompsburg Complex is believed to be 1.3 Ga (Visser, 1998). Hall (1932), Willemse (1969), and Hunter (1975) suggested that these intrusions might depict a north-northeast trending abyssal fracture (Tankard et al., 1982). Intermittent injection of magma occurred over a period of 1 400 Ma along this fracture. The Bushveld Complex is believed to have developed over a wide zone across this fracture (Visser, 1998).

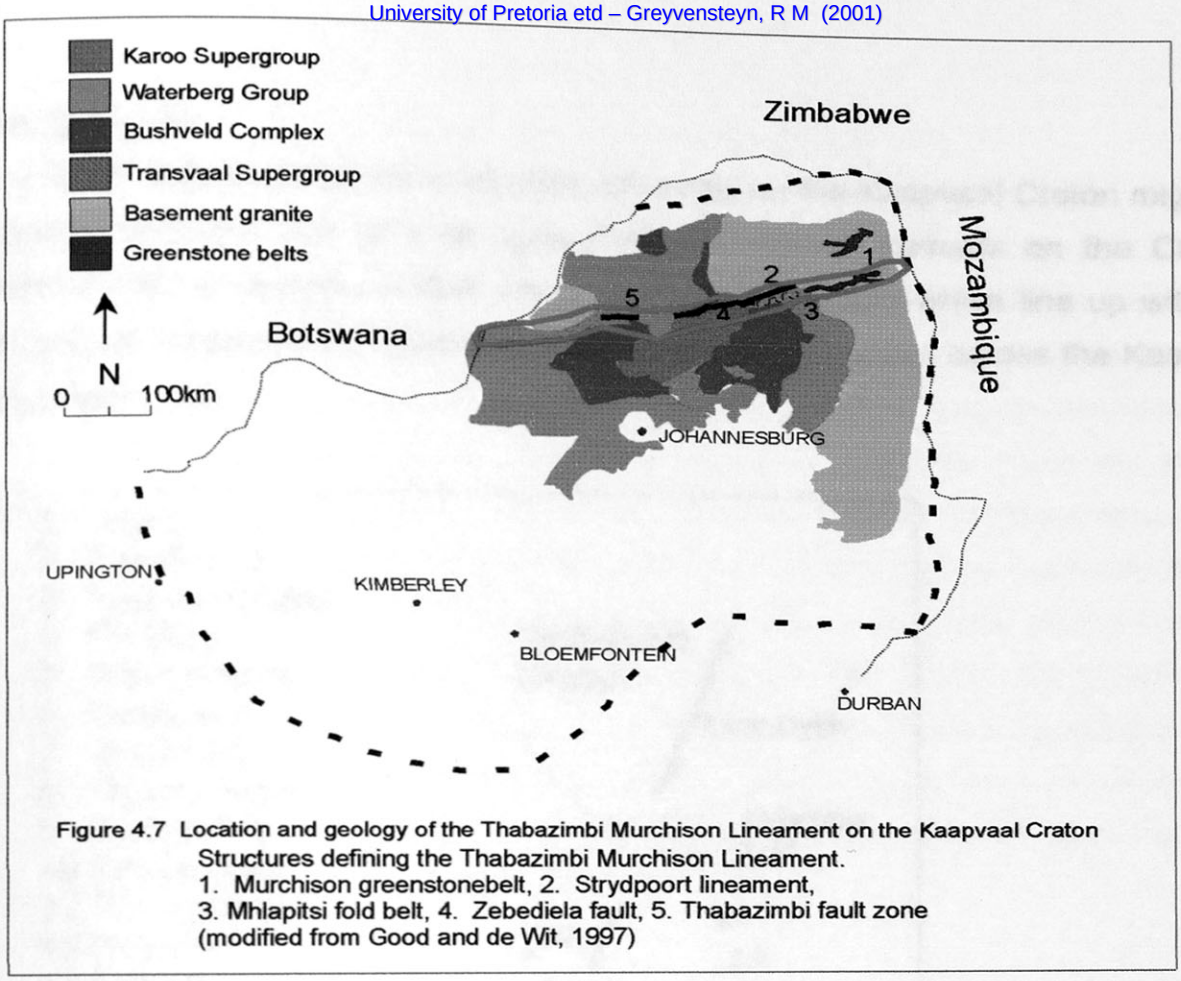

Figure 4.7 Location and geology of the Thabazimbi Murchison Lineament on the Kaapvaal Craton
Structures defining the Thabazimbi Murchison Lineament.
1. Murchison greenstonebelt, 2. Strydpoort lineament,
3. Mhlapitsi fold belt, 4. Zebediela fault, 5. Thabazimbi fault zone
(modified from Good and de Wit, 1997)

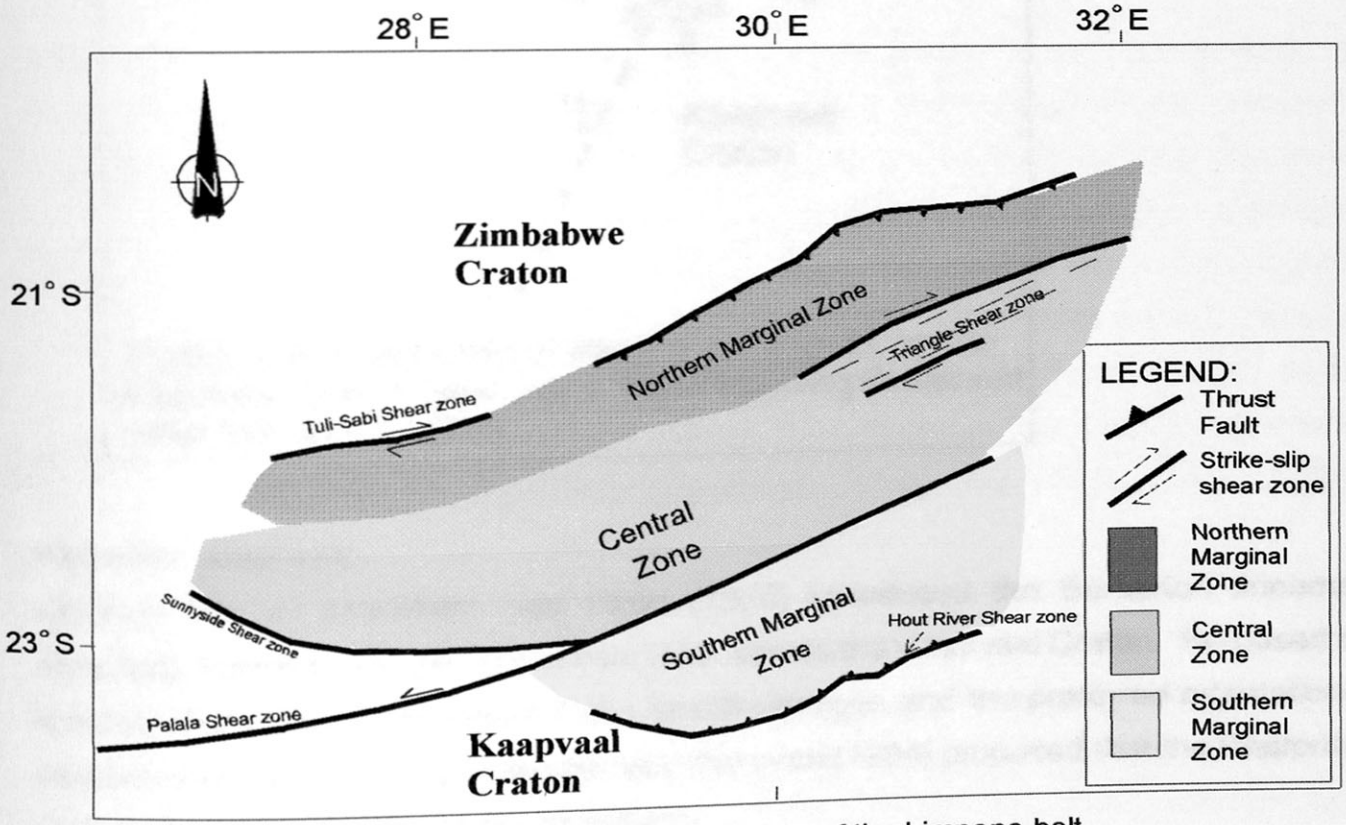

Figure 4.8. Southern, Central and Northern Zones of the Limpopo belt
(modified from Bumby, 2000)

Alkaline Intrusives

Visser (1998) proposed that some alkaline intrusives on the Kaapvaal Craton might be structurally controlled due to their ages and distributional patterns on the Craton. Verwoerd (1993) envisioned a NNE trending structural feature which line up with the Great Dyke of Zimbabwe for alkaline complexes and carbonatites across the Kaapvaal Craton, (Figure 4.9).

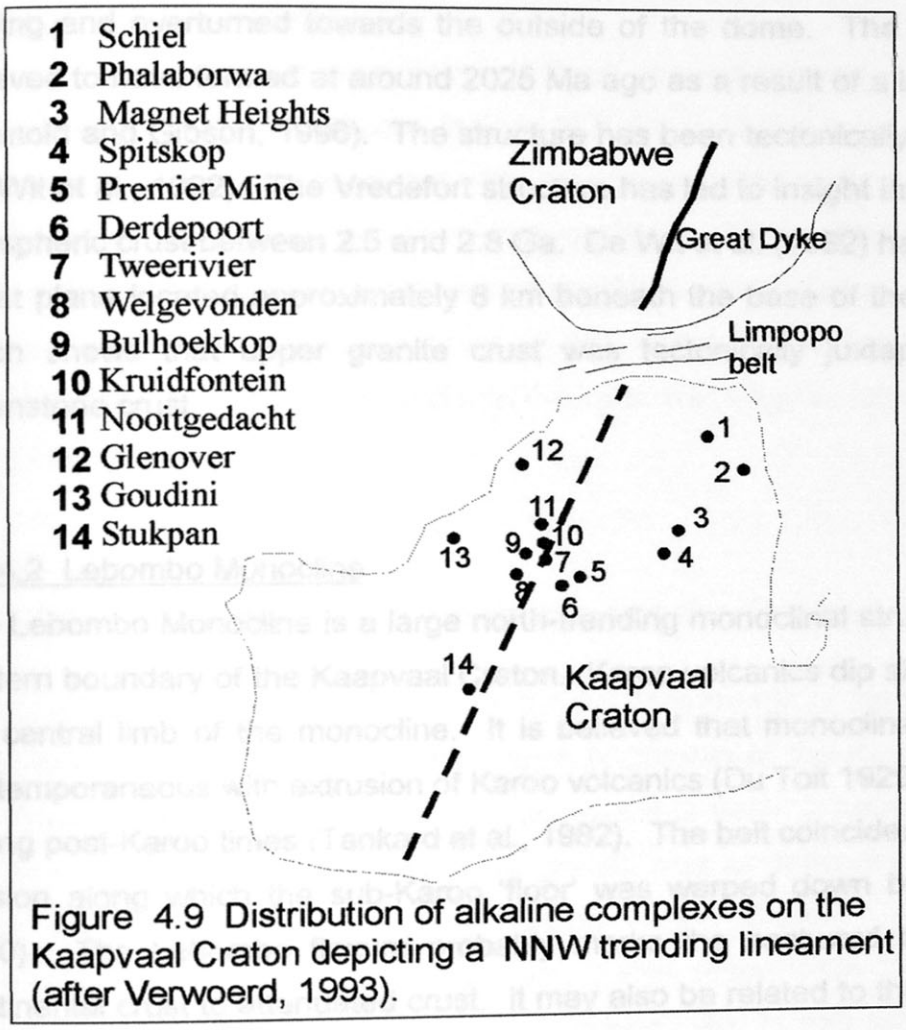

Figure 4.9 Distribution of alkaline complexes on the Kaapvaal Craton depicting a NNW trending lineament (after Verwoerd, 1993).

Barberton lineament

Although not so prominent, van Biljon (1976) introduced the Barberton lineament stretching from the Barberton Mountain land across the Kaapvaal Craton. He based the location of this lineament form ERTS-I satellite images and the preferred orientation of structures along this line. Du Plessis and Walravan (1994) proposed that the Rietfontein fault system is connected to the lineament.

4.1.4 Other important structures affecting the Kaapvaal Craton

4.1.4.1 Vredefort dome

The Vredefort dome, located in the center of the Craton is made up of a granitic core, approximately 50 km wide, with a roughly circular shaped rim 15-20 km wide (Reimold and Gibson, 1996). The rim or collar is made up of rocks belonging to the Dominion, Witwatersrand, Ventersdorp and the Transvaal sequences. These rocks are steeply dipping and overturned towards the outside of the dome. The Vredefort structure is believed to have formed at around 2025 Ma ago as a result of a large meteoritic impact (Reimold and Gibson, 1996). The structure has been tectonically tilted after the impact (de Wit et al., 1992). The Vredefort structure has led to insight into the formation of the lithospheric crust between 2.5 and 2.8 Ga. De Wit et al. (1992) have suggested a major thrust plane located approximately 8 km beneath the base of the Witwatersrand basin which shows that upper granite crust was tectonically juxtaposed above granite-greenstone crust.

4.1.4.2 Lebombo Monocline

The Lebombo Monocline is a large north-trending monoclinal structure which forms the eastern boundary of the Kaapvaal Craton. Karoo volcanics dip steeply east-ward along the central limb of the monocline. It is believed that monoclinal warping was in part contemporaneous with extrusion of Karoo volcanics (Du Toit 1929) but was accentuated during post-Karoo times (Tankard et al., 1982). The belt coincides with a zone of crustal tension along which the sub-Karoo 'floor' was warped down by at least 9 km (Cox, 1970). The Lebombo flexure probably marks the eastward transition from normal continental crust to attenuated crust. It may also be related to the junction between the Archaean Kaapvaal Craton and the Late Proterozoic Mozambique Belt (Visser, 1998).

4.1.4.3 Vryburg Arch

A broad belt of Archaean domal structures define what is known to be the Vryburg Arch (Hunter and Hamilton, 1978). The belt flanks the western margin of the Bushveld Complex, and Transvaal rocks attenuate across the Arch into Botswana, thus separating the Griqualand West and Transvaal basins (Tankard et al., 1982). All of the domes are

composed of granitic basement and include the Vredefort, Johannesburg, Makoppa, Gaberone, Molopo, Mafikeng and Klerksdorp domes. Thick Mesozoic and Proterozoic sedimentary sequences occur on either side of the Arch (Tankard et al., 1982). It is believed that the Arch has been active over a long period of time stretching from Archaean times to Pilanesberg times at 1300Ma (Visser, 1998).

4.1.4.4 Mafic dyke swarms

Uken and Watkeys (1997a) recognized three orientations of dyke swarms during Pre-Karoo times. These orientations include NW, NE and EW dyke events. They propose that the NW dykes are associated with Pongola and Witwatersrand rifting, whereas the NE dykes are associated with Ventersdorp rifting. They further proposed that Craton wide compression during the intrusion of the Bushveld Complex was responsible for the emplacement of EW orientated dykes. Karoo-age dyking is characterized by NNW, NE and NS trending dykes associated with the Mesozoic fragmentation of Gondwana (Uken and Watkeys 1997b).

4.1.5 Other marginal tectonic events affecting the Kaapvaal Craton

The Eburnian orogeny prevailed along the western margin of the Craton during the early Proterozoic. The convergent margin type sediments of the Richtersveld Province and the Kheis orogeny at 1.75 Ga both represent this event (Thomas et al., 1993). From mid-late Proterozoic major continental growth and accretionary processes dominated along the southern and western margins of the Craton. This is known as the approximately 1.2 Ga Kibaran event which was responsible for the formation of the Namaqua-Natal Metamorphic Province. Subsequent to this orogenesis was the Late Paleozoic Pan-African event (Thomas et al., 1993). This event is marked by a period of extensive continental fragmentation with geosynclinal deposition seen in the Gariep and Saldanian provinces (Thomas et al., 1993). By the early Palaeozoic the Kaapvaal Craton was situated in the center of the super-continent Gondwana. During this time the Cape Supergroup was deposited along the southern margin of the south African continent in an aborted rift type setting (Tankard et al., 1982). The Cape Supergroup was followed by the formation of the large intracratonic Karoo foreland basin. The Cape

and Karoo successions were deformed along the Cape fold belt, due to what is believed to be shallow subduction of oceanic crust at the supercontinental margin. The break-up of Gondwana then commenced in two stages around – 180 and 160 Ma and 135 Ma along lines of Proterozoic and Archaean crustal weakness (Dingle et al., 1983: Martin and Hartnady, 1986; Watkeys and Sweeney, 1988).

4.2 TECTONIC SETTING OF THE BUSHVELD COMPLEX

The Bushveld Complex is situated in the center of the main Transvaal basin (Figure 4.10). The main axis of the Complex trends roughly ENE, parallel to the long axis of the Transvaal basin. Transvaal rocks form the floor and roof of the Complex except towards the northern lobe where Bushveld rocks overlie granitoid-gneiss basement. The mafic phase of the Complex has been dated at 2061 ± 27 Ga (Walraven, 1990) and the acid phase at 2.05 Ga (Harmer and Von Gruenewaldt, 1991). Several models have been proposed for the distribution of the Complex. Du Plessis and Walraven (1990) summarized the models as follows:

- a complex basin-shaped continuous body (Willemse, 1969)
- a complex comprising four separate bodies (Cousins, 1959)
- a cruciform body comprising four separate lobes, each with its own center of intrusion (Hunter, 1975)
- a major body with interconnected compartments fed from seven centers of intrusion. (Von Gruenewaldt, 1979)

A regional gravity survey done by Smit et al. in 1962 has shown that the mafic rocks are not continuous beneath the younger cover rocks and therefore suggested that the Complex does not have a simple lopolithic form. Smit et al. (1962) proposed a four leaf clover shape for the Complex which represents four separate intrusions. The four lobes include (Figure 1.5);

1. The western lobe, extending from near Pretoria westward to Rustenburg and around the Pilanesberg Alkaline Complex to and along the southern flank of the Makopa Dome.
2. The southeastern lobe which is mostly covered by Mesozoic rocks.

3. The eastern lobe which continues northward from the southeastern lobe to about 50 km east of Potgietersrus.
4. The northern lobe which extends from south of Potgietersrus to Villa Nora.

Overall the Bushveld Complex is relatively undeformed. Dips of the layered sequence of basic and ultrabasic rocks in each of the lobes are toward the center, usually at low angles between 10° and 25°, except for in the northern lobe where it averages 60°. The current structural pattern of the Complex is characterized by three large and prominent faults. These faults include: in the west, the NW striking Rustenburg fault and Brits Graben, in the center, the NNE striking Wonderkop fault, and in the east the NE striking Steelpoort fault (Figure 1.4). Furthermore, the Bushveld Complex is intensely deformed along the Palala shear zone.

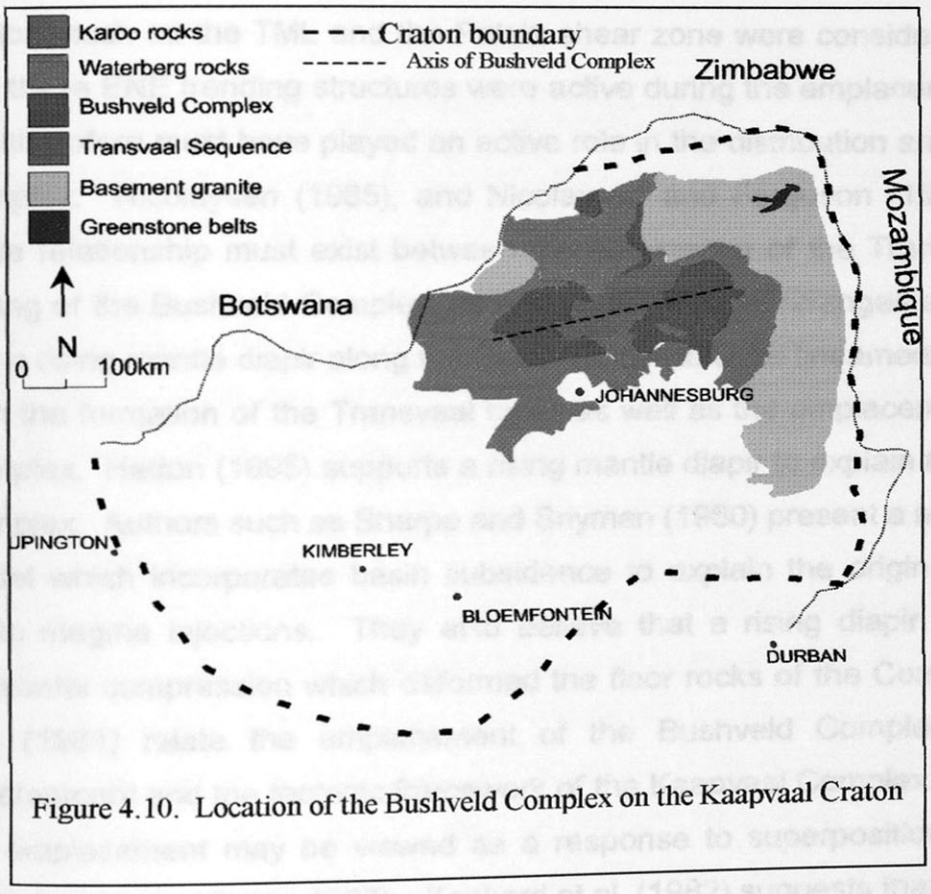

Figure 4.10. Location of the Bushveld Complex on the Kaapvaal Craton

Various models for the tectonic setting and emplacement of the Bushveld Complex have been proposed in the past. These models vary from stable cratonic settings to plate tectonic linked orogenies, as well as major crustal features controlling the emplacement

of the Complex (Du Plessis and Walraven 1990). The first author to speculate about the tectonic setting of the Bushveld Complex was probably Hall (1932). He suggested that a deep crustal fracture, the Bushveld-Great Dyke line of intrusion, was responsible for the emplacement of the Complex. Some authors have also speculated about the siting of the Complex at the intersection of the TML and the Bushveld-Great Dyke mega-fracture, (Visser, 1998). On the other hand, Lee and Sharpe (1986) have concluded by means of LANDSAT imaging that no deep seated crustal fractures were responsible for the emplacement of the Complex. Van Biljon (1976) relates the intrusion of the Complex to an active spreading center with major lineaments such as the TML and Barberton lineaments acting as major transform faults. Furthermore, Du Plessis and Walraven (1990) have suggested that the emplacement of the Complex was indeed structurally controlled. During their investigations major structural lineaments of the Kaapvaal Craton, such as the TML and the Palala shear zone were considered. They proposed that these ENE trending structures were active during the emplacement of the Complex and therefore must have played an active role in the distribution and deformation of the Complex. Nicolaysen (1985), and Nicolaysen and Ferguson (1980), suggested that some relationship must exist between the occurrence of the Transvaal basin and the setting of the Bushveld Complex, as well as its elliptical arrangement. They concluded that a rising mantle diapir along the Bushveld-Great Dyke lineament was responsible for both the formation of the Transvaal basin as well as the emplacement of the Bushveld Complex. Hatton (1995) supports a rising mantle diapir to explain the distribution of the Complex. Authors such as Sharpe and Snyman (1980) present a mathematically based model which incorporates basin subsidence to explain the origin of sill intrusion and mafic magma injections. They also believe that a rising diapir was responsible for horizontal compression which deformed the floor rocks of the Complex. Vermaak and Lee (1981) relate the emplacement of the Bushveld Complex to the geological development and the tectonic framework of the Kaapvaal Complex. They conclude that the emplacement may be viewed as a response to superposition of NNW and ENE crustal warps (in Visser, 1998). Tankard et al. (1982) suggests that the emplacement of the Bushveld Complex is probably due to a combination of the above mentioned mechanisms.

5: STRUCTURAL GEOLOGY OF THE BUSHVELD COMPLEX AND THE SURROUNDING AREAS

In this chapter the nature and geometry of all the major structures occurring in the eastern, northern and western Bushveld Complex and surrounding areas, as present in BOSGIS, are described. All the data were obtained from the literature and no additional fieldwork was done. Archaean structures are not discussed in detail and only major features are mentioned. The younger structures are discussed in more detail but due to the paucity of published data many descriptions are therefore incomplete. Structures are firstly organized into the separate areas of the Complex in which they are located, and then discussed according to the ages of the rocks which they deform.

5.1 THE WESTERN BUSHVELD COMPLEX

A geological map, including all the various structures, of the western Bushveld Complex area is shown in Figure 5.1.

5.1.1 ARCHAEAN STRUCTURES

Archaean structures are confined to the Makoppa dome and the Johannesburg dome. Both of these domes form part of the Vryburg Arch.

5.1.1.1 Makoppa dome

According to Beukes (1983) and Hunter (1975, 1976) the Makoppa dome might be the result of two intersecting fold directions which trends NW and NE. Fourie (1984) concluded that the dome formed a palaeo-high during the deposition of the Chuniespoort Group. Minor greenstone fragments are present in the dome but nothing is known about any structures contained within these greenstone fragments. A few minor shear zones orientated more or less EW are observed, (Figure 5.1). In addition, well defined NNE satellite lineaments can be traced, but it is unknown what these lineaments represent. However these lineaments do not cut across into adjacent younger strata.

Geological Map of the western Bushveld Complex and surrounding areas

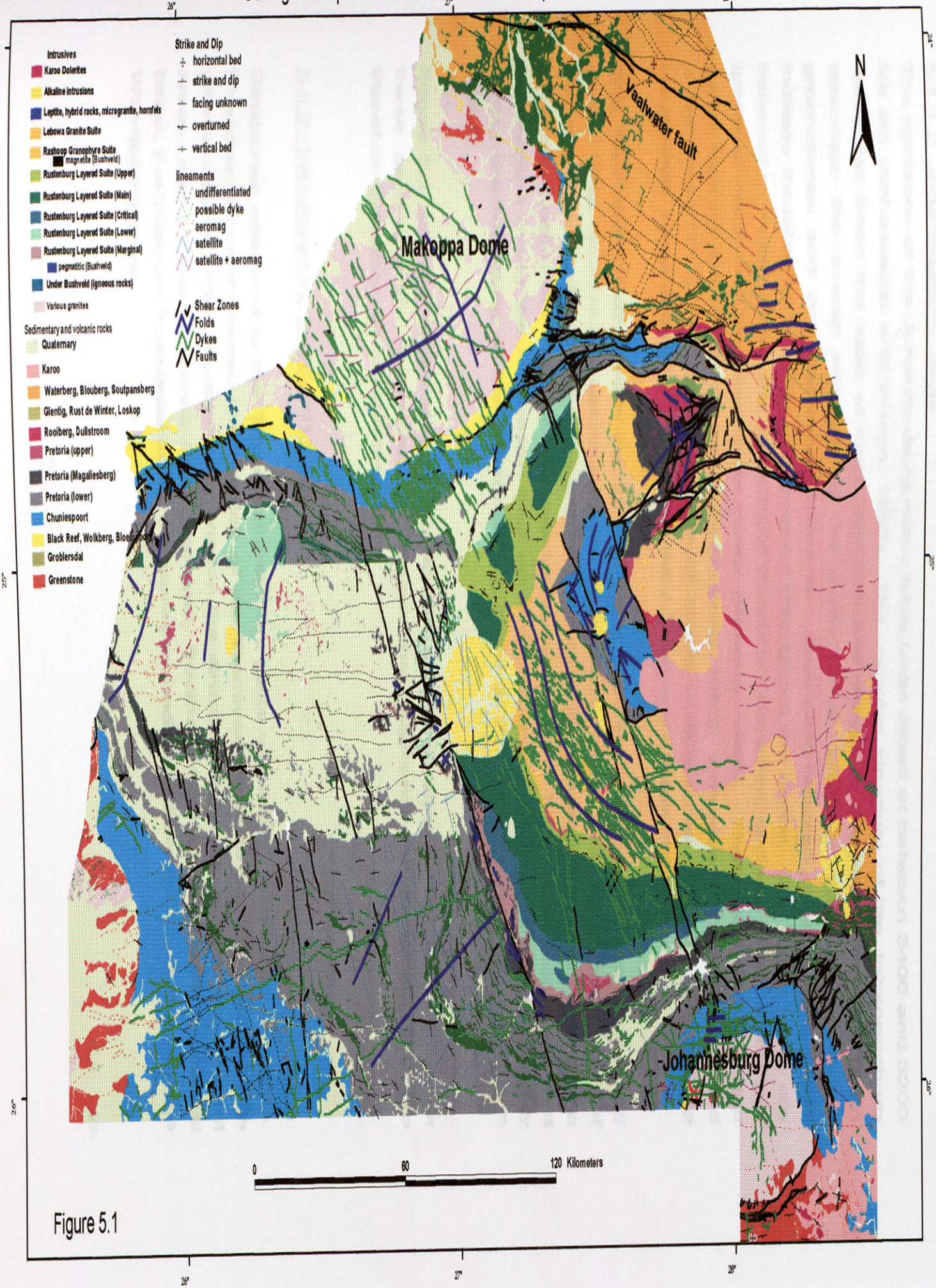

Figure 5.1

5.1.1.2 Johannesburg dome

The gneisses of the Johannesburg dome have been dated at between 3400 and 3200 Ma old (Anhaeusser and Wilson, 1981). The complex structure of the Johannesburg dome has been the topic of much research and debate in the past. Roering (1986) describes the overall structure of the dome as an imbricate stack of granitoids, greenstones and Witwatersrand sediments. East-west oriented shear zones, which indicate thrusting to the north are present throughout the dome. The thrust faults are believed to be older than the Black Reef Quartzite Formation, and are cut by a younger group of northeast trending shear zones (Roering, 1986). These NE striking shear zones indicate left lateral displacement (Roering, 1986). Anhaeusser (1973) also noted a prominent NE striking shear zone which shows vertical as well as dextral strike-slip movement. He proposed a post-Transvaal activation for these structures.

The *Rietfontein fault* system occurs along the southern margin of the Johannesburg dome. This sinuous approximately EW striking fault system, has had a long history of activation. According to Charlesworth et al. (1986) it has been continuously active as a left-lateral strike-slip fault during pre-Transvaal times. They also suggested that reactivation along the Rietfontein fault occurred during post-Transvaal times, possibly during the reheating of the Johannesburg dome at 2.1 Ga as postulated by Allsopp (1961).

Figure 5.1 also indicates EW trending satellite and aeromagnetic lineaments, however these aeromagnetic lineaments cut across into adjacent younger strata and are therefore probably not of Archaean age.

5.1.2 TRANSVAAL STRUCTURES

Structures observed in the Transvaal rocks are quite variable in orientation and style. Previous research proved deformation of the Transvaal rocks to be quite extensive in different areas. For convenient description the structures are grouped into six different areas, namely the Crocodile River fragment, Rooiberg fragment, Western Transvaal basin, Far Western Transvaal basin, structures around the Johannesburg dome, and the Warmbaths area.

5.1.2.1 Crocodile River fragment

The general geometry of the Crocodile River fragment is domal with rocks of the Transvaal Supergroup dipping towards the surrounding Bushveld Complex (Figure 5.2). The Transvaal rocks in the Crocodile River fragment are intensely deformed and a detail description of the deformation is provided by Hartzer (1987).

Faults

Two main NW striking faults can be traced in the fragment. Hartzer (1994) referred to these faults as V1 and V2. V1 is now named the Brits fault and V2 the Crocodile River fault. The faults are defined by a ferruginized breccia which mainly consists of chert, quartzite and dolomite fragments. Both these faults display dip-slip normal movement and dip very steeply towards the outside of the fragment. The central portion of the fragment moved upwards relative to the western portion and the Rooiberg fragment. Hartzer (1994) estimated the vertical displacement of the Brits fault to be in the order of 1 300m and that of the Crocodile River fault to be about 3000m. Crocker (1976) proposed the Crocodile River fault to be a right-lateral strike-slip fault with displacement of 1- 2 km which was superimposed on the downthrow to the NE. These faults are believed to have been active after the Bushveld Complex intrusion as a response to isostatic imbalances (Hartzer, 1994).

Folds

The Crocodile River fragment contains complex folding in which overfolding is common. Hartzer (1987) recognized three phases of folding. The first set of folds (F_1) trend northwest in the southern portion of the fragment and NE in the northern and central portion of the fragment. These F_1 folds were later refolded along an ENE trending axis (F_2), and later NW trending, F_3 folds, formed. F_1 and F_2 are believed to be of pre-Bushveld age, while F_3 are probably post-Bushveld in age.

5.1.2.2 Rooiberg fragment

The Rooiberg fragment occurs to the NE of the Crocodile River fragment but is not as intensely deformed as the Crocodile River fragment. The general shape of the Rooiberg fragment is that of a synform (Figure 5.2). A comprehensive overview of the Rooiberg fragment is provided by Hartzer (1994).

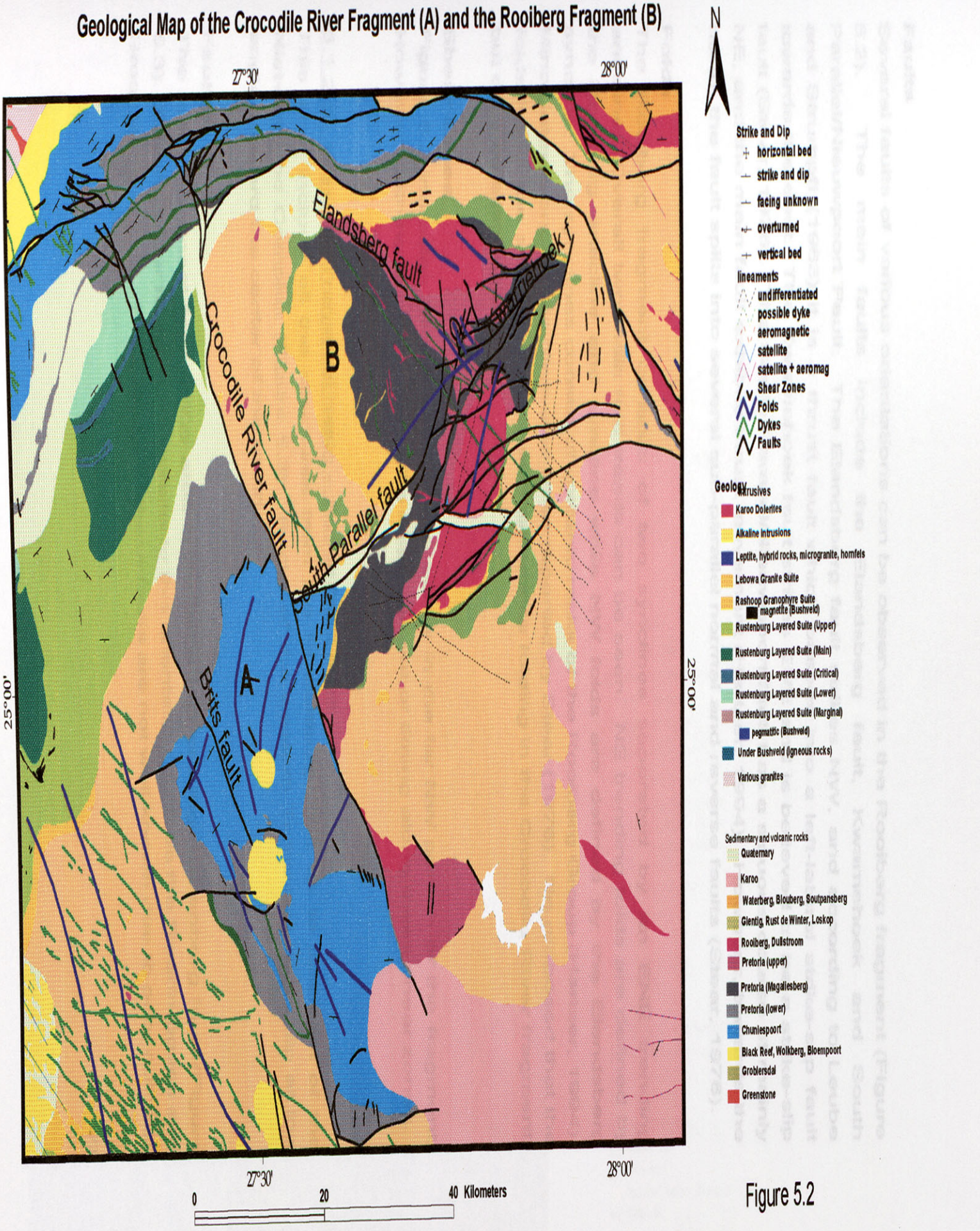

Figure 5.2

Faults

Several faults of various orientations can be observed in the Rooiberg fragment (Figure 5.2). The main faults include the Elandsberg fault, Kwarriehoek and South Parallel/Nieuwpoort Fault. The Elandsberg fault strikes NW, and according to Leube and Strumpfl (1963) it is a thrust fault which passes into a left-lateral strike-slip fault towards the east. The Kwarriehoek fault strikes ENE and is believed to be a strike-slip fault (Stear, 1976). The South Parallel/Nieuwpoort fault has a sinuous course of mainly NE, and the main fault exhibits thrust movement (Hartzer, 1994). However, towards the north, the fault splits into several sub-parallel normal and reverse faults (Stear, 1976).

Folds

The Rooiberg fragment consists of two synclines separated by an ENE trending anticline. Overall two main fold trends can be seen. NE trending folds are defined by the Rooiberg anticline and syncline while NW folds are defined by the Elandsberg syncline. The synclines consist of volcanic rocks of the Rooiberg Group (Hartzer, 1994). Minor interference folds have also been reported by Stear (1976). He proposed that the folds follow the same directions as interference folding in the Crocodile River fragment, but on a smaller scale.

Shear zones

Figure 5.2 indicates NNE trending shear zones in the far NW portion of the fragment. However, nothing is known about the displacement or timing along these shear zones.

5.1.2.3 Western Transvaal basin – Rustenburg area

This area include all the structures from the Rustenburg fault up to just east of the Nietverdiend Complex (Figure 5.3). Rocks of the western Transvaal basin dip at low angles toward the center of the basin.

Faults

The most prominent fault in the area is the large NW striking Rustenburg fault (Figure 5.3). Several other faults strike parallel to this orientation such as the Swartruggens and Groot Marico faults. The geology of these faults are not well known due to poor outcrop,

Geological Map of the structures of the western Transvaal basin

N

1: 846 000

Strike and Dip
- horizontal bed
- strike and dip
- facing unknown
- overturned
- vertical bed

lineaments
- undifferentiated
- possible dyke
- aeromagnetic
- satellite
- satellite + aeromag

Shear Zones
Folds
Dykes
Faults

Intrusives
- Karoo Dolerites
- Alkaline intrusions
- Leptite, hybrid rocks, microgranite, hornfels
- Lebowa Granite Suite
- Rashoop Granophyre Suite
  - magnetite (Bushveld)
- Rustenburg Layered Suite (Upper)
- Rustenburg Layered Suite (Main)
- Rustenburg Layered Suite (Critical)
- Rustenburg Layered Suite (Lower)
- Rustenburg Layered Suite (Marginal)
  - pegmatitic (Bushveld)
- Under Bushveld (igneous rocks)
- Various granites

Sedimentary and volcanic rocks
- Quaternary
- Karoo
- Waterberg, Blouberg, Soutpansberg
- Glentig, Rust de Winter, Loskop
- Rooiberg, Dullstroom
- Pretoria (upper)
- Pretoria (Magaliesberg)
- Pretoria (lower)
- Chuniespoort
- Black Reef, Wolkberg, Bloempoort
- Groblersdal
- Greenstone

Figure 5.3

but they have been documented as gravity faults (Visser, 1998). However, much research has been done on the Rustenburg and Liliput faults. The nature of these faults have been the subject of much debate in the past.

Rustenburg fault

The Rustenburg fault (Figure 5.3) has a NNW orientation and can be traced for approximately 200km. Various authors have described the Rustenburg fault and most interpretations are that it is a normal fault with downthrow to the east (Coertze, 1962; Vermaak, 1970; Du Plessis and Walraven, 1990), although a few interpretations favour strike-slip faulting (Bloy, 1986; Friese et al., 1995; Bumby, 1997). There is however much speculation about the timing of the fault with most authors proposing a post-Bushveld age. On the other hand, Bumby (1997) proposed a long reactivation history for the fault. He suggested that during Pretoria Group sedimentation the fault had normal displacement with downthrow to the west, as indicated by thickness differences observed on opposite sides of the fault. He further suggested that post-Transvaal but pre-Bushveld compressive events led to dextral strike-slip movement of the fault with a displacement of 10.6 km.

Liliput fault

The Liliput fault (Figure 5.3) is a northward extension of the Rustenburg fault (Bumby, 1997) which was later offset from the Rustenburg fault by faulting related to the intrusion of the Pilanesberg Alkaline Complex. Bumby (1997) has therefore also interpreted this fault as a strike-slip fault. Vermaak (1976) noted that the fault exhibits slight right-lateral movement in addition to the normal displacement. He however interpreted the fault as post-Bushveld in age.

Folds

Folding in the western Transvaal basin is uncommon although a few large antiform-synform pairs in the Pretoria Group sediments can be observed in the south (Figure 5.3). The axial trace trends NE, and the fold axis plunges in the same direction. Not much is known about the characteristics or timing of the folding. A few minor anticlines and synclines are also present along the southwestern margin of the Bushveld Complex in the Boshoek area. The axial traces of these folds trend 329° and 65° (Vermaak, 1970).

Bumby (1997) described the same interference fold pattern along the Rustenburg fault as were documented by Hartzer (1995) in the Transvaal inliers, namely NW orientated F_1 and NE orientated F_2 folds.

Lineaments

Numerous large undifferentiated lineaments are present in the area with generally poor outcrop. These lineaments exhibit a strong EW trend (Figure 5.3). Just to the south of these lineaments, various smaller NNW orientated aeromagnetic lineaments can clearly be traced in the upper Transvaal sequence.

Dykes and Sills

Only a few large dolerite dykes striking NE cut through the upper and lower Transvaal Supergroup in the southern part of the area (Figure 5.3). However, numerous concordant sills are present in the Pretoria Group. Studies done by Cawthorn et al. (1981) determined pre-, syn- and post-Bushveld ages for the sills based on their different compositions.

5.1.2.4 Far Western Transvaal basin – Nietverdiend-Zeerust area

Interpretation of the geology in this area is complicated due to limited outcrop (Figure 5.4). Previous research in this area was done by Engelbrecht (1986) and Crockett (1969, 1971). They proposed a syn or post-Transvaal, pre-Bushveld deformation event during which gravity-driven slides of upper Transvaal Supergroup rocks moved from east to west. This event is envisioned as a 'catastrophic' lowering of the Transvaal basin floor. Engelbrecht (1986) recorded intense folding and faulting of the overlying upper Transvaal slab, in contrast to the undeformed underling lower Transvaal sequence rocks.

Faults

Mannyelanong fault

This fault is located in the far western portion of the Transvaal basin and extends into Botswana (Figure 5.4). The fault has a NE strike and deforms rocks belonging to the Transvaal Supergroup, although small outcrops of what is believed to be Waterberg sediments have been found on the eastern side of this fault. The fault is proposed to be

Geological Map of the far western Transvaal basin

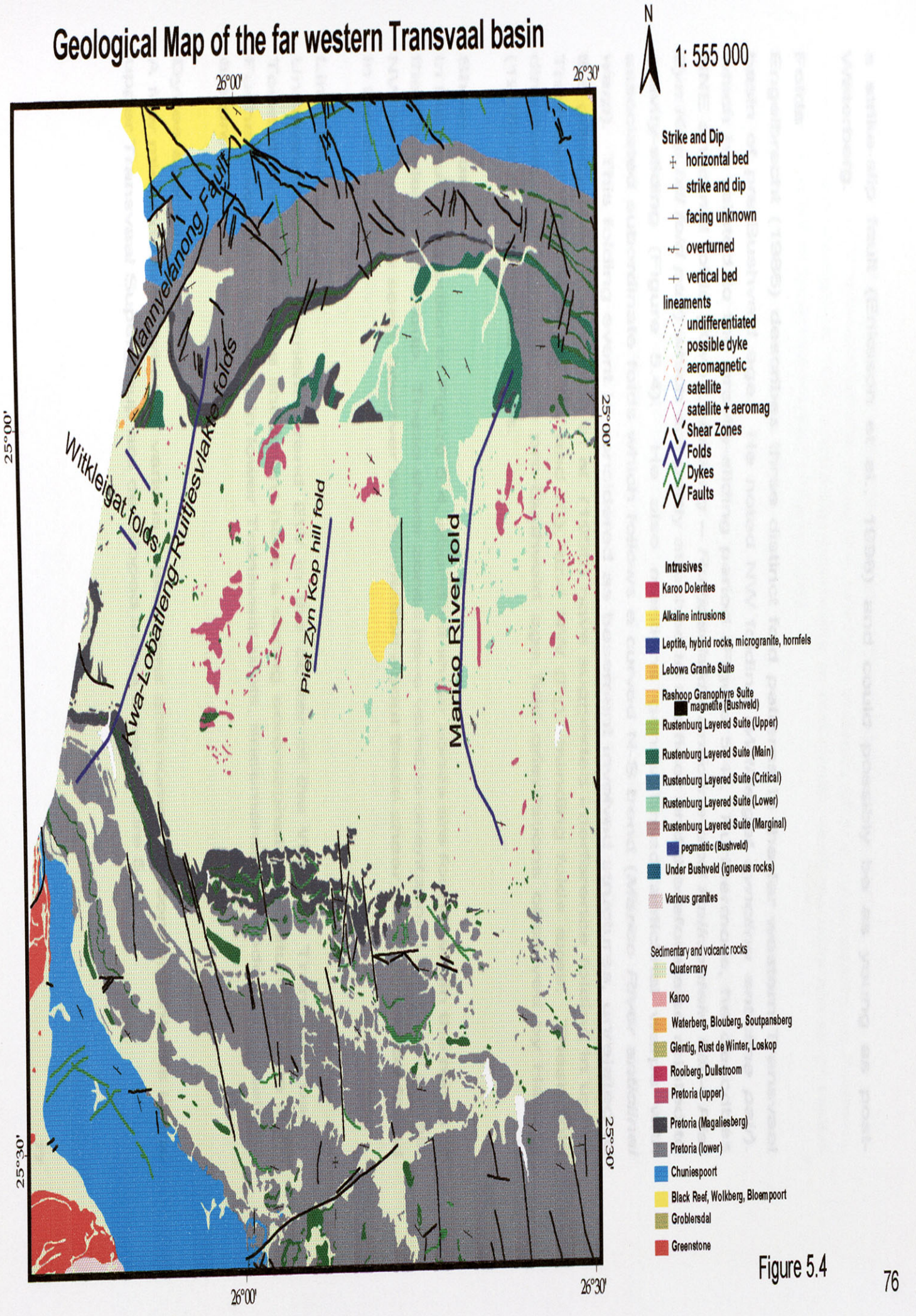

Figure 5.4

a strike-slip fault (Eriksson et al., 1998) and could possibly be as young as post-Waterberg.

Folds

Engelbrecht (1986) describes three distinct fold patterns in the far western Transvaal basin of pre-Bushveld age. He noted NW folding (*Witkleigat syncline anticline pair*). which he related to the gravity-sliding period (Figure 5.4). Furthermore, he describes NNE anticlinal folds *(Kwa-Lobatleng – Ruitjesvlakte anticline and Kalkfontein hill – Piet Zyn Kop hill fold pair*) which are partly attached to the floor and therefore also related to gravity-sliding (Figure 5.4). He also mentions gentle broad anticlinal warps with associated subordinate folds which follows a curved N-S trend (*Marico River anticlinal warp*). This folding event is considered as basement involved structures, unrelated to the gravity-sliding. Eriksson et al. (1998) have suggested interference folding in upper Transvaal rocks with NE (F_1 and F_3), and NW (F_2) trending folds axes. These fold directions also coincide with pre-Bushveld age fold orientations observed by Hartzer (1995) in the Transvaal inliers.

Shear zones

In the southern portion of Figure 5.4, abundant shear zones are found within the rocks of the Chuniespoort Group. These shear zones have variable orientations although a main NW trend can be seen, however no information about these shear zones could be found in the literature.

Lineaments

Undifferentiated lineaments trend EW in the center of the Western Transvaal basin. Towards the west these lineament have a strong aeromagnetic signature (Figure 5.4). Further towards the south, in lower Transvaal units, lineaments of random orientations are present.

Dykes and sills

A few minor dolerite dykes of various orientations and numerous concordant sills in the upper Transvaal Supergroup are developed in the area (Figure 5.4).

5.1.2.5 Transvaal structures around the Johannesburg-Pretoria dome

Deformation of Transvaal strata along the northern margin of the Johannesburg-Pretoria dome is fairly complex. The rocks dip generally to the north, and various types of faults and folding have been recorded (Figure 5.5).

Faults

Towards the northwest of the dome the faults have a NW trend. These faults are subvertical and display strike separations of up to 300m (Gibson et al., 1999). Gibson et al. (1999) noted evidence for both sinistral and dextral strike-slip and dip-slip movement. To the northeast of the dome the faults trend NE to ENE. The dominant sense of movement along these faults is right-lateral although one fault displays a reverse sense of movement (Visser, 1998). The faults along the northeastern rim of the dome are almost at right angles with respect to the strike of the bedding, with local horst and graben structures. Towards the east of the dome there is an approximately NS striking thrust fault. This fault has caused duplication of the Chuniespoort Group and lower parts of the Pretoria Group (Figure 5.5) .

Folds

The Black Reef Formation and Chuniespoort Group have been intensely folded along the northwestern part of the Johannesburg dome. Folds have been described by Gibson et al. (1999) as open to tight asymmetric, inclined to reclined, doubly plunging (periclinal) folds. He recorded wavelengths from a couple of meters to tens of meters with amplitudes of up to 1-2 m. Fold hinges plunge shallowly on an east-west trend, and axial planes dip shallow to moderately steep to the south. Gibson et al. (1999) also noted overturned bedding in some places along the steep northern limbs of anticlines. The age of this folding is not well constrained, however, Gibson et al. (1999) proposed a post-Bushveld pre-Pilanesberg age (related to the Vredefort event) to the folding. These folds trend parallel to Waterberg-age folds observed along the Thabazimbi belt and therefore, it might be possible that these folds formed during post-Waterberg times.

Geological Map of the Johannesburg Dome area

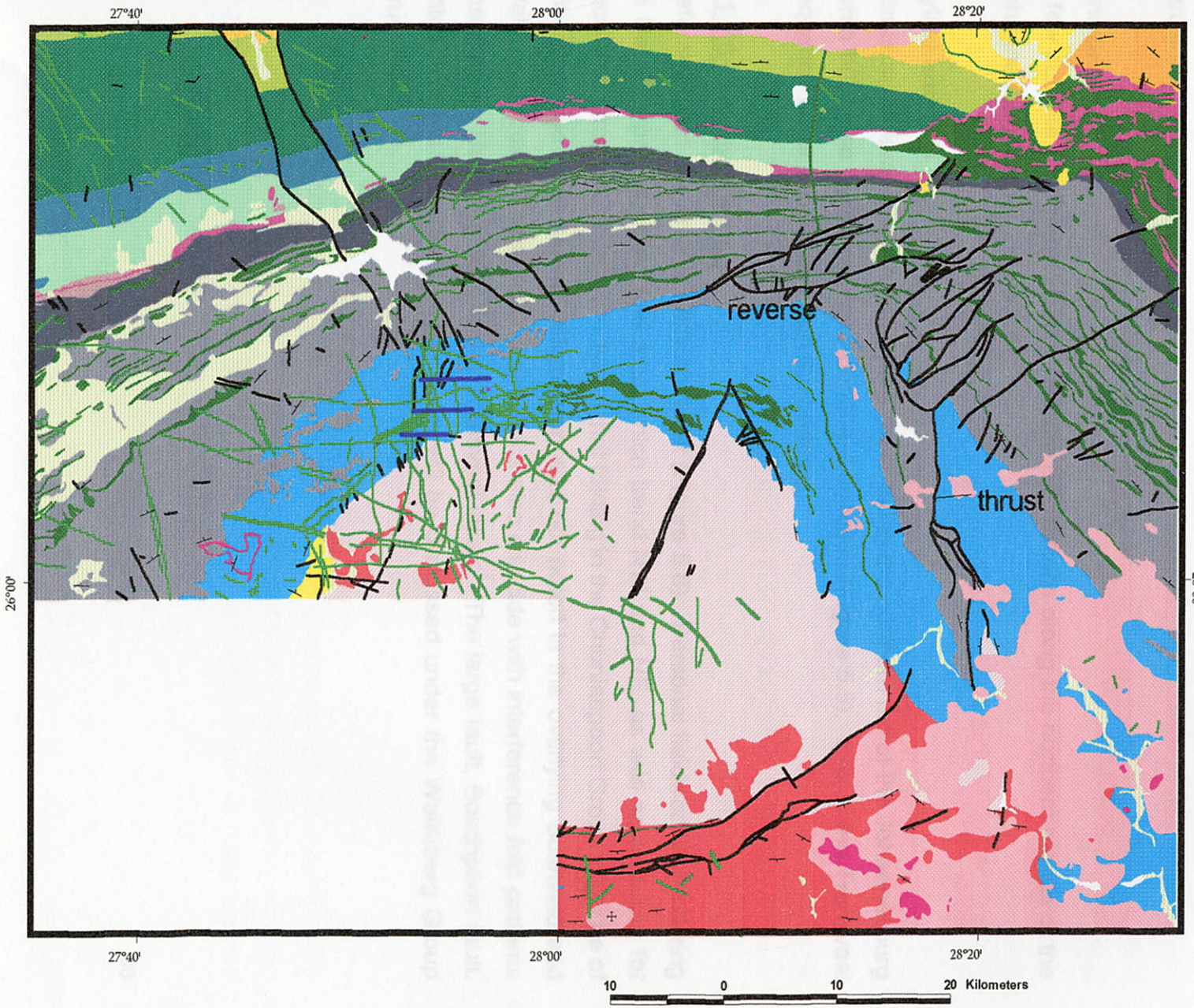

N
W E
S

Strike and Dip
- horizontal bed
- strike and dip
- facing unknown
- overturned
- vertical bed

lineaments
- undifferentiated
- possible dyke
- aeromagnetic
- satellite
- satellite + aeromag
- Shear Zones
- Folds
- Dykes
- Faults

Intrusives
- Karoo Dolerites
- Alkaline intrusions
- Leptite, hybrid rocks, microgranite, hornfels
- Lebowa Granite Suite
- Rashoop Granophyre Suite
  - magnetite (Bushveld)
- Rustenburg Layered Suite (Upper)
- Rustenburg Layered Suite (Main)
- Rustenburg Layered Suite (Critical)
- Rustenburg Layered Suite (Lower)
- Rustenburg Layered Suite (Marginal)
  - pegmatitic (Bushveld)
- Under Bushveld (igneous rocks)
- Various granites

Sedimentary and volcanic rocks
- Quaternary
- Karoo
- Waterberg, Blouberg, Soutpansberg
- Clentig, Rust de Winter, Loskop
- Rooiberg, Dullstroom
- Pretoria (upper)
- Pretoria (Magaliesberg)
- Pretoria (lower)
- Chuniespoort
- Black Reef, Wolkberg, Bloempoort
- Groblersdal
- Greenstone

Figure 5.5

Shear zones

A prominent NE striking shear zone in the Johannesburg dome can be traced into the adjacent Transvaal rocks where it passes into a left-lateral strike-slip fault (Visser, 1998). Other northward dipping and verging shear zones to the northwest of the Johannesburg dome have been noted by Gibson et al. (1999). However, Courtnage (1995) has stated that subsequent refolding of the bedding and shear zones resulted in localized dips to the south. Gibson et al. (1999) proposed the timing of this deformation to be related to outward-directed thrusting associated with the formation of the 2.023 Vredefort dome, since the deformation post-dates the 2.06 Bushveld metamorphism but predates the intrusion of Pilanesberg dykes.

Lineaments

A few satellite lineaments display random orientations along the northern margin of the Johannesburg dome (Figure 5.5).

Dykes and sills

Numerous dolerite and syenite dykes occur along the northern rim of the Johannesburg dome but these dykes show no dominant direction (Figure 5.5). Sills in the Transvaal sequence occur concordant with the bedding.

5.1.2.6 Warmbath's area

Deformation in this area is fairly complex (Figure 5.8). Personal fieldwork done during an Honours project noted fold axes which trend NW and NE, as well as evidence for ductile deformation. It was concluded that folding in the Chuniespoort Group might be of Transvaal age since similar deformation was not noted in the overlying Bushveld and Waterberg rocks. These folding directions also coincide with interference fold patterns observed by Hartzer (1995) in the Transvaal inliers. The large fault, Boschpoort fault, which deforms Waterberg Group rocks will be discussed under the Waterberg Group structures.

5.1.2.7 Thabazimbi area

The Transvaal rocks in the Thabazimbi area are intensely deformed and forms part of the TML. However, since this deformation involves Waterberg Group rocks the structures will be describe under the Waterberg structures.

5.1.3 WESTERN BUSHVELD COMPLEX STRUCTURES

The western lobe of the Bushveld Complex consists of two compartments: a far western Nietverdiend compartment and the main western compartment. It is yet uncertain if these two compartments are connected at depth (Visser, 1998). The main western compartment generally dips at low angles towards the center of the Complex, and gravity surveys of the Nietverdiend compartment reveal shallow centripetal dips (Biesheuvel, 1970). The dominant structural direction of the western Bushveld Complex is defined by the NNW trending Brits and Welgevonden Graben as well as antiformal-synformal structures observed in the granites (Figure 5.6).

Faults

The Brits and Welgevonden graben has a NNW strike (Figure 5.6), and appears to be a southward extension of the Crocodile River fault. These faults exhibit normal displacement with fault planes dipping outward at steep angles (Visser, 1998). However, seismic reflection modeling by Du Plessis and Levitt (1987) led them to conclude that these faults might have been active during pre-Bushveld times, controlling the emplacement of the Rustenburg Layered Suite. Another conspicuous set of faults occur along the northwestern margin of the Lobe. These faults are known as the Roodedam Graben and they strike parallel to other extensional faults such as the Brits and Welgevonden graben. Other smaller faults occur throughout the Rustenburg Layered Suite and are almost orientated at right angles with respect to the bedding of the Complex.

Folds

Figure 5.6 shows large anitformal and synformal structures present in the western lobe of the Bushveld Complex. The trend of these structures are mainly NW but curve to approximately follow the shape of the contact between the granites and the layered

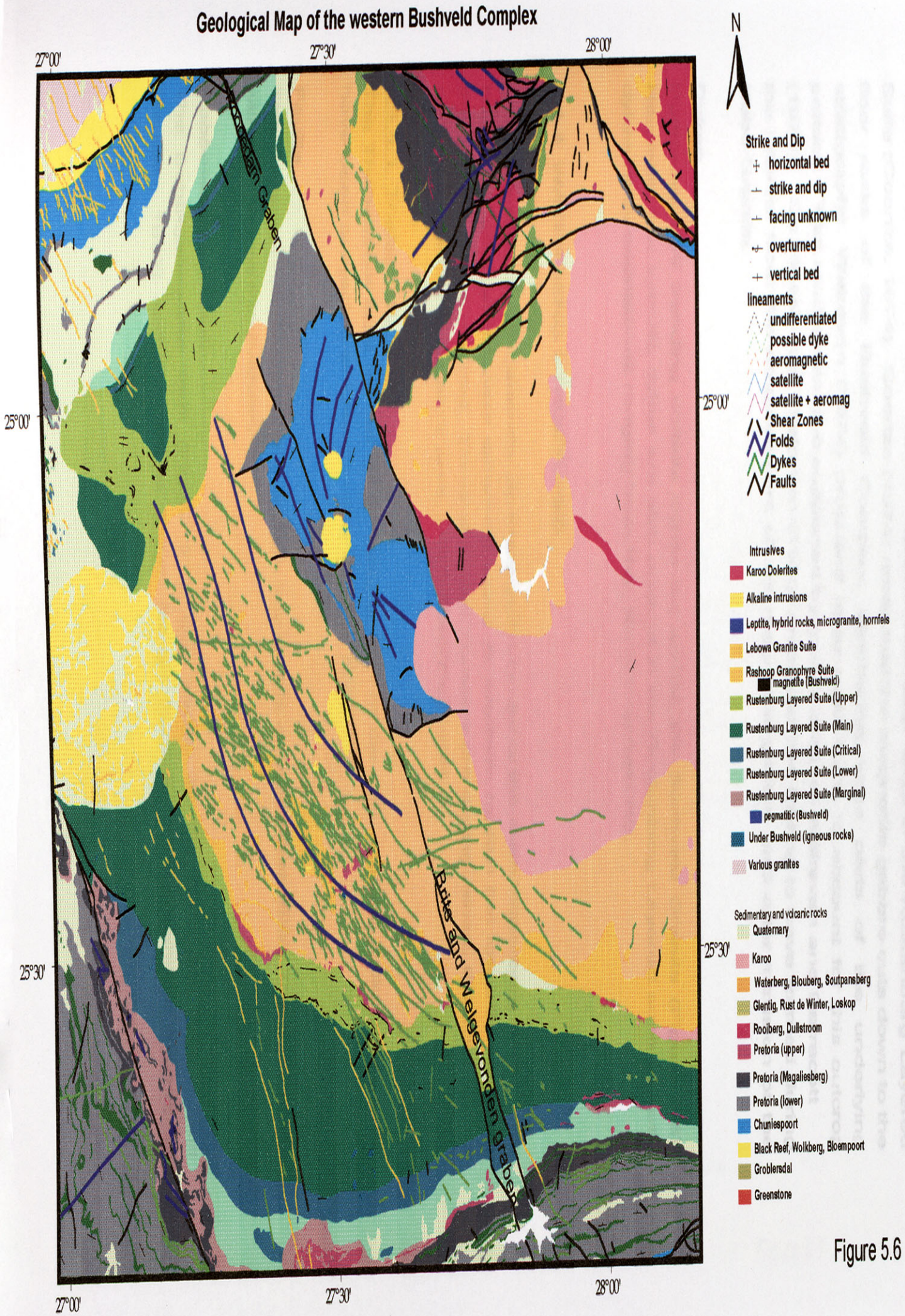
Geological Map of the western Bushveld Complex
27°00'
27°30'
28°00'
25°00'
25°30'
N
Rooiberg Graben
Brits and Welgevonden graben
Strike and Dip
horizontal bed
strike and dip
facing unknown
overturned
vertical bed
lineaments
undifferentiated
possible dyke
aeromagnetic
satellite
satellite + aeromag
Shear Zones
Folds
Dykes
Faults
Intrusives
Karoo Dolerites
Alkaline intrusions
Leptite, hybrid rocks, microgranite, hornfels
Lebowa Granite Suite
Rashoop Granophyre Suite
magnetite (Bushveld)
Rustenburg Layered Suite (Upper)
Rustenburg Layered Suite (Main)
Rustenburg Layered Suite (Critical)
Rustenburg Layered Suite (Lower)
Rustenburg Layered Suite (Marginal)
pegmatitic (Bushveld)
Under Bushveld (igneous rocks)
Various granites
Sedimentary and volcanic rocks
Quaternary
Karoo
Waterberg, Blouberg, Soutpansberg
Glentig, Rust de Winter, Loskop
Rooiberg, Dullstroom
Pretoria (upper)
Pretoria (Magaliesberg)
Pretoria (lower)
Chuniespoort
Black Reef, Wolkberg, Bloempoort
Groblersdal
Greenstone

Figure 5.6

mafic suite. These folds were recognized on the basis of a discordant intrusive relationship between the magnetite gabbro and older units of the Rustenburg Layered Suite (Coertze, 1974). Coertze (1974) noted that the magnetite gabbro cuts down to the floor rocks of the Bushveld Complex, eliminating large parts of the underlying stratigraphy. Walraven (1974) proposed large open folds to account for this outcrop pattern. This model was also supported by gravity data of Walraven and Darracott (1976). Du Plessis and Walraven (1990) proposed this folding to have formed during the interval from the emplacement of the magnetite gabbro until after intrusion of the Nebo Granite.

Dykes

Numerous NW trending dolerite dykes cut across the Bushveld Granite (Figure 5.6). However, few syenitic dykes are also present in the Rustenburg Layered suite. These dykes have orientations ranging from NW, NNW to almost NS.

5.1.4 WATERBERG STRUCTURES

The Waterberg rocks generally dip towards the center of the main Waterberg basin. The basin has been extensively deformed along its southern margin but towards the north the deformation is minimal. Three structural domains are distinguished, the Thabazimbi area, Nylstroom-Warmbath's area, and the Northern area.

5.1.4.1 Thabazimbi area

The Thabazimbi area makes up an integral part of the TML and the rocks in this area have been subjected to intense deformation (Figure 5.7).

Faults

The dominant orientation of the faults in this area is approximately EW. The main faults will be discussed individually:

Bobbejaanwater fault

The Bobbejaanwater fault (Figure 5.7), also known as the Crocodile Bridge fault (Jansen, 1982) and the Middle Thrust Range (Strauss, 1954), exhibits a complex

Geological Map of the Thabazimbi area

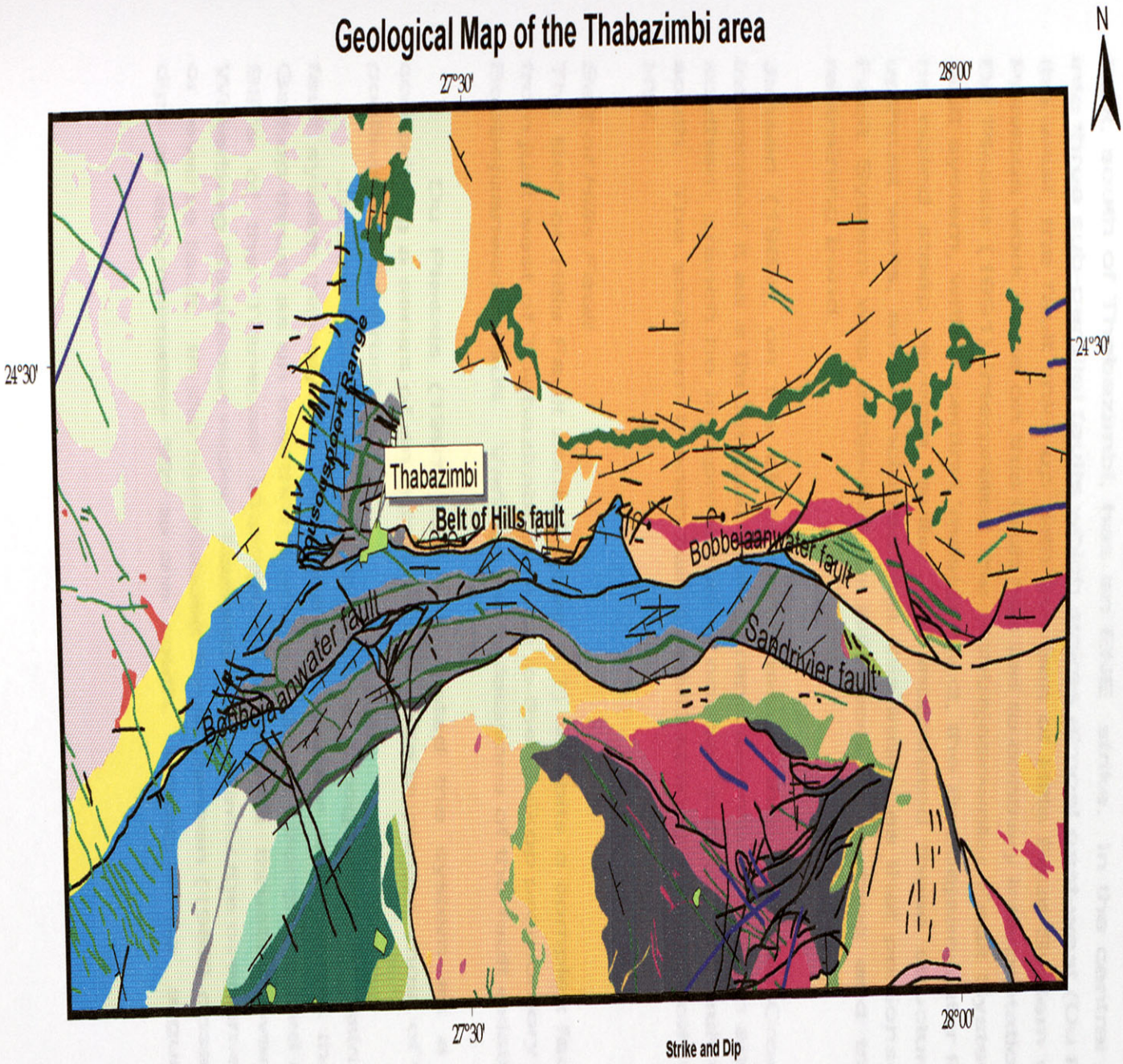

Figure 5.7

structural pattern. The fault has a approximate strike length of 120 km and can be traced from south-east of Thabazimbi until close to Loubad. The eastern portion of the fault, south of Thabazimbi, has an ENE strike. In the central portion, the fault splays into three sub-parallel faults which strikes almost east-west (Du Plessis, 1991). Towards the west, the fault links up with the Belt of Hills Fault System which strikes southeast. Previous work done on this fault has led to contrary interpretations:
Du Plessis (1991) interpreted the Bobbejaanwater Fault System as a major strike-slip fault system, with a central 'master' fault, the Bobbejaanwater Fault. Flanking the fault he noted steep reverse faults. He interpreted these structures as strike-slip duplex upthrust welts, and concluded that this indicates that portions of the Bobbejaanwater Fault System was subjected to left-lateral wrenching and transpression on a local restraining bend.

Jansen (1982), on the other hand named this fault the Crocodile Bridge Fault and interpreted it as a thrust fault which branches into a northern and southern branch. The southern branch he interpreted as a normal, sub-vertical fault with a downthrow to the south. The southern branch has two NE striking splays, both with down throws to the NW.

Belt of Hills Fault

The Belt of Hills Fault zone (Figure 5.7) exhibits a complex fault pattern and stretches from just west of Thabazimbi through to the Gatkop promontory where it merges with the Bobbejaanwater fault. Various interpretations of the fault exists:

Du Plessis (1991) has interpreted the system as a strike-slip fault system comprising a series of en echelon strike-slip duplexes, most of which are believed to be positive flower structures

Jansen (1982), on the other hand, recognized two main faults in the Belt of Hills fault system namely the Gatkop thrust and the Buffelshoek thrust. He interpreted the Gatkop thrust as an overthrust which involves strongly faulted and folded dolomite and BIF's of the Transvaal Supergroup which is thrusted over Bushveld granite and Waterberg Sequence rocks. Towards Thabazimbi the overthrust grades into an upthrust or reverse fault. In the Buffelshoek thrust Jansen (1982) observed a fault plane which dips at approximately 30° to the south. However, he argued that the presence of

slickensides not parallel with this dip direction suggests that the fault might be a reactivated tear fault.

Strauss (1954) has interpreted the area as being intensely faulted, the main components being low-angle strike faults (Gatkop thrust and Middle Range thrust) caused by overthrusting from the south. He noted that the fault plane of the Gatkop thrust dips at progressively lower angles in an eastward direction, until the Gatkop promontory, where it is practically horizontal.

Rousouspoort Range

Field work done by Du Plessis (1991) has noted shears orientated in an arrangement similar to a left-lateral strike-slip regime. Therefore he concluded that the east west striking faults must all be left-lateral strike-slip faults.

Folding

Du Plessis (1991) described a large fold in Pretoria Group sedimentary rocks in the area between the Bobbejaanwater fault and the Belt of Hills fault. This fold is however not indicated in the BOSGIS data base. The northern limb of the fold dips to the south, the fold axis plunges towards the ESE. Du Plessis (1991) interpreted the fold as a possible drag fold in response to left-lateral strike-slip faulting along the Bobbejaanwater Fault System.

5.1.4.2 Nylstroom-Warmbath's area

In this area Waterberg, Bushveld and Transvaal rocks occur in a complex arrangement, and numerous faults and folds are responsible for the current structural pattern (Figure 5.8).

Faults

Boschpoort fault

The Boschpoort fault has a northwest strike and is responsible for the contact of overturned Waterberg sediments against Rooiberg Felsites. The fault dips southward at an estimated 65°, and is interpreted as a normal fault (Pringle, 1986). The faults has a speculative age of late-Waterberg.

Geological Map of Nylstroom-Warmbath's area

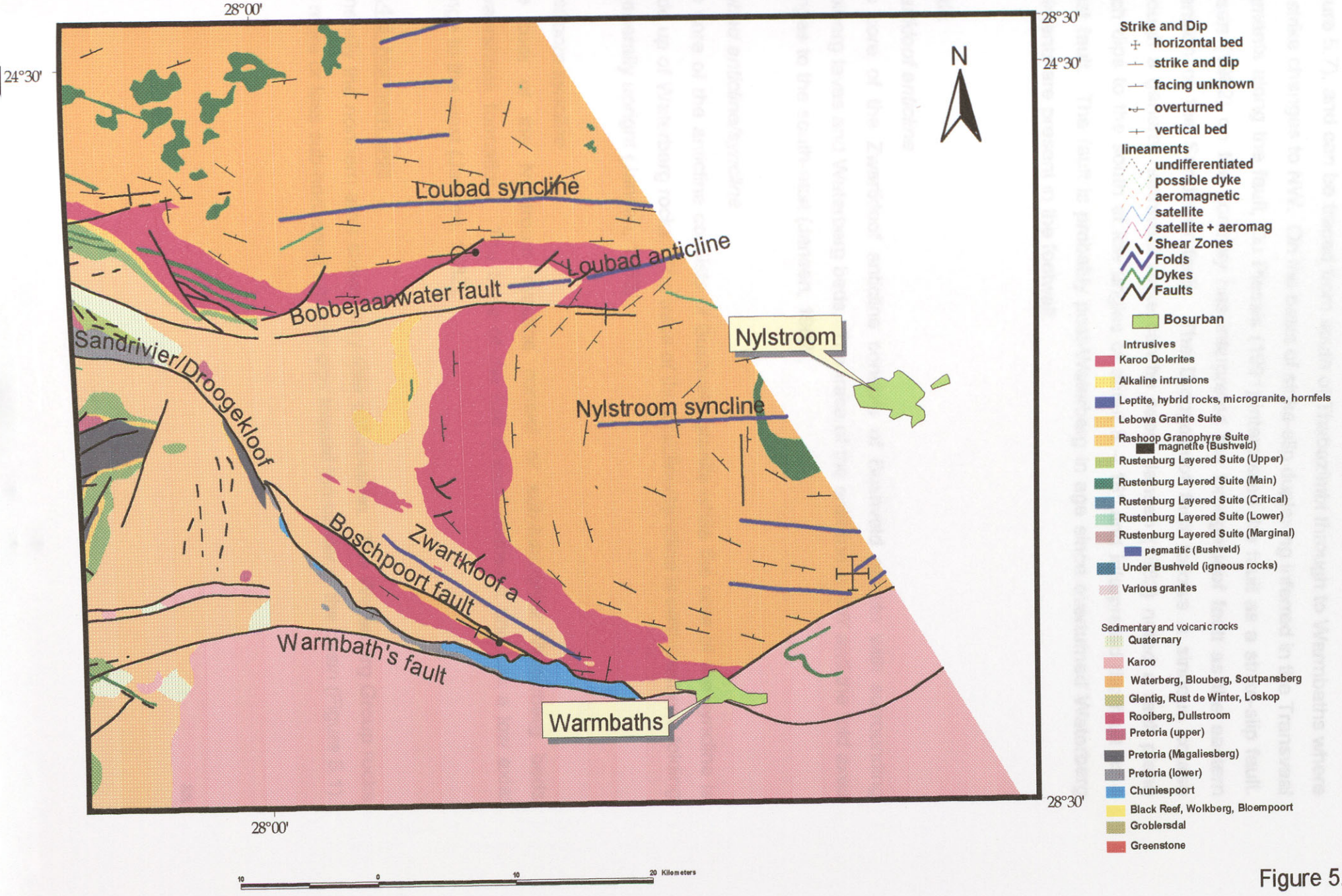

Figure 5.8

Sandrivier fault /Droogekloof thrust

The Sandrivier fault strikes parallel to the Bobbejaanwater and Belt of Hills fault systems (Figure 5.7), and can be traced from south of Thabazimbi through to Warmbaths where the strike changes to NW. On the basis of strike-slip duplexing inferred in the Transvaal fragments along the fault, Du Plessis (1991) interpreted the fault as a strike-slip fault. Jansen (1982) on the contrary has interpreted the Droogekloof fault as the eastern extension of the Sandrivier fault. The Droogekloof fault follows a sinuous course although a general northwest strike can be seen. Jansen (1982) noted a fault plane which dips to the south at low angles of about 5 – 15° and interpreted the fault as a thrust fault. The fault is probably post-Waterberg in age since overturned Waterberg sediments are present in the footwall.

Folds

Zwartkloof anticline

The core of the Zwartkloof anticline consists of Bushveld granite with surrounding Rooiberg lavas and Waterberg beds. The trace of the anticline is NW and the fold axes plunges to the south-east (Jansen, 1982).

Loubad anticline/syncline

The core of the anticline consists of Bushveld granite while the core of the syncline is made up of Waterberg rocks. The trace of the anticline/syncline is east-west and folding is generally upright (Jansen, 1982).

Nylstroom syncline

The core of the Nylstroom syncline consist of sub-horizontal Waterberg beds (Swaershoek formation). The trace of the fold is east-northeast and has a low axial plunge to the west (Jansen, 1982).

5.1.4.3 Northern area

Generally the northern area shows very little deformation. The Waterberg Group rocks are more or less sub-horizontal with low dips toward the center of the basin (Figure 5.1).

Faults

The only fault in this area is the large NW trending Vaalwater fault zone. This fault is probably a normal fault of post-Waterberg age (Jansen, 1982).

Lineaments

Numerous undifferentiated lineaments are present in this area. The lineaments have mainly NW and NNE orientations.

Sills

Extensive sills can be seen in this area which are probably related to tension during post-Waterberg times.

5.1.5 PILANESBERG STRUCTURES

The Pilanesberg Alkaline Complex intruded along the margin of the Rustenburg Layered Suite and the Granitic rocks of the Bushveld Complex (Figure 5.9). The intrusion caused local deformation of the complex in the form of radial normal faults which are prominent towards the west of the complex. The emplacement of the Pilanesberg Complex might have caused reactivation of earlier formed structures (Vermaak, 1976). These structures are represented by the two faulting directions, the ENE Vlakfontein trend, and the NW Gevonden trend (Vermaak, 1976). Van Zyl (pers. comm.) noted dome and basin structures in the Transvaal and lower Bushveld rocks on the western side of the Pilanesberg Complex. He propose this deformation to be post-Bushveld but pre-Pilanesberg in age as a response to the formation of a periclinal type basin. The complex fault pattern around the Complex is therefore due to this basining. The faults were then later reactivated during the intrusion of the Pilanesberg Complex.

Syenite dykes are a characteristic feature associated with the Pilanesberg Complex. NW trending syenite dykes cut across the Bushveld Complex.

Geological Map of Pilanesberg area

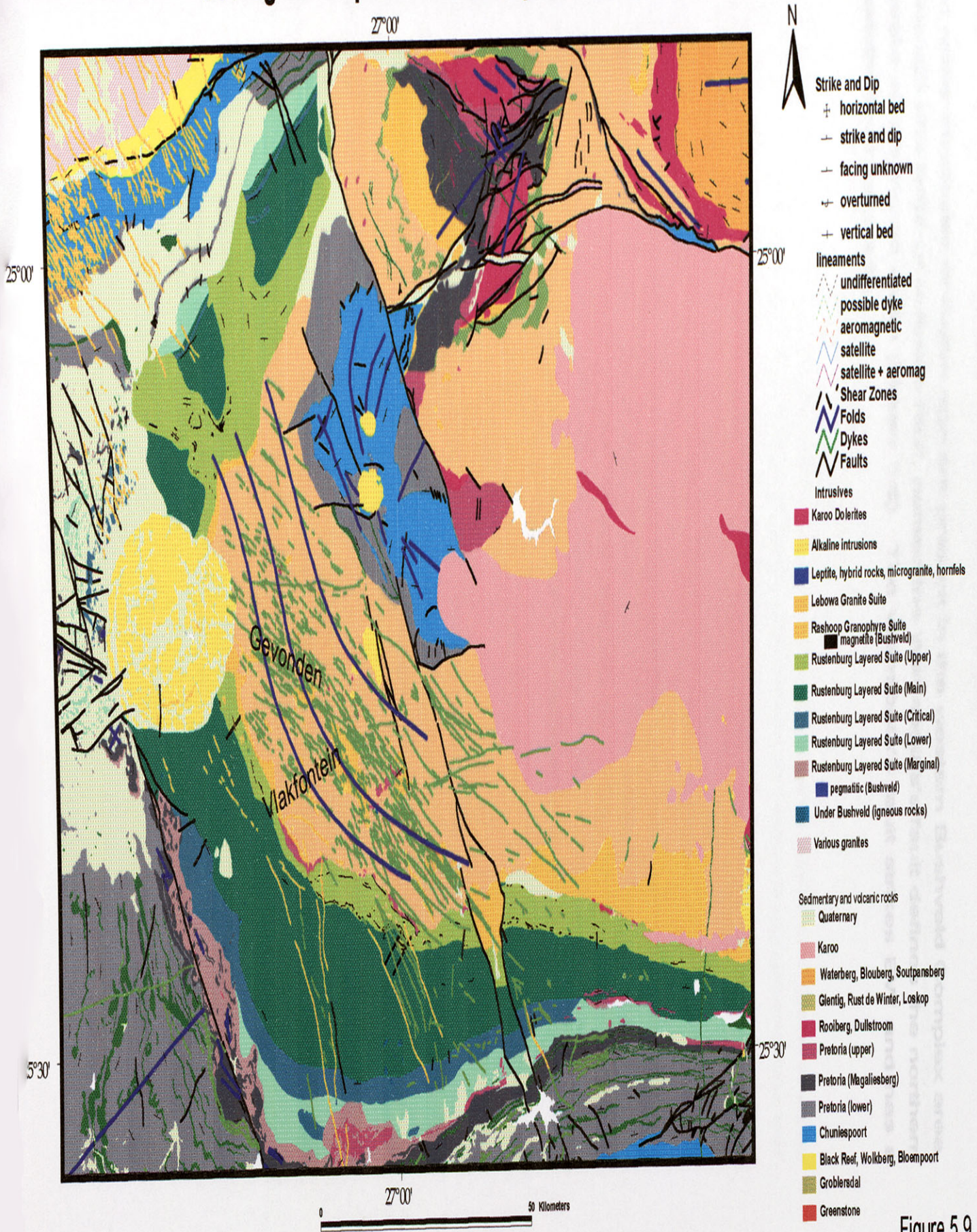

Figure 5.9

5.1.6 KAROO STRUCTURES

Not many structures of Karoo age are present in the western Bushveld Complex area. Although one large post-Karoo fault, named the Warmbaths's fault defines the northern margin of the Karoo basin (Figure 5.8). The Warmbath's fault strikes EW and has a downthrow to the south.

5.2 THE NORTHERN BUSHVELD COMPLEX

A geological map including all the various structures of the northern Bushveld Complex area is shown in Figure 5.10.

5.2.1 ARCHAEAN STRUCTURES

Archaean structures in this area include the Southern Marginal Zone and Central Zone of the Limpopo Belt. Even though just a small portion of the Pietersburg greenstone belt occurs in this area its structures will be discussed as part of the northern Bushveld Complex.

5.2.1.1 Limpopo Belt

Part of the Central and Southern Marginal Zone of the Limpopo Belt is contained within the Northern Bushveld Complex area (Figure 5.11). The Central Zone is characterized by granulite-grade gneiss of the Beitbridge Complex (S.A.C.S., 1980) as well as pelite, quartzite and carbonates (McCourt and Vearncombe, 1992). In contrast, the Southern Zone consists of granite and greenstone material metamorphosed at granulite facies (van Reenen et al., 1992).

Central Zone

Isotopic signatures, lithology and structural characteristics have shown that the Central Zone formed independent of the Limpopo Belt (McCourt and Vearncombe, 1992). The Zone was later thrusted into the heart of the orogen by SW directed thrusting as an allochthonous thrust sheet during peak collision of the two cratons (Van Reenen et al., 1988; McCourt and Vearncombe, 1987: 1992; McCourt and Wilson, 1992; Treloar et al., 1992). The Central Zone has been deformed by several deformational events. Many authors (Barton et al., 1979; Fripp et al., 1980; Fripp, 1981; Watkeys, 1984) have done extensive research on the Central Zone. Tankard et al. (1982) summarizes four main deformational periods, all older than 2.5 Ga:

- An early D_1 deformational event younger than 3.2 Ga (pre-Messina Intrusive) which was responsible for isoclinal recumbent folding and flat-lying ductile shearing.

Geological map of the northern Bushveld Complex

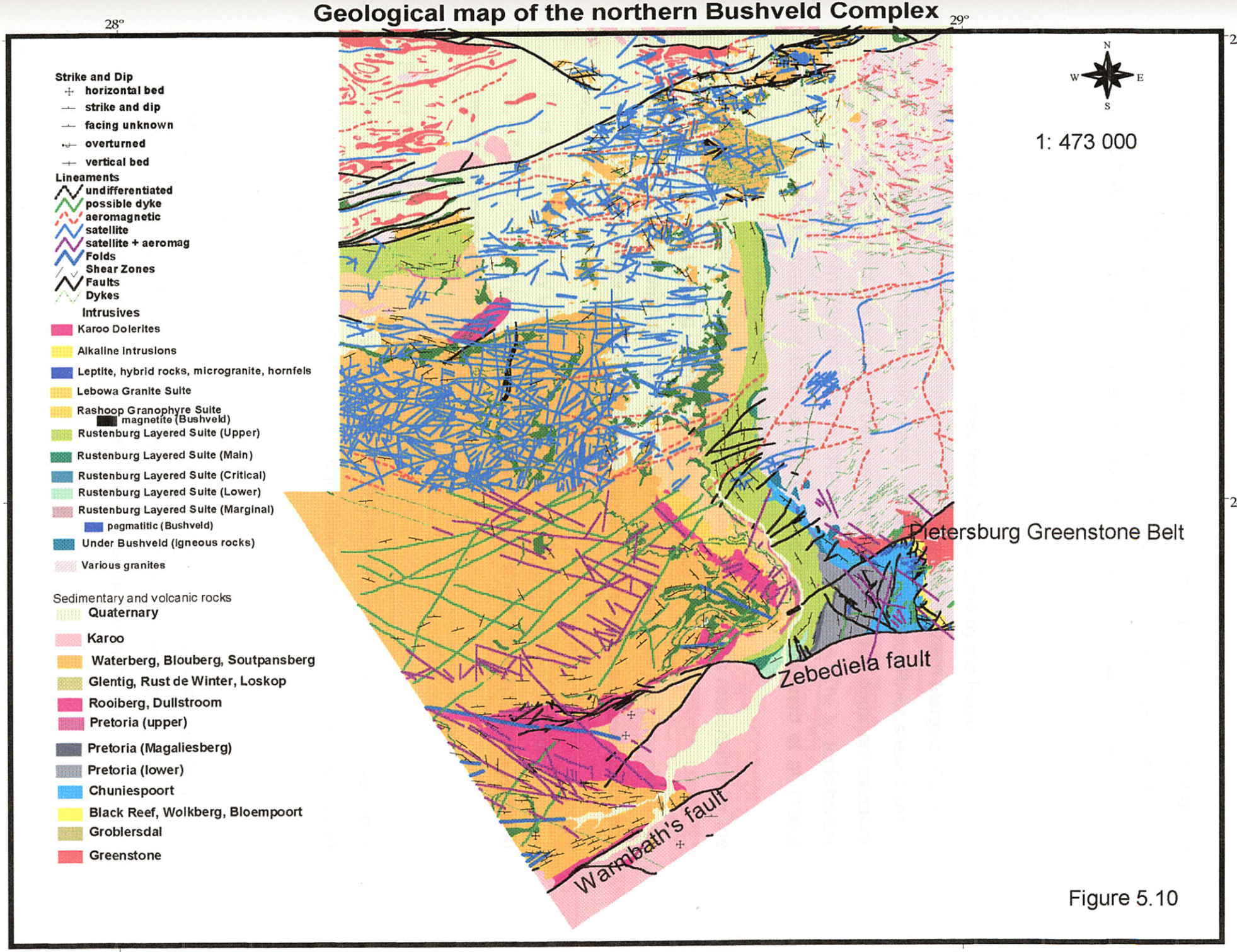

Figure 5.10

- A D_2 period of intense crustal shortening just after 2.7 Ga. This event is characterized by tight, isoclinal upright folds with NE axial trends and intense ductile shearing.
- A final D_3 and D_4 event which was responsible for the present outcrop pattern of interference folding between D_3 and D_4 folds. NE trending F_3 folds were refolded around NW trending F_4 axial surfaces. This resulted in a periclinal interference set of folds.

The Southern Marginal Zone

The Southern Marginal Zone is separated from Central Zone by the Palala shear zone, while the boundary between the Kaapvaal Craton and the Southern Marginal Zone is a gradational transition of metamorphic grade. However, the Hout River shear zone is generally taken to depict the boundary between the two zones. The dominant structural direction of the Southern Marginal Zone is ENE-trending structures. The tectonic history of the Zone can be bracketed between 2.6 Ga and 2.5, and Tankard et al. (1982) summarizes four main deformational events:

- D_1 is characterized by early regional NS shortening. This was responsible for the formation of ENE trending upright horizontal synclines
- During D_2 at approximately 2.58 Ga continuing NS compression (slightly oblique to D_1) produced the regional fabric of upright transecting cleavage and steeply plunging folds.
- D_3 is characterized by upright folding and periclinal interference structures.
- D_4 followed during which large south dipping ductile shear zones marked by sinistral movement formed.

Shear zones

Studies done by McCourt and Vearncombe (1992) have found that crustal shortening in the Limpopo Belt was accommodated by large-scale ductile shear zones which trend approximately ENE-WSW.

Palala Shear Zone

The Palala shear zone represents one of these zones of crustal compression and is proposed to be a crustal scale lateral ramp (McCourt and Vearncombe, 1992). The shear zone is approximately 10-km wide and forms the northern boundary of the

Geological map of the southern portion of the Limpopo Belt

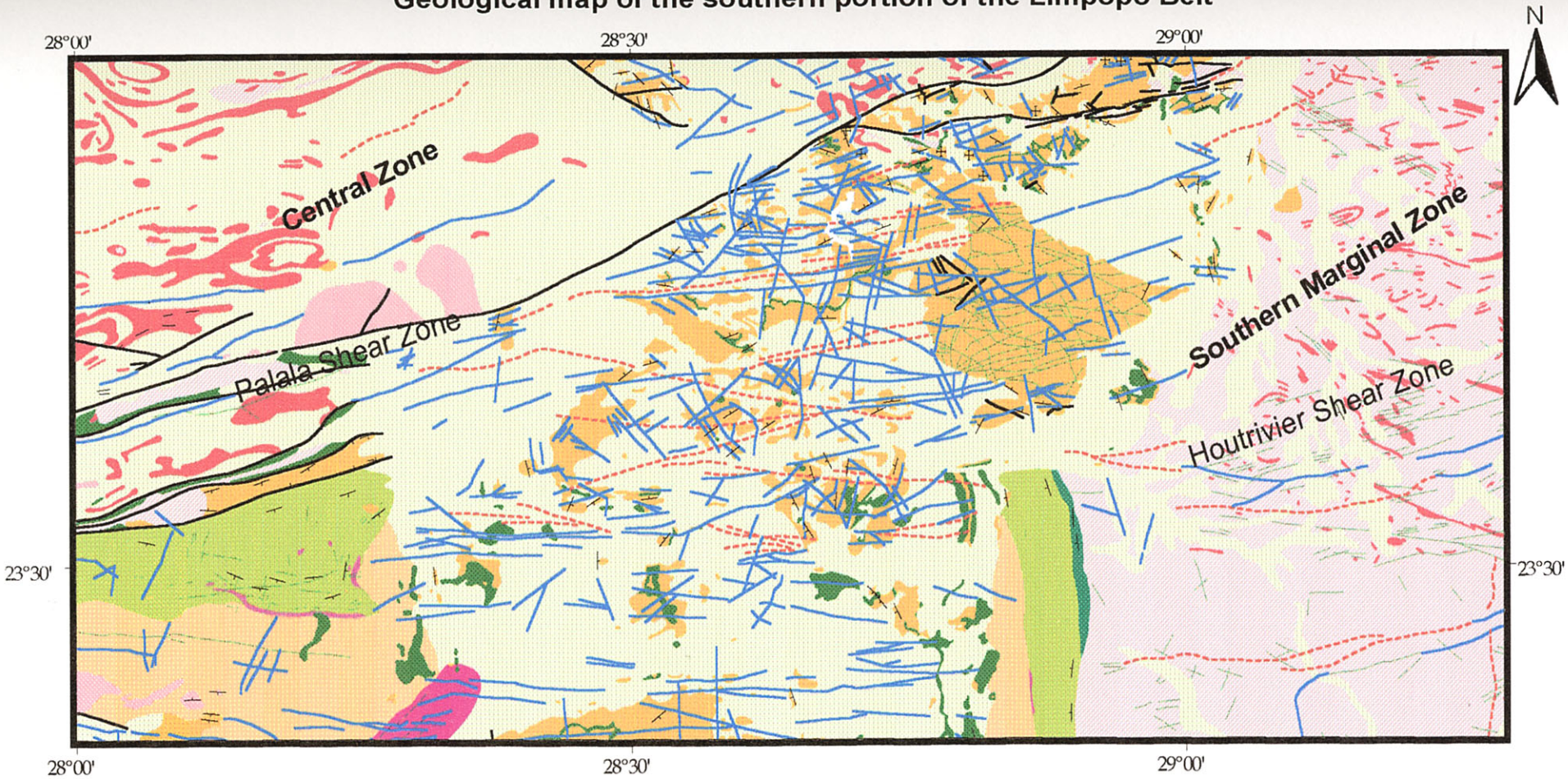

Figure 5.11

Southern Marginal Zone. N-ward dipping mylonitized rocks of Archaean gneiss, Transvaal, and Bushveld Complex rocks depict this zone of intense deformation. The Palala shear zone is believed to have been constantly reactivated, the oldest deformation marking the collision of the Central Zone of the Limpopo belt and the Southern Marginal Zone. This ductile deformation event was responsible for strong left-lateral shearing which pre-dates the intrusion of the Bushveld Complex. In addition, tight, south verging, ENE trending faults are present in this zone. McCourt and Vearncombe (1992) also recorded changes in mineral elongation lineation along the southern margin of the zone which implies an overall thrust geometry. The age of the last ductile deformational event in this zone is believed to have ceased at 2042 Ma (Brandl and Reimold, 1990). Later deformation along the shear zone is observed along the Melinda and Abbotspoort faults. These faults, however will be discussed under Karoo structures.

Hout River shear zone

The Hout River shear zone is generally taken to form the boundary of the Southern Marginal Zone and the Kaapvaal Craton, marking the transition of granulite facies rocks to low-grade granite greenstone rocks (Smit et al., 1992). The shear zone system dips steeply to the north, and C-S kinematic indicators imply SW-directed thrusting at around 2.67 Ga (McCourt and Vearncombe, 1992). McCourt and Vearncombe (1992) further described the shear zone as an anastomising network which defines a series of 10 km scale structural domains characterized by steeply NE-plunging folds, probably sheath-folds. Estimates of the displacement along the shear zone is unknown but McCourt and Vearncombe (1992) suggested a vertical displacement in the order of at least 10 - 15km.

Dykes

Numerous small dykes occur in the granite-gneiss terrain. Although various orientations of dykes are present, a vague NE trend can be seen (Figure 5.11).

Lineaments

Various large aeromagnetic and satellite lineaments transect the granite-gneiss terrain in the northern Bushveld Complex area. These lineaments have various orientations although a ENE trend, resembling the Limpopo Belt trend, can be distinguished. It is

interesting to note that these satellite and aeromagnetic lineaments occur at the boundary between the Southern Marginal Zone and the Kaapvaal Craton (Figure 5.11).

5.2.1.2 Pietersburg Greenstone belt

The Pietersburg Greenstone belt has an approximate NE trend and is dominated by northwest verging thrust tectonics (de Wit, 1991) (Figure 5.11). De Wit (1991) ascribes a maximum age of 2.88 Ga to the deformation and relates it to terrane accretion along the northern margin of the Mid-Archaean core of the Kaapvaal Craton. Grobler (1972) recognized three periods of deformation. The first deformation precedes the deposition of the Uitkyk Formation (upper sequence of the Pietersburg Greenstone Belt). The second period is characterized by isoclinal overfolding to the NW during which pronounced slaty cleavage and schistosity developed. The last deformational event was the crenulation of existing foliation. However, Visser (1998) mentions only two main deformational events. A D_1 event during which open EW trending anticlines and synclines formed, and a later D_2 event during which these folds were tightened.

5.2.2 TRANSVAAL STRUCTURES

The Transvaal rocks in the northern Bushveld Complex area strike NS to NW and dip west to southwest, and have been deformed along the TML (Figure 5.13).

Faults

NE, NW and NS orientated faults are prominent in Transvaal rocks and these faults were active at various times (Potgieter, 1992).

NE trending faults – Ysterberg fault

The Ysterberg fault trends NE and cuts obliquely through Bushveld rocks, Transvaal strata, the Pietersburg Greenstone belt and Archaean gneiss (Figure 5.13). The fault displays about an 8 km left-lateral displacement. The earliest movement along this fault is believed to be pre-Transvaal, possibly lateral movement (De Wit and Roering, 1990). Grobler (1972) proposed the fault to be a wrench fault which was genetically associated with the Pietersburg greenstone belt, but reactivated during Bushveld times, or an oblique-slip fault associated with the formation of the Bushveld Complex.

Geological Map of the Pietersburg Greenstone Belt

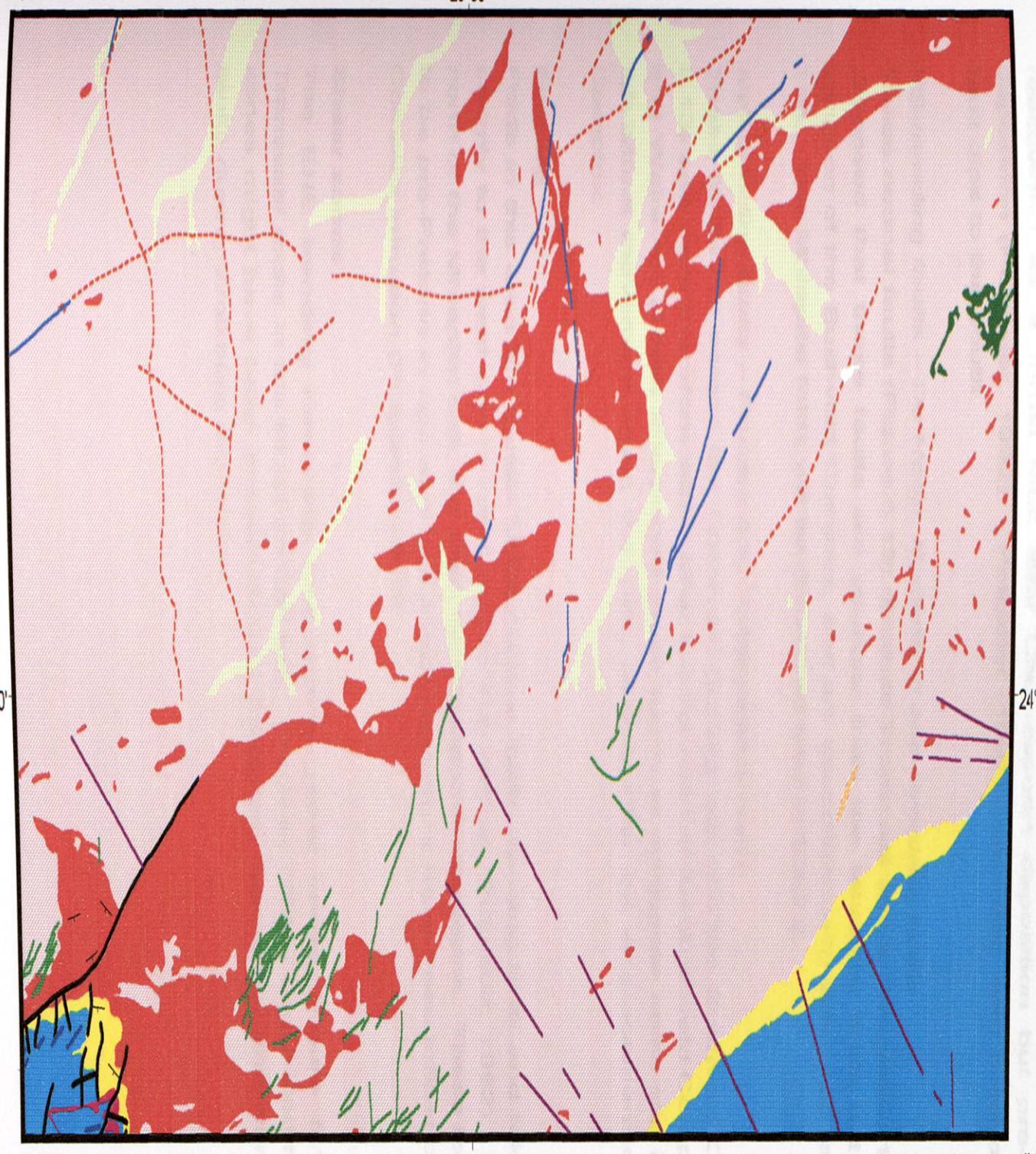

Strike and Dip
- horizontal bed
- strike and dip
- facing unknown
- overturned
- vertical bed

Lineaments
- undifferentiated
- possible dyke
- aeromagnetic
- satellite
- satellite + aeromag
- Folds
- Shear Zones
- Faults
- Dykes

Intrusives
- Karoo Dolerites
- Alkaline intrusions
- Leptite, hybrid rocks, microgranite, hornfels
- Lebowa Granite Suite
- Rashoop Granophyre Suite
  - magnetite (Bushveld)
- Rustenburg Layered Suite (Upper)
- Rustenburg Layered Suite (Main)
- Rustenburg Layered Suite (Critical)
- Rustenburg Layered Suite (Lower)
- Rustenburg Layered Suite (Marginal)
  - pegmatitic (Bushveld)
- Under Bushveld (igneous rocks)
- Various granites

Sedimentary and volcanic rocks
- Quaternary
- Karoo
- Waterberg, Blouberg, Soutpansberg
- Glentig, Rust de Winter, Loskop
- Rooiberg, Dullstroom
- Pretoria (upper)
- Pretoria (Magaliesberg)
- Pretoria (lower)
- Chuniespoort
- Black Reef, Wolkberg, Bloempoort
- Groblersdal
- Greenstone

Figure 5.12

Potgieter (1992) noted post-Wolkberg Group reactivation as a growth fault, as indicated by stratigraphic thickness differences across the fault. The fault was then again reactivated as a thrust fault after Chuniespoort deposition but pre-Pretoria Group deposition (Potgieter, 1992). Potgieter (1992) concluded from borehole data that the fault dips to the south.

NS-trending faults – De Hoop, Nederland and Grootvlei faults

These normal faults (Figure 5.13) displace Transvaal strata (Potgieter, 1992). Potgieter proposed that these faults are younger than the Mhlapitsi folds but older than the intrusion of the Bushveld Complex, and are associated with strike-slip faulting along the TML. The Mhlapitsi folds will be discussed later in 5.3.2.2.

NW-trending faults – Pruizen and Potgietersrus faults

These faults cut across the Transvaal Supergroup and the Bushveld Complex (Figure 5.13) and were therefore active after the intrusion of the Bushveld Complex. Du Plessis and Walraven (1990) interpreted these faults as conjugate strike-slip faults related to left-lateral movement along the TML, directly after the emplacement of the Bushveld Complex.

Folding

Folds in this area are typical Mhlapitsi-type folds, trending ENE and fold axes plunging steeply to the west and in some places sub-vertical (Potgieter, 1992). However, to the north of the Mhlapitsi belt, the folds have random orientations. These folds are believed to be pre-Pretoria in age and fold axes orientations have been influenced by Bushveld Complex intrusion (Potgieter, 1992).

Shear zones

The ENE trending Eersteling and Spanje shear zones (Figure 5.13) deform the Transvaal rocks in the Mhlapitsi fold belt. Potgieter (1992) suggested that these shear zones might have been present before Transvaal deposition, and were active growth faults during Wolkberg deposition.

Geological Map of Transvaal rocks in the northern Bushveld Complex area

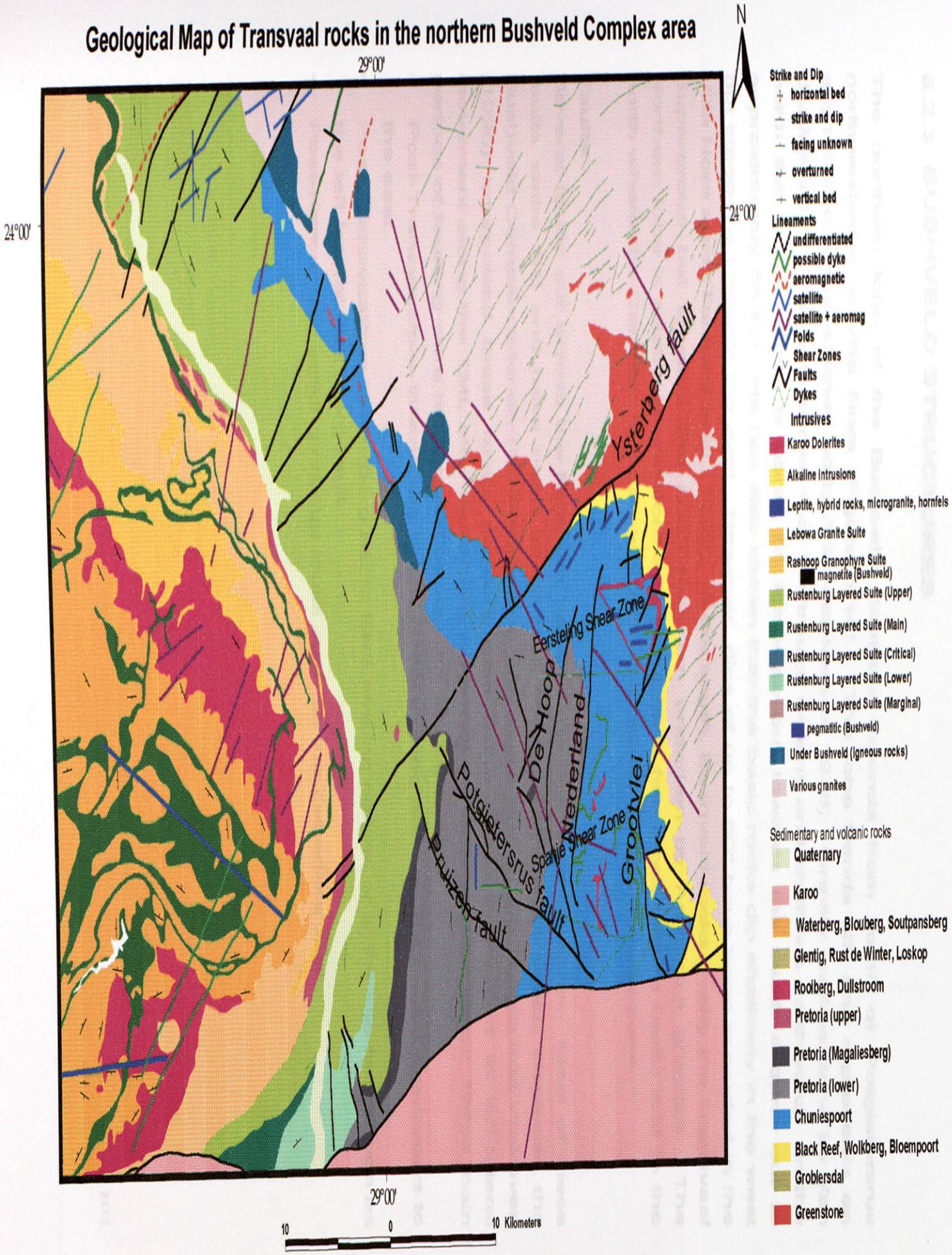

Figure 5.13

5.2.3 BUSHVELD STRUCTURES

The northern lobe of the Bushveld Complex extends from south of Potgietersrus northwestward to Villa Nora (Figure 5.14). The lobe trends NS and represents an asymmetric trough-shaped body (Van der Merwe, 1976). Gravity profiles done by Van der Merwe (1976) have shown that the trough widens and shallows northward. In the north the cross-section is about 85 km wide but towards the south it thins out to approximately 35 km. He has also shown that the basic rocks dip shallowly in the west but steepens towards the east. However, dips of up to 60° have been recorded in the Villa Nora area (Tankard et al., 1982). In the south, Bushveld rocks overly the Transvaal Supergroup but towards the north they are underlain by Archaean granites. The Northern lobe is relatively undeformed except for a few cross-cutting faults and to the north where the Complex is deformed by the NE trending Palala shear zone.

Faults

Several faults cut across the Northern Lobe of the Bushveld Complex. Most of these faults strike NE and have been interpreted as strike-slip faults which displaces the Bushveld Complex laterally (Du Plessis and Walraven, 1990). Du Plessis and Walraven (1990) interpreted these faults as conjugate strike-slip faults related to left-lateral movement along the TML after the emplacement of the Bushveld Complex. Three main periods of faulting were recognized by van der Merwe (1976).

- Post-Transvaal/pre-Waterberg N and NNW striking normal faults with downthrows to the east.
- Post-Transvaal/pre-Waterberg NE to ENE striking normal or strike-slip faults such as the left-lateral Ysterberg fault.
- Post-Karoo, NW striking normal faults such as the Zebediela fault.

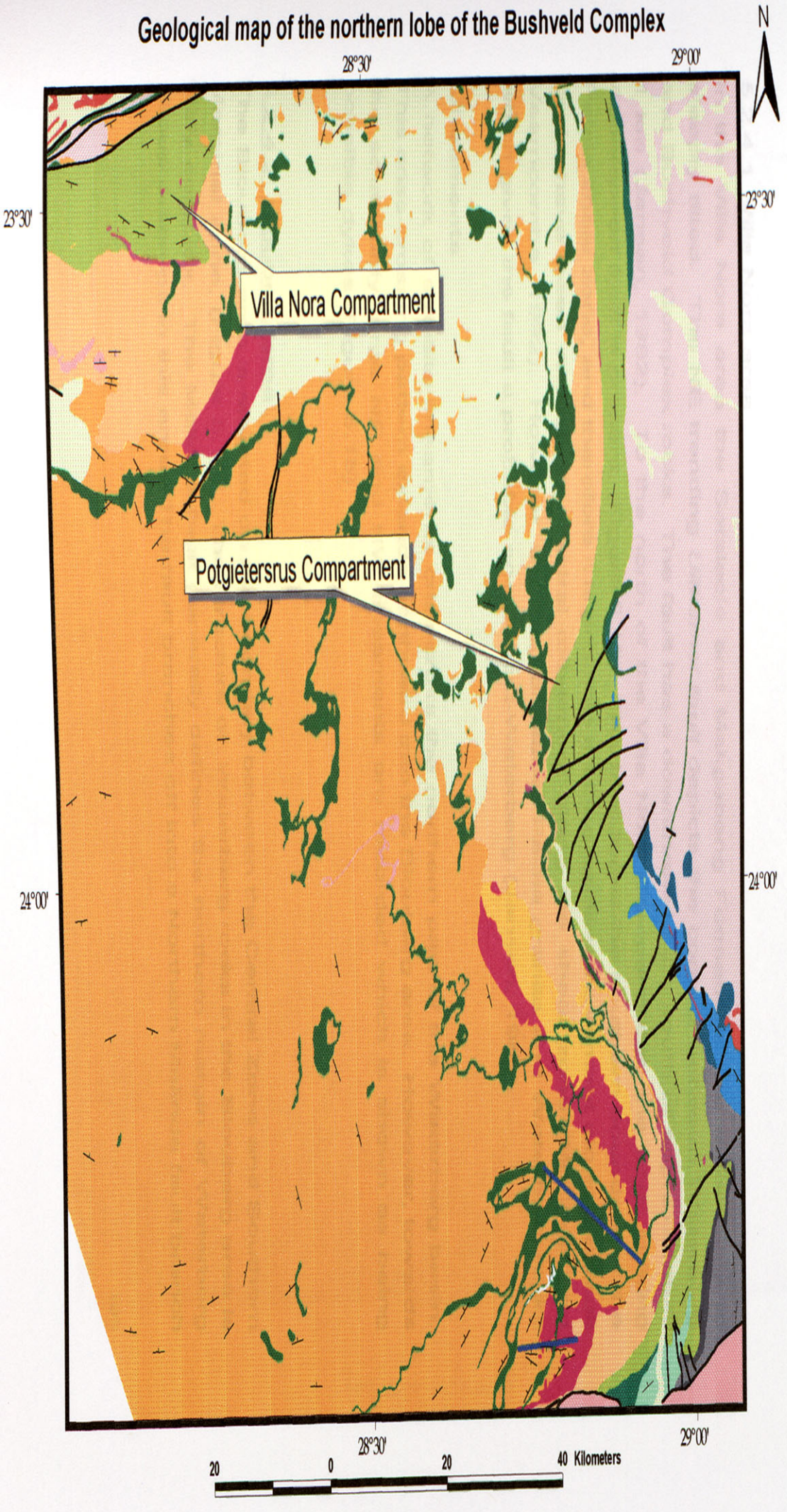

Figure 5.14

5.2.4 WATERBERG STRUCTURES

The structures described in this section deform both Waterberg, Blouberg and Soutpansberg group rocks. However, as mentioned previously, the various groups are collectively referred to as Waterberg Group rocks. In general the Waterberg rocks in this area are relatively undeformed with dips averaging 5°. However, areas such as in the vicinity of Villa Nora, Blouberg and the Swaershoek mountains (Figure 5.15), have experienced mild to intense deformation.

5.2.4.1 Villa Nora area

In the Villa Nora area the Setalaole and Makgabeng Formations are moderately to steeply tilted. The NE trending *Uitkomst fault* depicts the contact between Waterberg and Bushveld Complex rocks. The fault has a downthrow to the south of approximately 1 km (Jansen, 1982). To the north of the Villa Nora Compartment, the ENE striking *Abbotspoort fault* is present, (Figure 5.15). This fault forms the southern boundary of the Palala shear zone, and therefore it is possible that the earliest movement along this fault could have been related to sinistral movement along the shear zone (McCourt and Vearncombe, 1992). However, the fault displaces Palala granite and Waterberg rocks which gives the fault a probable age of post-Waterberg (Jansen, 1982).

Lineaments

A network of satellite lineaments criss-cross the northern part of the Waterberg basin. This criss-crossing pattern extends northward into the Blouberg area. However, towards the south only large NE and NW lineaments are recorded which is shown as being possible dykes (Figure 5.15).

5.2.4.2 Blouberg area

The Blouberg area is situated on the boundary between the Central Zone and Southern Marginal Zone, (Figure 5.15). The structure of Waterberg rocks in the Blouberg area is fairly complex. The Melinda fault generally defines the northern margin of Waterberg Group outcrops in this area. The fault branches off into a Northern Melinda fault branch

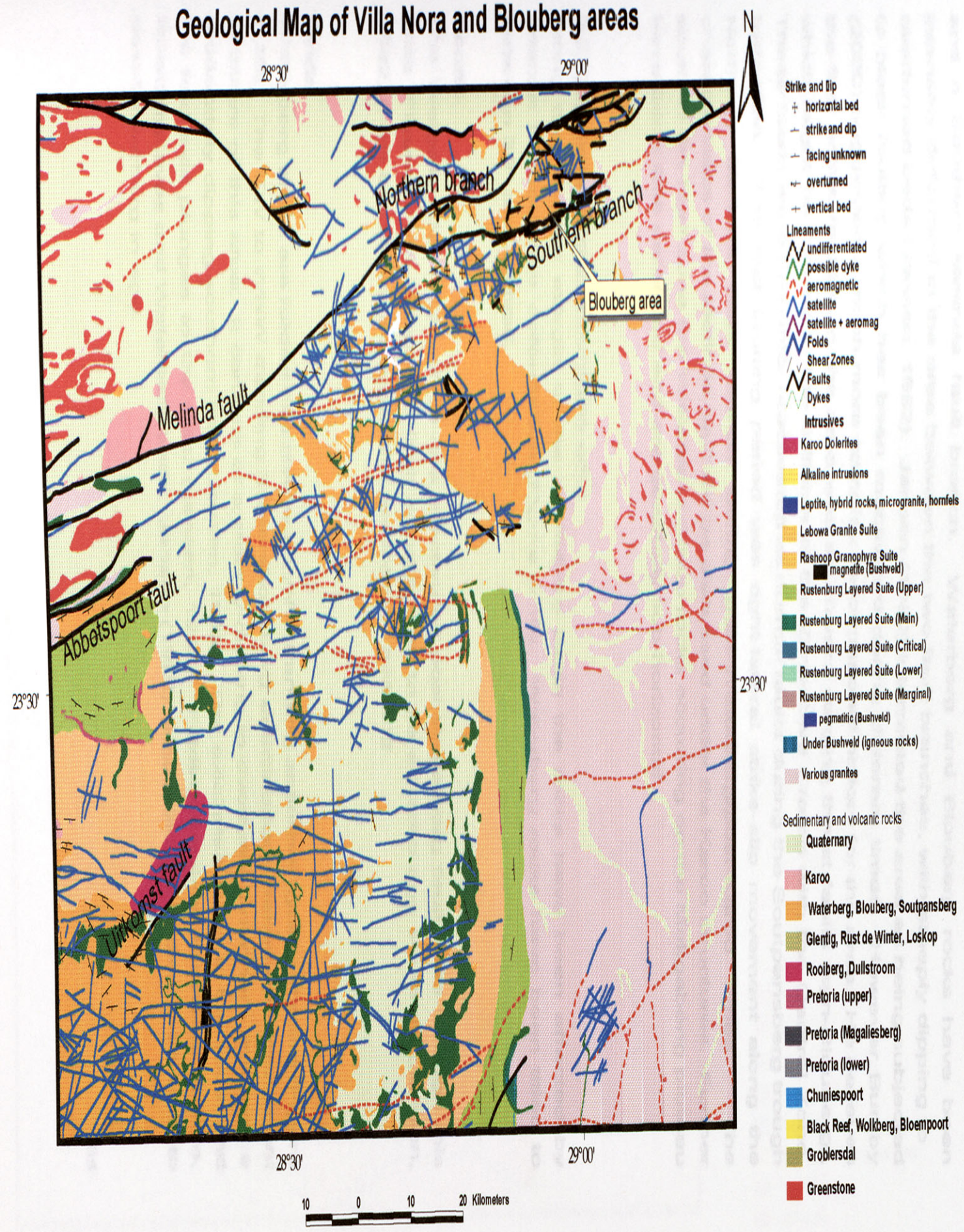

Figure 5.15

and a Southern Melinda fault branch. Waterberg and Blouberg rocks have been intensely deformed in the area between the two fault branches, with steeply dipping to overturned beds (Jansen, 1982). Jansen (1982) interpreted the area as being subjected to block faulting which has been reactivated during different times. However Bumby (2000) suggested a much more complex deformational history for the area. He believes the first active faulting in the area was southward verging thrust faults (syn-Blouberg), which might be related to the collision of the Zimbabwe Craton with the Central Zone. These faults were then later reactivated as normal faults during the Soutpansberg trough formation. The last faulting period was right-lateral strike-slip movement along the Northern Melinda fault branch during post-Waterberg/post-Karoo times. The characteristics of the Melinda fault will be discussed under the Karoo structures. Further south of the fault zone the Waterberg Group rocks occurring on the Makgabeng plateau have been little deformed and are generally sub-horizontal.

5.2.4.3 Swaershoek mountains area

Along the eastern margin of the Waterberg basin the rocks have been affected by intense to moderate deformation (Figure 5.16). Waterberg rocks have been titled to between 30° and vertical.

Faults

The Welgevonden fault, which is a reactivated post-Waterberg fault, cuts through this area (Figure 5.16). Since the fault is suggested to be a Karoo age structure (Jansen, 1982) it will be discussed under the appropriate heading.

Folds

Waterberg strata are folded into NW and WNW trending anticlinal-synclinal pairs (Figure 5.16). The EW to WNW trending Swaershoekberg anticlinorium makes up a prominent structure of this area. It consists of a steeply-dipping to overturned northern limb and a moderately dipping southern limb (Jansen, 1982). The axial plane dips to the south and the fold axis plunges to the west (Jansen, 1982). Folding involves Bushveld granite, Rooiberg lavas and Waterberg beds. Jansen (1982) suggested the folding to be early to post-Waterberg in age.

Geological map of the Swaershoek area

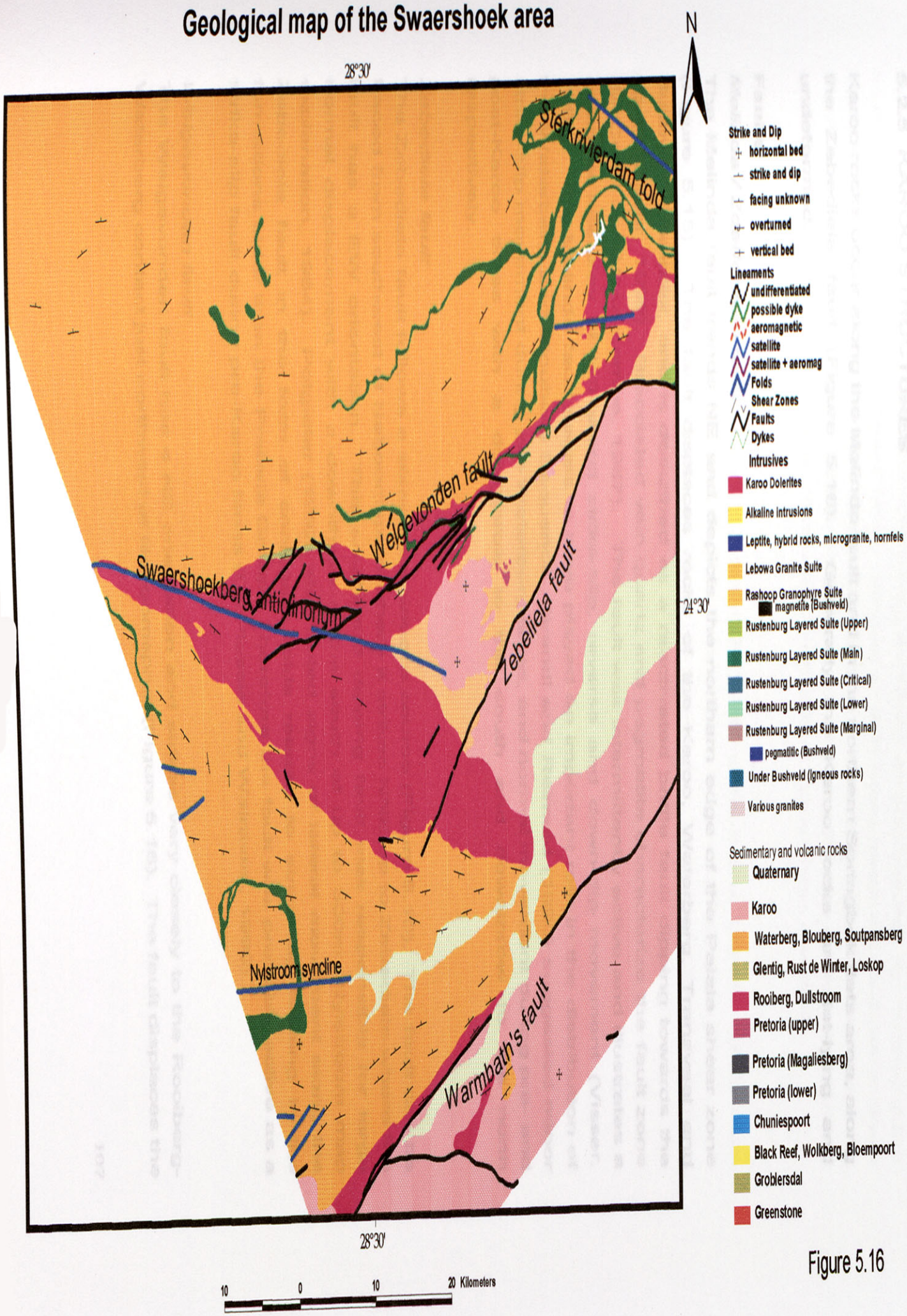

Figure 5.16

5.2.5 KAROO STRUCTURES

Karoo rocks occur along the Melinda fault and in the northern Springbok flats area, along the Zebediela fault (Figure 5.16). Generally the Karoo rocks are flat-lying and undeformed.

Faults

Melinda / Zoetfontein fault

The Melinda fault trends NE and depicts the northern edge of the Palala shear zone (Figure 5.15). The fault displaces rocks of the Karoo, Waterberg, Transvaal and Bushveld Complex, and is described as a reactivated brittle fault dipping towards the north (Visser, 1998). Brecciated vein quartz and pegmatite characterize the fault zone (McCourt and Vearncombe, 1987). The fault was intermittently active and illustrates a complex interplay of left-lateral strike-slip, reverse and down-dip movement (Visser, 1998). The Melinda fault seems to have played an important role in the distribution of the Waterberg and Blouberg Sequence. Brandl and Reimold (1990) suggested minor strike-slip movement during pre-Waterberg times, and normal movement during pre- and post-Karoo times with a downthrow to the south and downthrow to the north respectively.

Zebediela fault

The Zebediela fault follows a somewhat sinuous course (Figure 5.10). The fault can be traced from southwest of Naboomspruit where it strikes NNE up to Zebediela where the fault has a EW orientation. This southward dipping fault was responsible for large normal displacement with a downthrow to the south of up to 300m (Nylstroom map explanation, 1984). Potgieter (1992) also noted signs of lateral movement along the Zebediela fault in the form of conjugate folds related to strike-slip faulting in the formations older than the Pretoria Group. Therefore the fault was probably active as a strike-slip fault during pre-Karoo times (Du Plessis and Walraven, 1990).

Welgevonden fault

The Welgevonden fault has a NE orientation and strikes very closely to the Rooiberg-Waterberg contact just northwest of Naboomspruit (Figure 5.16). The fault displaces the

Bushveld Complex, Waterberg Sequence and Karoo rocks. To the west the fault extends into the core of the Swaershoekberg anticlinorium and towards the northeast the fault merges with the Zebediela fault. Jansen (1982) interpreted the fault as a steep reverse fault which dips north. However, towards the north he noted a breccia zone dipping at 80° S. He explains this abnormal behaviour of the fault as being a reactivated post-Waterberg thrust fault, with movement on the fault plane being reversed.

Warmbaths fault

The Warmbaths fault is a large generally EW striking fault and can be traced from Warmbaths, through the Springbok flats, up to the Stavoren fragment. The fault probably has a downthrow to the south and is responsible for the contact of Transvaal rocks with Karoo rocks (Figure 5.10).

5.3 THE EASTERN BUSHVELD COMPLEX

A geological map including all the various structures of the eastern Bushveld Complex area is shown in (Figure 5.17).

5.3.1 ARCHAEAN STRUCTURES

Archaean structures are generally confined to the Barberton, Murchison and Pietersburg Greenstone belts. However, the structure of the Pietersburg belt has already been discussed as part of the northern Bushveld Complex area.

5.3.1.1 Murchison Greenstone belt

The Murchison Greenstone belt trends east-northeast and makes up the eastern most component of the TML (Figure 5.18). Visser (1998) summarizes three deformational events in the belt:

- D1 is characterized by upright, tight to isoclinal folds with steep ENE-plunging axes.
- During a later D2 event these folds were refolded about E-trending axes.
- Finally during D3 local kink bands and crenulation cleavages developed.

Shear zones

The *Letaba shear zone* strikes NE and separates the northern and southern part of the belt. The shear zone has been interpreted by Fripp et al. (1980) to exhibit dextral movement, but Vearncombe (1988, 1991) suggests sinistral movement. Late vertical movement along the shear zone has also been mentioned by Visser (1990).

The *Constantia shear zone*, just to the north, trends parallel to the Letaba shear zone and exhibits dextral sense of movement (Brandl, 1987).

The economically important *Antimony line* is also considered to be a ductile shear zone with a north-over-south sense of movement related to D1 (Visser, 1990). Vearncombe (1988) noted nappe-like structures in the hangingwall, and attributed it to SW-directed oblique (reverse-sinistral) shear movement.

5.3.1.2 The Barberton Greenstone belt

Only a portion of the Barberton Greenstone belt is exposed in the eastern Bushveld Complex area. However the Barberton belt forms an integral part of the tectonic

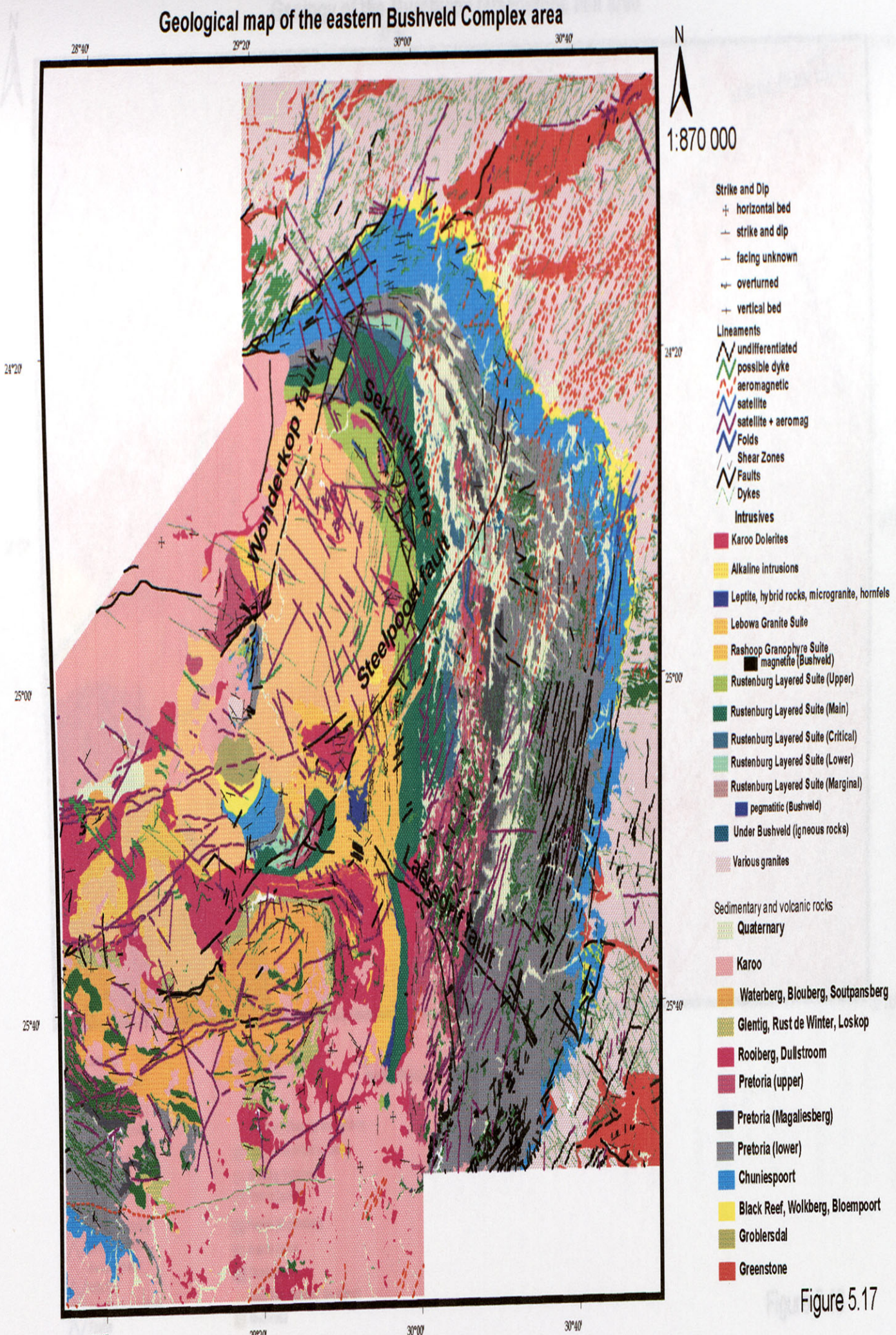
Geological map of the eastern Bushveld Complex area
28°40'
29°20'
30°00'
30°40'
24°20'
25°00'
25°40'
N
1:870 000
Wonderkop fault
Sekhukhune
Steelpoort fault
Lebowa fault
Strike and Dip
horizontal bed
strike and dip
facing unknown
overturned
vertical bed
Lineaments
undifferentiated
possible dyke
aeromagnetic
satellite
satellite + aeromag
Folds
Shear Zones
Faults
Dykes
Intrusives
Karoo Dolerites
Alkaline intrusions
Leptite, hybrid rocks, microgranite, hornfels
Lebowa Granite Suite
Rashoop Granophyre Suite
magnetite (Bushveld)
Rustenburg Layered Suite (Upper)
Rustenburg Layered Suite (Main)
Rustenburg Layered Suite (Critical)
Rustenburg Layered Suite (Lower)
Rustenburg Layered Suite (Marginal)
pegmatitic (Bushveld)
Under Bushveld (igneous rocks)
Various granites
Sedimentary and volcanic rocks
Quaternary
Karoo
Waterberg, Blouberg, Soutpansberg
Glentig, Rust de Winter, Loskop
Rooiberg, Dullstroom
Pretoria (upper)
Pretoria (Magaliesberg)
Pretoria (lower)
Chuniespoort
Black Reef, Wolkberg, Bloempoort
Groblersdal
Greenstone

Figure 5.17

Geology of the Murchison Greenstone belt area

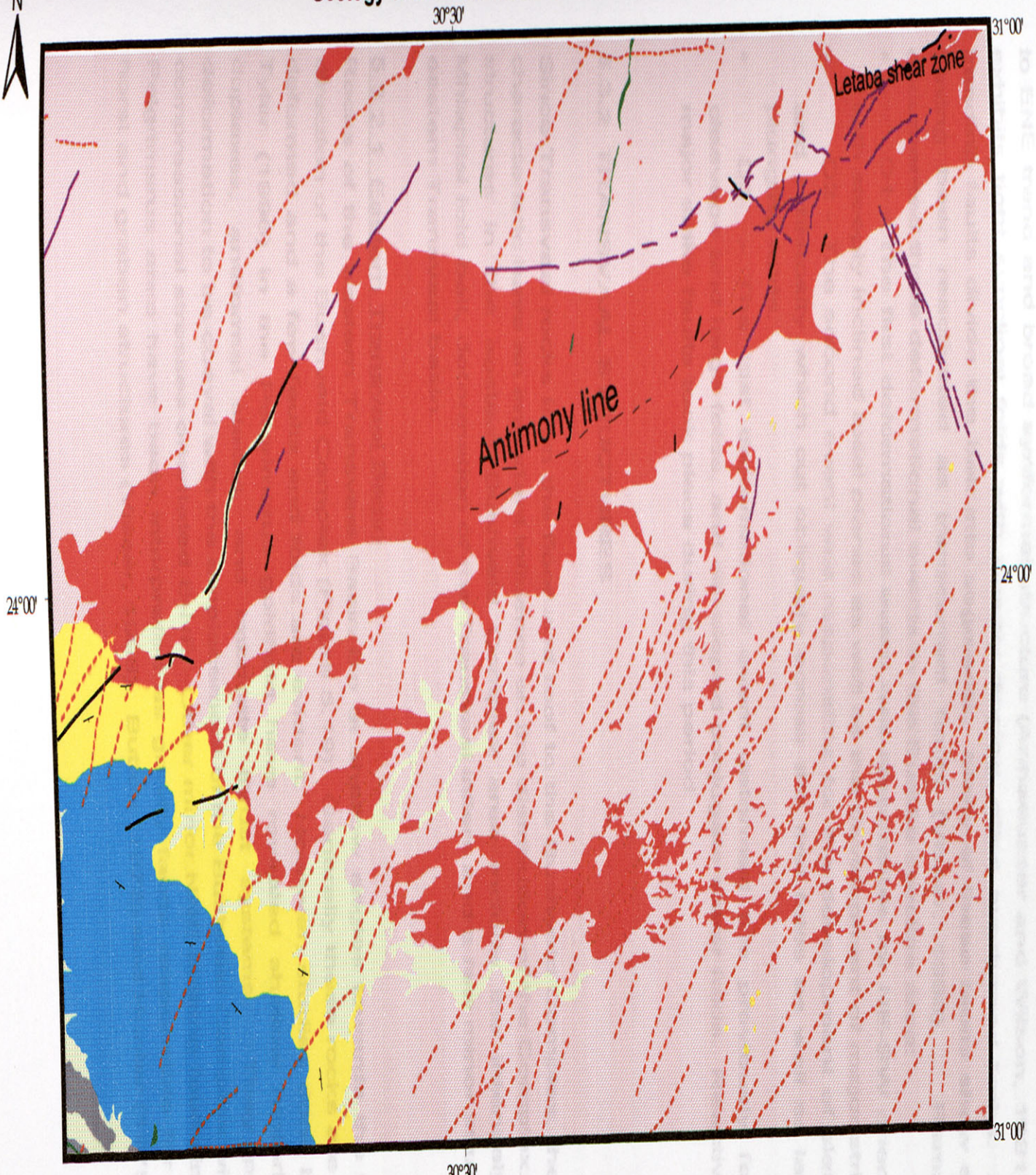

Strike and dip
- horizontal bed
- strike and dip
- facing unknown
- overturned
- vertical bed

lineaments
- undifferentiated
- possible dyke
- aeromagnetic
- satellite
- satellite + aeromag
- Faults
- Faults

Sedimentary and volcanic rocks
- Quaternary
- Karoo
- Waterberg, Blouberg, Soutpansberg
- Glentig, Rust de Winter, Loskop
- Rooiberg, Dullstroom
- Pretoria (upper)
- Pretoria (Magaliesberg)
- Pretoria (lower)
- Chuniespoort
- Black Reef, Wolkberg, Bloempoort
- Groblersdal
- Greenstone

Figure 5.18

evolution of the Kaapvaal Craton and is therefore worth mentioning. The belt has a NNE to ENE trend and broad synformal structure (Anhaeusser and Wilson, 1981). The belt exhibits tight synclinal folds with steeply dipping, often overturned limbs. Major ENE trending faults divide the belt into segments. Many of these faults show evidence of having been reactivated as transcurrent faults (Visser, 1998). Ramsay (1963) documented three deformational events in the Eureka syncline area:

- D1 - The first deformational event was responsible for NE-SW orientated folds with steeply inclined axial planes as well as the development of major strike faults.
- D2 - The second event was responsible for the development of slaty cleavage and schistosity which cut obliquely across the first folds as well as large steeply plunging folds.
- D3 - The last deformational event deformed the previously formed slaty cleavage and large folds, and developed conjugate shear folds. Reactivation of the major strike faults took place during this period.

5.3.2 TRANSVAAL STRUCTURES

Since Transvaal rocks form the floor and roof to the Bushveld Complex, their structural characteristic have an important influence on the distribution of the Complex. Transvaal structures in the eastern Bushveld Complex area include the intensely deformed Mhlapitsi fold belt, deformation of the Transvaal inliers and a few minor structures in the eastern Transvaal basin.

5.3.2.1 Eastern Transvaal Basin

Rocks of the eastern Transvaal Basin dip at shallow angles towards the west, in the direction of the Bushveld Complex (Figure 5.19). Generally these rocks are only slightly deformed and a few faults and folds are evident. However, studies done by Tyler and Tyler (1996) in the Pelgrimsrus goldfield have revealed shallow hinterland-dipping duplexes, antiformal stacks, and imbricate thrust systems. They propose this deformation to be coeval with the emplacement of the Bushveld Complex with maximum compressional stresses orientated E-NE. Other minor NNE striking faults in the Penge-Pelgrimsrus area have been interpreted as gravity faults responsible for the present horst and graben structures (Visser, 1998). Button (1973) and Hunter (1975) have

proposed large scale anticlinal and synclinal warps based on the outcrop pattern of the Transvaal rocks along the NE margin of the basin. They suggested that the intrusion of the Bushveld Complex was controlled by these pre-existing folds in the Transvaal rocks. In addition various prominent NNE trending lineaments are present in the eastern Transvaal rocks. Figure 5.18 shows some of these lineaments as undifferentiated, aeromagnetic and satellite lineaments. These lineaments exhibit a definite curve towards the NE as it enters the adjacent Archaean rocks.

5.3.2.2 The Mhlapitsi fold belt

The Mhlapitsi fold belt trends NE and Transvaal rocks are intensely deformed along the belt (Figure 5.20). The belt dips towards the Bushveld Complex (south) at steep angles. Faulting, folding and shearing are characteristical structural features of the belt.

Faults

Faults trend mainly ENE and include, the *Welkommyn, Serala, Wolkberg* and *Acre Faults* respectively (Figure 5.20). These faults are interpreted by Potgieter (1992) as dip-slip faults which were active during and after Wolkberg deposition, and then later reactivated as thrust faults, before Pretoria Group, but after Chuniespoort Group deposition (Potgieter, 1992). However, a very prominent fault, the *Strydpoort fault*, forms the northern boundary of the fold belt. The fault strikes ENE and can be followed for approximately 70 km along the contact between Transvaal and Archaean rocks (Potgieter, 1992). This fault dips to the south and was a strike-slip fault before deposition of the Transvaal Supergroup. During deposition of the Wolkberg Group the fault was reactivated as a normal fault and then later again reactivated as a thrust fault after the deposition of the Chuniespoort Group but before Pretoria Group deposition (Potgieter, 1992).

Folds

Fold axes are mainly orientated ENE and folding involves the Black Reef Formation and Chuniespoort Group. Potgieter (1992) named the folds the *Acre, Wolkberg, Serala, The Downs, Moltke, and Welkommyn folds* respectively (Figure 5.20). According to Potgieter these folds are closely related to thrust movement along faults after Chuniespoort, but

Geological Map of the eastern Transvaal basin

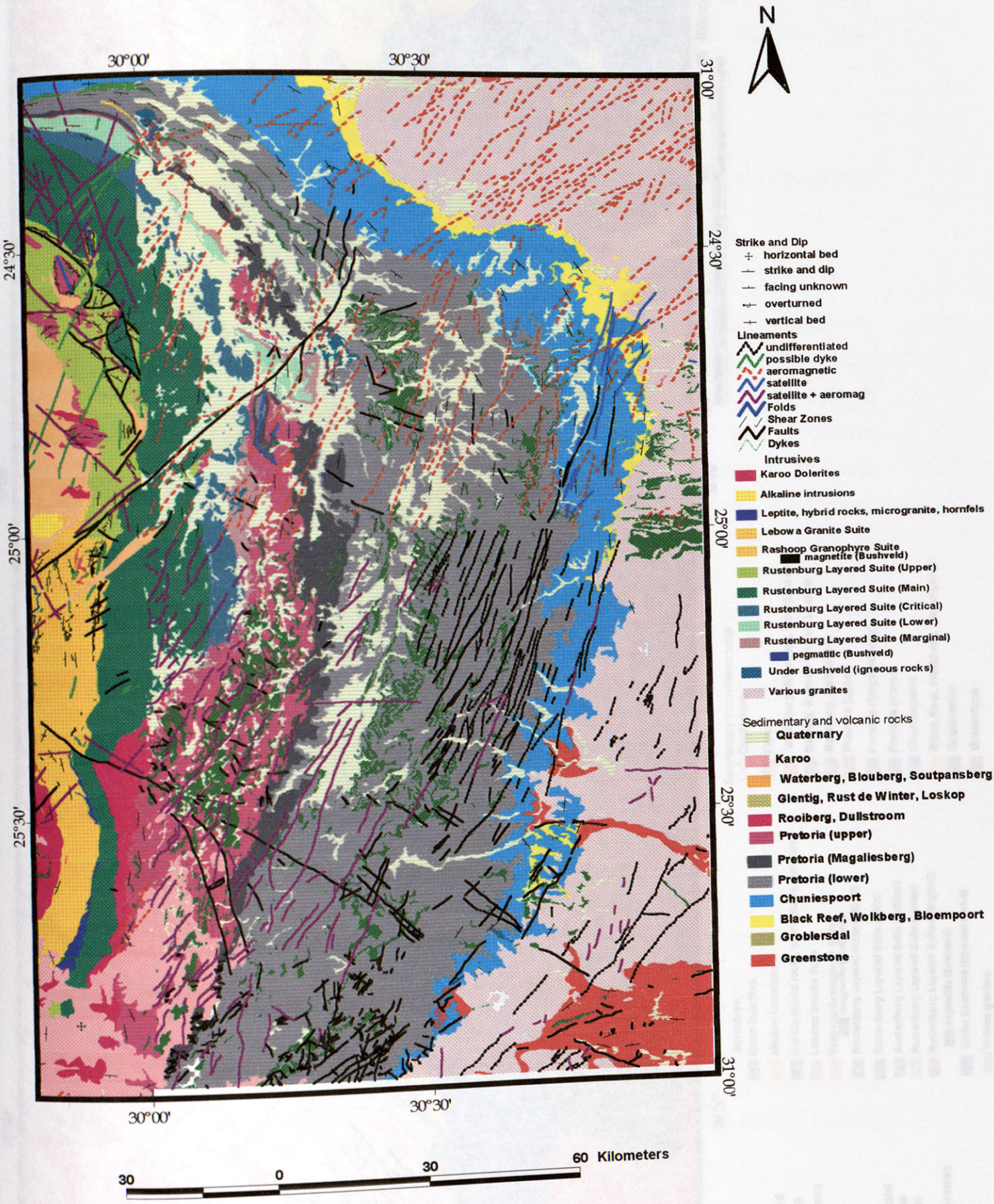

Figure 5.19

Figure 5.20

Geological map of the Mhlapitsi fold belt area (after Potgieter, 1992)

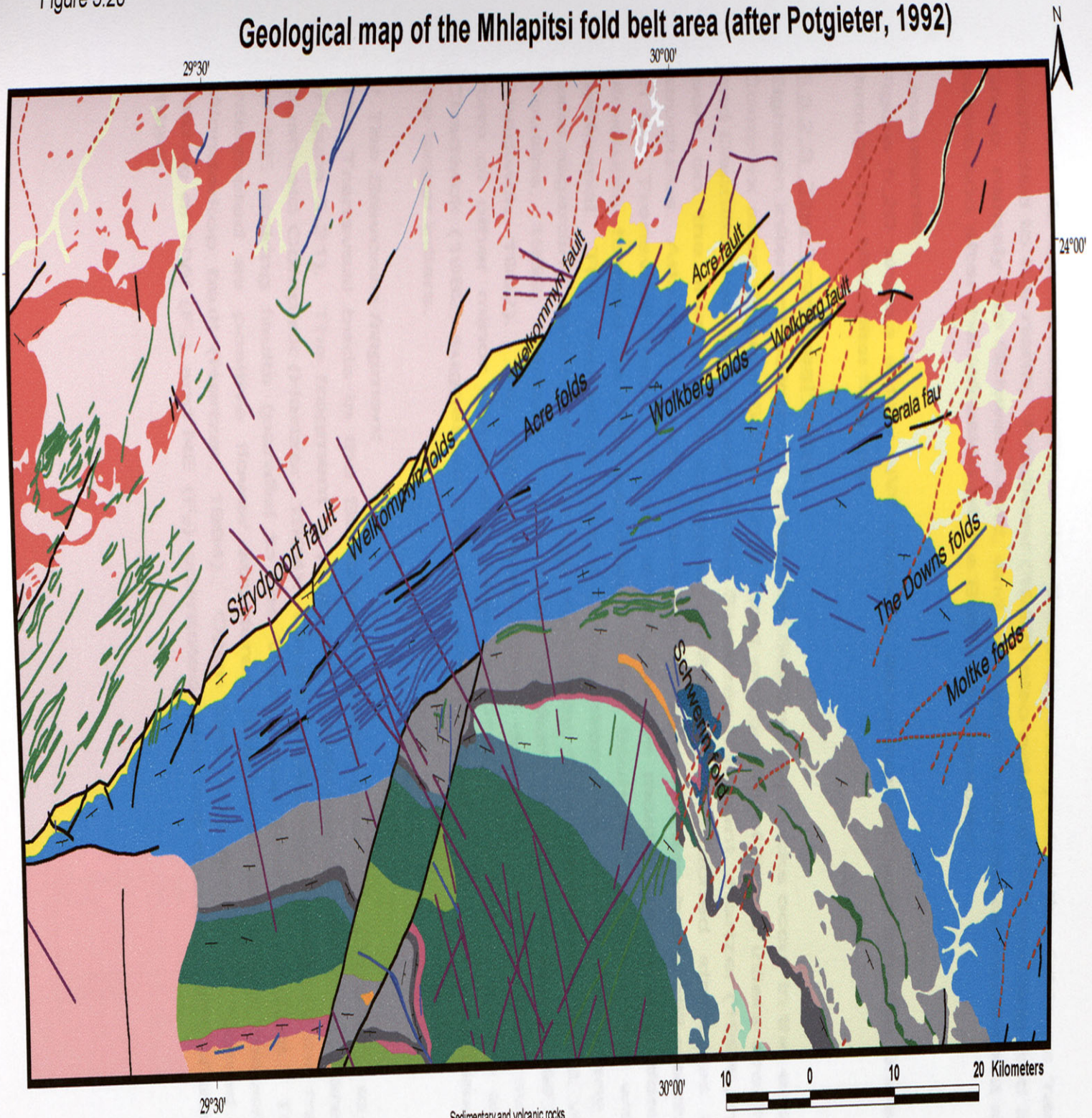

Strike and dip
- horizontal bed
- strike and dip
- facing unknown
- overturned
- vertical bed

lineaments
- undifferentiated
- possible dyke
- aeromagnetic
- satellite
- satellite + aeromag
- Folds
- Faults

Intrusives
- Karoo Dolerites
- Alkaline Intrusions
- Leptite, hybrid rocks, microgranite, hornfels
- Lebowa Granite Suite
- Rashoop Granophyre Suite
  - magnetite (Bushveld)
- Rustenburg Layered Suite (Upper)
- Rustenburg Layered Suite (Main)
- Rustenburg Layered Suite (Critical)
- Rustenburg Layered Suite (Lower)
- Rustenburg Layered Suite (Marginal)
  - pegmatitic (Bushveld)
- Under Bushveld (igneous rocks)
- Various granites

Sedimentary and volcanic rocks
- Quaternary
- Karoo
- Waterberg, Blouberg, Soutpansberg
- Glentig, Rust de Winter, Loskop
- Roolberg, Duilstroom
- Pretoria (upper)
- Pretoria (Magaliesberg)
- Pretoria (lower)
- Chuniespoort
- Black Reef, Wolkberg, Bloempoort
- Groblersdal
- Greenstone

pre-Pretoria Group deposition. He therefore interpreted the folds as 'ramp anticlines' overfolded to the north. Potgieter (1992) also noted a NW trending fold in the Pretoria Group, namely the Schwerin fold, and related it to left-lateral movement along the TML before and after the intrusion of the Bushveld Complex.

Lineaments

Figure 5.20 shows a few NW trending aeromagnetic and satellite lineaments cutting through the Mhlapitsi fold bet.

5.3.2.3 The Transvaal inliers

Eighteen inliers of deformed Transvaal Supergroup rocks occur in the eastern Bushveld Complex area (Figure 5.21). The most prominent of these inliers are the Marble Hall and Dennilton domes as well as the Stavoren fragment. Hartzer (1994), has done detail work on the inliers and categorized them into attached structures and detached structures. Attached structures include all the inliers which are still attached to the floor of the Transvaal basin. These structures are mostly anticlinal or domal. Detached structures formed as roof pendants to the Bushveld Complex and would mainly be synformal. The internal structures of the inliers are variable and many interpretations exist regarding their formation (e.g. Humphrey, 1906, 1908; Daly, 1928; Willemse, 1959; Cousins, 1959; Hartzer, 1987, 1994; Button, 1986; Hamilton, 1977; Sharpe and Chadwick, 1982). The major inliers will be discussed briefly and a summary in table form of other minor inliers are given in Table 5.1. Hartzer (1994) and Sharpe and Chadwick (1982) suggested that the smaller inliers have the same structural trends as the larger inliers.

1.The Stavoren fragment

The Transvaal beds in the Stavoren fragment generally dip gently to the south-east (Figure 5.21). The fragment is probably completely underlain by granitic rocks of the Bushveld Complex (Hartzer, 1994). On the southeastern edge of the fragment a series of NE striking faults (parallel to the Wonderkop fault) is present. These faults are interpreted as positive flower structures related to left-lateral movement along the Wonderkop fault (Hartzer, 1994). Open syn- and anticlines, formed by interference folding of NW (F_1) and NE (F_2) orientated folds are characteristic of this inlier (Hartzer, 1994).

Tabel 5.1. Summary of Transvaal Inliers in the eastern Bushveld Complex area. (After Hartzer (1994) and Sharpe and Chadwick (1982).

Inlier Name	General form	Geological setting	Fault trends	Fold trends	linear trends	Deformation age	Class
Malope	Dome (3 antiforms)	Surrounded by Bushveld Complex granite and gabbro		interference NE, NW (elongated along 015° axial plane)	shear zones with northerly trend	pre-, syn- and post-Bushveld	Dome (fault bounded, not updomed floor, (Sharpe Chadwick)/Diapir [upfolding of basement rocks pre-Bush, (Meyer and De Beer, 1987)]
Adriaanskop	Sheet	Within Bushveld Complex granite	along the Wonderkop fault	ENE		syn-Bushveld	Xenolith (Sharpe and Chadwick)
Fortdraai/ M'Phatlele	Anticline	Surrounded by Bushveld Complex gabbro, partially fault-bounded	Wonderkop fault forms western margin. Secondary fault, linked to Wonderkop fault, cuts through central part	NW, small scale tight folds plunging to the SE	shear zones	pre- to mid Main Zone	Dome/ Diapir
Katkloof	Anticline	At contact between Bushveld Complex gabbro and the Transvaal Supergroup, partially fault-bounded	Wonderkop fault forms northwestern margin	Plunging anticline, fold axis NNW		pre-Bushveld to top of Critical zone	Dome/Diapir
Schwerin	Anticline	At contact between the Bushveld complex gabbro and the Transvaal Supergroup		interference folds NW, ENE		pre- to lower Main Zone	Dome
Paradys	domal structure	Surrounded by Bushveld Complex gabbro		F1: (anticlinal axis) N-S TO NNW F2; ENE - intensly folded	shear zones	pre and syn Bushveld	Dome/Diapir
Potosenyane	Fragment - structure dips towards NE	At contact between the Bushveld Complex gabbro and granite	block faults	ENE fold axis, NW trending syncline and ?, small scale folds (rotated)		pre-and syn-Bushveld	Xenolith
Lezwete	Fragment/synform - dipping towards the N and E	In Bushveld Complex gabbros		gently folded around NW, ENE		pre- and syn-Bushveld	Xenolith
Parys	Fragment - random dips	In Bushveld Complex gabbros		(situated on an anticline)		pre- and syn-Bushveld	Xenolith
Signal Hill-Boschpoort	Fragment	At contact between the Bushveld Complex gabbro and granite		E-ENE, gently folded		pre- and syn-Bushveld	Xenolith

Dwars River	Anticline (double plunging anticline and syncline)	In the Bushveld Complex gabbro, near contact with the Transvaal Supergroup. Partially fault-bounded		axial traces NNW - small scale folds also plunge NNW, curved axial plane = refolding around ENE	shear zones	syn-Bushveld	Dome
Steelpoort	Anticline	At contact between the Bushveld complex gabbro and the Transvaal Supergroup		NW-NNE, D2 ENE - small scale folds		pre-Bushveld	Dome
Derde Gelid	Anticline (pericline)	At contact between the Bushveld complex gabbro and the Transvaal Supergroup		NNW-NE, sligthly refolded along E-ENE (parallel to Steelpoort F)		pre- and syn-Bushveld	Dome
De Berg	Syncline	At contact between the Bushveld complex gabbro and the Transvaal Supergroup, but surrounded by the Critical Zone of the Rustenburg Suite		NW, ENE		syn-Bushveld	Dome
Stoffberg	Sheet	At contact between the Main and Upeer Zones of the Rustenburg Suite					Xenolith

Hartzer (1994) proposed the following deformational history for the Stavoren fragment:

1. During phase 1 (post-Pretoria but pre-Bushveld), folds with axial planes in a NW-SE direction formed due to compression from the NE and SW.
2. During phase 2 (post-Pretoria but pre-Bushveld), folds with axial planes in a NE-SW direction developed due to compression from the NW and SE.
3. The Wonderkop fault zone caused lateral and vertical displacement of the Stavoren succession along a wide zone. Displacement took place along a pre-existing line of weakness and in close association with the intrusion of the Bushveld Complex. Internal right-lateral displacement took place within the fault zone.
4. Secondary faults developed in the Wonderkop fault zone which were partially filled with pegmatitic vein material.
5. The intrusion of Bushveld granite lifted the fragment relative to adjacent Marble Hall dome. Isostatic adjustment after emplacement of the Bushveld caused normal faulting along the Wonderkop fault zone.

2. Marble Hall dome

The Marble Hall dome is separated from the Stavoren fragment by the left-lateral Wonderkop fault zone (Figure 5.21). The general shape of the inlier is domal with rocks of the Transvaal Supergroup dipping outward, (Hartzer, 1994). Several NNE striking faults are present, and the fold pattern of the dome is fairly complex. A general NNE trending anticline, the Swartkop-Marble Hall anticline, exist in the center of the dome. Hartzer (1994) noted that parasitic folding caused severe thickening in the center of the anticline, and that parallel folding and faulting are responsible for the very complex outcrop pattern. Hartzer (1994) noted several NW (F_1) fold axes that have been refolded about a NE (F_2) axes. Snyman (1956) suggested the folding was linked to the intrusion of the Nebo Granite. However, Clubley-Armstrong and Sharpe (1979) proposed structural irregularities in the Transvaal floor which was reactivated during Bushveld intrusion. Hartzer (1994), on the other hand, suggested that most of the folding took place before the emplacement of the Bushveld Complex.

Figure 5.21

Geolgical map of the distribution of the Transvaal Inliers, (after Hartzer, 1994)

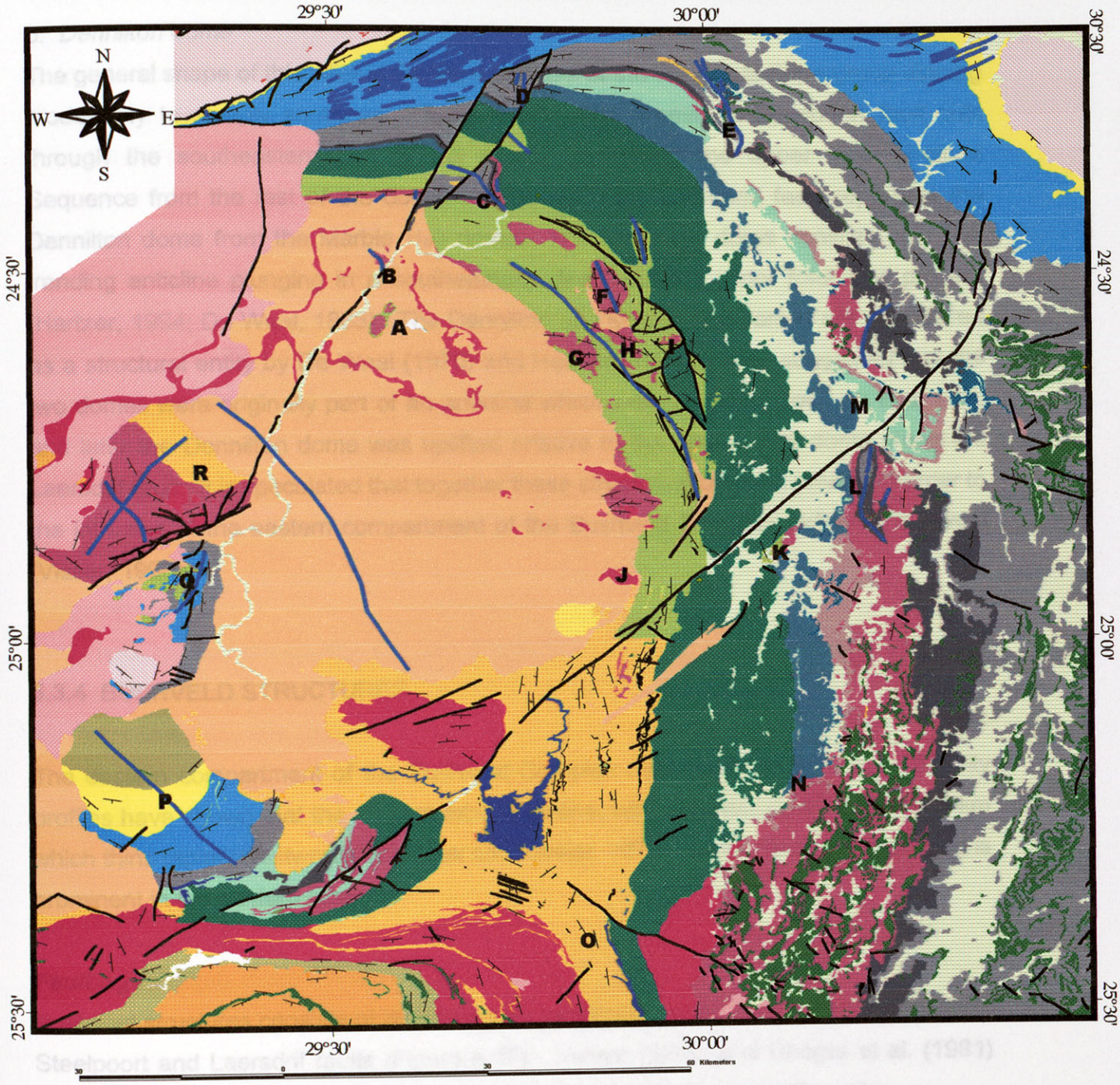

A. Malope structure
B. Adriaanskop structure
C. M'Phatele/Fortdraai structure
D. Katkloof structure
E. Schwerin structure
F. Paradys structure
G. Potosenyane structure
H. Lezwete structure
I. Parys structure
J. Signal Hill - Boschpoort structure
K. Derde Gelid structure
L. Steelpoort structure
M. Dwars River structure
N. De Berg structure
O. Stoffberg structure
P. Dennilton structure
Q. Marble Hall dome
R. Stavoren fragment

3. *Dennilton dome*

The general shape of this inlier is domal, with rocks of the Transvaal Supergroup dipping moderately to steeply southeast (Figure 5.21). The prominent Steelpoort fault cuts through the southeastern part of the dome, separating the upper most Pretoria Sequence from the rest of the dome. In the north the Laersdrift fault separates the Dennilton dome from the Marble Hall dome. The Dennilton dome consists of a NW trending anticline plunging in a southeasterly direction, and minor folding is present (Hartzer, 1994; De Waal, 1963). The Dennilton and Marble Hall domes are considered as a structural entity by De Waal (1970) and Hartzer (1994). They suggested that the two domes were originally part of an anticline which were refolded along an ENE axis, and later the Dennilton dome was uplifted relative to the Marble Hall dome along the Laersdrif fault. It is speculated that together these structures formed a physical barrier to the intrusion of the eastern compartment of the Bushveld Complex further to the west (Visser, 1998).

5.3.4 BUSHVELD STRUCTURES

The eastern compartment of the Bushveld Complex dips mainly to the west. Gravity profiles have shown that the eastern lobe is sill-like, with a maximum thickness of 5 km which thins rapidly westward (Molyneux and Klinker, 1978). Large faulting and folding is prominent in the eastern lobe.

Faulting

Bushveld structures consists of the three very prominent faults, namely the Wonderkop, Steelpoort and Laersdrif faults (Figure 5.17). Hunter (1976) and Sharpe et al. (1981) considered these faults as presumed feeder fissures to the Bushveld Complex.

Wonderkop fault

The Wonderkop fault strikes over a distance of more than 120 km and has a general NNE strike. Some authors suggests that the fault extends beyond the Chuniespoort Group towards the northeast (Schwellnus et al., 1962). The fault is not very well exposed but based on outcrops in the Stavoren fragment and along the northern rim of

the Bushveld Complex, Hartzer (1994) interpreted the fault to be a left-lateral strike-slip fault with some internal right-lateral movements. The Wonderkop fault has been active over a long period, stretching from pre-Bushveld times to post-Bushveld times. Du Plessis and Walraven (1990) mentions post-Bushveld normal faulting, and Visser (1998) ascribes the normal displacement to thermal collapse after the intrusion of the Complex.

Steelpoort fault

The Steelpoort fault strikes NE and can be followed for approximately 95km. Even though the fault is a very prominent structure cutting through the Bushveld Complex very little research has been done on the fault. Shearing in places along the fault zone indicates right-lateral movement (Visser, 1998). In contrast, Sharpe and Chadwick (1982) suggested that the Dwars River fragment is a horst block related to vertical movement along the fault. The fault is believed to be post-Bushveld in age, however pre-Bushveld movement might have been possible (Visser, 1998).

Laersdrif fault

The Laersdrif fault strikes NW and cuts trough the upper Transvaal Supergroup and the Lower Bushveld Complex. The northwestern continuation of the fault is uncertain although some authors consider it to be responsible for the separation of the Dennilton and Marble Hall domes (De Waal, 1970). Up to date no detail study of the Laersdrif fault has been done. The timing of the fault can be constrained to post-Bushveld due to cross-cutting relationships. However, pre-Bushveld activation should not be discarded.

Sekhukhune fault

The Sekhukhune Fault (Figure 5.17) displaces the upper and lower zones of the Rustenburg Layered Sequence. The fault has a very sinuous nature but mainly follows the outcrop pattern of the Rustenburg Sequence. Molyneux (1970) noted vertical displacement along the fault zone. The type of faulting however is uncertain.

Folding

A few NW trending anticlines and synclines are present in the eastern Bushveld Complex area. Molyneux (1970) noted the existence of an anticline in the Rustenburg Layered Sequence close to Magnet Heights. Walraven (1986) proved through trace-element distribution indexes, which indicates stratigraphic height, that a large NW

orientated open synclinal structure is present in the Nebo Granites of the eastern compartment of the Complex (Figure 5.21). Other workers such as Lenthall (1975) and MacCaskie (1983) reported the same structure.

Lineaments

Numerous lineaments can be traced through the eastern compartment of the Bushveld Complex (Figure 5.17). BOSGIS show these lineaments as satellite and aeromagnetic lineaments and some possible dykes. During an Honours project undertaken by Hoffmann (1997) on the Nebo granites of the eastern Bushveld Complex, five different orientations of fractures were recorded. They include the following orientations from oldest to youngest (Hofmann, 1997):

- 170°-180°
- 40°-50° and 140°-150° (Same orientation as Wonderkop and Sekhukhune fault)
- 80°-90°
- 120°-130° (possibly post-Karoo age)

Although many different orientations of fractures exist, Hofmann noticed that most of the displacement along shear fractures indicate right-lateral shearing.

5.3.5 WATERBERG STRUCTURES

Waterberg rocks in the Cullinan-Waterberg basin are relatively undeformed and dip towards the center of the basin (Figure 5.22). However, prominent faulting and small scale folding have been observed along the northern margin of the basin (Van der Neut, 2000). The most prominent structure is the large E to ENE trending Wilgerivier fault, extending for approximately 75 km. The fault displays a very complex geology with Waterberg rocks dipping steeply towards the north, south, vertical, and overturned. Van der Neut (pers. Comm.) describes ramp flat geometry for the fault zone with fault planes dipping south. Small-scale NE trending folds and thrusts are developed in shale layers, whereas approximately E-W orientated mullion structures are present in local quartzite layers. Van der Neut (pers. Comm.) attribute the structures of the fault zone to thrust movement towards the north during post-Waterberg but pre-Karoo times.

5.3.6 KAROO STRUCTURES

Karoo rocks occur to the south of the Bushveld Complex as well as in the center of the Complex, known as the Springbok flats. The Karoo rocks in this area is relatively undeformed and no major Karoo structures are present in the eastern Bushveld Complex area. A few satellite and aeromagnetic lineaments have been recorded in the Karoo rocks occurring to the south of the Complex (Figure 5.17). These lineaments show various orientations and cut through adjacent Waterberg rocks.

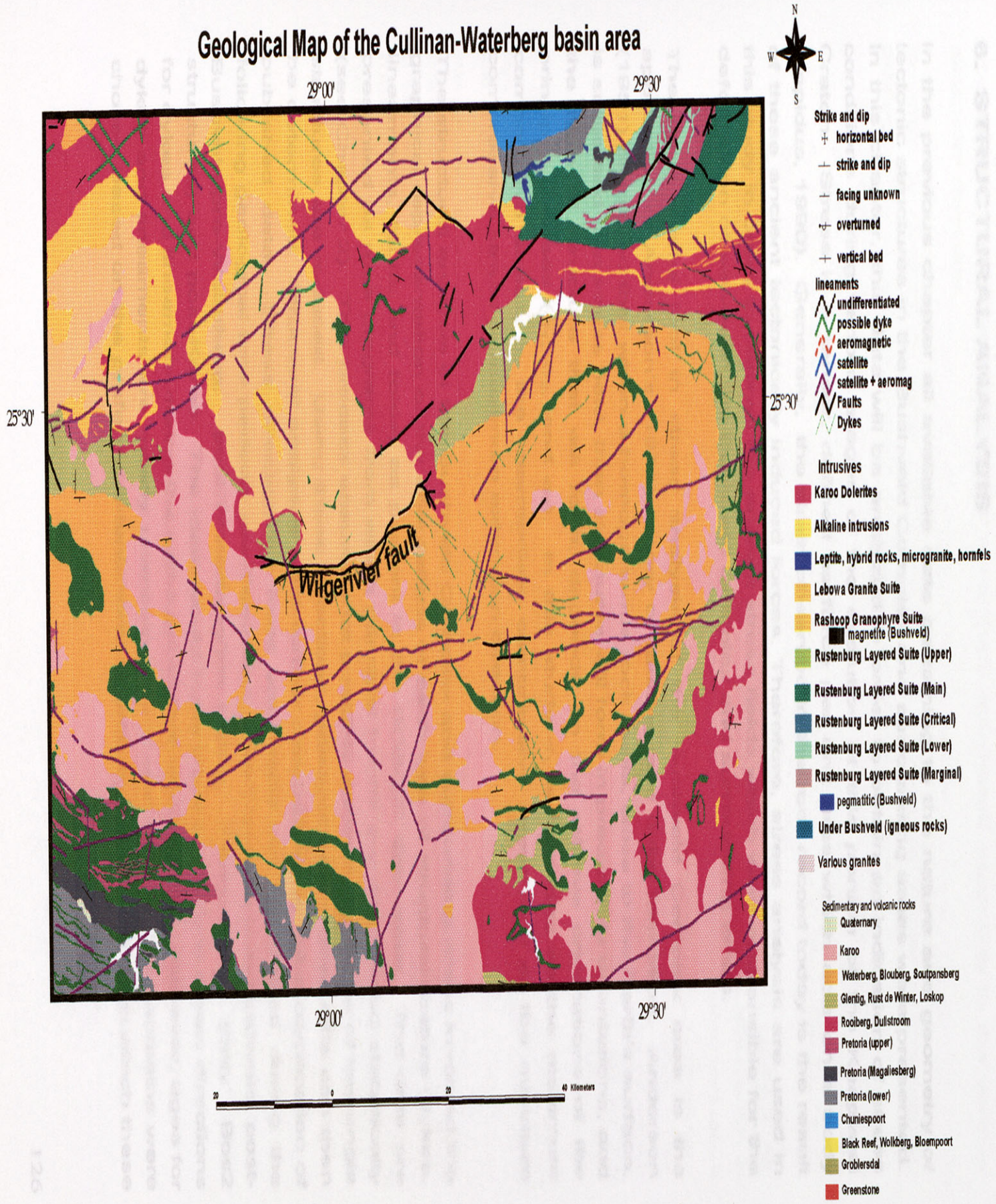

Figure 5.22

6. STRUCTURAL ANALYSIS

In the previous chapter all available data pertaining to the nature and geometry of tectonic structures in the Bushveld Complex and surrounding areas were presented. In this chapter, this data will be analyzed in order to obtain an indication of stress conditions during various stages of the evolution of this portion of the Kaapvaal Craton. Stress is a tensor, defined as force per unit area which acts on a body (Lapidus, 1990). Generally, the strain observed in the rock record today is the result of these ancient tectonically induced forces. Therefore, stress analysis are used in this study in order to unravel the ancient stress fields which were responsible for the deformation observed in the Bushveld Complex and surrounding areas.

The most useful tool in stress analysis of the Bushveld Complex area is the application of Anderson's (1951) theory of faulting and dyke formation. Anderson (1951) proposed that when a homogeneous rock mass, close to the Earth's surface, is subjected to a stress field, then structures will form in predictable orientations, and the type of structure that will form, depends on the relative orientations of the principal stresses (σ_1, σ_2, and σ_3). In this study σ_1 is regarded as the maximum compressive stress, σ_2 the intermediate compressive stress and σ_3 the minimum compressive stress or maximum extension direction.

The structural analysis of the Bushveld Complex and surrounding areas involved the graphical representation of the orientations of each type of structural feature (dykes, lineaments, faults and folds) as present in the BOSGIS data base. The data are presented as rose diagrams from which principal trends are determined statistically (see Chapter 2). This process ensures that possible errors in the strike of low-angle structures are reduced. Using these directions, principal stress directions can then be determined. Structural analyses were further constrained by the incorporation of published data. Stress direction for folds and faults are interpreted during the following geological time periods; pre-Transvaal, post-Transvaal/pre-Bushveld, post-Bushveld/pre-Waterberg, post-Waterberg/pre-Karoo, Pilanesberg (only Bos2 structures) and post-Karoo. The ideal would have been to analyse stress directions for dykes and lineament during the same geological time periods. However, ages for dykes and lineaments are mostly unknown, and therefore structural domains were chosen based on the preferred orientations as well as the rock types in which these

structures occur. Stress directions were then interpreted according to the various structural domains.

In order to determine stress conditions for the various structures at the various geological times periods, certain assumptions had to be made:

1. The intersection of any specific feature with the map surface is the true strike of the feature. This is always true for vertical structures such as dykes, but may give erroneous results for low-angle structures such as thrust faults, or axial planes of folds, especially in areas of high relief.
2. Rocks are homogeneous and no pre-existing weaknesses are present (cf. Anderson, 1951). This is rarely the case, and many structures are known to have reactivated along pre-existing weaknesses. Therefore, even though a stress is not applied in the optimum orientation according to Anderson's (1951) theory, a pre-existing weakness might reactivate in response to an oblique stress direction. In this study, stress directions for structures which are known to have reactivated, are interpreted to have formed under the proposed stresses of Anderson's (1951) theory for homogenous rocks.

In the second part of this chapter the strike and dip data of the BOSGIS data base are analyzed by means of stereographical plots. Generally, stereographical plots were made according to the ages of the rocks in which strike-and–dip values were measured, thereby defining structural domains. Density distribution analysis and principal direction analysis are the main methods by which these plots were analysed. The regional geometry of the various areas could be determined by means of this type of analysis. However, structural analysis was somewhat handicapped due to the irregular distribution of strike and dip values in the data base.

6.1 Stress analysis from Dykes

Dykes are generally considered to be vertical features which formed as a result of horizontal extension. Anderson's (1951) theory of dyke formation is illustrated in Figure 6.1. In this case σ_3 is perpendicular to the strike of the dyke, i.e. horizontal, while the dyke itself lies in the σ_1 -σ_2 plane. Thus, either σ_1 or σ_2 can be vertical.

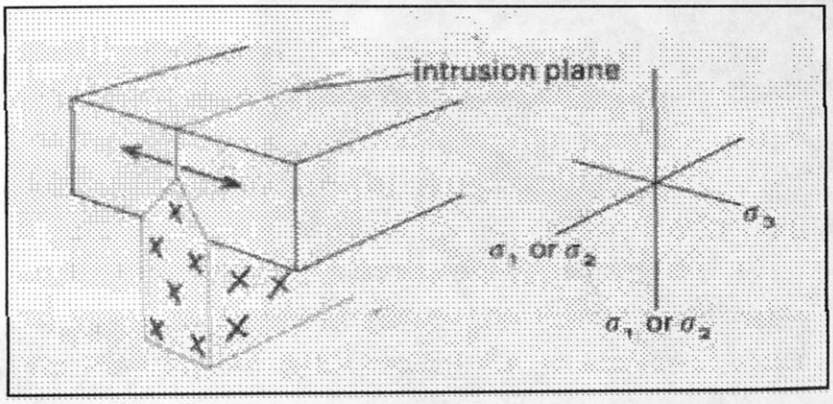

Figure 6.1. The emplacement of a dyke and the predictable stress directions according to Anderson (1951) (after Park, 1997).

A geological map of the Bushveld Complex and surrounding areas with all the dykes included in the BOSGIS database is shown in Figure 6.2. Dyke orientations for each structural domains of the respective Bos areas were analysed separately. Due to uncertainty of σ_1 and σ_2 directions, only σ_3 directions are mentioned in the text and indicated on the rose diagrams.

6.1.1 Bos2

Dykes occurring in the Bos2 area (Figure 6.3) were grouped based on their compositions obtained from the BOSGIS data base, namely dolerite dykes (A) and syenite dykes (B). The majority of the dykes are situated in granites, however syenitic dykes are more restricted to the granites of the Makoppa dome, whereas dolerite dykes appear more frequently in the granites of the Bushveld Complex. Dolerite dykes are interpreted to have intruded during post-Karoo times and syenite dykes are related to the intrusion of the Pilanesberg Complex (Keyser, 1997).

Both types of dykes are orientated more or less in the same direction (Figure 6.3). However, closer evaluation indicates that the dolerite dykes have a preferred orientation of 300° whereas the syenite dykes are orientated along a 320° direction. The following principal stress directions are therefore interpreted for the respective

Figure 6.2

Bosgis Dyke Map

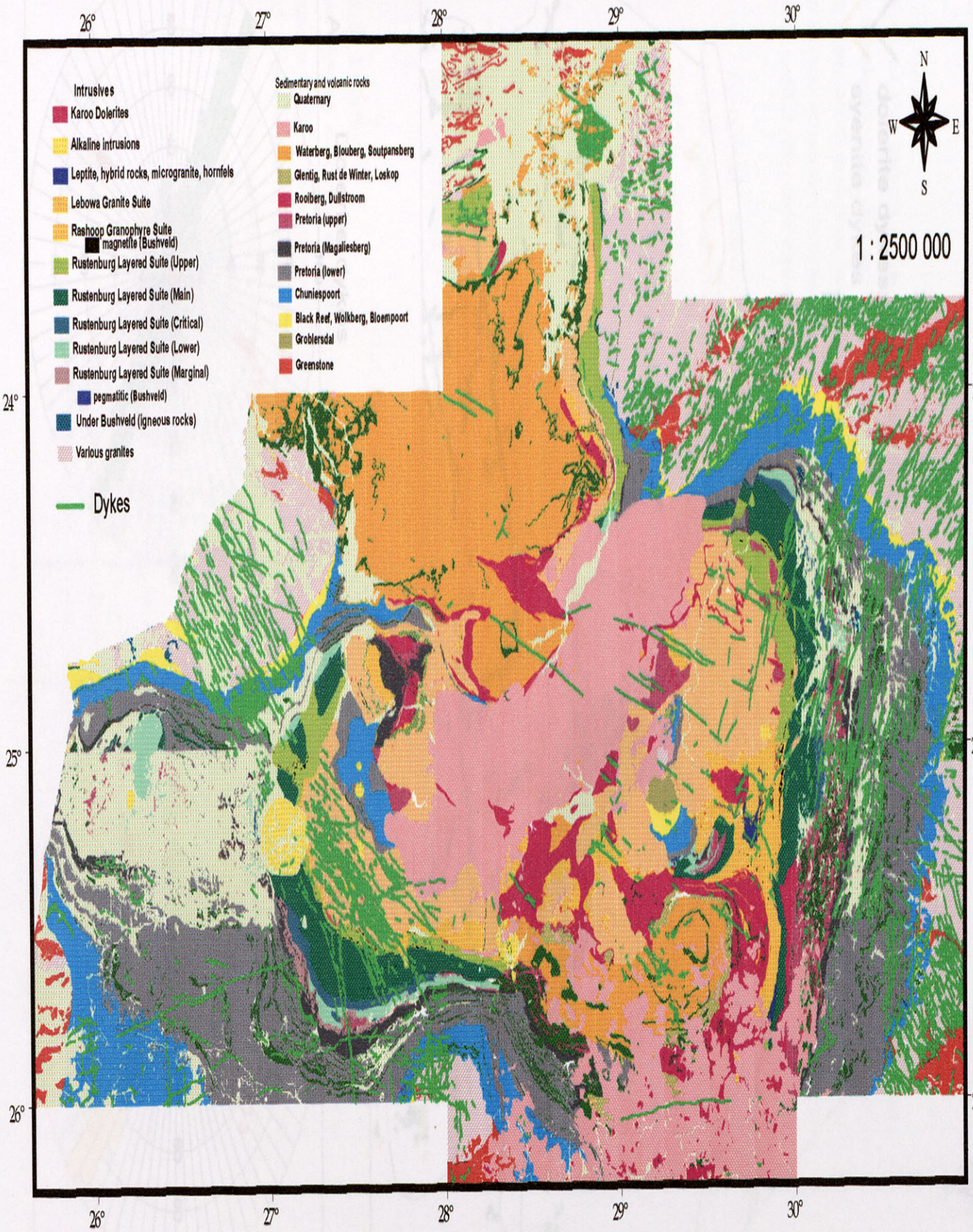

Figure 6.3

Bos2 Dyke Map

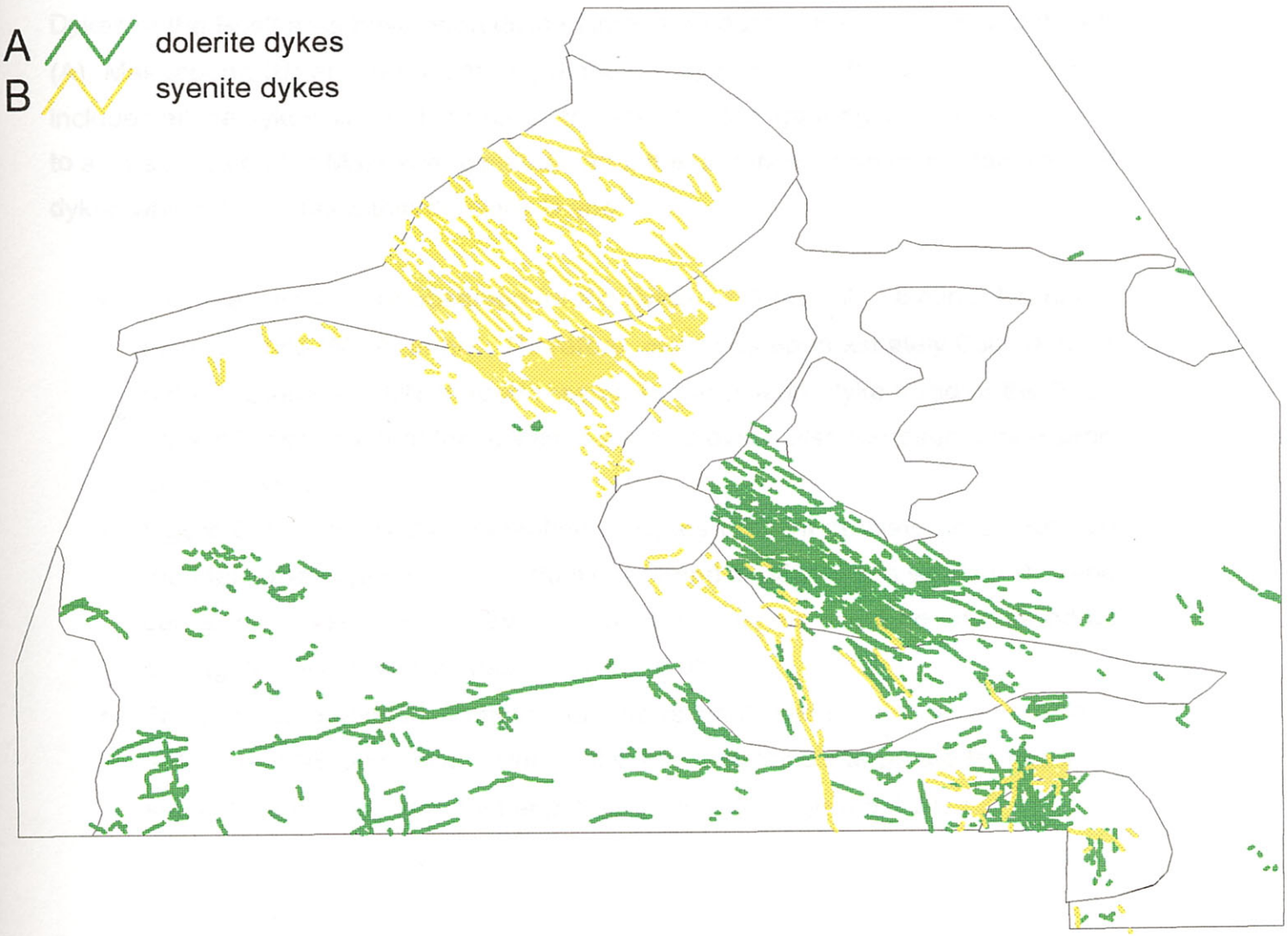

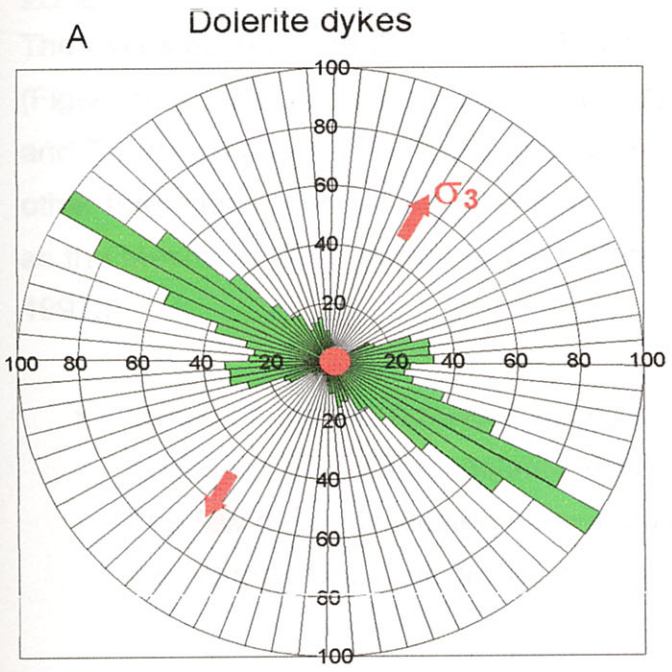

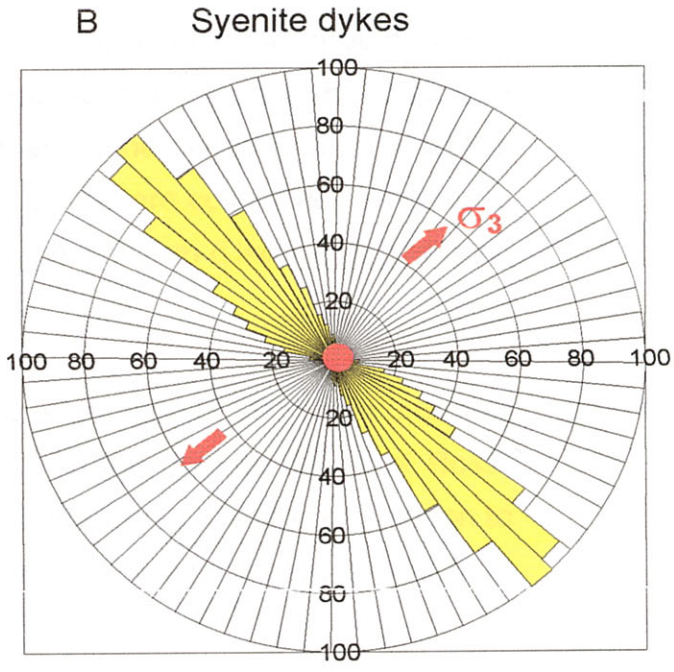

dyke sets: σ_3 trends 030° in the case of the dolerite dykes, and 050° for the syenite dykes (Figure 6.3 A and B).

6.1.2 Bos3

Dykes of the Bos3 area have been divided into three domains, namely an undefined, (A), Makgabeng (B) and Archaean (C) domain (Figure 6.4). The Archaean domain includes all the dykes situated in Archaean rocks, the Makgabeng domain is confined to a small area on the Makgabeng plateau and, the undefined domain contains all the dykes which do not fall within domains B and C.

- Two main trends are observed for the dykes of domain A , a minor NE and a more definite WNW trend. Therefore, σ_3 trends approximately 030° (Figure 6.4 A). Since the WNW trend resembles the dolerite dyke trend of the Bos2 area, it is possible that these WNW trending dykes also represent post-Karoo dolerite dykes.
- Figure 6.4 B shows the orientation of dykes present in Waterberg strata on the Makgabeng plateau. The dominant trend is 080° and a weak 100° trend can also be seen. These two orientations of dykes might be interpreted as conjugate sets, in which case σ_3 will trend 0°.
- The Archaean domain (C) hosts numerous small dykes which appear to have a dominant NE orientation. Principal stress directions interpreted for this dyke set, indicates a σ_3 orientated approximately 330° (Figure 6.4 C).

6.1.3 Bos5

The dykes occurring in the eastern Bushveld Complex area occur in three domains (Figure 6.5). The domains include all the dykes situated in the Archaean (domain C) and Transvaal (domain B) rocks respectively, as well as the dykes present in all the other formations (domain A). Dykes of domains B and C are collectively referred to as the Mesozoic Dyke swarm or the Olifants River dyke swarm (Uken and Watkeys, 1997a).

- Dykes of domain A have a strong preferred orientation of 290°, and probably represent post-Karoo dolerite dykes, similar to the dolerite dykes of Bos2. The few dykes orientated between 040° and 050° have a similar orientation to the Wonderkop fault trend, and are therefore possibly related to the fault

Figure 6.4

Bos3 Dyke Map

A Undefined

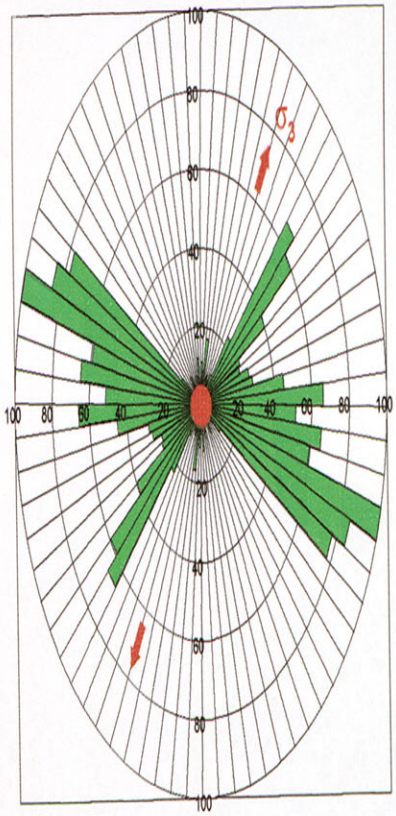

B Makgabeng

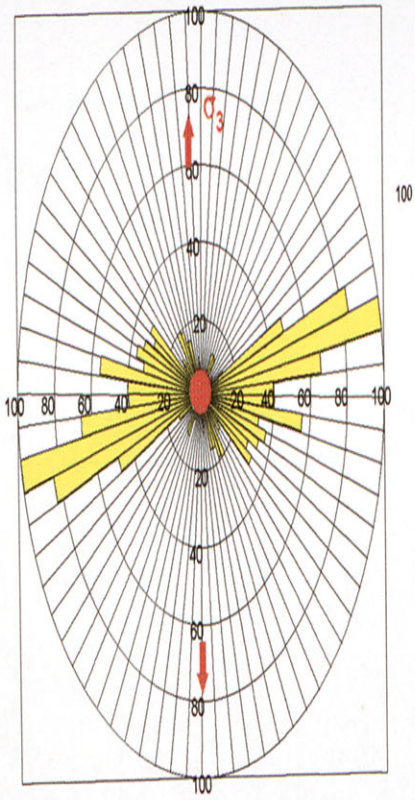

C Archaean

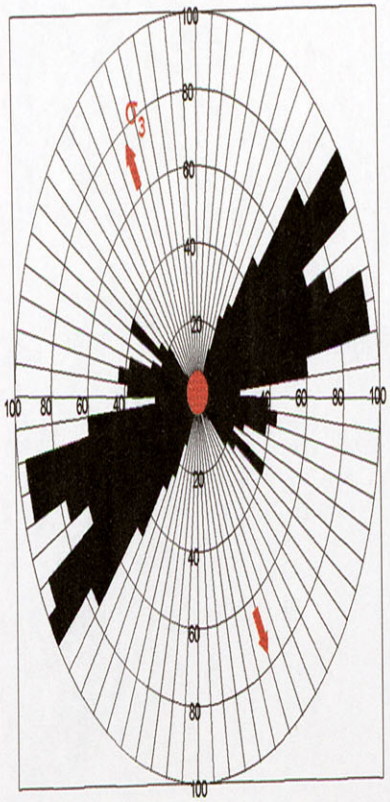

- formation. σ_3 for the post-Karoo dolerite dykes is interpreted to be orientated at 030°.
- Dykes occurring in the Transvaal rocks (domain B) are orientated in a clear 040° direction (Figure 6.5 B). σ_3 for these dykes have an orientation of 310°.
- Dykes present in the adjacent Archaean granites, domain C, are almost orientated in the same direction as the dykes in the Transvaal rocks, with a dominant 050° trend. σ_3 for the Archaean dykes is postulated to be orientated at 320° (Figure 6.5 C).

A Undefined

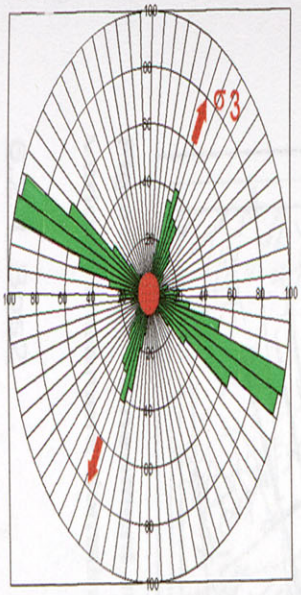

B Transvaal

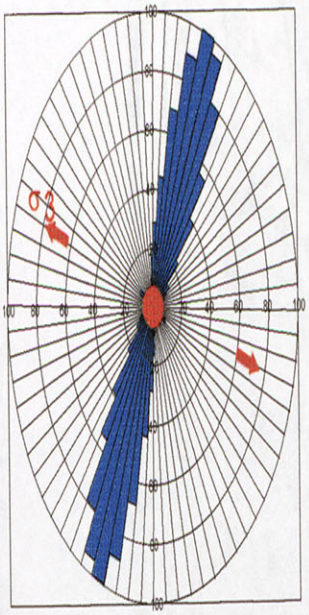

C Archaean

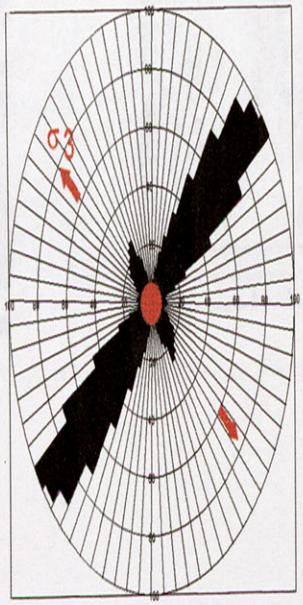

Figure 6.5 **Bos5 Dyke Map**

A undefined
B Transvaal domain
C Archaean domain

6.2 Stress analysis from Lineaments

A lineament can be defined as a linear feature prominent enough to be recognized by regional observation techniques such as aerial photos, LANDSAT images, aeromagnetics, etc. In many cases it is unknown what these linear features represent, but in this study the assumption is made that lineaments reflect vertical joints, fractures, or dykes. Therefore, the interpretation of stress directions responsible for lineaments will be the same as for dykes.

Figure 6.6 shows a geological map with the locations of different types of lineaments in the Bushveld Complex area. The lineaments of each Bos area were considered separately according to the various structural domains. Sharpe and Lee (1990) presented a lineament domain map, defining six lineament domains (Figure 6.7), which are broadly similar to domains chosen for this study.

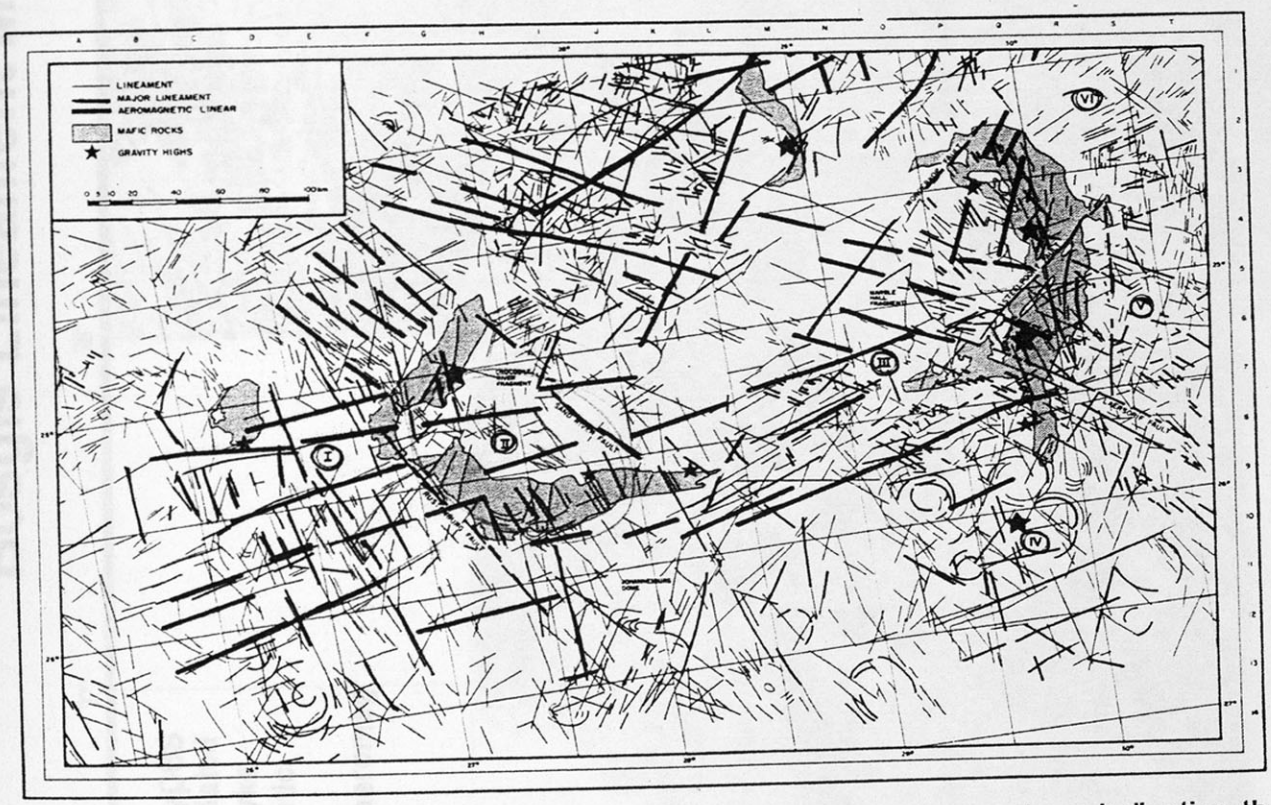

Figure 6.7. Lineament map of Sharpe and Lee (1990) with roman numbers indicating the various lineament domains.

6.2.1 Bos2

Figure 6.8 shows the eight lineament domains of the Bos2 area, they include a Karoo (A), Pilanesberg (B), Waterberg (C), far western Province (D), western

Figure 6.6

Bosgis Lineament Map

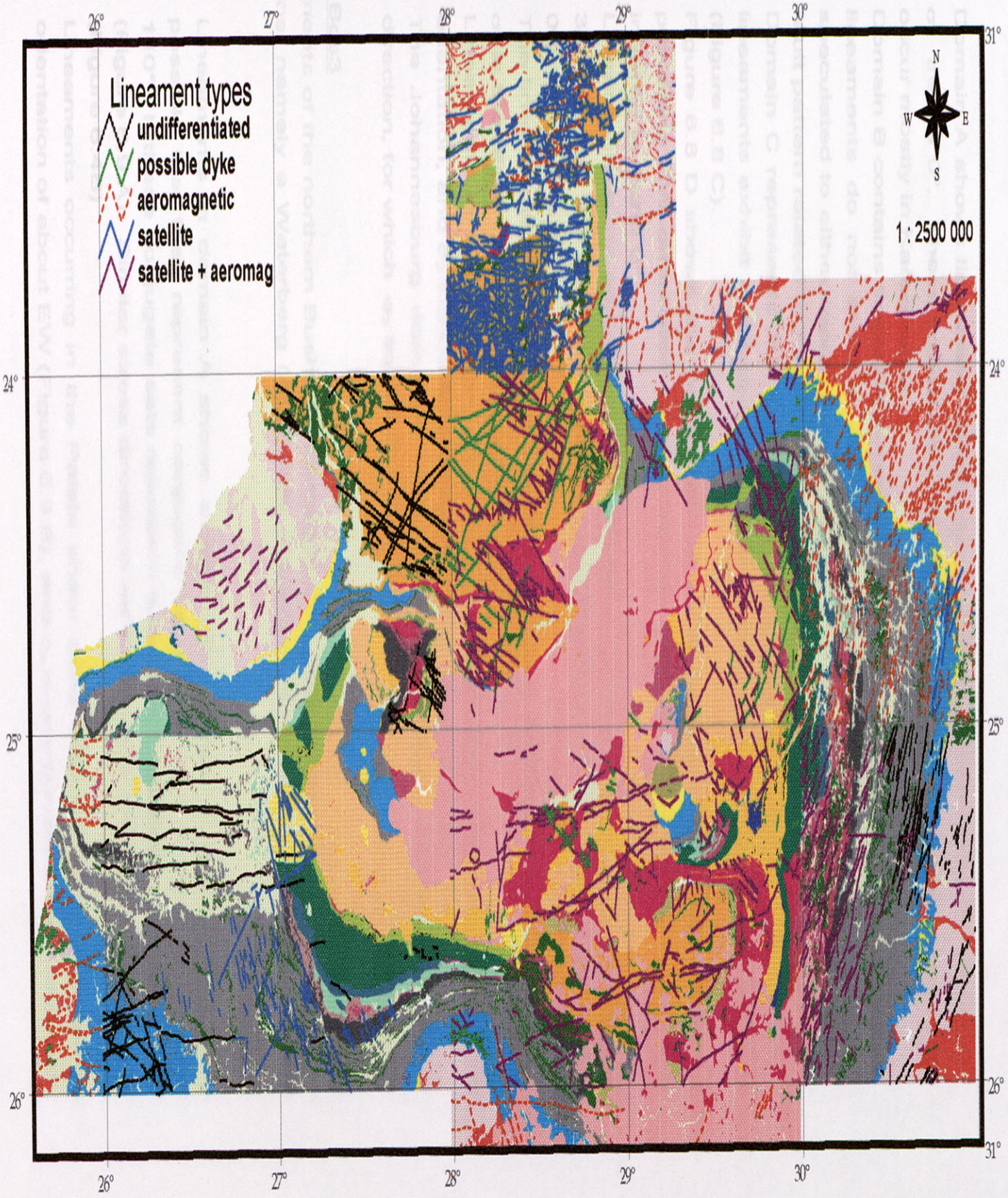

- Domain A shows lineament orientated about 90° (Figure 6.8 A). Therefore, σ_3 trends 0°. These lineaments are probably post-Karoo in age since they occur mostly in Karoo rocks.
- Domain B contains lineaments occurring in the Pilanesberg Complex. These lineaments do not show a preferred orientation and their significance is speculated to either represent conjugate joint sets, veins or might be a radial fault pattern related to the Pilanesberg Complex (Figure 6.8 B).
- Domain C represents lineaments occurring in the Waterberg rocks. These lineaments exhibit a strong trend of 290° and a σ_3 trending 020° is deduced (Figure 6.8 C).
- Figure 6.8 D shows the lineaments of the far western Transvaal basin. A prevailing EW orientation of aeromagnetic lineaments is present and σ_3 is inferred to trend 0°.
- Lineaments in the adjacent domain (E) have two main orientations of EW and 330° (Figure 6.8 E). σ_3 directions would therefore trend 0° and more or less 060° (Figure 6.8 E).
- The lineaments of the Rooiberg domain (F) have a general trend of 300° and σ_3 is therefore directed towards 030° (Figure 6.8 F).
- Lineaments in the Makoppa dome (G) are short and have a general ENE orientation, and σ_3 trends approximately 330° (Figure 6.8 G).
- The Johannesburg dome (H) host longer lineaments orientated in a EW direction, for which σ_3 trends 0° (Figure 6.8 H).

6.2.2 Bos3

Lineaments of the northern Bushveld Complex area are grouped into three structural domains, namely a Waterberg (A), Palala (B) and a Archaean (C) domain (Figure 6.9).

- Lineaments in domain A shows a wide EW spread of orientations. It is possible that they represent conjugate sets orientated at roughly 60° and 110°. If these conjugate sets represent extensional features, σ_3 will trend 0° (Figure 6.9 A). Similar stress directions were obtained from Waterberg dykes (Figure 6.4B)
- Lineaments occurring in the Palala shear zone area (B) have a preferred orientation of about EW (Figure 6.9 B), and σ_3 is interpreted to be directed 0°.

Figure 6.8 **Bos2 Lineament Map**

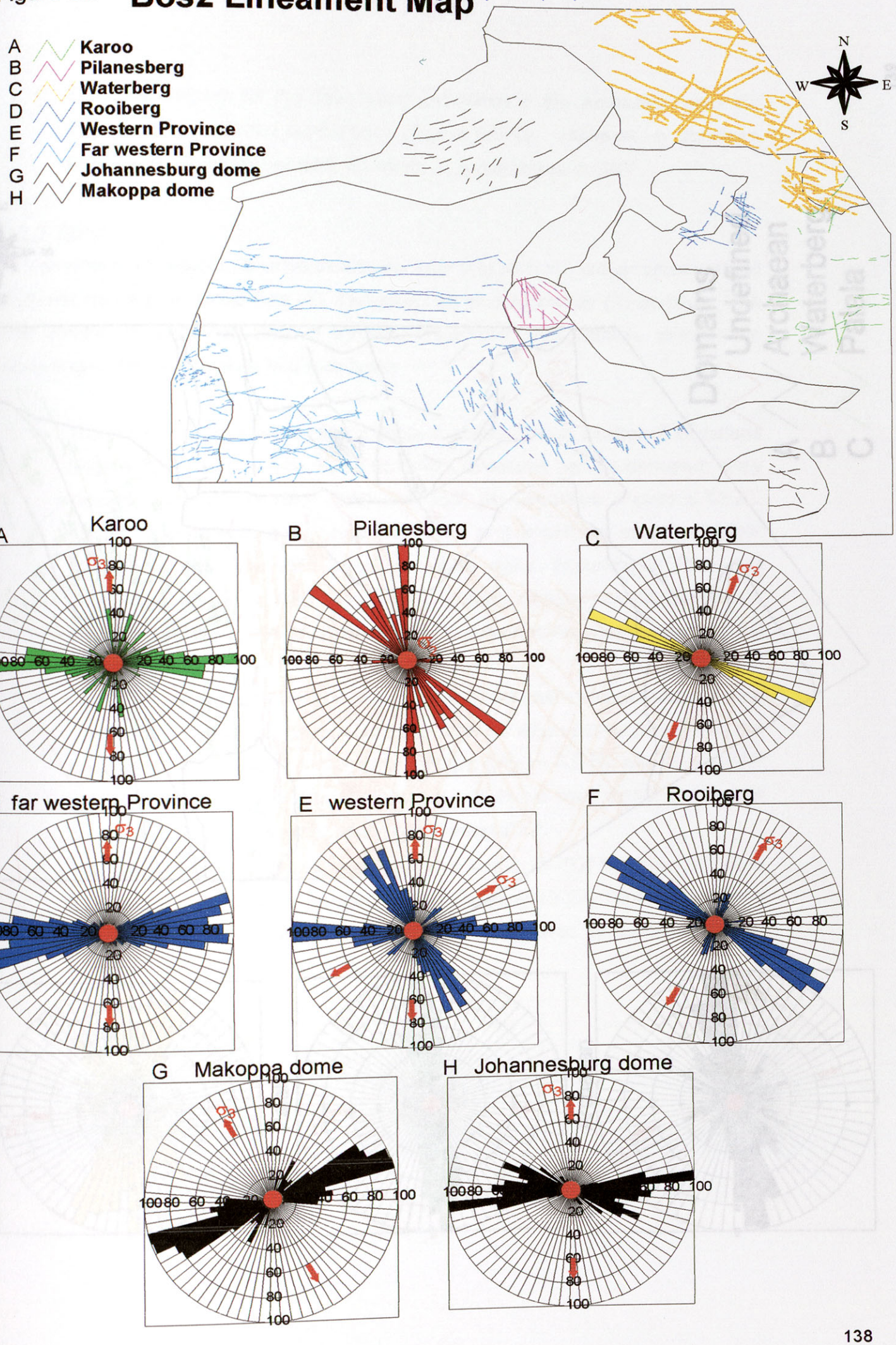

Figure 6.9

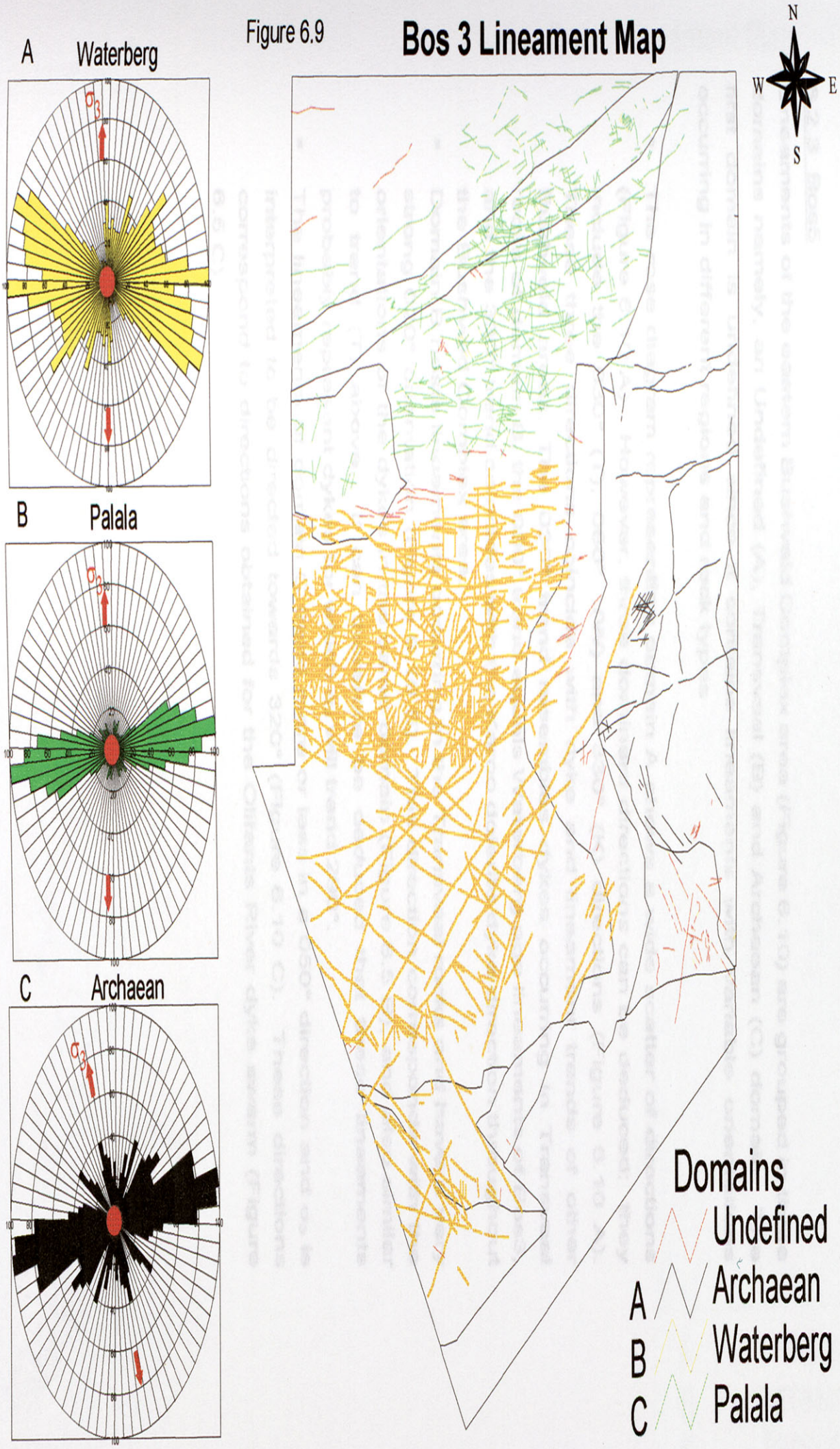

- The rose diagram for the lineaments positioned in the Archaean rocks (C) display fairly scattered orientations (Figure 6.9 C). However, a dominant 080° trend can be recognized, for which σ_3 is orientated at 350°.

6.2.3 Bos5

Lineaments of the eastern Bushveld Complex area (Figure 6.10) are grouped in three domains namely, an Undefined (A), Transvaal (B) and Archaean (C) domain. The first domain is undefined since it contains lineaments with variable orientations occurring in different regions and rock types

- The rose diagram representing domain A shows a wide scatter of directions (Figure 6.10 A). However, three dominant directions can be deduced; they include the 030° (T), 080° (W) and 330° (K) directions (Figure 6.10 A). These three directions coincide with dyke and lineament trends of other Bushveld areas. The 030° trend resembles dykes occurring in Transvaal rocks of domain B, the 080° trend equals Waterberg age lineaments of Bos3, and the 330° trend coincides with the Karoo dolerite dyke direction throughout the Bushveld Complex area.
- Domain B hosts lineaments occurring in the Transvaal rocks and have a very strong 020° orientation (Figure 6.10 B). This direction corresponds with the orientations of the dykes in the same domain (Figure 6.5 B), and also similar to trend (T) above. It can therefore be deduced that these lineaments probably represent dykes for which σ_3 will trend 290°.
- The lineaments of domain C trend more or less in a 050° direction and σ_3 is interpreted to be directed towards 320° (Figure 6.10 C). These directions correspond to directions obtained for the Olifants River dyke swarm (Figure 6.5 C).

Figure 6.10

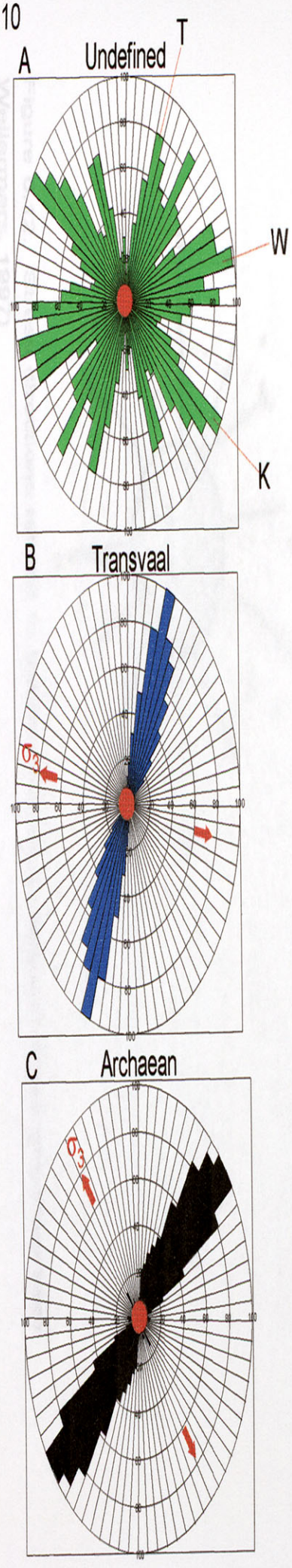

6.3 Stress analysis from Faults

Many different types of faults occur in the Bushveld Complex and surrounding areas. Anderson's (1951) theory of faulting was used to derive stress directions for the faults in the study area (Figure 6.11).

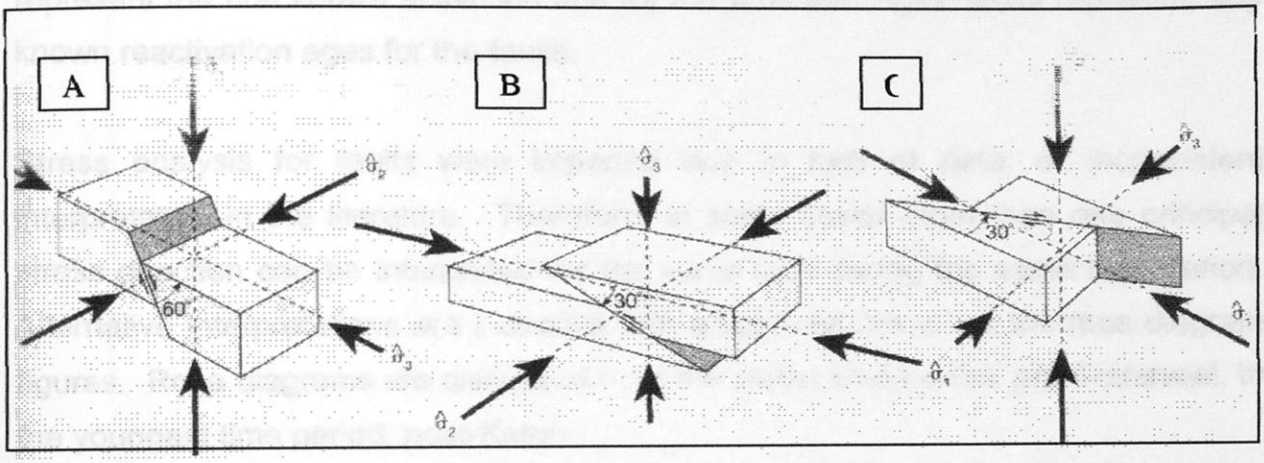

Figure 6.11. Anderson's (1951) theory of faulting, showing the relationship between the orientation of the principal stresses and the different ideal fault types. A. Normal fault with maximum compressive stress σ_1 vertical. B. Thrust fault with minimum compressive stress σ_3 vertical. C. Strike-slip fault with intermediate compressive stress σ_2 vertical (after Twiss and Moores, 1992).

Special consideration is necessary when analysing the stress directions for faults resulting from the intrusion of a magmatic dome, such as Pilanesberg. Generally faults will occur in a radial pattern around the intrusion (Figure 6.12). Principal stress direction, σ_1 and σ_2 might be vertical depending on the distance from the dome. Around the dome faults are the result of a vertical σ_2 and horizontal σ_1 and σ_3 (Figure 6.12).

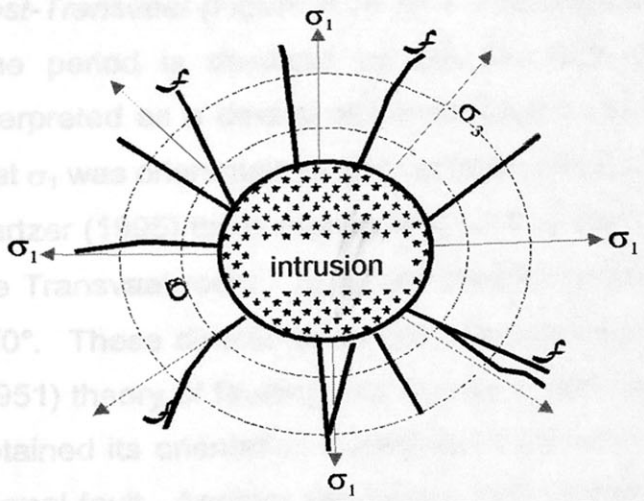

Figure 6.12. Stress directions related to the intrusion of a magmatic dome (modified from Weijermars, 1997)

Figure 6.13 is a geological map illustrating the distribution of faults present in the Bushveld Complex and surrounding areas. Rose diagrams of the orientation of the faults were generated according to various geological time periods. However, many faults are known to have been reactivated during geological history. Therefore, for each Bos area, rose diagrams of Age1 and Age2 faults are created. Age1 faults represent the first known activation age for the fault and Age2 faults represent any known reactivation ages for the faults.

Stress analysis for faults were impeded due to lack of data, or inconsistent interpretation in the literature. Therefore, in some cases more than one principal stress direction can be interpreted for the same fault during the same time period. Alternative interpretations are indicated with a light red colour on the rose diagram figures. Rose diagrams are discussed from the oldest time period, pre-Transvaal, to the youngest time period, post-Karoo.

6.3.1 Bos2

Fault Age1

Figure 6.14 shows a colour map of the faults for Age1 according to the various time periods they occur in, as well as a rose diagram of orientations of faults for each time period. Rose diagrams A through F show the stress orientation interpretation for each time period of Age1. They are interpreted as follows:

- *Pre-Transvaal (Figure 6.14 A)* - faults of this age in the Bos2 area include the Rietfontein fault system. This fault has been interpreted as a left-lateral strike-slip fault (Charlesworth et al., 1986) and therefore σ_1 will be orientated approximately 030°, σ_2 vertical, and σ_3 about 300°.
- *Post-Transvaal (Figure 6.14 B)* – The dominant faulting direction during this time period is depicted by the Rustenburg fault. The fault has been interpreted as a dextral strike-slip fault by Bumby (1997) and he suggested that σ_1 was orientated roughly at 340°, parallel to the D_2 direction proposed by Hartzer (1995) to be responsible for the interference fold pattern observed in the Transvaal rocks; σ_2 would then have been vertical and σ_3 orientated at 070°. These directions do not coincide with those predicted by Anderson's (1951) theory of faulting, but Bumby (1997) argued that the Rustenburg fault obtained its orientation during syn-Transvaal times when it was active as a normal fault. Another secondary fault pattern which is evident are the radial faults around the Johannesburg dome. It is possible that these faults reflect

Figure 6.13

Bosgis Fault Map

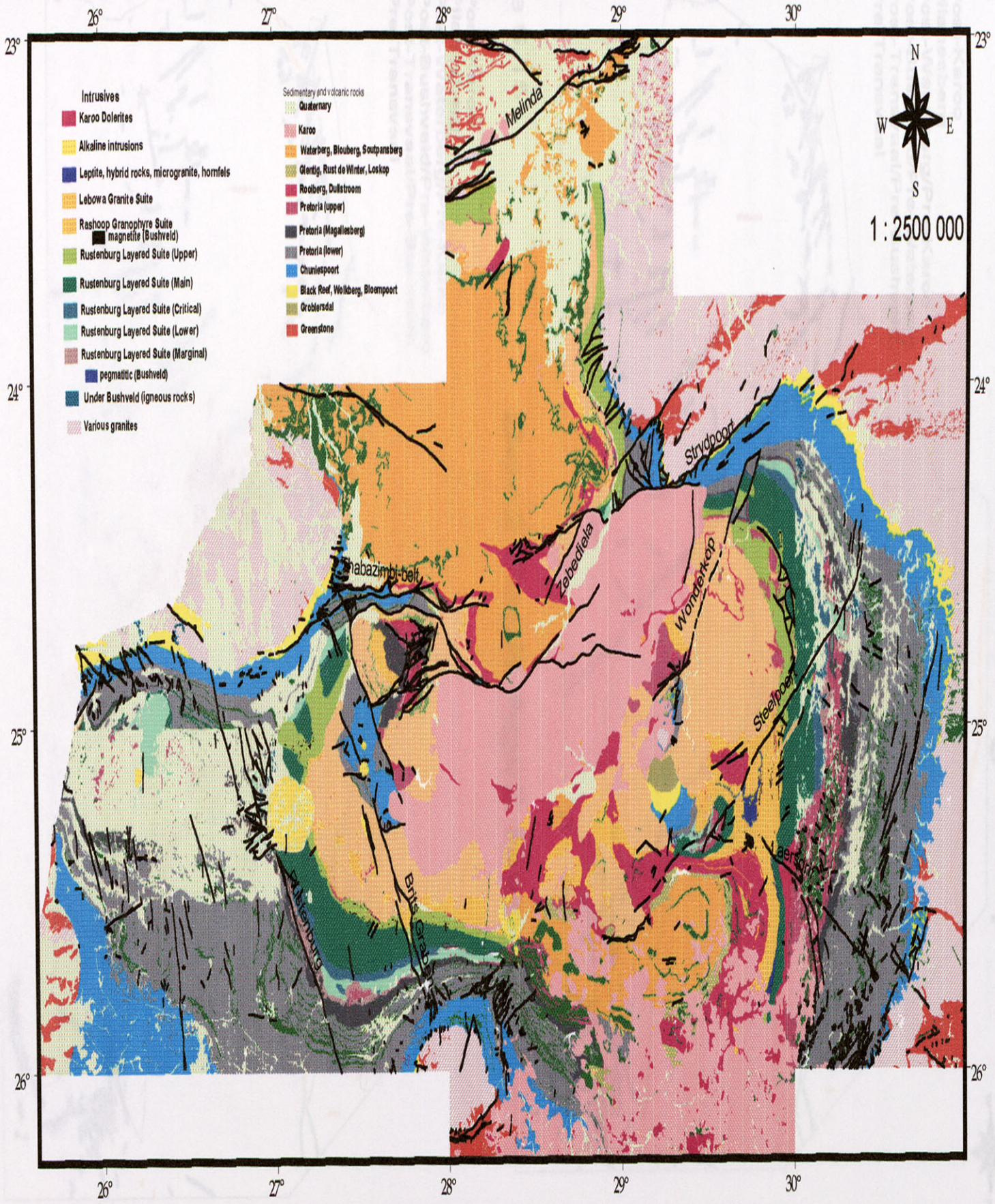

Figure 6.14

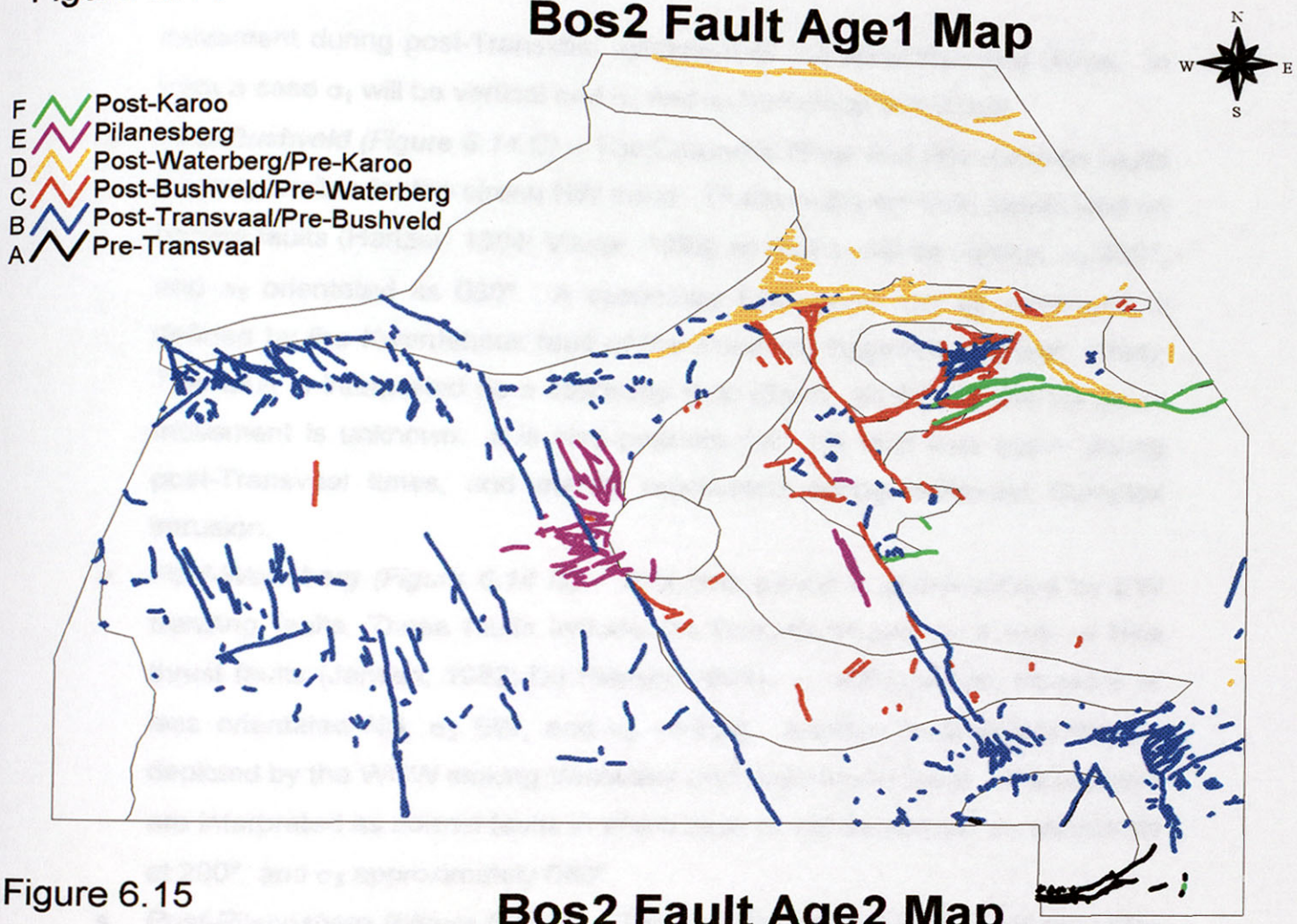

Figure 6.15

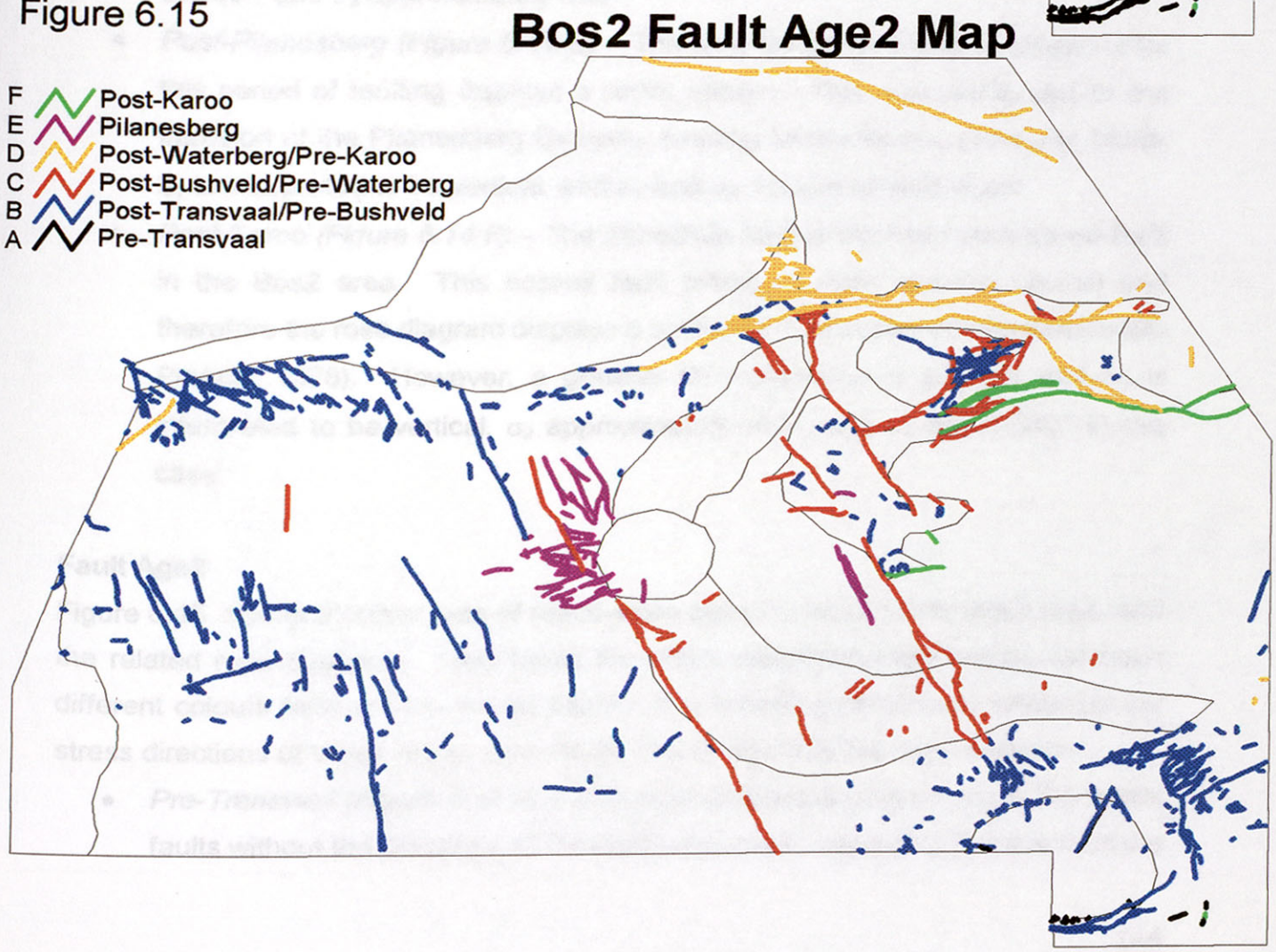

movement during post-Transvaal upliftment of the Johannesburg dome. In such a case σ_1 will be vertical and σ_2 and σ_3 horizontal and equal.

- *Post-Bushveld (Figure 6.14 C)* – The Crocodile River and Brits Graben faults are responsible for the strong NW trend. These faults are both interpreted as normal faults (Hartzer, 1994; Visser, 1998) so that σ_1 will be vertical, σ_2 330°, and σ_3 orientated as 060°. A secondary ENE trend can be seen and is defined by the Kwarriehoek fault of the Rooiberg fragment (Hartzer, 1994). This fault is interpreted as a strike-slip fault (Stear, 1976), but the sense of movement is unknown. It is also possible that this fault was active during post-Transvaal times, and merely reactivated during Bushveld Complex intrusion.
- *Post-Waterberg (Figure 6.14 D)* – This time period is characterized by EW trending faults. These faults include the Bobbejaanwater and Belt of Hills thrust faults (Jansen, 1982; Du Plessis, 1991); σ_1 will therefore be more or less orientated NS, σ_2 EW, and σ_3 vertical. Another faulting direction is depicted by the WNW striking Vaalwater and Boschpoort faults. These faults are interpreted as normal faults in which case σ_1 will be vertical, σ_2 orientated at 290°, and σ_3 approximately 040°.
- *Post-Pilanesberg (Figure 6.14 E)* – The rose diagram of fault orientations for this period of faulting displays a radial pattern. This is probably due to the intrusion of the Pilanesberg Complex causing tensional and strike-slip faults. σ_2 is interpreted to be vertical, and σ_1 and σ_3 horizontal and equal.
- *Post-Karoo (Figure 6.14 F)* – The Zebediela fault is the main post-Karoo fault in the Bos2 area. This normal fault follows a fairly sinuous course and therefore the rose diagram displays a scattered distribution of orientations (Du Plessis, 1978). However, a general NE orientation is present and σ_1 is interpreted to be vertical, σ_2 approximately 060°, and σ_3 about 330° in this case.

Fault Age2

Figure 6.15 shows a colour map of reactivation ages for faults in the Bos2 area, and the related rose diagrams. Only faults for which reactivation are known will have different colours from the Fault Age1faults. The following discussion interprets the stress directions of these reactivation faults as portrayed by the rose diagrams.

- *Pre-Transvaal (Figure 6.15 A)* – This rose diagram displays the pre-Transvaal faults without the presence of the Rietfontein fault, assuming that the fault did

Interpretation of stress directions of Bos2 Fault Age1

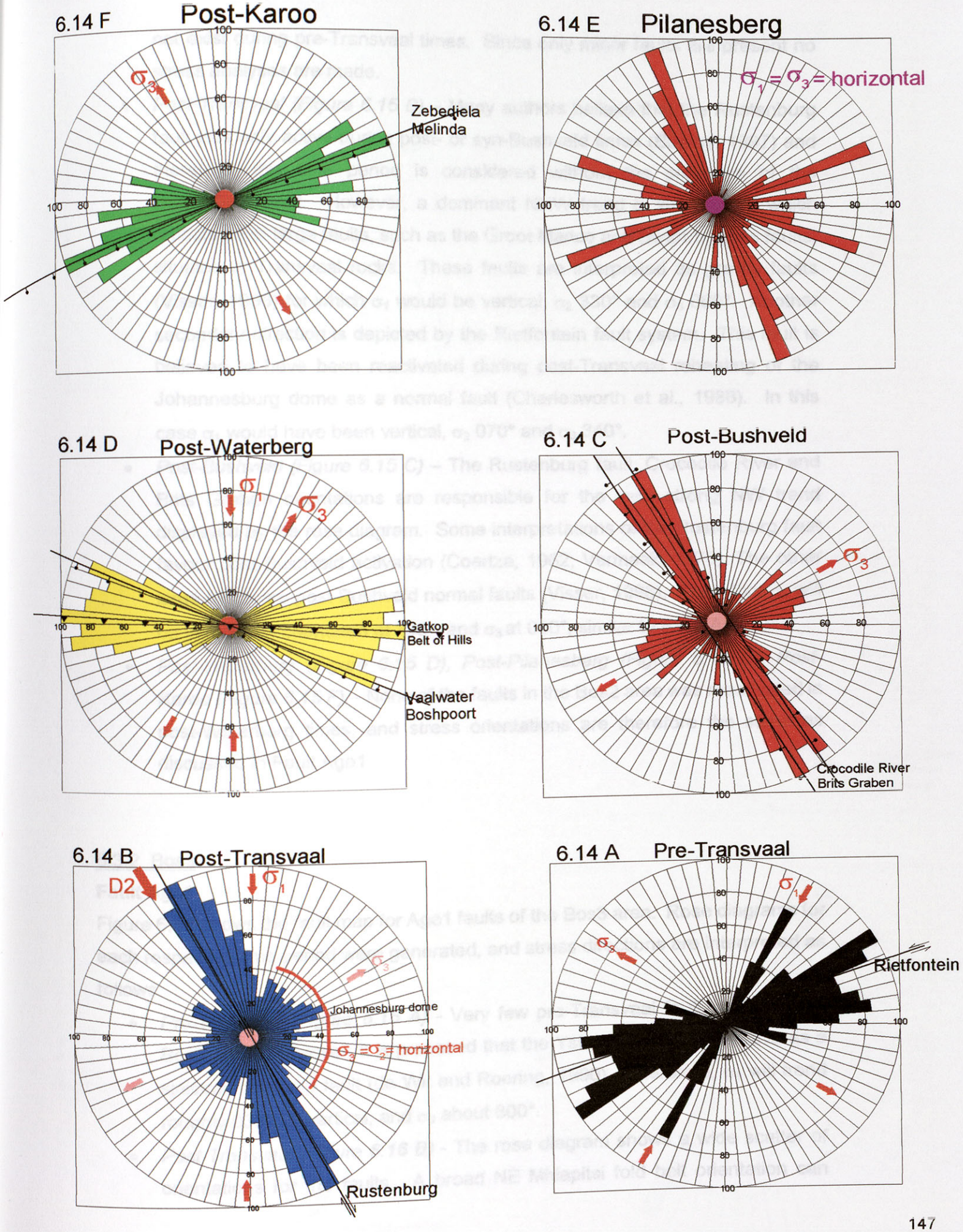

not exist during pre-Transvaal times. Since only minor faults are present no stress analyses are made.

- *Post-Transvaal (Figure 6.15 B)* – Many authors believe that the Rustenburg fault was only active during post- or syn-Bushveld times (Bumby, 1997) and therefore, this time period is considered without the presence of the Rustenburg fault. However, a dominant NNW trend is still present which reflects other large faults, such as the Groot Marico and Swartruggens faults, situated in Transvaal rocks. These faults are interpreted as gravity faults (Visser, 1998) for which σ_1 would be vertical, σ_2 330° and σ_3 060°. Another secondary direction is depicted by the Rietfontein fault system. This fault is believed to have been reactivated during post-Transvaal reheating of the Johannesburg dome as a normal fault (Charlesworth et al., 1986). In this case σ_1 would have been vertical, σ_2 070° and σ_3 340°.
- *Post-Bushveld (Figure 6.15 C)* – The Rustenburg fault, Crocodile River and Brits Graben orientations are responsible for the very strong NW trend displayed by the rose diagram. Some interpretations of the Rustenburg fault favour post-Bushveld activation (Coertze, 1962; Vermaak, 1970). The other large faults are post-Bushveld normal faults (Visser, 1998). Therefore σ_1 will be vertical, σ_2 orientated at 330°, and σ_3 at 060°, similar to Fault Age 1.
- *Post-Waterberg (Figure 6.15 D), Post-Pilanesberg (Figure 6.15 E), Post-Karoo (Figure 6.15 F),* - None of the faults in the Bos2 area was reactivated in post-Waterberg times, and stress orientations are therefore the same as discussed in Fault Age1.

6.3.2 Bos3

Fault Age1

Figure 6.16 shows the fault map for Age1 faults of the Bos3 area. Rose diagrams for each respective time period were generated, and stress directions are interpreted as follows:

- *Pre-Transvaal (Figure 6.16 A)* - Very few pre-Transvaal faults occur in the Bos3 area. However, it is proposed that the Ysterberg fault was active as a sinistral strike-slip fault (de Wit and Roering, 1990). Therefore, σ_1 will trend roughly 030°, σ_2 vertical, and σ_3 about 300°.
- *Post-Transvaal (Figure 6.16 B)* - The rose diagram shows a wide scatter of orientations for the faults. A broad NE Mhlapitsi fold belt orientation can

Interpretation of stress directions of Bos2 Fault Age2

6.15 F Post-Karoo

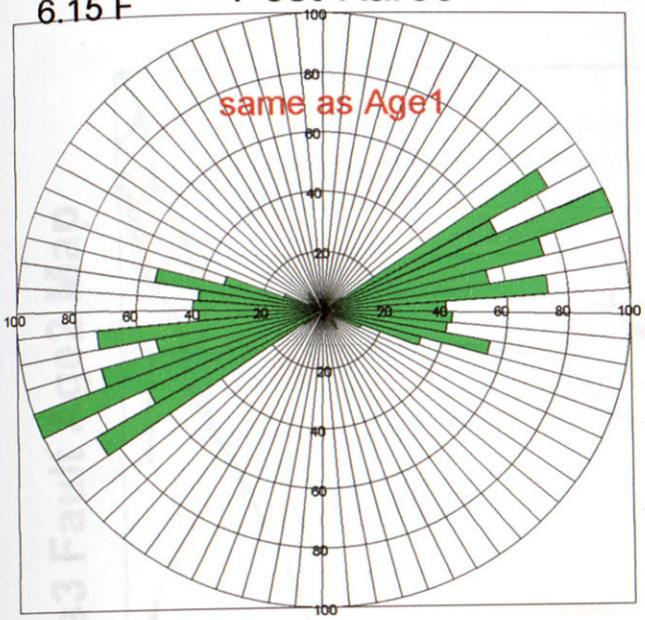

6.15 E Pilanesberg

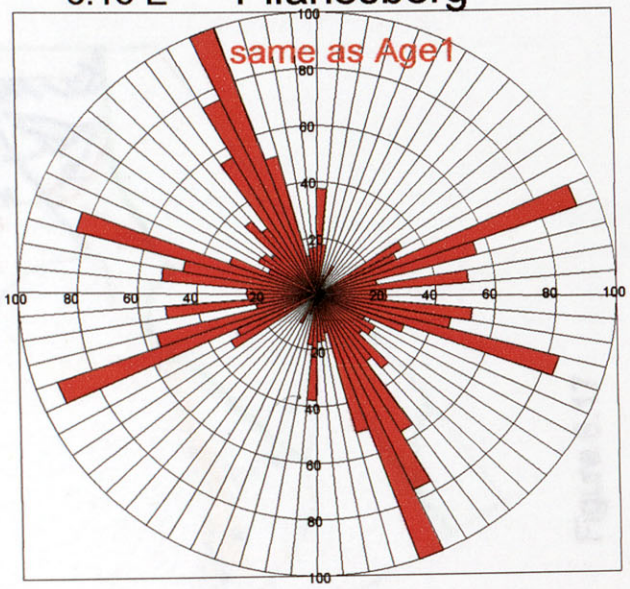

6.15 D Post-Waterberg

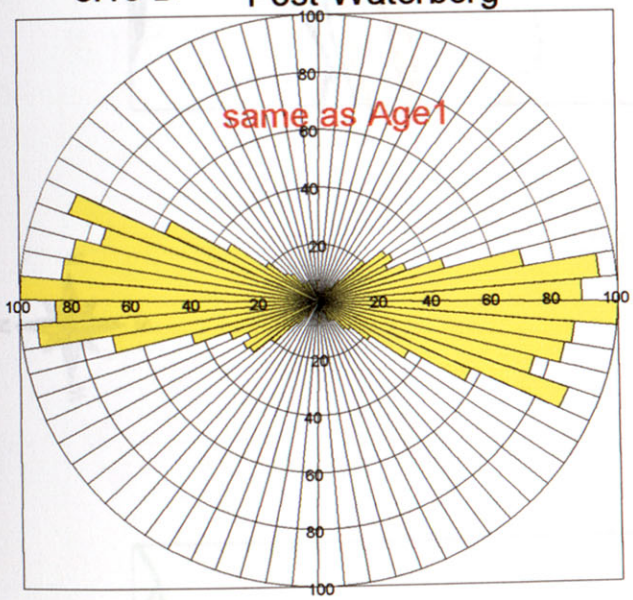

6.15 C Post-Bushveld

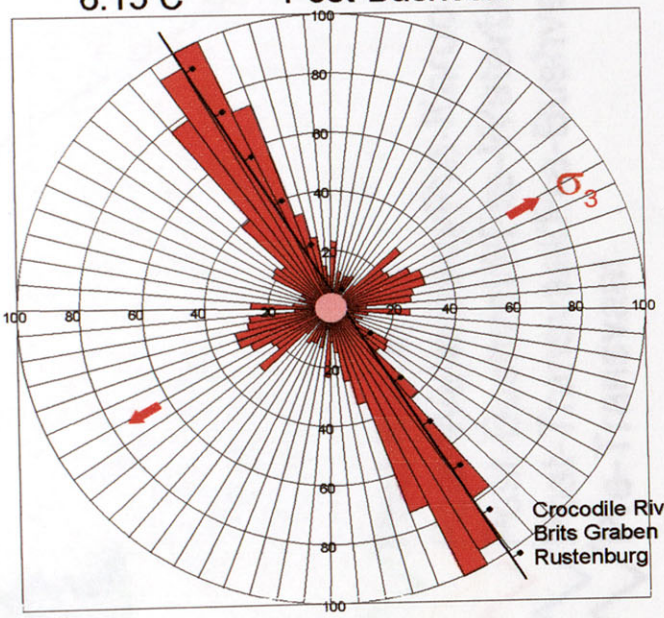

6.15 B Post-Transvaal

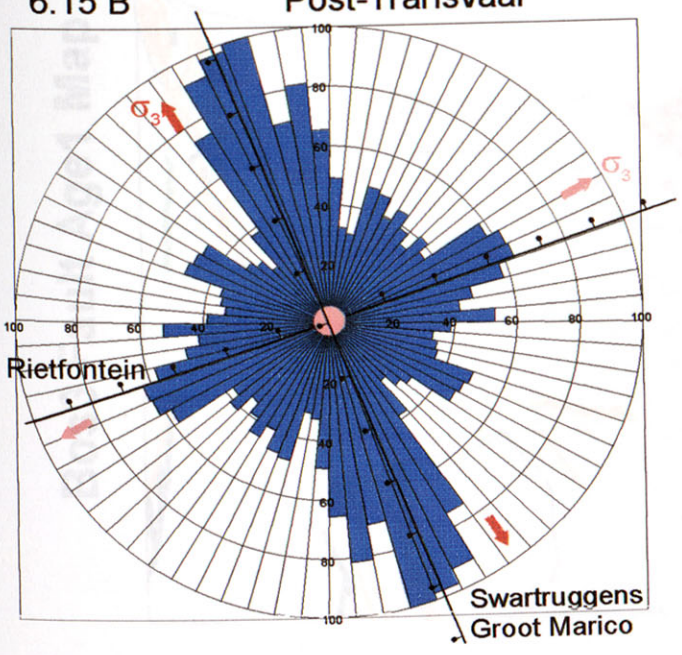

6.15 A Pre-Transvaal

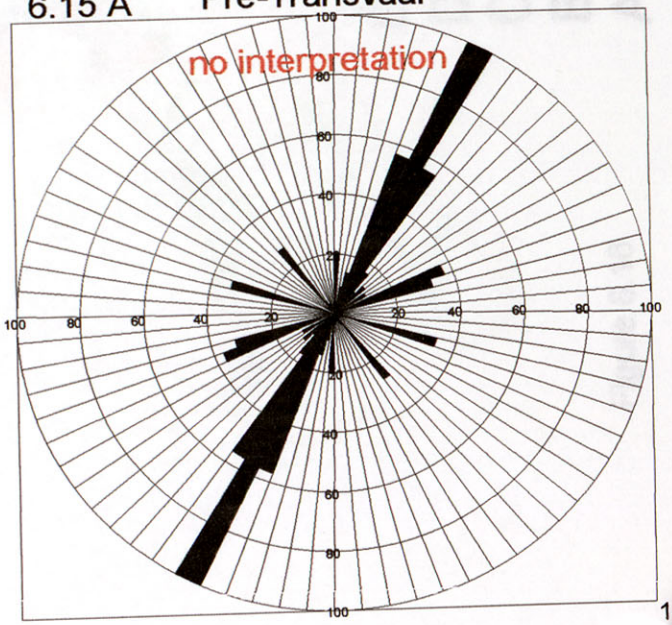

Figure 6.16

Figure 6.17

E Post Karoo
D Post-Waterberg/Pre-Karoo
C Post-Bushveld/Pre-Waterberg
B Post-Transvaal/Pre-Bushveld
A Pre-Transvaal

Interpretation of stress orientations for Bos3 Age1

6. 16 E Post-Karoo

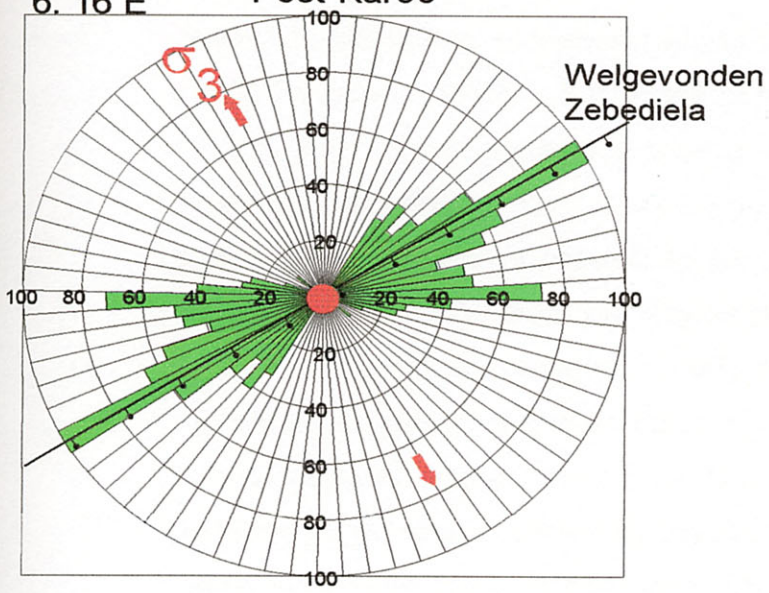

6. 16 D Post-Waterberg

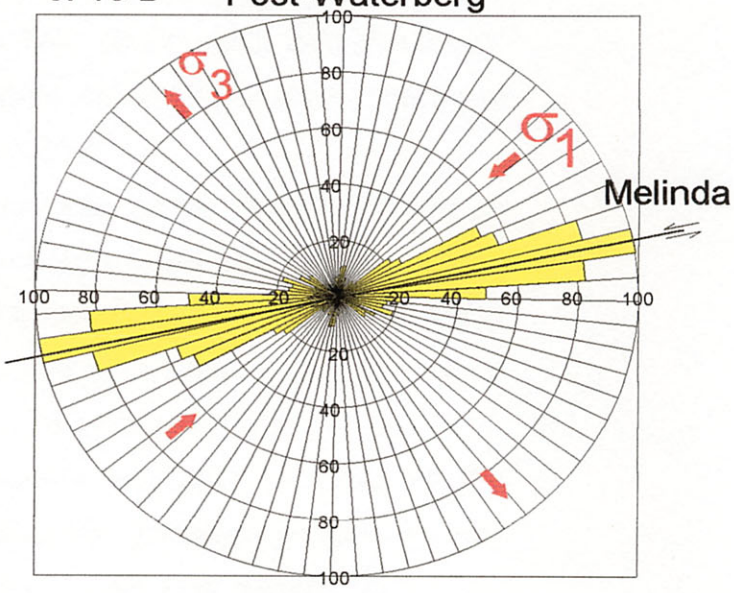

6. 16 C Post-Bushveld

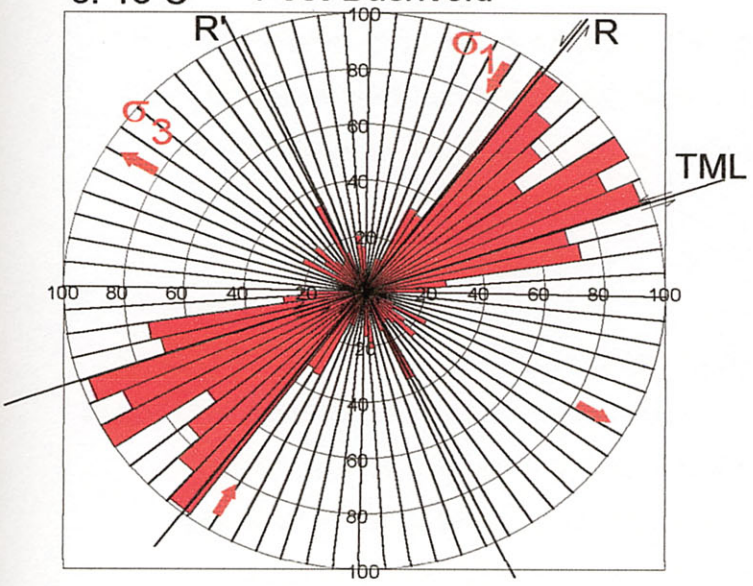

6. 16 B Post-Transvaal

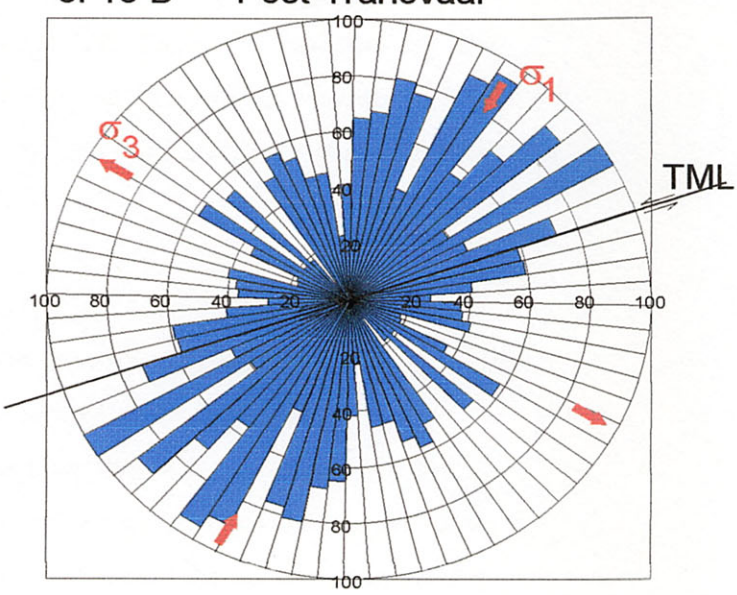

6. 16 A Pre-Transvaal

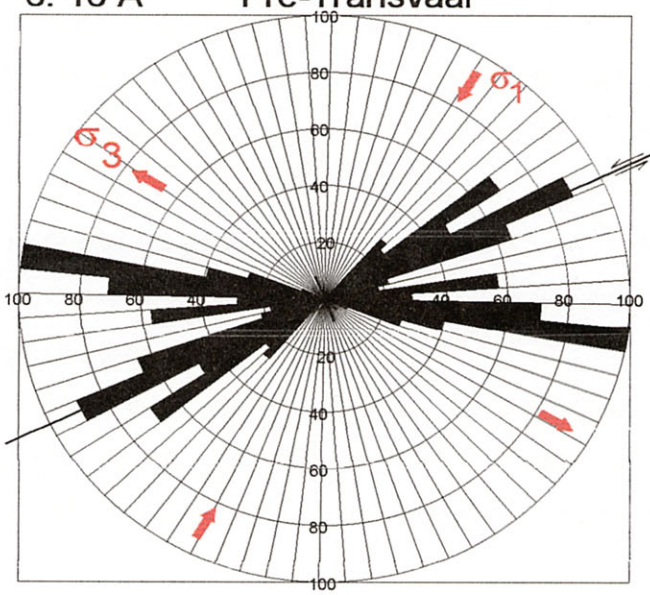

however be recognized. Other main faults could be conjugate strike-slip faults related to left-lateral movement along the TML (Du Plessis and Walraven, 1990; Potgieter, 1992). For these conjugate strike-slip faults σ_1 will trend roughly 030°, σ_2 vertical, and σ_3 orientated at 330°.

- *Post-Bushveld (Figure 6.16 C)* - The northern lobe of the Bushveld Complex contains several NE orientated faults as can be seen by the orientations displayed on the rose diagram. These faults are interpreted as Riedel shears related to left-lateral movement along the TML (Du Plessis, 1991). σ_1 will therefore be orientated around 030°, σ_2 vertical, and σ_3 at 300°.
- *Post-Waterberg (Figure 6.16 D)* - The Melinda fault is responsible for the dominant ENE trend depicted by the rose diagram. The Melinda fault is a left-lateral strike-slip fault (Brandl and Reimold, 1990) and would have been caused by a σ_1 orientated approximately 050°, a vertical σ_2 , and a σ_3 trending 320°.
- *Post-Karoo (Figure 6.16 E)* - the dominant NE trend is caused by the Zebediela and Welgevonden faults. These normal faults (Du Plessis, 1978) would have been caused by a vertical σ_1, σ_2 directed 070°, and σ_3 directed 340°.

Fault Age2

Figures 6.17 A-E shows the reactivation ages of the Bos3 faults where known. The stress directions for the reactivation histories are interpreted as follows:

- *Pre-Transvaal (Figure 6.17 A)* – If the Ysterberg fault was not active during pre-Transvaal times, the orientation of other supposedly pre-Transvaal faults are depicted by Figure 6.17 A. It is uncertain whether these are truly of pre-Transvaal age or if they are younger. Also, since only minor faults are present no stress orientations were interpreted.
- *Syn-Transvaal (Figure 6.17 B)* - This time period is characterized by the post-Chuniespoort/pre-Pretoria reactivation of the Ysterberg fault. The fault is suggested to have been a thrust fault (Potgieter, 1992) and therefore, σ_1 would have been orientated at 330°, σ_2 060°, and σ_3 vertically.
- *Post-Bushveld (Figure 6.17 C)* – Stress orientations for this time period is the same as Fault Age1(Figure 6.16 C).
- *Post-Waterberg (Figure 6.17 D)* – The main faulting directions of this time period are depicted by the Abbotspoort and Welgevonden faults. The possibly left-lateral Abbotspoort fault (McCourt and Vearncombe, 1992) would

Interpretation of stress orientations for Bos3 Age2

6. 17 E Post-Karoo

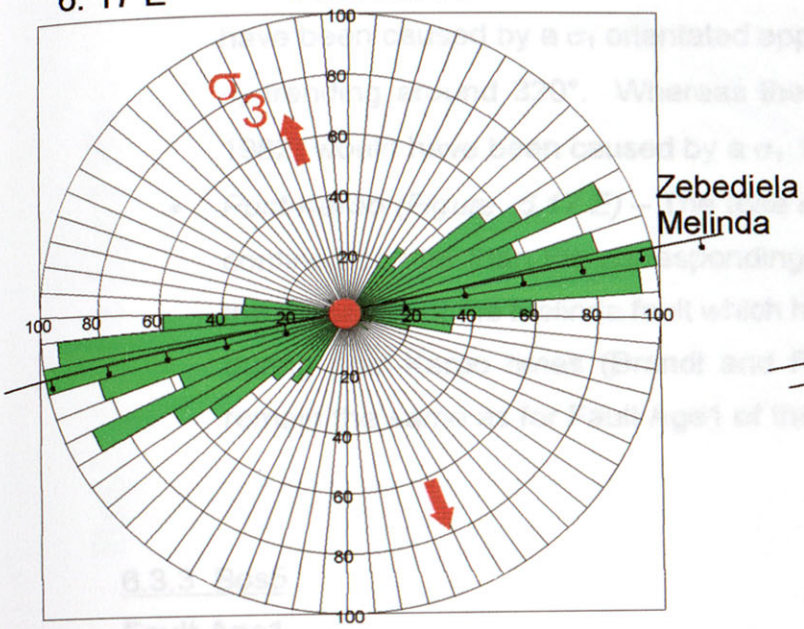

6. 17 D Post-Waterberg

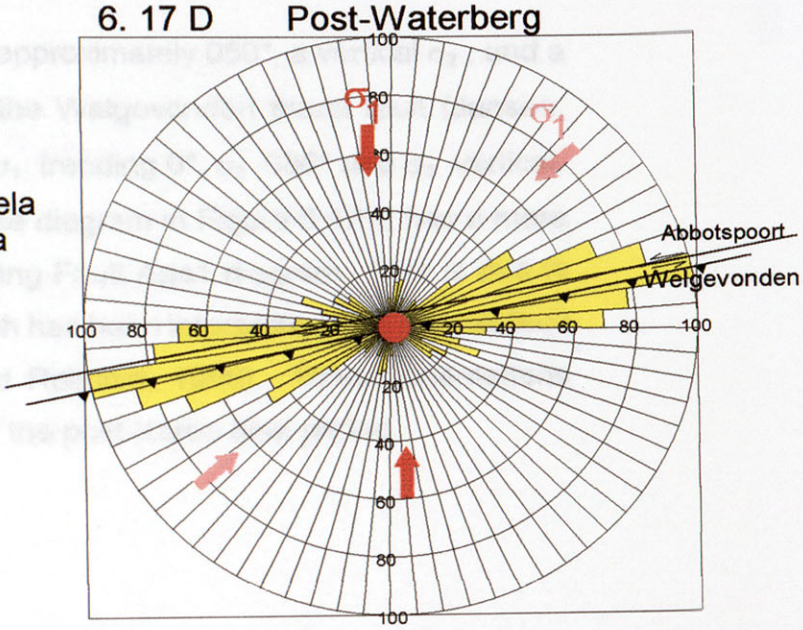

6. 17 C Post-Bushveld

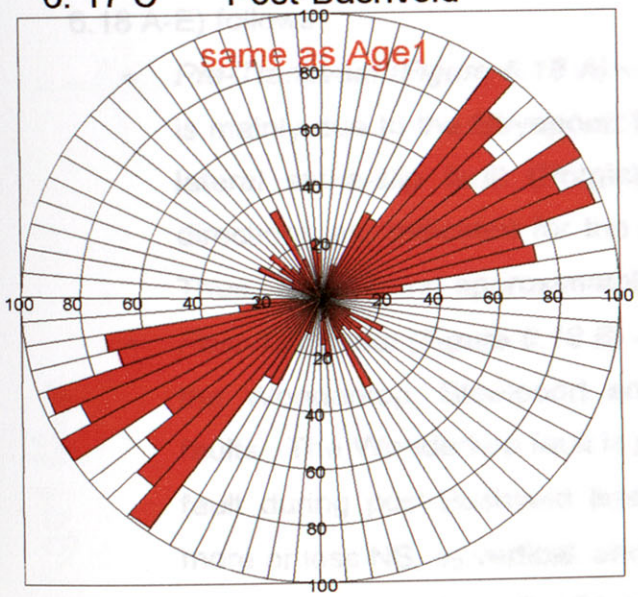

6. 17 B Syn-Transvaal

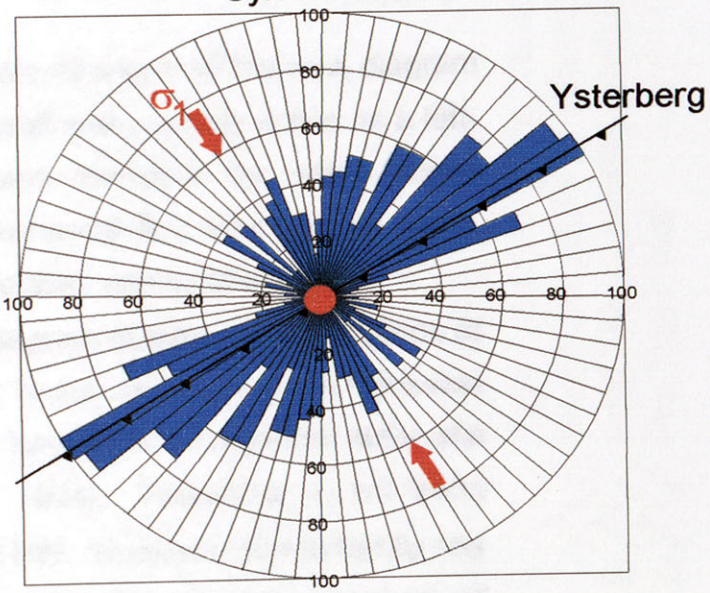

6. 17 A Pre-Transvaal

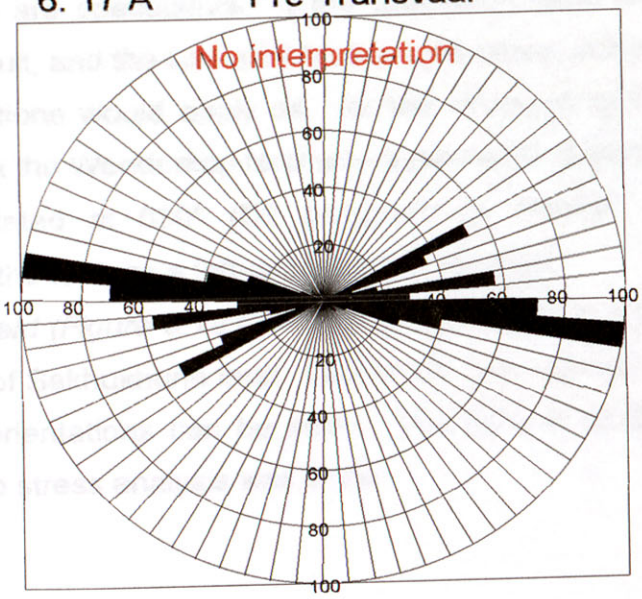

have been caused by a σ_1 orientated approximately 050°, a vertical σ_2 , and a σ_3 trending around 320°. Whereas the Welgevonden thrust fault (Jansen, 1982) would have been caused by a σ_1 trending 0°, σ_2 080° and σ_3 vertical.

- *Post-Karoo (Figure 6.17 E)* – The rose diagram in Figure 6.17 E has a more confined scatter than the corresponding Fault Age1 diagram. This is due to the presence of the Melinda fault which has been interpreted as a normal fault during post-Karoo times (Brandl and Reimold, 1990). Stress orientations remain the same as for Fault Age1 of the post-Karoo time period.

6.3.3 Bos5

Fault Age1

Figure 6.18 shows the fault map and rose diagrams of fault orientations of the Bos5 area. A discussion of the stress directions derived from the rose diagrams (Figures 6.18 A-E) follows:

- *Pre-Transvaal (Figure 6.18 A)* – The dominant direction on the rose diagram is mainly due to the Strydpoort fault. This fault was possibly active as a left-lateral strike-slip fault (Potgieter, 1992) and therefore the same stress directions as indicated for the other pre-Transvaal Bos areas would apply. Thus, σ_1 will trend approximately 020°, σ_2 vertical, and σ_3 trends 290°.
- *Post-Transvaal (Figure 6.18 B)* –The rose diagram depicts the orientations of the Wonderkop, Steelpoort and Laersdrif faults as active post-Transvaal faults. The Wonderkop fault is proposed to have been a left-lateral strike-slip fault during post-Bushveld times (Hartzer, 1994). Therefore, σ_1 will trend more or less NS, σ_2 vertical, and σ_3 directed EW. However, due to hardly any published research on the Steelpoort and Laersdrif faults, stress analyses of these faults are speculative. If the Steelpoort fault was also a left-lateral strike-slip fault, and the Laersdrif fault a right-lateral strike-slip fault, the same stress directions would apply as for the Wonderkop fault. However, it is possible that the Wonderkop fault was a pre-existing weakness, in which case a σ_1 orientated at 030° (D2 proposed by Hartzer, 1994) would have reactivated the fault as a left-lateral strike-slip fault.
- *Post-Bushveld (Figure 6.18 C)* – The rose diagram is a representation of the orientation of Sekhukhune fault. Due to the sinuous nature of the fault a wide scatter of orientations can be seen. The type of faulting is unknown and therefore no stress analysis was done.

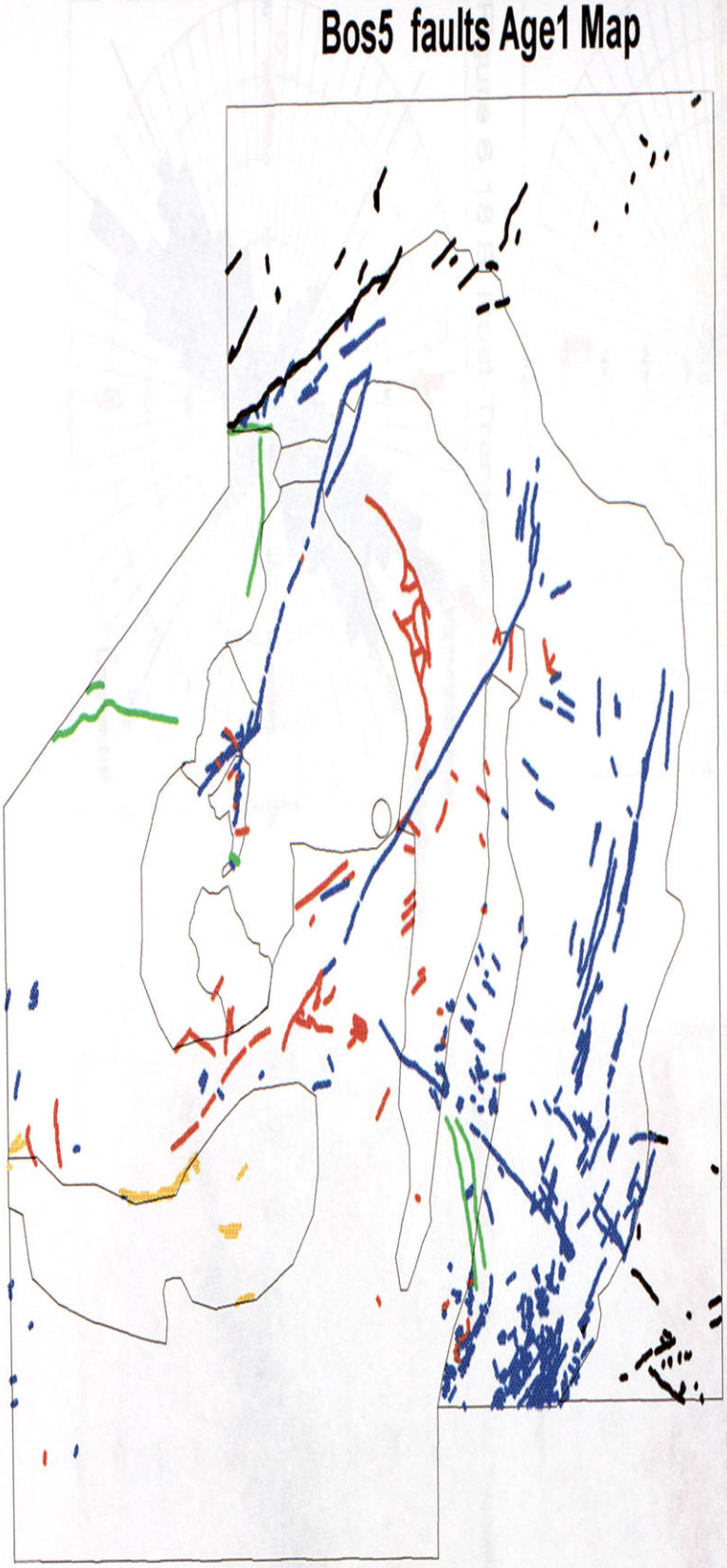

Figure 6.18

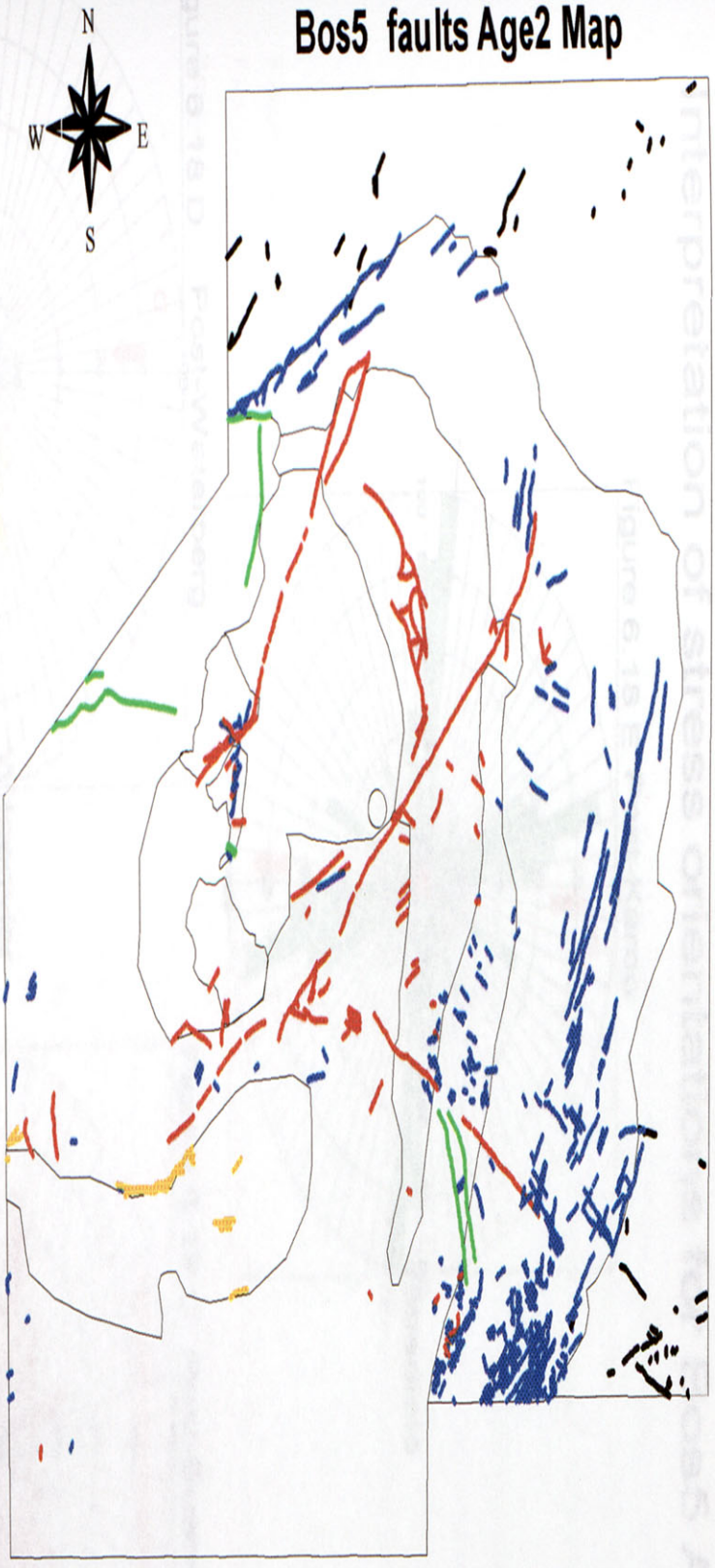

Figure 6.19

E Post Karoo
D Post Waterberg/Pre Karoo
C Post Bushveld/Pre Waterberg
B Post Transvaal/Pre Bushveld
A Pre Transvaal

Interpretation of stress orientations for Bos5 Age1

Figure 6.18 E Post-Karoo

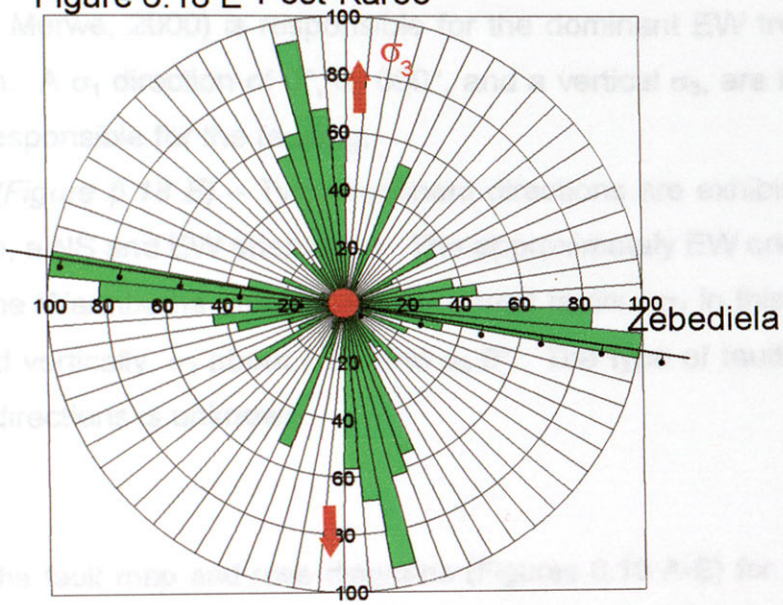

Figure 6.18 D Post-Waterberg

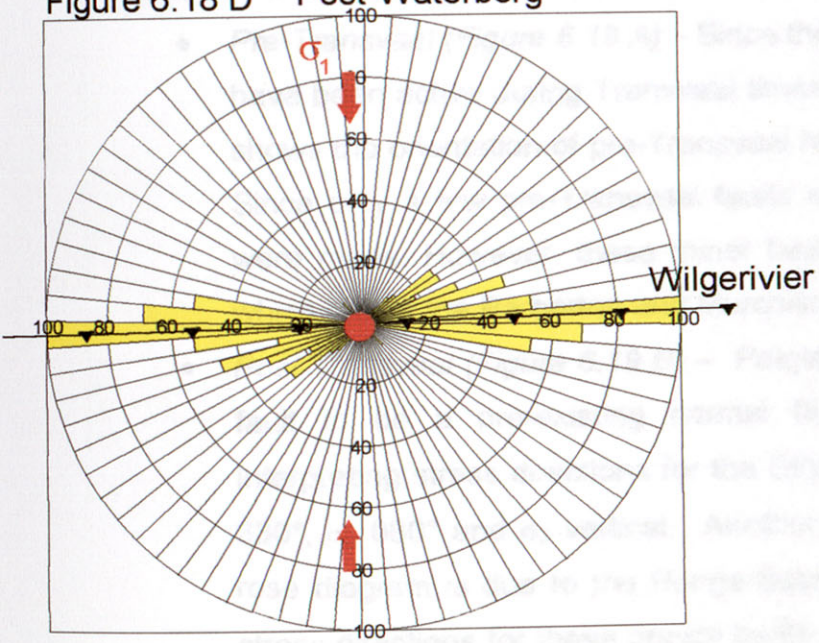

Figure 6.18 C Post-Bushveld

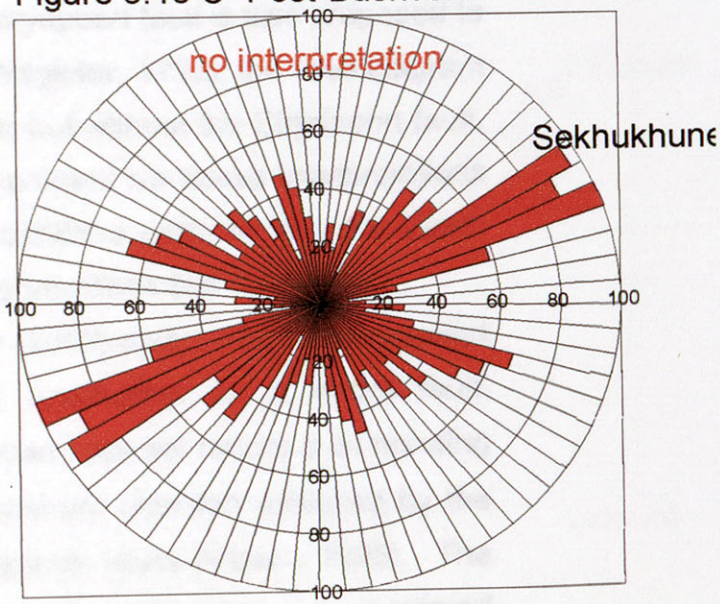

Figure 6.18 B Post-Transvaal

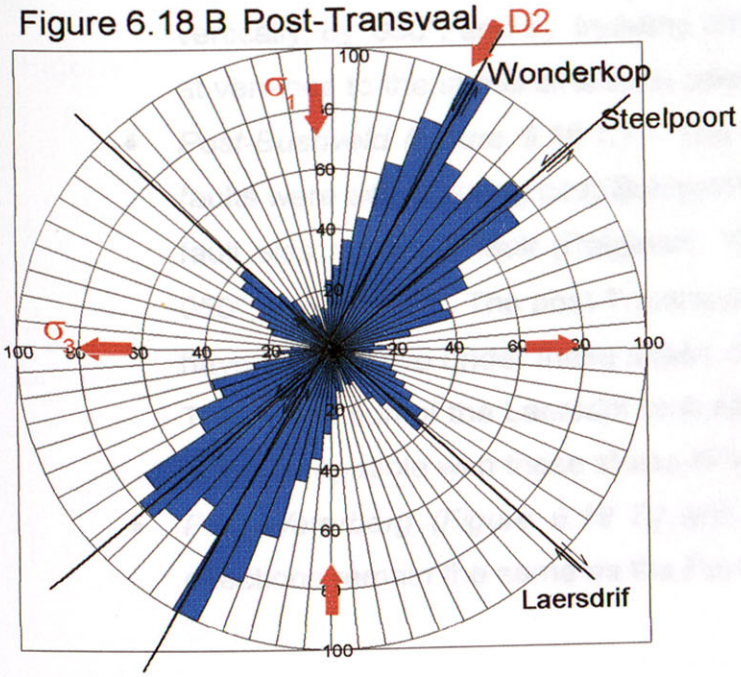

Figure 6.18 A Pre-Transvaal

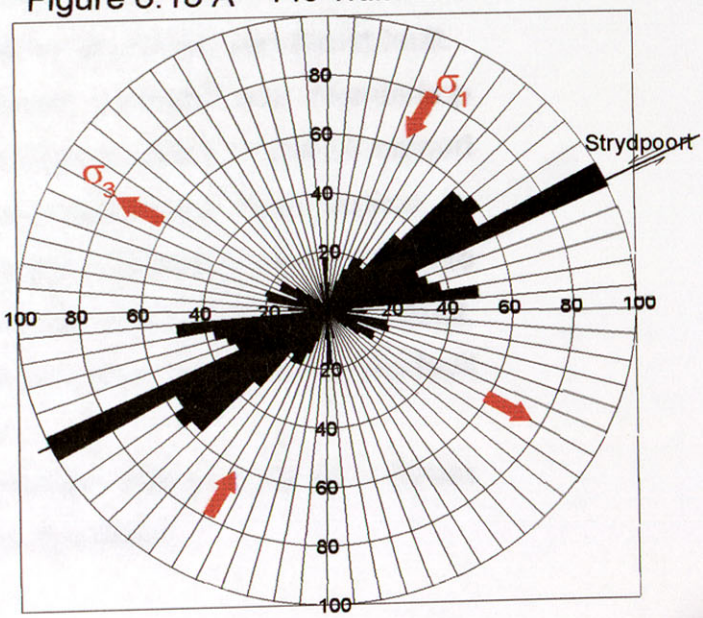

- *Post-Waterberg (Figure 6.18 D)* – The Wilgerivier thrust fault (Van der Neut and Van der Merwe, 2000) is responsible for the dominant EW trend in the rose diagram. A σ_1 direction of 0°, σ_2 090°, and a vertical σ_3, are inferred to have been responsible for the faulting.
- *Post-Karoo (Figure 6.18 E)* – Two prominent directions are exhibited by the rose diagram, a NS and EW orientation. The approximately EW orientation is the due to the Warmbaths and Zebediela normal faults. σ_1 in this case will be orientated vertically, σ_2 about EW, and σ_3 0°. The type of faulting for the NS faulting directions is unknown.

Fault Age2

Figure 6.19 shows the fault map and rose diagrams (Figures 6.19 A-E) for reactivated faults in the Bos5 area. Stress directions for these faults are interpreted as follows:

- *Pre-Transvaal (Figure 6.19 A)* – Since the Strydpoort fault is also proposed to have been active during Transvaal times (Potgieter, 1992), the rose diagram shows the orientation of pre-Transvaal faults but without the Strydpoort fault. Since only a few pre-Transvaal faults are present no stress interpretations were made. However, these minor faults exhibit a more or less NE trend, which reflect the Barberton and Murchison greenstone belt directions.
- *Post-Transvaal (Figure 6.19 B)* – Potgieter (1992) suggested the Strydpoort fault to be a pre-existing normal fault, reactivated as a thrust fault. Interpreting stress directions for the Strydpoort fault will render a σ_1 trending 330°, σ_2 060° and σ_3 vertical. Another dominant direction exhibited by the rose diagram is due to the Penge-Sabie gravity faults (Visser, 1998). The stress directions for these gravity faults are interpreted to be a σ_1, orientated vertically, σ_2 030°, and σ_3 trending 300°. These stress directions are clearly at variance to the stress directions interpreted for the Strydpoort thrust fault.
- *Post-Bushveld (Figure 6.19 C)* – The Steelpoort, Laersdrif and Wonderkop faults were active during post-Bushveld times (Visser, 1998). If the Steelpoort fault was a normal fault (Potgieter, 1992), σ_1 would have been vertical, σ_2 050°, and σ_3 320°. The post-Transvaal strike-slip Wonderkop fault could also have been active under these stress directions as a reactivated normal fault. The orientation of the Laersdrif fault either as a normal or as a strike-slip fault is not compatible with these stress directions.
- *Post-Waterberg (Figure 6.19 D)* and *Post-Karoo (Figure 6.19 E)* - Stress directions remain the same as the Fault Age1 directions.

Interpretation of stress orientations for Bos5 Age2

Figure 6.19 E Post-Karoo

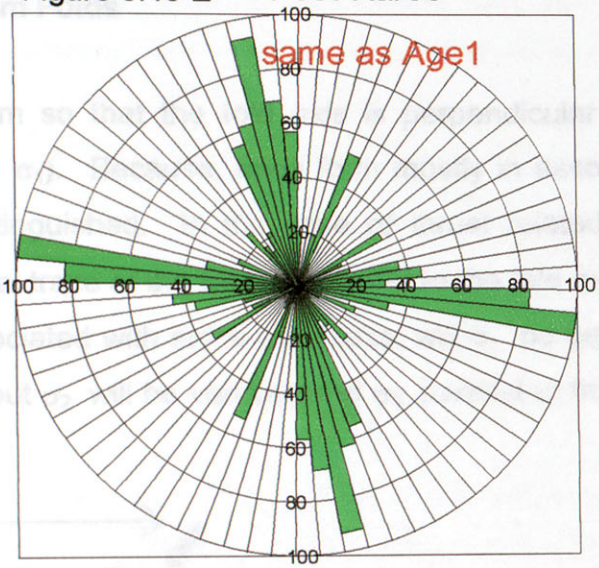

Figure 6.19 D Post-Waterberg

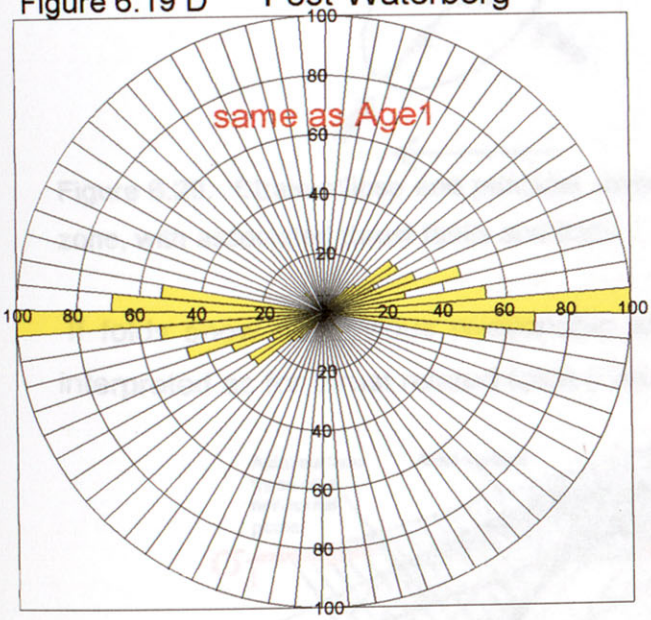

Figure 6.19 C Post-Bushveld

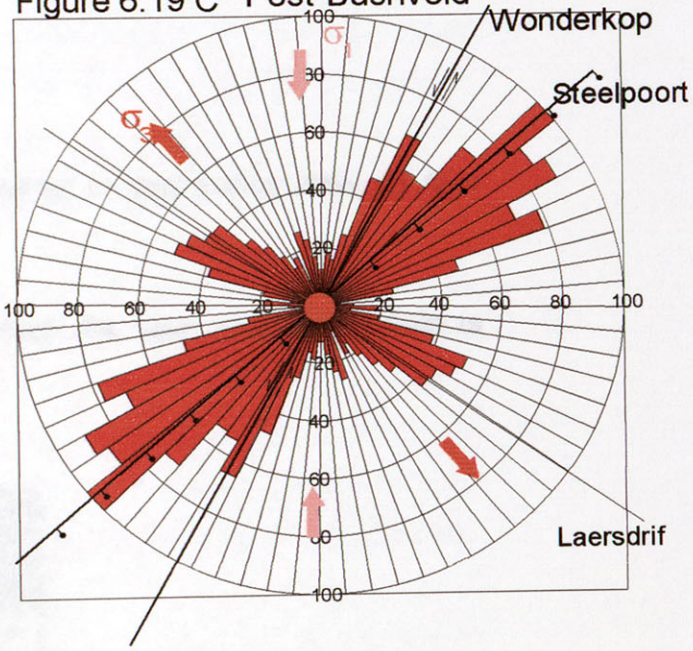

Figure 6.19 B Post-Transvaal

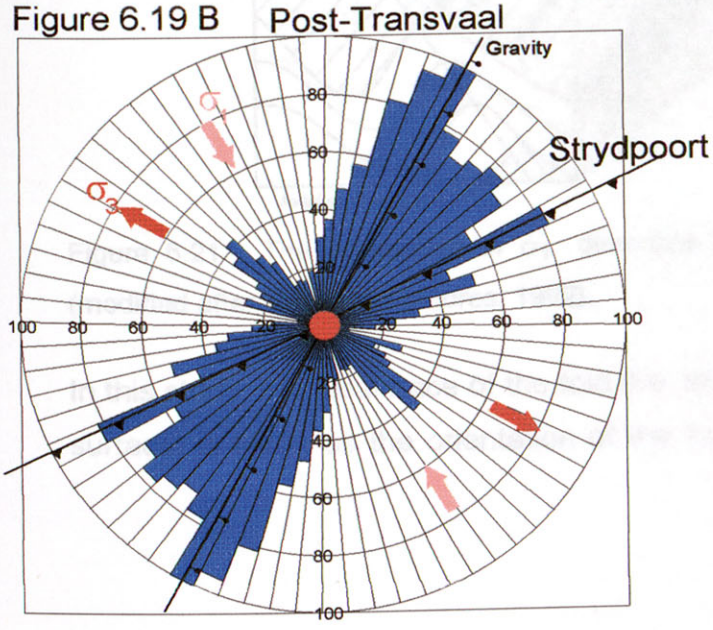

Figure 6.19 A Pre-Transvaal

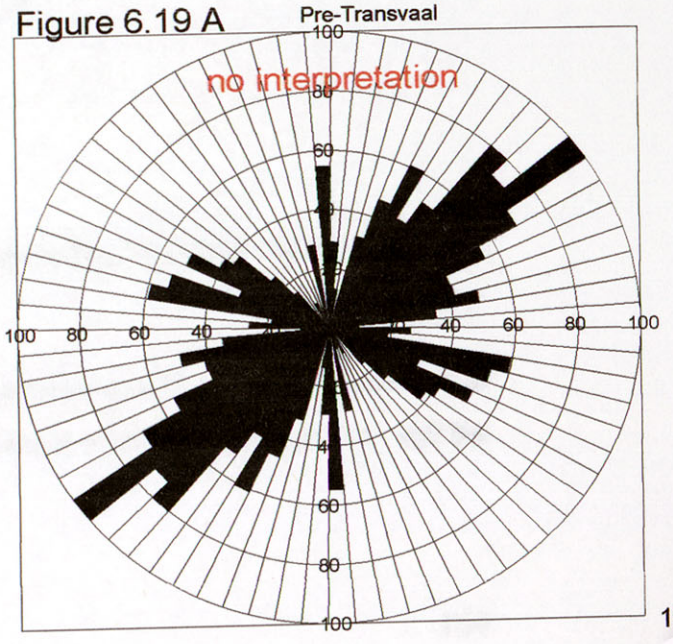

6.4 Stress analysis from Folds

Folds will generally form so that the fold axis is perpendicular to the maximum compressive stress (i.e. σ_1). Because, folds form mostly in association with faults two cases may be distinguished. In the case of thrust related folds, will σ_1 be perpendicular to the axial trace of the fold, σ_2 parallel to the fold axis, and σ_3 vertical. However, for folds associated with strike-slip faults, will σ_1 be perpendicular to the axial trace of the fold, but σ_2 will be vertical, and σ_3 parallel to the fold axis (Figure 6.20).

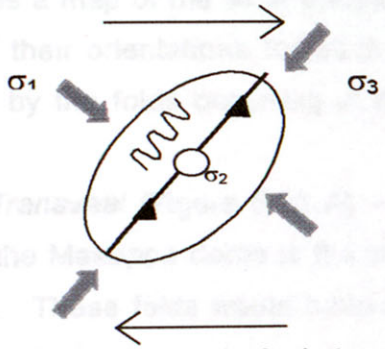

Figure 6.20. Strain ellipse and principal stress directions for an ideal dextral strike-slip fault zone, with associated thrust faults and folds.

If folds show no obvious relationship to faults, then the causative stress field is interpreted as for thrust related folds (Figure 6.21).

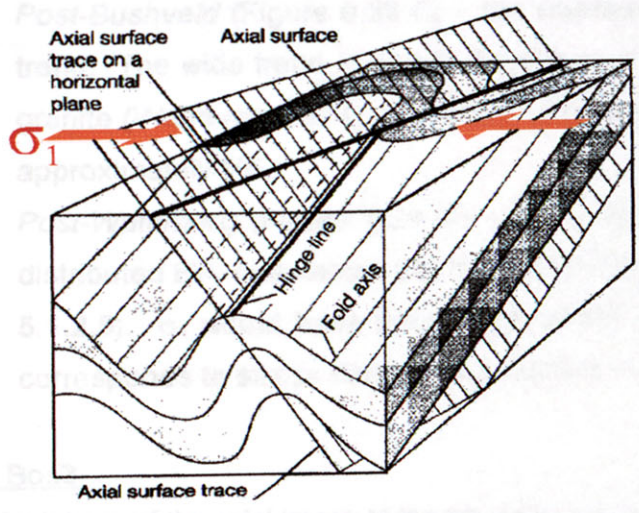

Figure 6.21. The orientation of σ_1 directions as interpreted for folds during this study (modified after Twiss and Moores, 1992).

In this study, the axial trace of the fold (i.e. the intersection of the axial plane with the surface) is taken as the orientation of the fold (Figure 6.21). Therefore, σ_1 will be

horizontal for both thrust and strike-slip fault related folds and also for non-fault related folds. Only σ_1 directions are mentioned and indicated on the figures.

Axial traces of folds occurring in the Bushveld Complex and surrounding areas are illustrated in Figure 6.22. Stress orientations for the folds are interpreted according to the Bos area they occur in, and according to the various time periods during which the folds formed.

6.4.1 Bos2

Figure 6.23 is a map of the axial traces of folds as well as the corresponding rose diagrams of their orientations for each folding period. Four fold generations are represented by the folds occurring in the Bos2 area, and they are interpreted as follows:

- *Pre-Transvaal* (Figure 6.23 A) – Some authors believe (e.g. Hunter, 1974) that the Makoppa dome is the product of NW and NE trending interference folds. These folds would have been caused by σ_1 orientated NE and NW respectively.
- *Post-Transvaal* (Figure 6.23 B) – The same two folding directions as discussed above characterizes the post-Transvaal folds, especially the folds present in the Transvaal inliers (Hartzer, 1995). These folds are also the response to σ_1 orientated NE (D1) and NW (D2) respectively, (Hartzer, 1995).
- *Post-Bushveld* (Figure 6.23 C) – the orientation of folds define a broad NW trend. The wide trend is due to the sinuous folds contained in the Bushveld granite (Walraven, 1974). σ_1 for this folding event is inferred to be orientated approximately NE.
- *Post-Waterberg* (Figure 6.23 D) – these folds are orientated in a narrowly distributed EW orientation, but the age of the folds are not well constraint (see 5.1.2.5). σ_1 would have been directed NS during this folding event, which corresponds to stress directions analysed for faults during this time period.

6.4.2 Bos3

The orientations of the axial traces of the few folds present in the Bos3 area are illustrated in Figure 6.24 and the corresponding rose diagram. A few small NE trending Mhlapitsi folds occur in the Transvaal rocks, for which σ_1 trends 320°. The principal stress direction for the formation of the post-Waterberg folds is inferred to be a NS directed σ_1.

Figure 6.22

Bosgis Fold Map

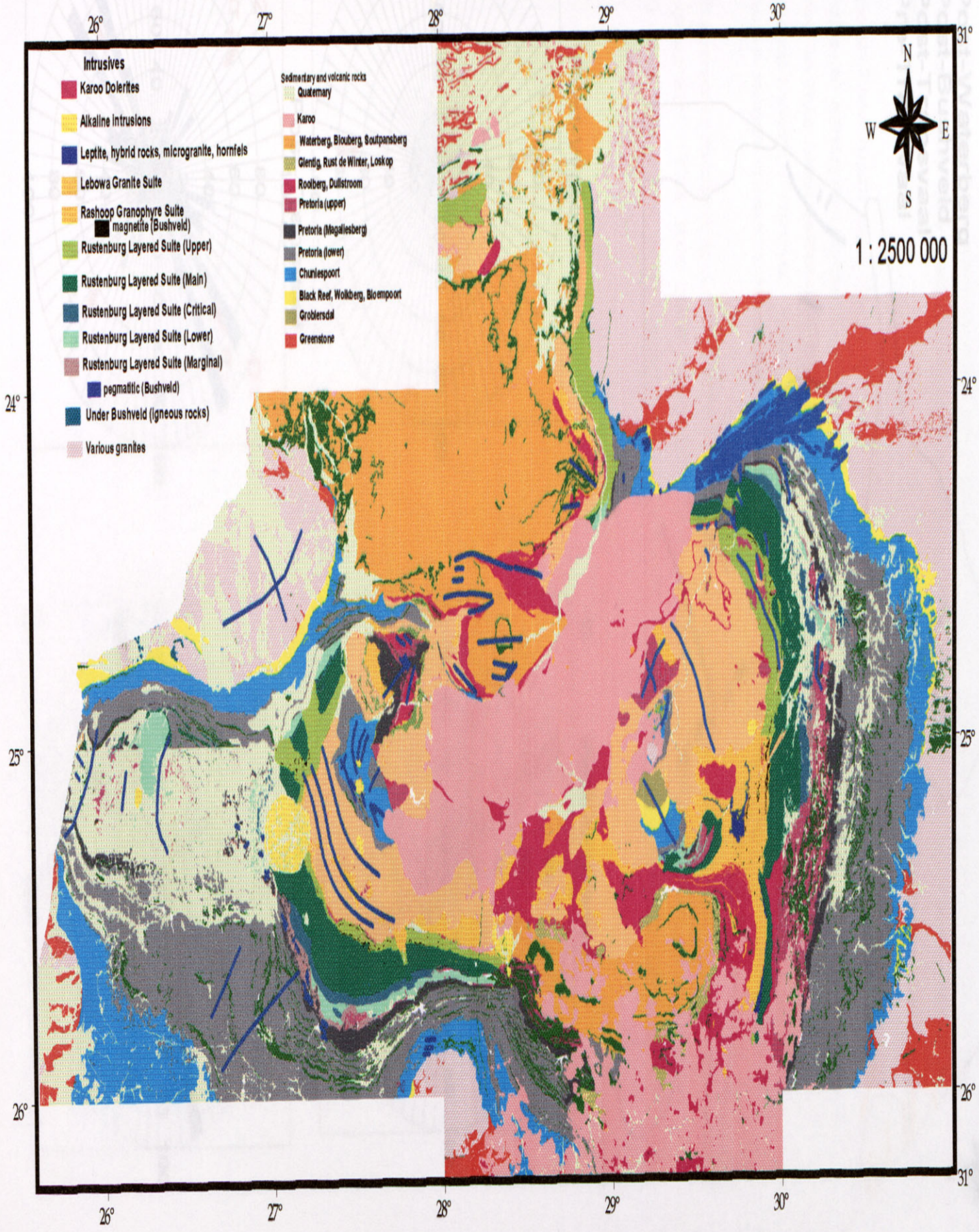

Figure 6.23

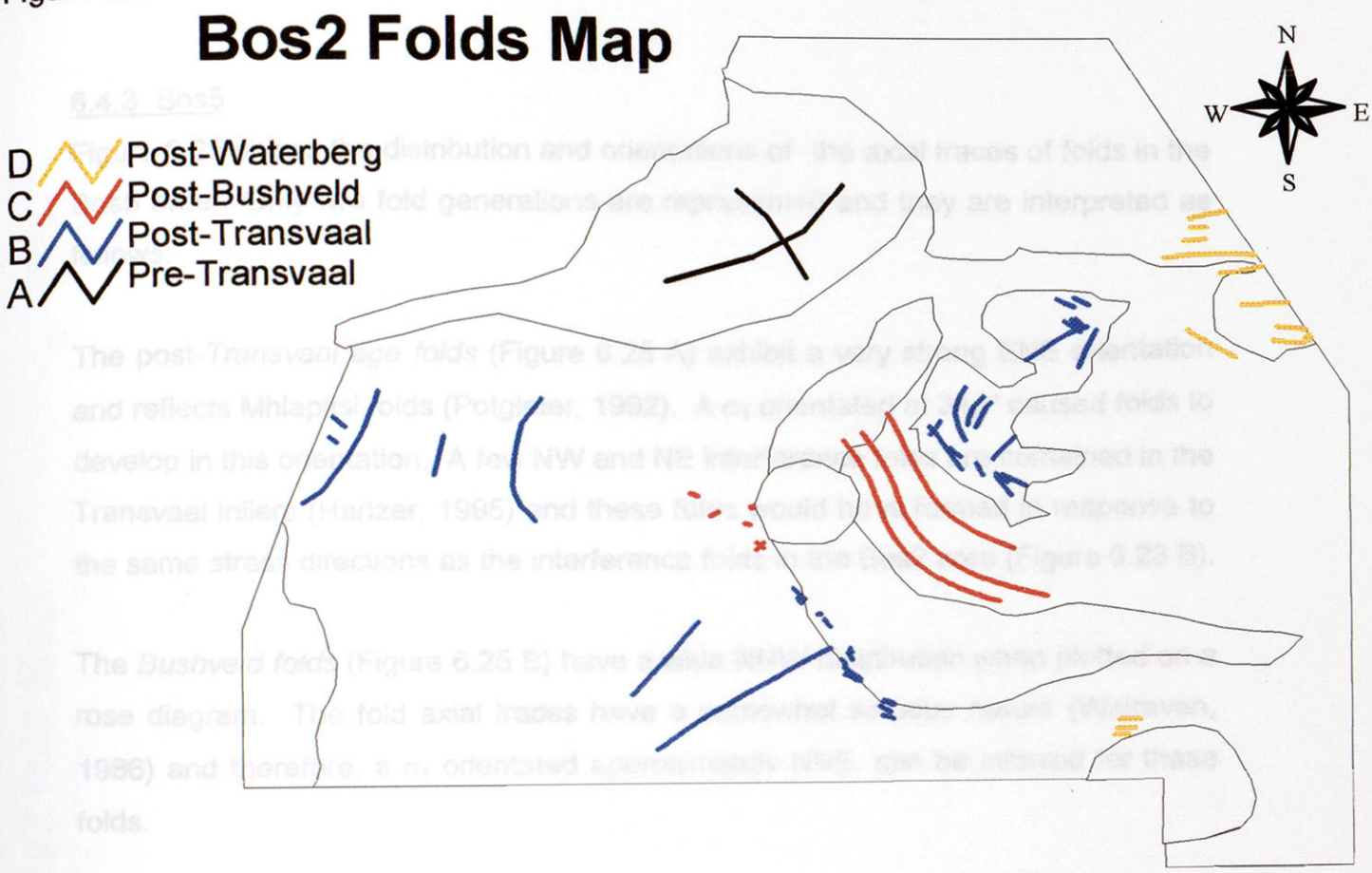
Bos2 Folds Map
D Post-Waterberg
C Post-Bushveld
B Post-Transvaal
A Pre-Transvaal
N
W
E
S

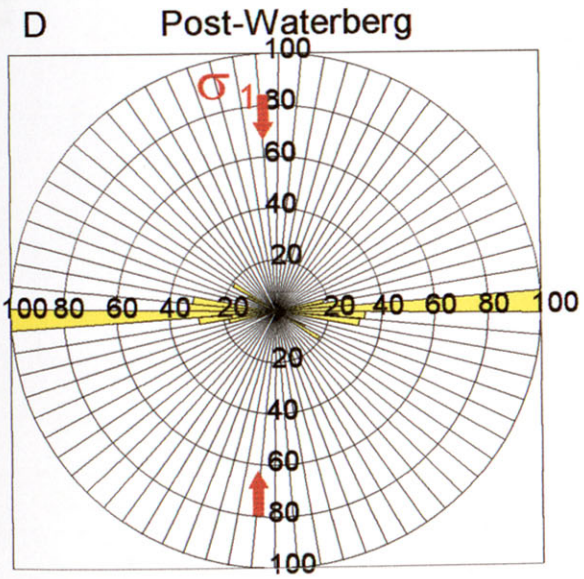
D
Post-Waterberg
σ1
100 80 60 40 20 20 40 60 80 100

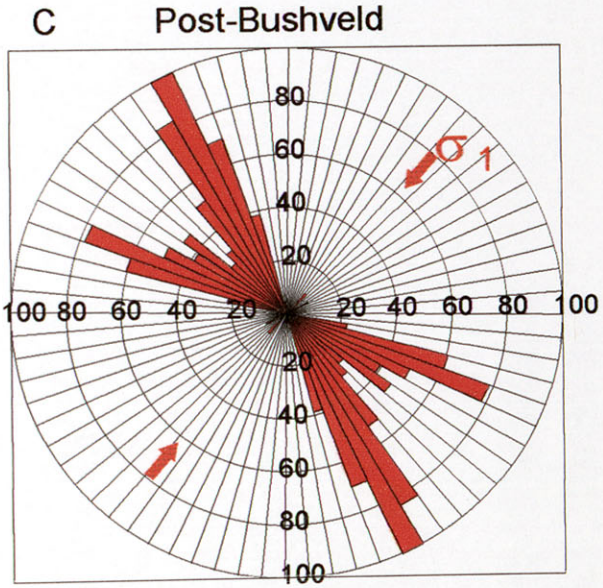
C
Post-Bushveld
σ1
100 80 60 40 20 20 40 60 80 100

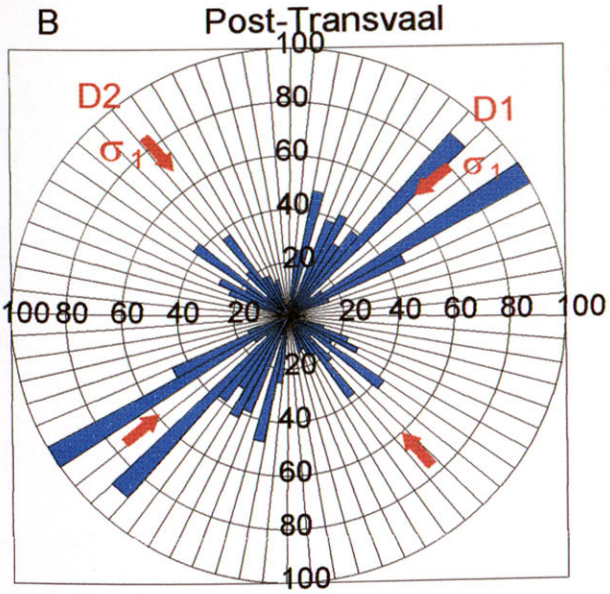
B
Post-Transvaal
D2
D1
σ1
σ1
100 80 60 40 20 20 40 60 80 100

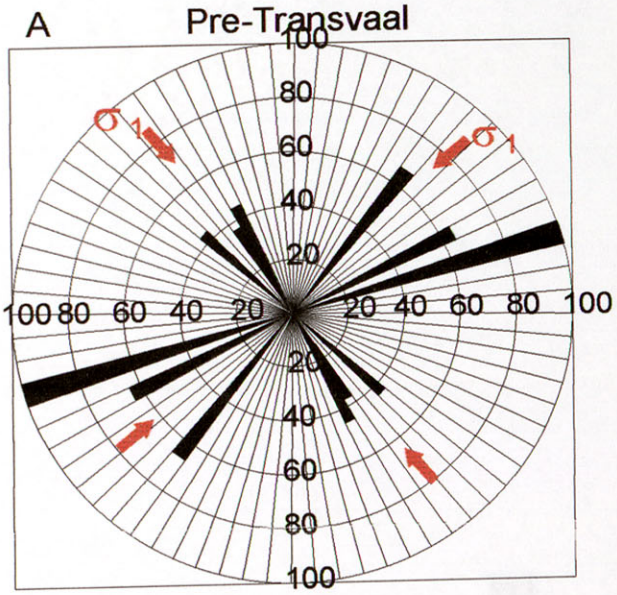
A
Pre-Transvaal
σ1
σ1
100 80 60 40 20 20 40 60 80 100

6.4.3 Bos5

Figure 6.25 shows the distribution and orientations of the axial traces of folds in the Bos5 area. Only two fold generations are represented and they are interpreted as follows:

The post-*Transvaal age folds* (Figure 6.25 A) exhibit a very strong ENE orientation and reflects Mhlapitsi folds (Potgieter, 1992). A σ_1 orientated at 340° caused folds to develop in this orientation. A few NW and NE interference folds are contained in the Transvaal inliers (Hartzer, 1995) and these folds would have formed in response to the same stress directions as the interference folds in the Bos2 area (Figure 6.23 B).

The *Bushveld folds* (Figure 6.25 B) have a wide NNW distribution when plotted on a rose diagram. The fold axial traces have a somewhat sinuous nature (Walraven, 1986) and therefore, a σ_1 orientated approximately NNE, can be inferred for these folds.

Figure 6.24

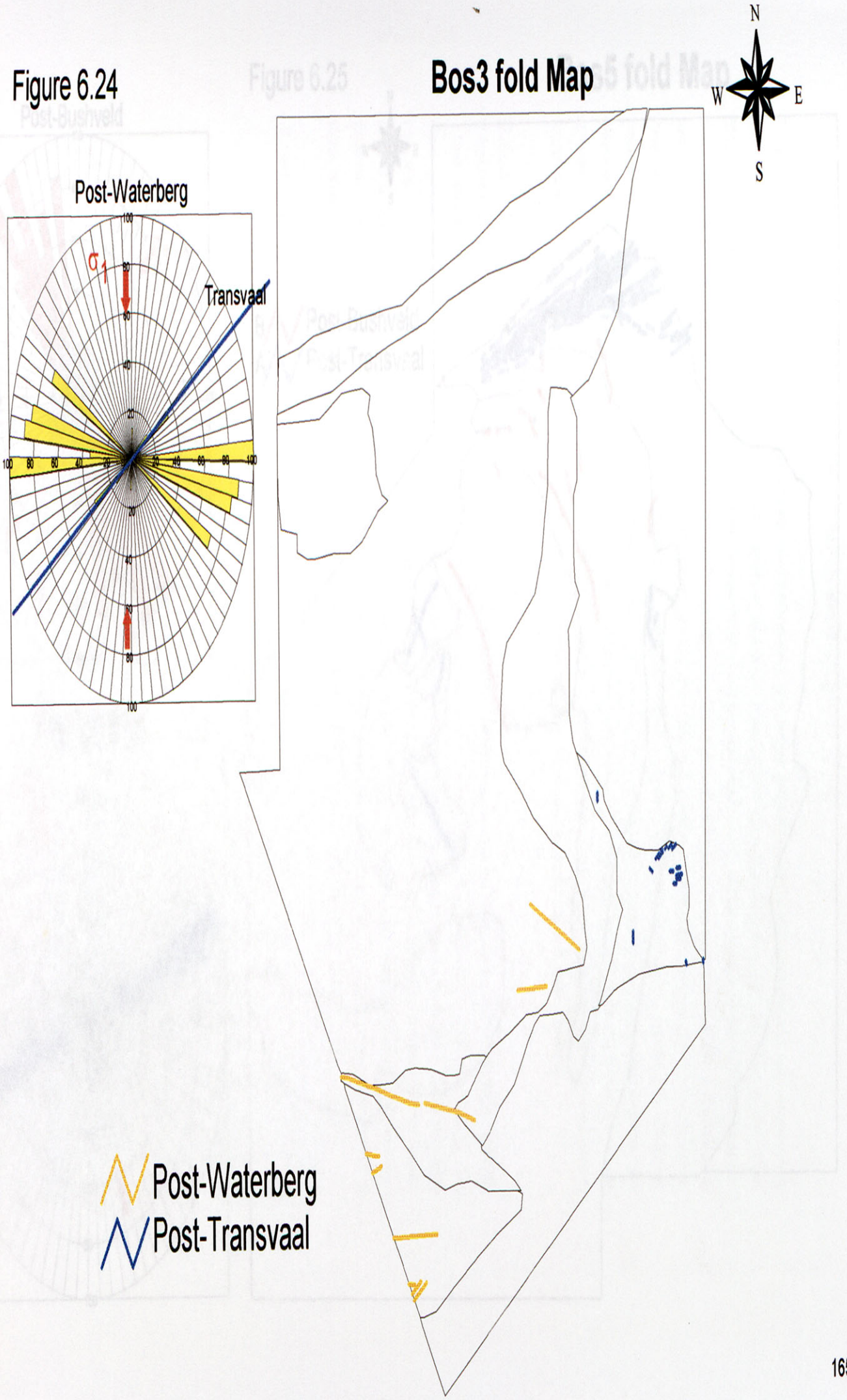

Figure 6.25

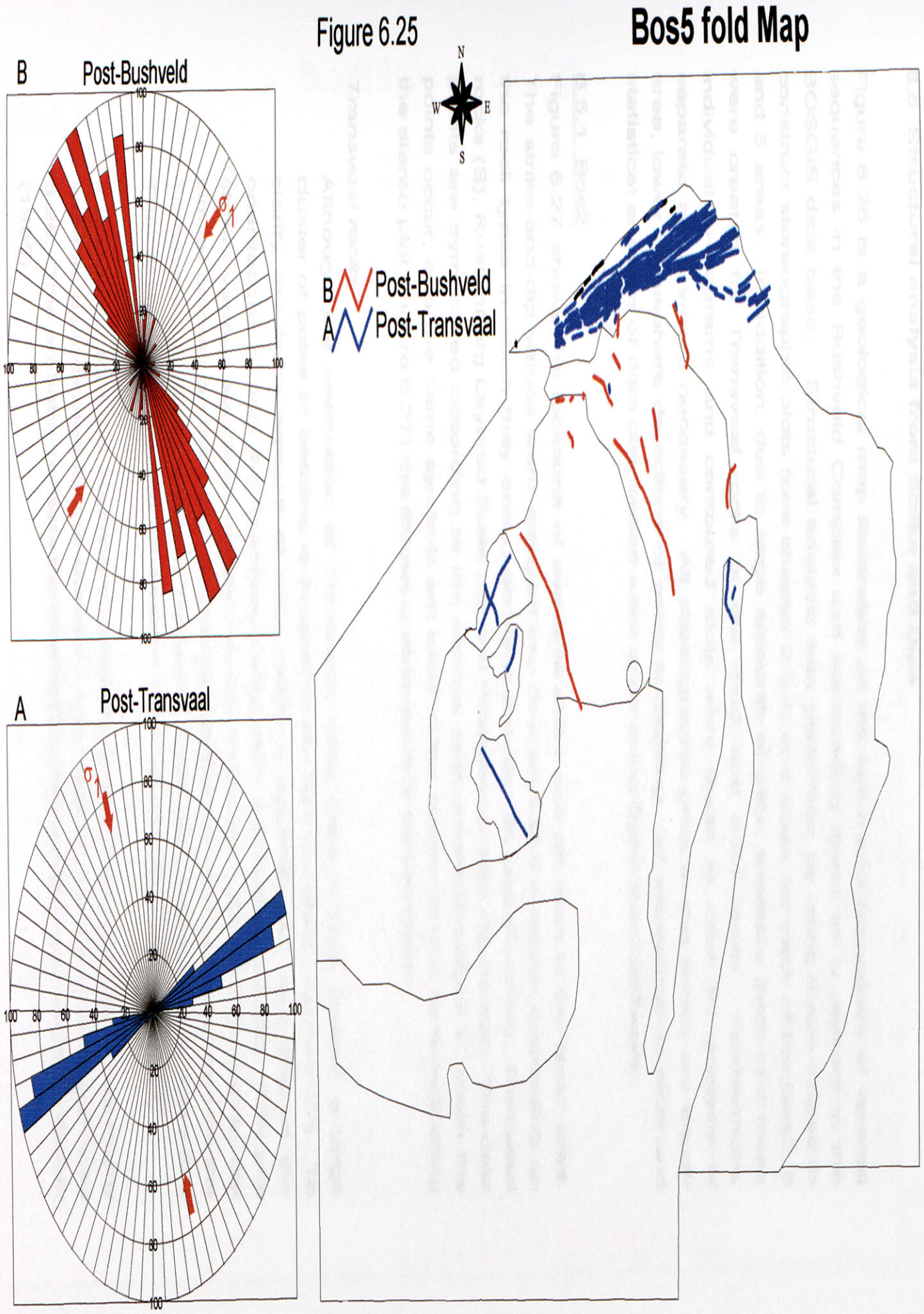

6.5 Structural analysis from Strike and Dips

Figure 6.26 is a geological map illustrating all the strike and dip values of layered sequences in the Bushveld Complex and surrounding areas as is present in the BOSGIS data base. Structural analysis was performed by using these values to construct stereographic plots (see chapter 2.3.4) and maps for each of the Bos2, 3 and 5 areas. In addition, due to large amounts of data, separate plots and maps were created for Transvaal rocks of the Bos2 and Bos5 areas. Furthermore, individual pi-diagrams and contoured plots were made to allow for analysis of separate areas where necessary. All stereographic plots in this thesis are equal-area, lower hemisphere depictions of poles to bedding. All stereographic plots and statistical analysis of data distribution were done using Spherical 2 software.

6.5.1 Bos2

Figure 6.27 shows the locations of available strike and dip data in the Bos2 area. The strike-and-dip values were grouped into four structural domains depending on the rock types in which they occur, domains include: an undefined (A), Transvaal rocks (B), Rustenburg Layered Suite (C) and Waterberg rocks (D) domain. The data points are symbolized according to the various stratigraphic horizons in which the points occur, and the same symbols are used in the stereonet plot from evaluating the stereo plot (Figure 6.27) the following observations can be made:

Transvaal rocks

Although the orientation of Transvaal rocks have a wide scatter, a large cluster of poles to bedding is present in the SW quadrant (Figure 6.27). To clarify the large amount of data points a separate plot and map of the orientations of only the Transvaal rocks were made (Figure 6.28). This plot shows various structural domains of the Transvaal rocks as indicated by the similar colours on the map. Structural domains for the Bos2 area include the Transvaal inliers (A), western Transvaal basin (B), Johannesburg dome (C), Thabazimbi area (D) and far western Transvaal basin (E) (Figure 6.28).

It is evident that the bedding orientations in the Transvaal Inliers are highly variable as indicated by the scattered occurrence of poles to bedding (Figure 6.28. This probably reflects the interference fold pattern described by Hartzer (1995).

Bosgis Strike and Dip Map

Figure 6.26

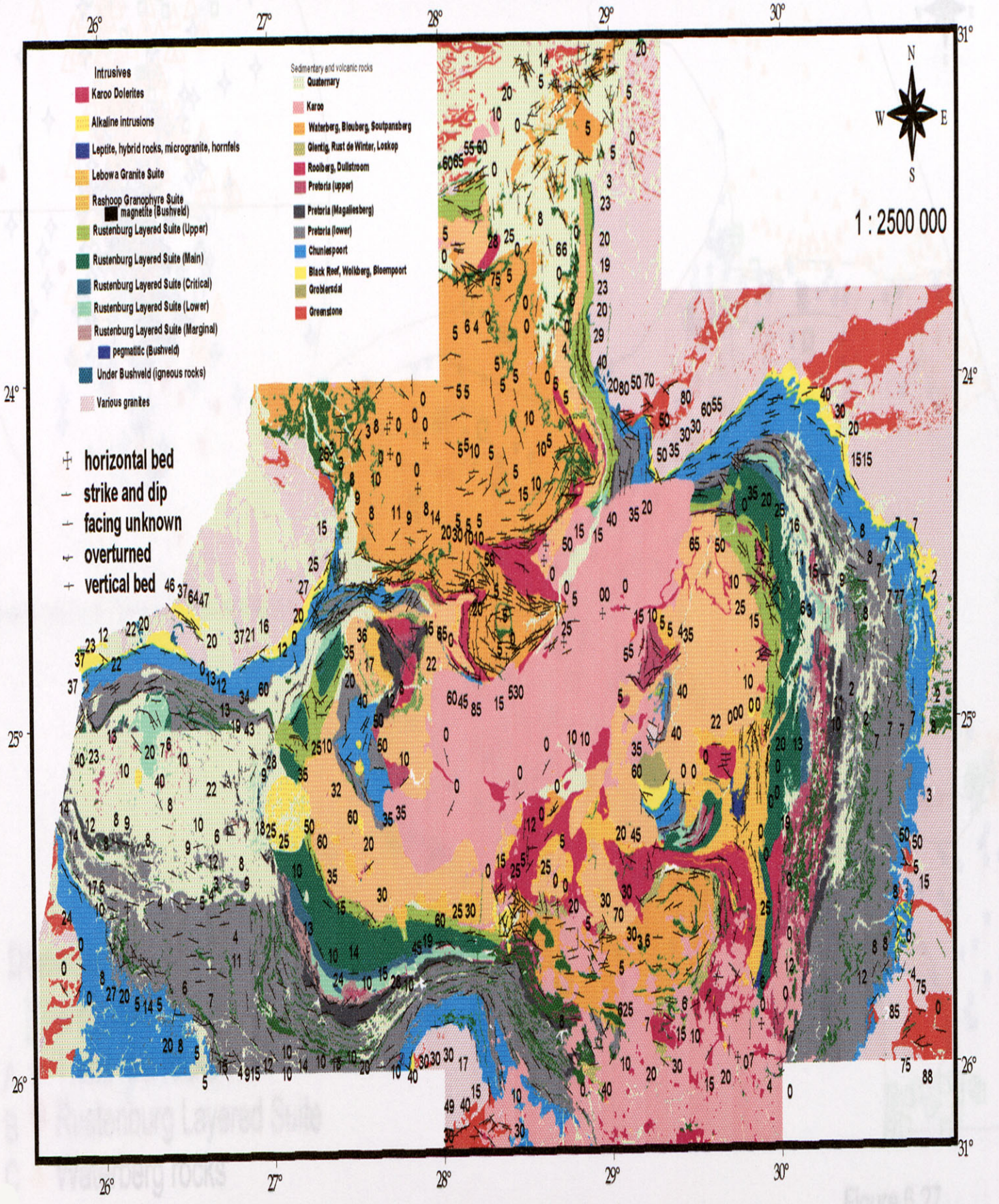

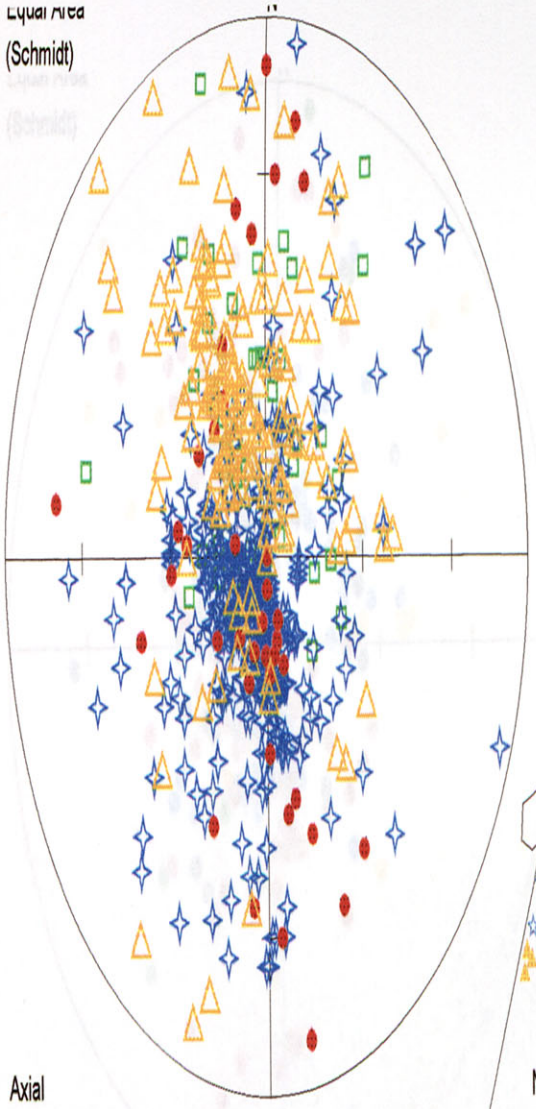

Stereographical plot of poles to bedding of rocks in the Bos2 area

Map of the distribution of strike-and-dip values of Bos2

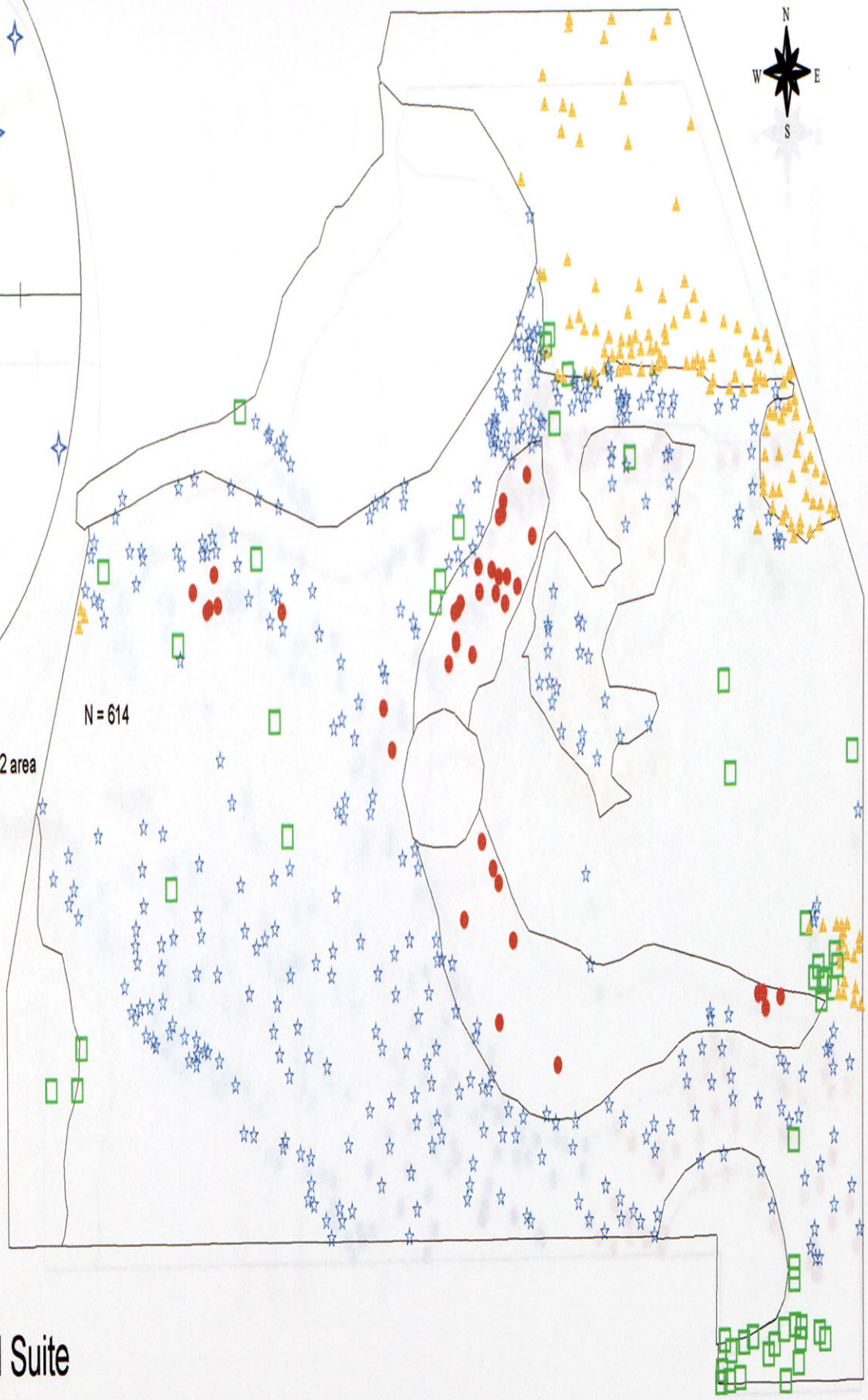

Domains

- undefined
- A Transvaal rocks
- B Rustenburg Layered Suite
- C Waterberg rocks

Figure 6.27

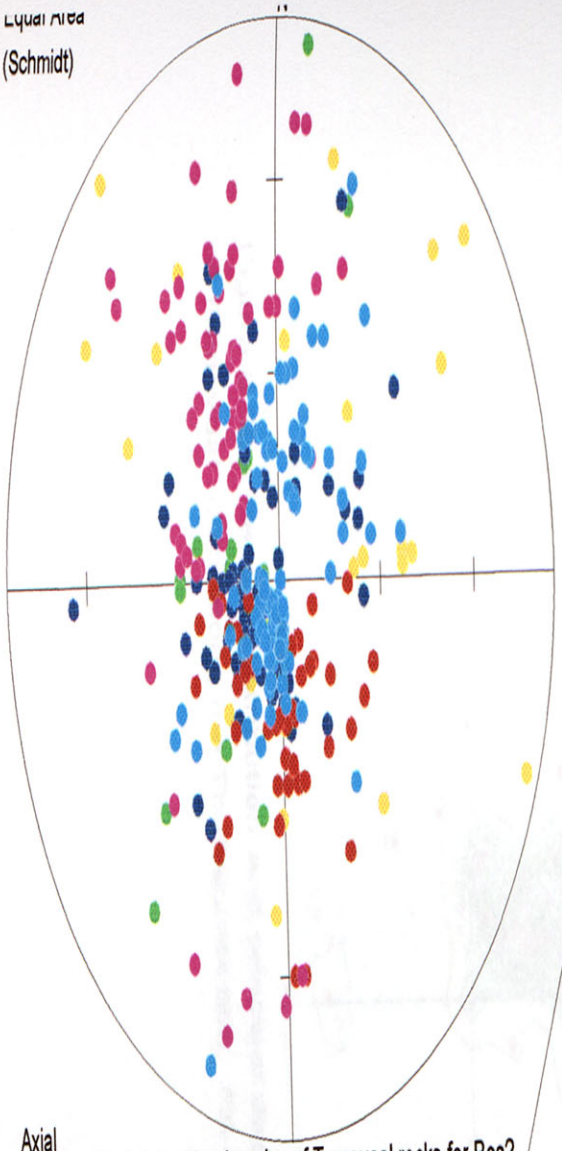

Axial
Stereographical plot of the domains of Transvaal rocks for Bos2

Strike and dip domains of Transvaal rocks for Bos2

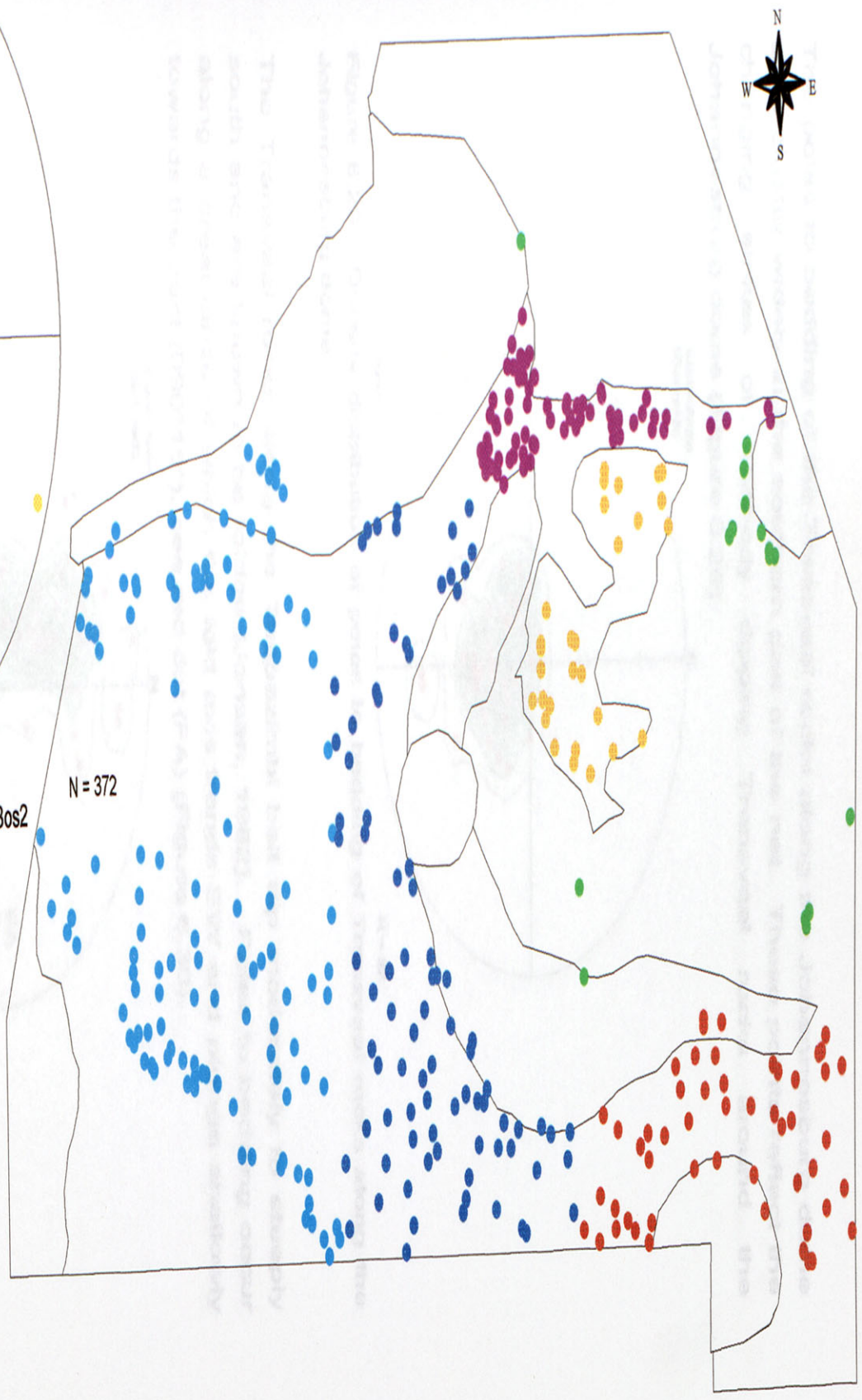

Domains

- undefined
- A Inliers
- B western Transvaal
- C Johannesburg dome
- D Thabazimbi
- E far western Transvaal

Figure 6.28

The poles to bedding of the Transvaal rocks along the Johannesburg dome area cluster widely in the southern part of the net. These points reflect the changing strikes of northerly dipping Transvaal rocks around the Johannesburg dome (Figure 6.29).

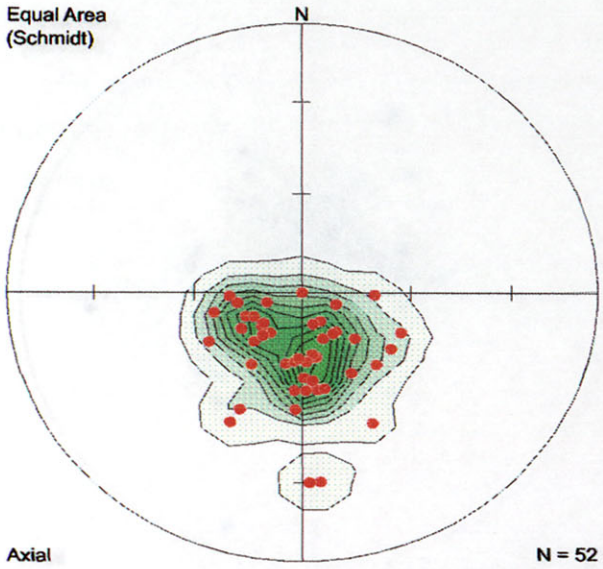

Figure 6.29. Density distribution of poles to bedding of Transvaal rocks along the Johannesburg dome.

The Transvaal rocks along the Thabazimbi belt dip moderately to steeply south and are known to be folded (Jansen, 1982). Poles to bedding occur along a great circle of which the fold axis trends EW and plunge shallowly towards the east (090°19°), see red dot (FA) (Figure 6.30).

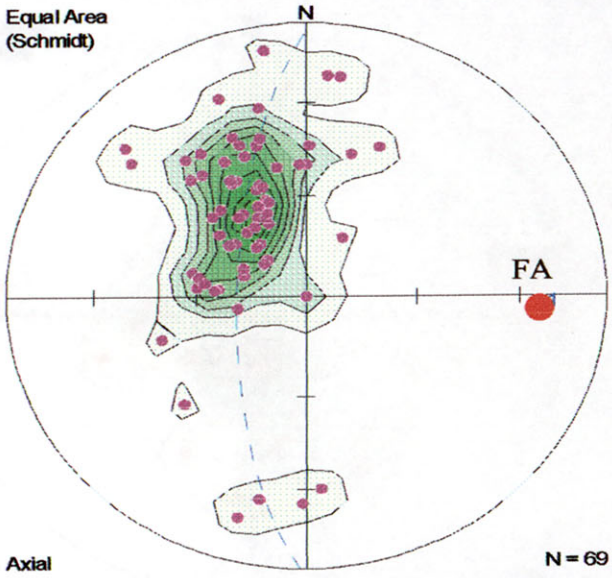

Figure 6.30. Density distribution and principal direction analysis of poles to bedding of Transvaal rocks along the Thabazimbi belt. FA = fold axis.

Poles to bedding of Transvaal rocks in the western and far western Transvaal basin (domains B + E) cluster in the center of the stereonet (Figure 6.31). This reflects Transvaal layers dipping of moderate angles towards the center of the main Transvaal basin.

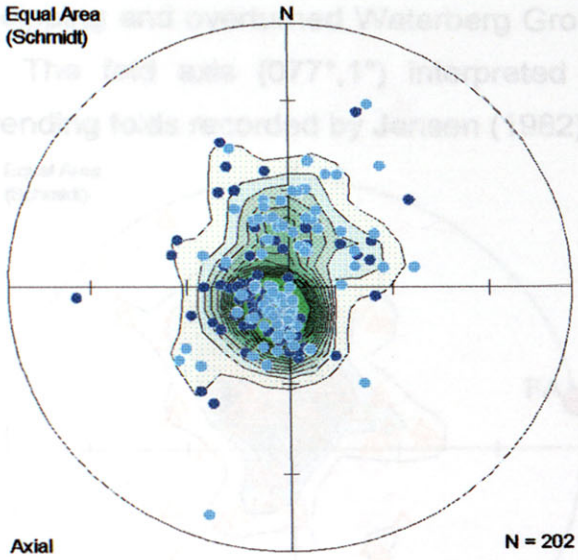

Figure 6.31. Density distribution analysis of poles to bedding of the western and far western Transvaal basin.

Bushveld Complex rocks

Poles to the layered sequences of the Bushveld Complex plot along a great circle as illustrated in Figure 6.32. A fold axis trending approximately EW and plunging shallowly E (080°,8°) can be interpreted from the available data.

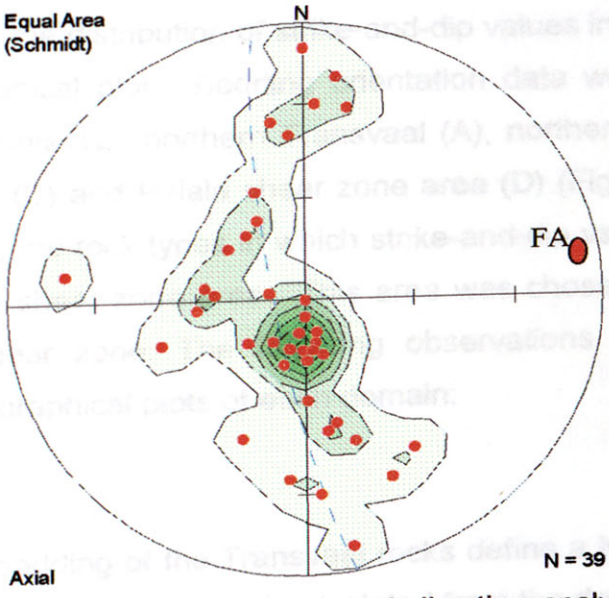

Figure 6.32. Density distribution and principal direction analysis of poles to layered sequences of the western lobe of the Bushveld Complex. FA = fold axis.

Waterberg Group rocks

Although the poles to bedding of Waterberg rocks cluster in the upper quadrants of the net, it also falls along a vague NS striking great circle (Figure 6.33). These poles generally signify EW striking and shallow southerly dipping to steeply dipping and overturned Waterberg Group rocks along the Thabazimbi belt. The fold axis (077°,1°) interpreted from Figure 6.33 confirms the EW trending folds recorded by Jansen (1982).

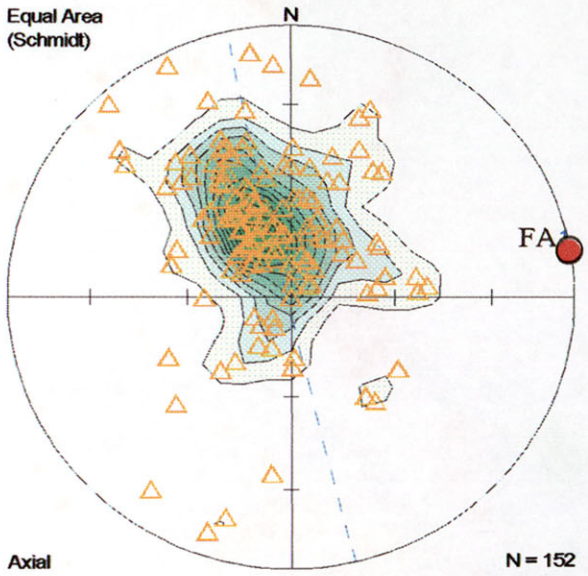

Figure 6.33. Density distribution and principal direction analysis of poles to bedding for Waterberg Group rocks of the Thabazimbi belt. FA = fold axis.

6.5.2 Bos3

Figure 6.34 illustrates the distribution of strike-and-dip values in the Bos3 area with a composite stereographical plot. Bedding orientation data were grouped into the following structural domains; northern Transvaal (A), northern Bushveld Complex (B), Waterberg basin (C) and Palala shear zone area (D) (Figure 6.34). Domains are chosen according the rock types in which strike-and-dip values were measured, except for the Palala shear zone area. This area was chosen based on outcrops along the Palala shear zone. The following observations can be made when evaluating the stereographical plots of each domain:

Transvaal rocks

The poles to bedding of the Transvaal rocks define a NS striking great circle (Figure 6.35). The fold axis (FA) calculated from the data distribution indicate a EW trending, shallow westerly plunging axis (273°19°). This reflects the folds in the Swaershoek area (Jansen, 1982) as well as Mhlapitsi-type folds

Figure 6.34

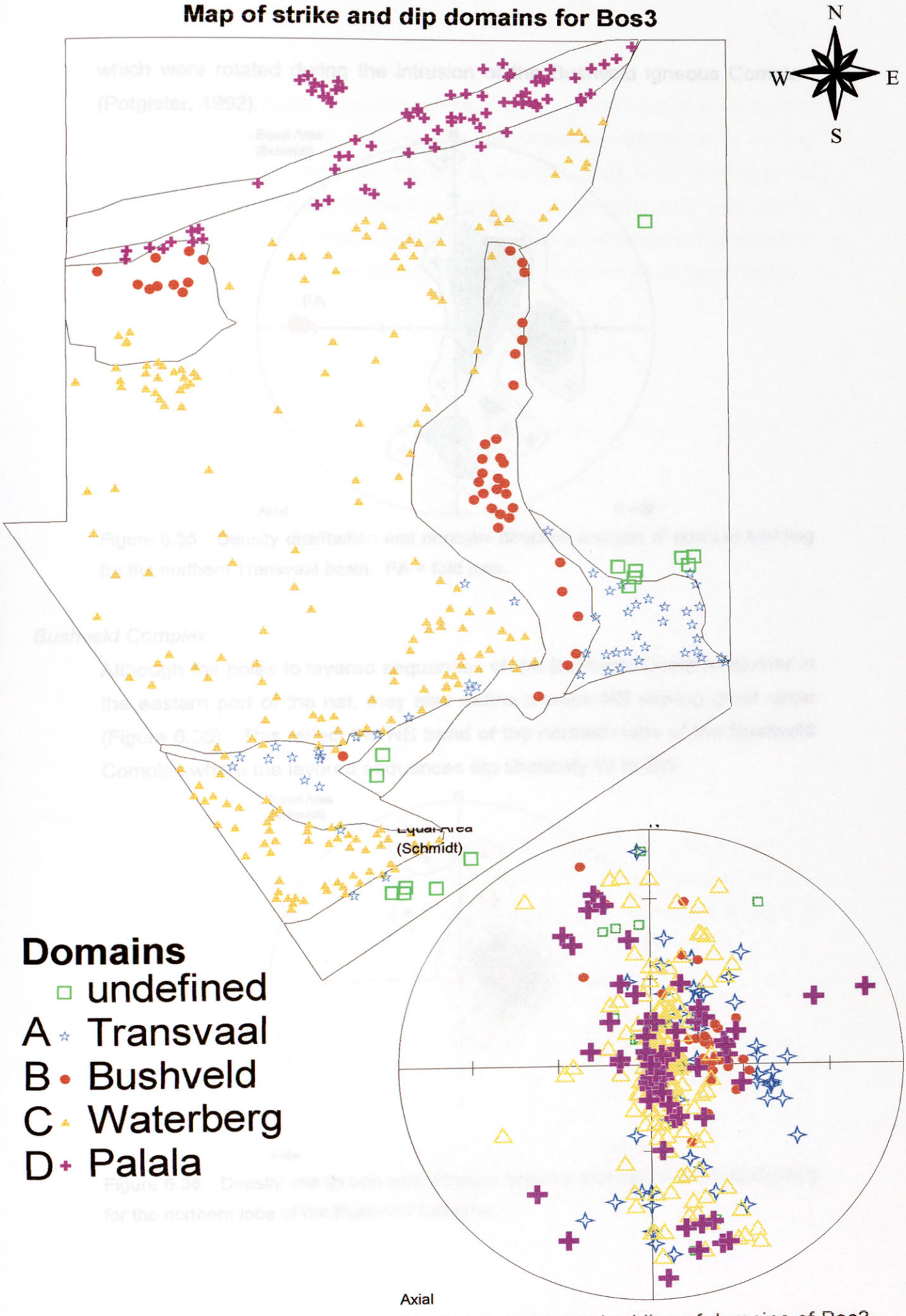

Sterographical plot of poles to bedding of domains of Bos3

which were rotated during the intrusion of the Bushveld igneous Complex (Potgieter, 1992).

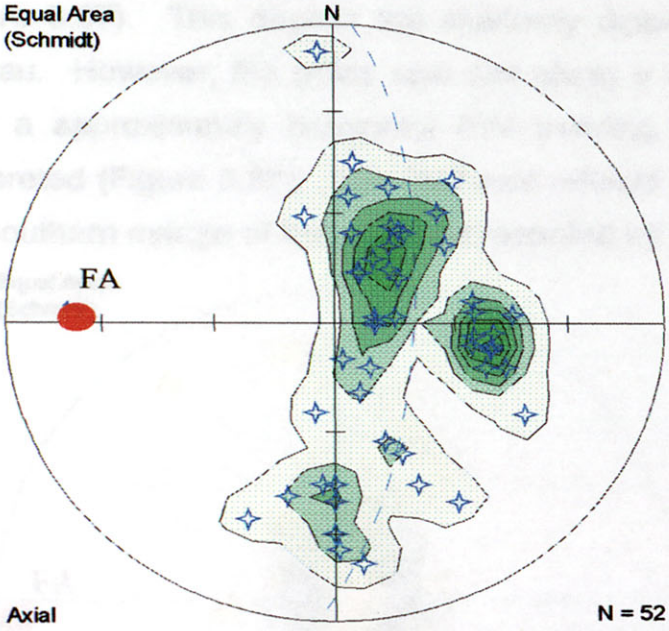

Figure 6.35. Density distribution and principal direction analysis of poles to bedding for the northern Transvaal basin. FA = fold axis.

Bushveld Complex

Although the poles to layered sequences of the Bushveld Complex cluster in the eastern part of the net, they also define a weak NS striking great circle (Figure 6.36). This reflect the NS trend of the northern lobe of the Bushveld Complex where the layered sequences dip shallowly W to SW.

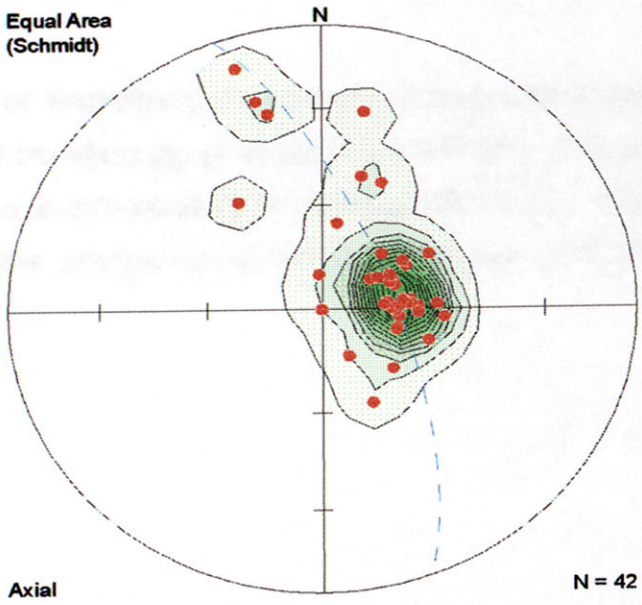

Figure 6.36. Density distribution and principal direction analysis of poles to layering for the northern lobe of the Bushveld Complex.

Waterberg Group

A large cluster of poles to bedding of the Waterberg rocks occur in the center of the net (Figure 6.37). This depicts the shallowly dipping rocks on the Waterberg plateau. However, the poles also plot along a NS striking great circle for which a approximately horizontal EW trending fold axis (FA = 266°,4°) is interpreted (Figure 6.37). This fold axis reflects the EW trending folds along the southern margin of the basin as recorded by Jansen (1982).

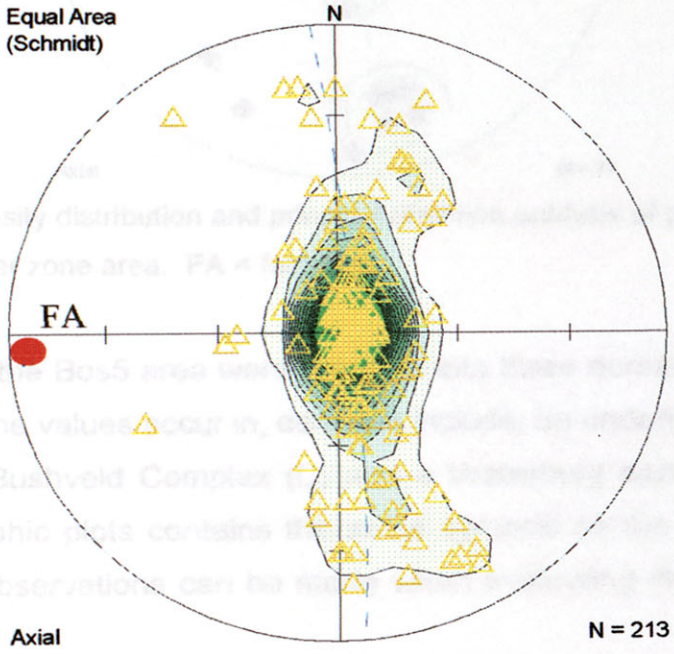

Figure 6.37. Density distribution and principal direction analysis of poles to bedding for the Waterberg plateau. FA = fold axis.

Palala shear zone area

Poles to bedding of Waterberg rocks in the Palala shear zone area define an approximately NS trending great circle (Figure 6.38). The calculated fold axis trends ENE and is approximately horizontal (261°,3°). The trend of the fold axis is parallel to the orientation of the Palala shear zone (Figure 4.5).

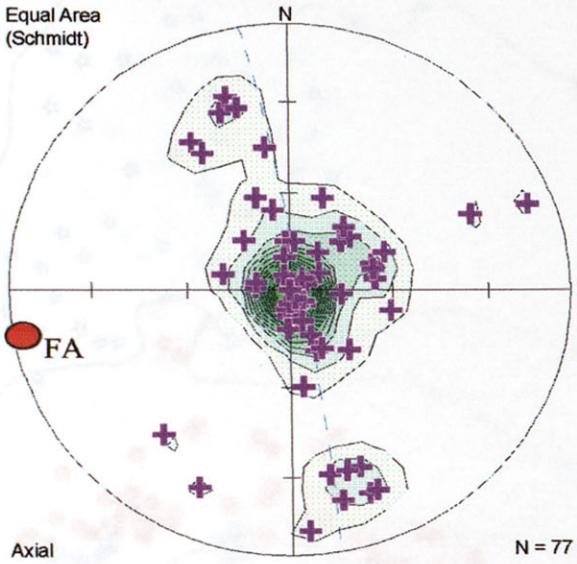

Figure 6.38. Density distribution and principal direction analysis of poles to bedding in the Palala shear zone area. FA = fold axis.

6.5.3 Bos5

Strike and dip data of the Bos5 area were grouped into three domains according to the ages of the rocks the values occur in, domains include; an undefined domain (A), Transvaal rocks (B), Bushveld Complex (C) and a Waterberg domain (D) (Figure 6.39). The stereographic plots contains the same symbols as the domains of the map. The following observations can be made when evaluating the stereographic plots.

Transvaal rocks

Structural domains for the Transvaal rocks were further subdivided and include the Mhlapitsi fold belt (A), Transvaal inliers (B) and eastern Transvaal basin (C) (Figure 6.40). Similar to Transvaal inliers in the Bos2 area, the poles to bedding of the inliers occurring in the eastern Bushveld Complex are scattered throughout the stereonet (Figure 6.40). The scatter probably reflects the interference fold pattern of the inliers as documented by Hartzer (1995).

The poles to bedding of Transvaal rocks along the Mhlapitsi fold belt cluster in the NNW area of the stereonet, but also lie along a weak NNW great circle (Figure 6.41). A horizontal ENE trending fold axis (FA = 075°/0°) calculated from this data. Mhlapitsi-type folds recorded by Potgieter (1992) differs from the fold axis of Figure 6.41, in that Mhlapitsi-folds trend more NE and plunges steeply west. This variance might be due to the lack of data in the BOSGIS database.

Figure 6.39 **Map of the distribution of strike-and-dip values of Bos5**

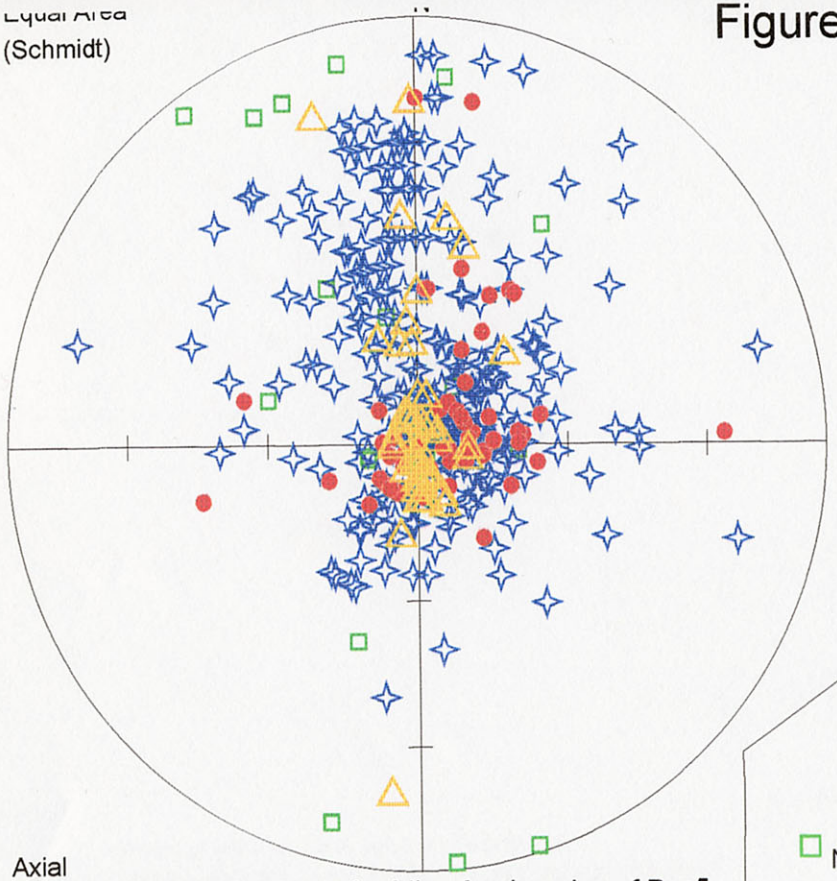

Stereograhical plot of poles to bedding for domains of Bos5

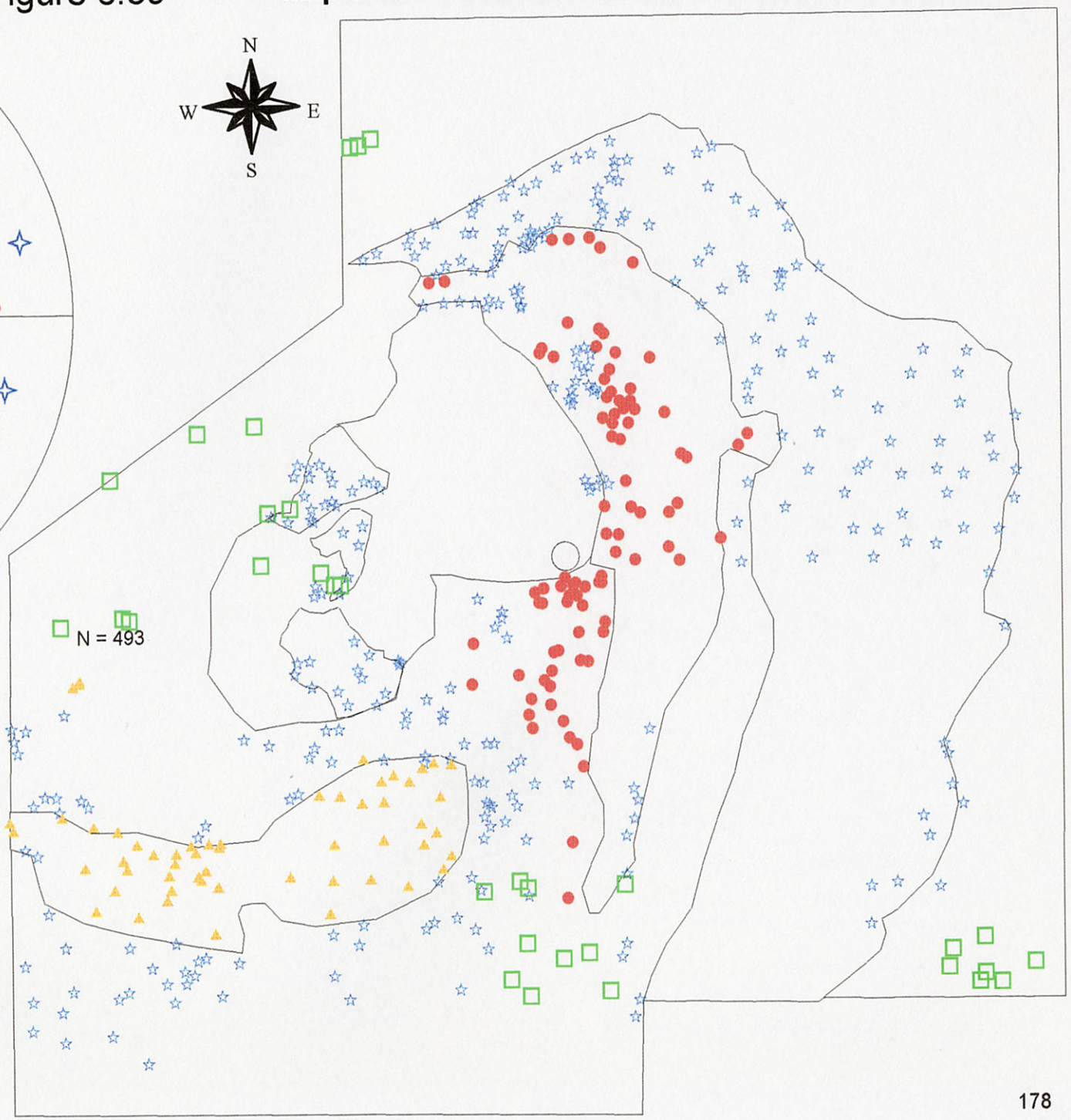

A □ **undefined**
B ☆ **Transvaal**
C ● **Bushveld Complex**
D ▲ **Waterberg**

Figure 6.40 Map of strike and dip domains of Transvaal rocks for Bos5

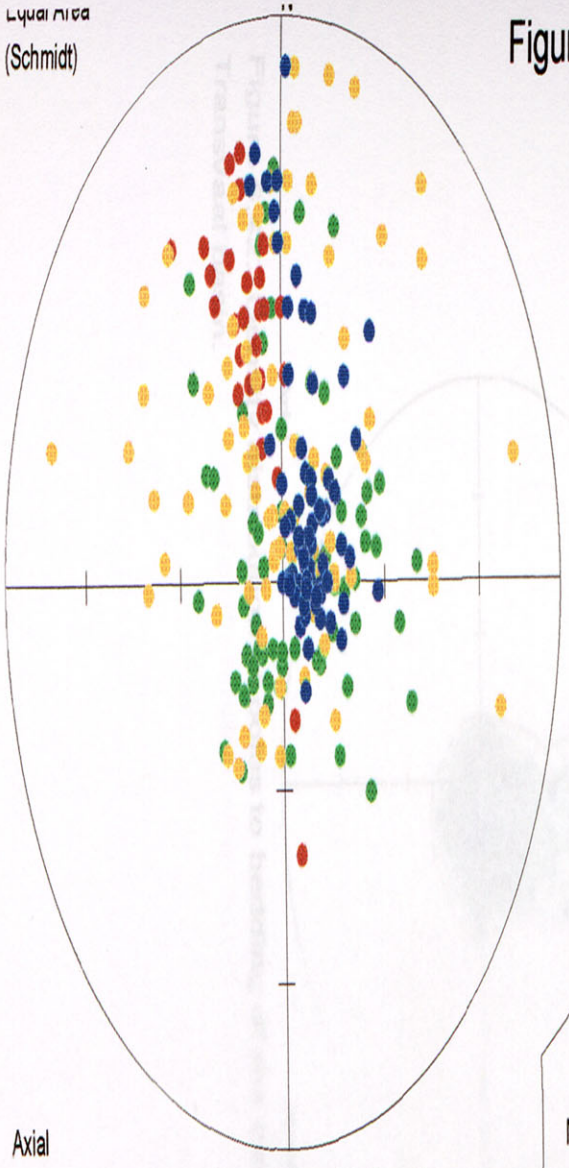

Stereographical plot of poles to bedding of Transvaal rocks illustrating the various domains for Bos5

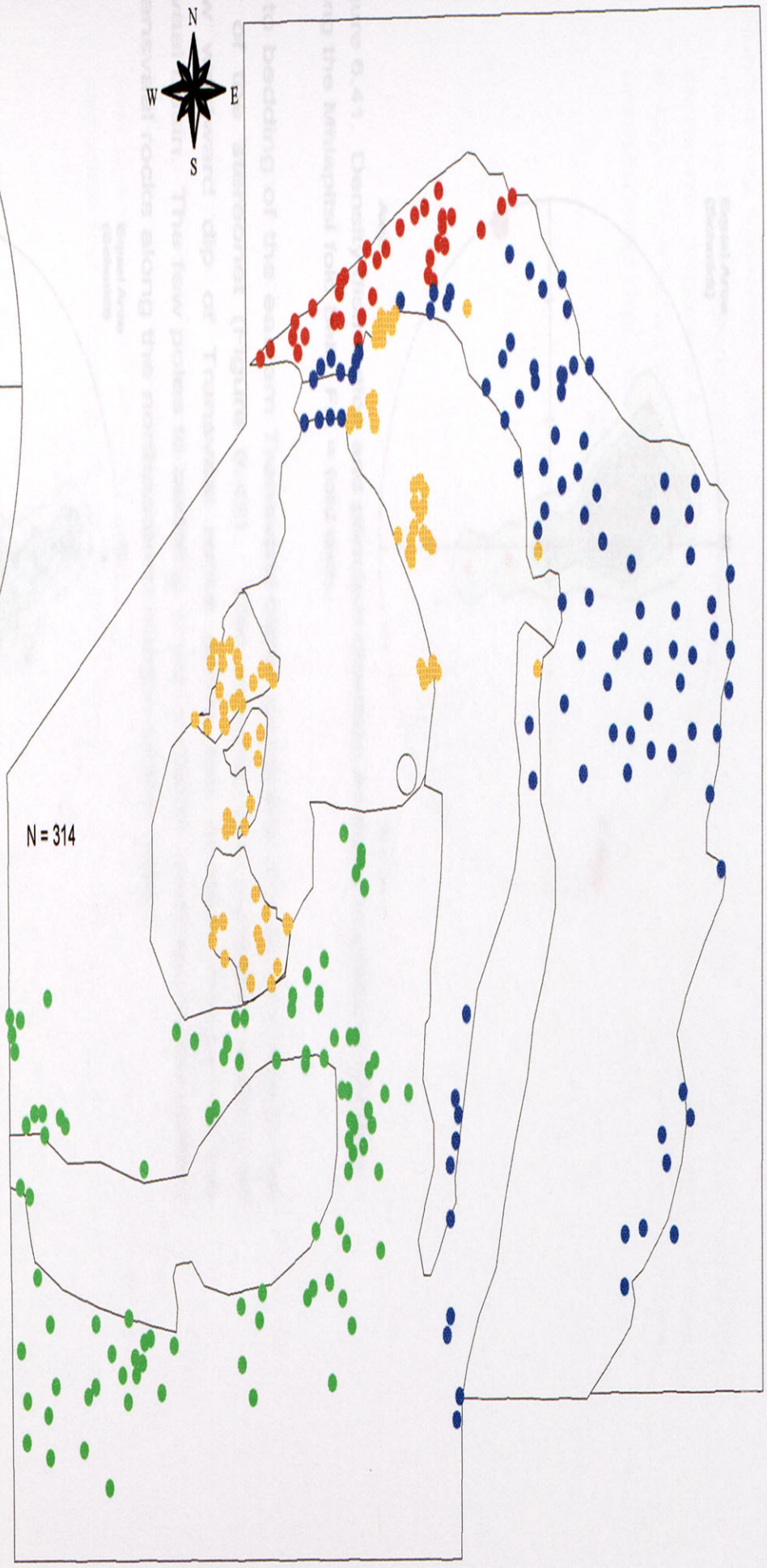

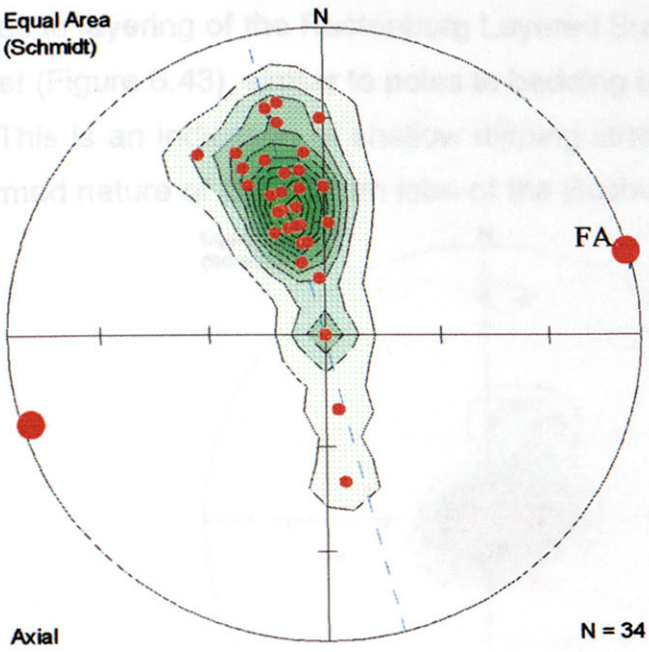

Figure 6.41. Density distribution and principal direction analysis of poles to bedding along the Mhlapitsi fold belt. FA = fold axis.

Poles to bedding of the eastern Transvaal basin generally cluster strongly in the center of the stereonet (Figure 6.42). This reflects the constant strike and shallow westward dip of Transvaal rocks along the eastern margin of the Transvaal basin. The few poles to bedding which indicate southward dips reflect the Transvaal rocks along the northeastern margin of the basin.

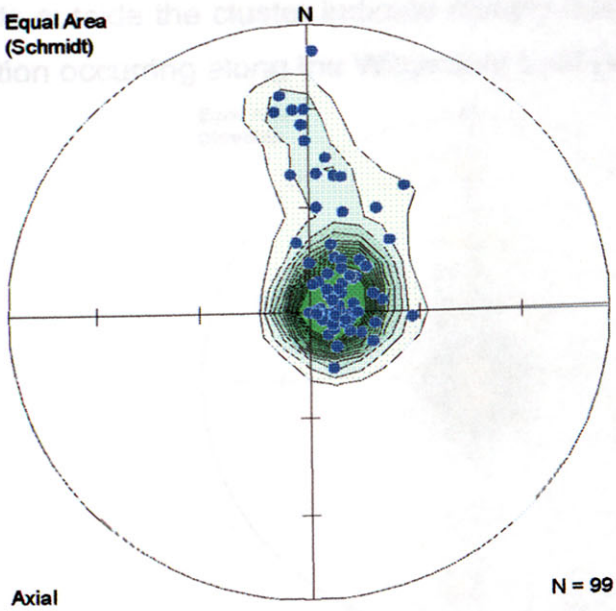

Figure 6.42. Density distribution of poles to bedding of the eastern margin of the Transvaal basin.

Rustenburg Layered Suite

The poles to layering of the Rustenburg Layered Suite cluster in the center of the stereonet (Figure 6.43), similar to poles to bedding of the Transvaal rocks (Figure 6.42). This is an indication of shallow dipping strata, and reflects the generally undeformed nature of the eastern lobe of the Bushveld Complex.

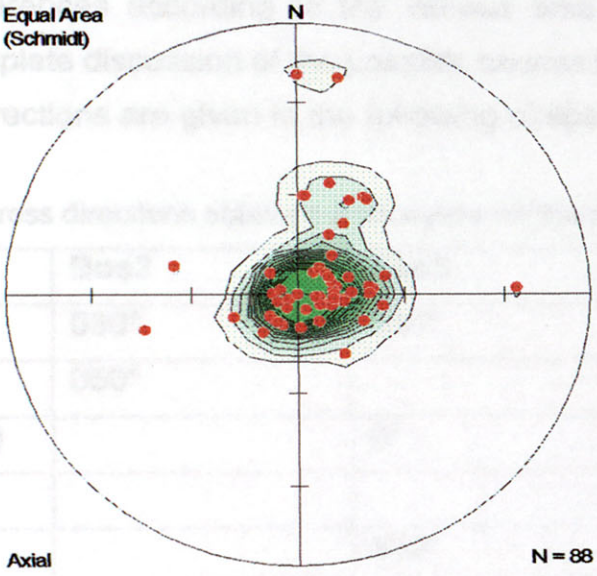

Figure 6.43. Density distribution of poles to layering of the eastern lobe of the Bushveld Complex.

Waterberg rocks

The poles to bedding of Waterberg rocks cluster more or less in the center of the net (Figure 6.44) signifying the shallow dips of the Cullinan-Waterberg basin. A few points outside the cluster indicate steeply dipping strata associated with the deformation occurring along the Wilgerivier fault (Van der Neut, 2000).

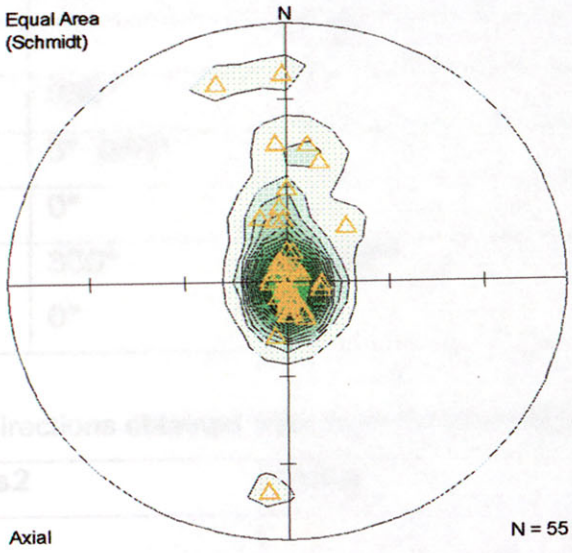

Figure 6.44. Density distribution of poles to bedding of Cullinan-Waterberg basin.

6.6 Summary of stress orientations derived from all the structural features

Stress directions obtained from the various structures, in the different regions and of the same age are summarized in Tables 6.1 – 6.4. These directions are compared for similarities and differences according to the various time periods considered during this study. A complete discussion of the possible causes and regional tectonic histories of the stress directions are given in the following chapter.

Table 6.1 Summary of σ_3 stress directions obtained from dykes for the respective Bos areas.

Domains	Bos2	Bos3	Bos5
Dolerite (post-Karoo)	030°	030°	030°
Syenite (Pilanesberg)	050°		
Makgabeng (Waterberg)		0°	
Transvaal rocks			310°
Archaean rocks		330°	320°

Table 6.2 Summary of σ_3 directions obtained from lineaments for the respective Bos areas.

Domains	Bos2	Bos3	Bos5
Undefined	0°		
Pilanesberg	radial		
Waterberg	020°	0°	
Palala		0°	
Rooiberg	030°		
Western Transvaal	0° 060°		
Far western Transvaal	0°		290°
Archaean	330° 0°	350°	350°

Table 6.3 Summary of σ_1 directions obtained from folds for the respective Bos areas.

Age	Bos2	Bos3	Bos5
Post-Waterberg	NS	NS	
Post-Bushveld	NE		NE
Post-Transvaal	NW and NE		340° NW
Pre-Transvaal	NW and NE		

Table 6.4

Summary of stress orientations of the respective Bos areas obtained from faults.

Age	Bos2					Bos3					Bos5				
	Age1			Age2		Age1			Age2			Age1			Age2	
	σ_1	σ_2	σ_3	σ_1	σ_2	σ_1	σ_2	σ_3	σ_1	σ_2	σ_3	σ_1	σ_2	σ_3	σ_1	σ_2	σ_3
Post-Karoo	v	60°	330°			v	70°	340°				v	90°	0°			
Post-Pilanesberg	v	h	h														
Post-Waterberg	0°	90°	v						50°	v	320°	0°	90°	v			
	v	290°	40°						0°	080°	v						
Post-Bushveld	v	330°	60°						30°	v	300°				v	50°	320°
Post-Transvaal	340°	v	70°	v	340°	60°	30°	v	300°				0°	v	270°	v	60°	330°
	v	h	h														
Syn-Transvaal	v	330°	60°						330°	60°	v				330°	60°	v
Pre-Transvaal	30°	v	300°			30°	v	300°	90°	v	0°	30°	v	300°			

Pre-Transvaal

Although, structural line data for the pre-Transvaal period is scarce, the stress directions indicated by analyses of available dykes, lineaments and faults in all the Bos areas display fairly similar σ_3 directions of between 300° and 350°. A secondary, σ_3 direction of 0° obtained for Bos2 lineaments and Bos3 Age2 faults are also evident.

Syn-Transvaal

Syn-Transvaal σ_1 directions of 330° from faults for the Bos3 and Bos5 areas correspond with each other, but not the stress directions of the faults of the Bos2 area. However, the stress directions of the Bos2 area matches post-Transvaal directions derived from the Bos2 Age2 faults. It is however interesting to note that more or less the same stress directions are constantly repeated by σ_1 , σ_2 and σ_3 stresses during syn-Transvaal and post-Transvaal times. These directions are 330/340° and 60/70°.

Post-Transvaal

Most of the dykes and lineaments occurring in Transvaal rocks indicate σ_3 directions varying between 290° and 0°. Stress directions interpreted from faults during this time period also rendered σ_3 directions varying between 270° and 330°. However, a second σ_3 direction varying between 060° and 070° is also evident from post-Transvaal faults and lineaments. In addition σ_1 directions trending NW and NE corresponds to σ_1 directions of 340° and 30° of Bos2 and Bos3 areas respectively.

Post-Bushveld

Stress directions obtained from the faults varying between 030° to 060° and are constantly repeated by σ_1 , σ_2 and σ_3 directions. However, NE trending σ_1 directions obtained form fold analysis of the Bos2 and Bos5 areas are at variance with stresses obtained from the fault analysis.

Post-Waterberg

Dykes and lineaments occurring in the Waterberg domains exhibit σ_3 directions of 0°, whereas stress analyses from faults and folds indicates σ_1 trending generally 0°. However, some stress directions from Waterberg faults in the Bos3 area do not correspond to any of the above mentioned directions.

Pilanesberg

Stress directions interpreted for the Pilanesberg age were only obtained form the Bos3 area. The syenite dykes indicates a σ_3 direction of 050° and a vertical σ_1, whereas stress directions for the faults and lineaments around the dome indicate a radial horizontal σ_3 pattern, and also a vertical σ_1.

Post-Karoo

Post-Karoo dolerite dykes in each of the Bos areas rendered a σ_3 direction of 030°. However, stress directions obtained from fault analyses do not confirm this direction, and indicates a σ_3 directions between 330° to 0°.

7. DISCUSSION

This chapter combines the stress directions derived in Chapter 6, together with structural data obtained from the literature study presented in Chapter 5, and the tectonic history of the Kaapvaal Craton discussed in Chapter 4. The aim is to attain an understanding of the possible stress fields which existed in and around the Bushveld Complex region during different time periods. Attempts are made to construct a single stress ellipse which can accommodate the stress directions, as well as incorporate the orientations of all the various structures, of a specific age. By doing so it is possible to see if a single stress field prevailed during a specific time period, or if different stress fields existed during the proposed time bracket. Finally, regional tectonic events affecting the Kaapvaal Craton are used to provide possible explanations for the causes of these stress fields. However, due to the lack of detailed structural information about certain structures, different possibilities of stress ellipses are considered and alternatives regarding the timing and displacement style of such structures are discussed.

The time periods which are considered include, pre-Transvaal, syn-Transvaal, post-Transvaal/pre-Bushveld, post-Bushveld/pre-Waterberg, post-Waterberg/pre-Karoo, Pilanesberg and post-Karoo periods. Tables 7.1 – 7.4, summarize the regional tectonic events, local events, the stratigraphy of the Bushveld Complex area, and present the possible stress ellipses for each time period.

7.1 Pre-Transvaal

The pre-Transvaal time bracket stretches over a long time period during which the Kaapvaal Craton was subjected to many deformational events (e.g. McCourt, 1995). During this time variously orientated stress fields existed, causing basin formation and subsequent basin inversion. It is also evident that since the Craton's early evolution prominent structural grains developed which played an important role throughout the later history of the Craton. These structural grains are exemplified by greenstone belts as well as important lineaments such as the TML, Limpopo belt, and Barberton lineament. Prominent Archaean structural trends include ENE to NE as well as NNW orientated structures. Unfortunately, due to the lack of sufficient pre-Transvaal structures in the BOSGIS database, the stress fields which existed during this time are not well represented in this study. Only a few strike-slip faults

namely the, Strydpoort, Ysterberg and Rietfontein faults, depict pre-Transvaal deformation in the study area. In addition, based on cross-cutting relationships, the NE-trending dykes developed in Archaean granites of the eastern Kaapvaal Craton might have formed during pre-Transvaal times.

A single stress ellipse (stress ellipse A, Table 7.1) can be constructed which accommodates left-lateral movement along the major faults (Charlesworth et al., 1986; de Wit and Roering, 1990; Potgieter, 1992), and the orientation of the dykes. It is therefore suggested that dyke formation and the strike-slip faults might have formed at the same time. However, it can be concluded that this single stress ellipse (Table 7.1) is an oversimplification of the stress fields existing during pre-Transvaal times in the Bushveld Complex area, but it can explain the ENE Archaean grain along which ancient crustal blocks accreted (de Wit et al., 1992; de Wit and Hart, 1993) and which controlled the formation of younger sedimentary basins.

7.2 Syn-Transvaal

The syn-Transvaal period can be grouped into three major stages, proto-basin development, post-Chuniespoort Group, and syn-Pretoria to post-Pretoria Group stage.

Eriksson et al. (1996) suggested that Transvaal proto-basin development was probably linked to strike-slip movement along the TML. The Ysterberg and Strydpoort faults have been interpreted as active growth faults during Wolkberg Group deposition (Potgieter, 1992). Stress directions derived for these faults indicate extension in a NNW-SSE direction (Figure 6.17 B). In a left-lateral strike-slip system, this NNW-SSE extension would have prevailed to accommodate movement along the Ysterberg and Strydpoort growth faults (stress ellipse A, Table 7.2). This ellipse is similar to the ellipse determined for the pre-Transvaal time period (stress ellipse A, Table 7.1), and therefore it can be concluded that Archaean stress fields influenced Transvaal proto-basin development.

Potgieter (1992) suggested that after deposition of the Chuniespoort Group, a major period of regional NNW-SSE directed compression resulted in the uplift of the Chuniespoort basin, causing a sedimentary hiatus of 150 Ma. This deformation resulted in the ENE trending folds of the Mhlapitsi fold belt as well as ENE trending

strike-slip and thrust faults. Stress directions derived from these structures indicate a strong NNW compressional direction (Figure 6.25). However, no other evidence for this regional compression has been recorded in other parts of the Chuniespoort basin. It is therefore suggested that the deformation might have been linked to right-lateral movement along the TML as illustrated by stress ellipse B (Table 7.2).

The Pretoria basin is interpreted as a rift related basin (Schreiber et al., 1992) or as the result of half-grabens, controlled by the TML. During syn-Pretoria times, the Rustenburg fault displays normal movement (Bumby, 1997). Extension directed towards the NE could have accommodated this type of faulting (Figure 6.15 B). The Groot Marico and Swartruggens faults follow the same orientation as the Rustenburg fault, and therefore might also have been syn-Pretoria normal faults. If right-lateral movement along the TML prevailed during syn-Pretoria times, then stress ellipse B (Table 7.2) would remain valid, and can explain the Rustenburg fault developing as a secondary normal fault with in a large strike-slip system. On the other hand, stress ellipse C (Table 7.2) illustrates the orientation of the stress field if the Rustenburg fault developed as a primary normal fault, perhaps due to extensional stresses related to rifting.

It seems as if ongoing movement along the TML played a fundamental role during deposition and deformation of the Transvaal basin. In addition, the same directions (NE and NW) for extension and compression are constantly reutilized. These are the same directions which were established early on in the evolution of the Kaapvaal Craton.

7.3 Post-Transvaal/Pre-Bushveld

The post-Transvaal/pre-Bushveld time bracket is relatively short and no evidence of regional tectonic events of this age, except for the Eburnian orogeny along the SW margin of the Craton, have been documented (Thomas et al., 1993). Also, based on the constant strike-and-dip values of the Transvaal basin it appears as if the Transvaal basin was not subjected to any large scale regional deformational events. Yet, the presence of several large faults (Rustenburg, Wonderkop, Steelpoort and Laersdrif faults), as well as the interference fold patterns documented by Hartzer (1994) and Bumby (1997) need to be accounted for. Hartzer (1994) proposed two deformational events during post-Transvaal but pre-Bushveld times. The first period (D_1) implies compression towards the NE, while D_2 is characterized by a NW directed

compression, possibly related to the Eburnian orogeny. Some workers (Potgieter, 1992; Du Plessis, 1990) proposed left-lateral movement along the TML during pre-Bushveld times.

Several large faults of post-Transvaal age are present in the Bushveld Complex and surrounding Transvaal rocks. These faults include the right-lateral Rustenburg (Bumby, 1997), normal Rietfontein (Charlsworth et al., 1986), left-lateral Wonderkop (Hartzer, 1994), right-lateral or normal Steelpoort (Visser, 1998; Sharpe and Snyman, 1980) and Laersdrif fault. In addition, the well documented interference fold patterns of the Transvaal Inliers (Hartzer, 1994) are also a characteristic feature of this time period. To accommodate these structures into one stress ellipse is a bit more problematic, partly due to a lack of geological information for most of the major faults. Therefore, several possible stress ellipses were considered.

The only stress ellipse which can accommodate the NW trending Rustenburg and NE trending Wonderkop fault into a single stress field is illustrated in stress ellipse D (Table 7.2). This would require a σ_1 directed NS, during which the Rustenburg and Wonderkop faults were conjugate strike-slip faults. This stress ellipse requires right-lateral movement along the Rustenburg fault and left-lateral movement along the Wonderkop fault. These faulting styles have been proposed for both faults (Hartzer, 1994; Bumby, 1997). However, this stress ellipse fails to explain the interference fold pattern observed in the Transvaal rocks observed by Hartzer (1994).

Stress ellipse E (Table 7.2) can accommodate folds with NW orientated fold axes, and normal faults orientated in a northeasterly direction as secondary structures related to a large ENE trending left-lateral strike-slip system. Hartzer (1994) and Bumby (1997) both recorded F_1 folds with NW trending fold axes in the Transvaal rocks, also, if the Wonderkop and Steelpoort faults were pre-Bushveld normal faults, then they might have formed under these stress conditions. However, if the Wonderkop fault was a pre-existing weakness, left-lateral movement along the fault could also have occurred under these stress conditions.

Stress ellipse F (Table 7.2) accommodate NE orientated fold axes, and NW orientated normal faults as secondary structures related to right-lateral movement in a large ENE strike-slip system. Large NE trending anticline and syncline pairs occur in the western Transvaal basin, but no documentation of NW orientated post-Transvaal normal faults exist. However, according to Bumby (1997) extensive right-

lateral displacement along the pre-existing Rustenburg fault, could have occurred under these stresses (ellipse F Table 7.2).

The last set of structures that needs to conform to the stress fields active during post-Transvaal times, are the radial faults around the Johannesburg dome. These faults might be due to post-Transvaal uplift of the dome (Allsop, 1961) which would have resulted in only a localized stress field. However, the uplift might be due to post-Transvaal normal movement along the Rietfontein fault (Charlsworth et al., 1986). The Rietfontein fault trends NE and would therefore fit well into stress ellipse E (Table 7.2).

It is almost impossible to attribute a single stress field to the different orientations and styles of the various faults. The proposed stress fields can only be accurate if structures formed as secondary structures resulting from a major strike-slip system. Such a strike-slip system might have existed between the TML and the Barberton lineament. Prolonged left-lateral (D_1) and right-lateral (D_2) movement within this strike-slip zone would have been the cause of the opposing stress directions observed during this time. If this supposed lateral movement can be ascribed to the Eburnian orogeny remains speculative. However, it might also be possible that only localized stress fields deformed the Transvaal basin during pre-Bushveld times. Stresses might have been imposed by the updoming of the Bushveld Complex, and therefore intense deformation do not extend across the entire Transvaal basin. However, Bumby (1997) argues that most of the stress imposed by the Eburnian orgogeny was accommodated by the Rustenburg fault and therefore no large scale deformation is present further towards the east.

7.4 Post-Bushveld/Pre-Waterberg

The poorly documented structures present in the Bushveld Complex contributes to the uncertainty about the tectonic setting of this large layered intrusion. Opinions vary greatly (see Chapter 4.2) from an active tectonic environment in which rifting allowed for the intrusion of such a large igneous body to a stable cratonic setting into which a rising mantle diapir was responsible for the emplacement of the Bushveld Complex. Du Plessis and Walraven (1990) suggested left-lateral movement along the TML during and after the emplacement of the Bushveld Complex. On the other hand, some workers (Uken and Watkeys, 1997b) believe that EW compression and NS extension prevailed during the intrusion of the Bushveld Complex. In contrast,

Van Biljon (1976) suggested EW extension during the emplacement of the Complex. Not enough structural information is available to constrain the stress conditions existing during syn-Bushveld times.

EW compression (Uken and Watkeys, 1997b) would result in stress fields illustrated by stress ellipse G (Table 7.2). These directions could explain the large EW striking lineaments present in the western Transvaal basin. However, EW compression (van Biljon, 1976) would result in opposite stress fields (ellipse K, Table 7.2) and can possibly explain the NS trend of the northern lobe of the Bushveld Complex.

Understanding the stress fields which existed during post-Bushveld times are just as problematic as the pre-Bushveld and syn-Bushveld stress fields. Again, this is due to the poorly constrained ages and faulting styles for the Wonderkop, Brits Graben, Steelpoort and Laersdrif faults. Based on cross-cutting relationships, these faults may have a minimum age of post-Karoo. However, in this study these faults are considered as at least pre-Waterberg in age. The Rustenburg fault is not considered as a post-Bushveld fault since Bumby (1997) suggested that the pre-existing Rustenburg fault did not reactivate during Bushveld times since recrystalization of the fault zone during the intrusion of the Bushveld Complex caused the fault zone to be more competent than the host rock. It appears however, as if the eastern compartment of the Complex is dominated by NE orientated faults (Steelpoort, Wonderkop faults), whereas the western compartment is dominated by NW trending faults (Brits Graben, Crocodile River faults). Other prominent structures which need to conform to the stress fields of post-Bushveld times are the large NW orientated folds observed in the granites of both compartments (Walraven, 1974; Walraven, 1986). The following question thus arises: was the Bushveld Complex subjected to opposing stress fields of the same age, or did two separate stress fields of different ages affect the Complex?

Stress conditions as illustrated by stress ellipse G (Table 7.2) and would explain normal movement of the NE orientated Wonderkop, and Steelpoort faults, as well as the NW orientated folds observed in the Bushveld granites of both compartments. The sinuous nature of these folds might indicate syn-Bushveld folding when magma was still unsolidified and the fold axes probably rotated. Investigations by Tyler and Tyler (1996) in the marginal rocks of the eastern Bushveld Complex confirms ENE orientated compression during syn-Bushveld times.

Normal movement along the Crocodile River fault and Brits Graben (Hartzer, 1994; Visser, 1998) are not reconcilable with the proposed left-lateral movement along the TML, or EW extension or compression. Therefore, two separate stress fields are proposed to have existed in the eastern and western compartments. They are portrayed by stress ellipse I (western lobe) and J (eastern lobe) (Table 7.2) which implies NE and NW extension respectively. However, the proposed stress fields existing in the eastern compartment still fails to explain the orientation of the Laersdrif fault. A possible explanation might be that the fault is not post-Bushveld in age.

Stress analysis of this time period, suggests that at least two different stress fields must have existed during post-Bushveld times. It is possible that left-lateral movement along the TML existed during syn-Bushveld times till shortly after (ellipse H, Table 7.2). The stress fields as illustrated by ellipses I and J then existed simultaneously after the left-lateral movement of the TML.. A possible cause for these opposing stress fields existing of the same time, might be due to locally induced stresses during thermal collapse of the Bushveld Complex (Visser, 1998). Therefore, similarly to the Transvaal basin, it appears as if the deformation of the Bushveld Complex was not the result of regional scale tectonic events, but was deformed by locally induced stress fields. Also, the strikingly similar strike-and-dip pattern of the Transvaal basin and Bushveld Complex, points to the fact that both sequences must have been subjected to similar regional tectonic events.

7.5 Post-Waterberg/Pre-Karoo

The post-Waterberg/pre-Karoo period has a very long time span (1800Ma – 350Ma). The absence of preserved sedimentary sequences during this time makes it difficult to place a more narrow time constraint on the deformational events affecting the Bushveld Complex and surrounding areas. In addition, no evidence exists for major tectonic processes affecting the Kaapvaal Craton during this time. The Waterberg basin is believed to formed in a half-graben setting with the TML marking the southern boundary (Callaghan et al., 1991). Du Plessis (1990) suggested left-lateral movement along the TML during proto-basin development. In addition tensional conditions existed on the Kaapvaal Craton due to cooling of the crust after the intrusion of the Bushveld Complex (Jansen, 1982). Two main theories exist regarding the deformation of the Waterberg basin, one favouring strike-slip movement (Du Plessis, 1990) and the other favouring mostly thrust movement

(Jansen, 1982) along the southern margin of the Waterberg basin. Stress interpretations of post-Waterberg times rely much on the geological evidence observed in the Waterberg rocks along the Thabazimbi-belt, which include EW orientated faults and folds. The smaller Cullinan-Middelburg basin is also characterized by EW striking faults. Other structures of the large Waterberg basin include some NW orientated faults and lineaments (Figure 6.8 C).

Du Plessis (1990) interpreted the large EW striking faults as strike-slip faults caused by post-Waterberg left-lateral movement along the TML. Stress ellipse A (Table 7.3) illustrates the possible stress field existing during this time. The complex interplay of faults was interpreted by Du Plessis (1990) as conjugate shears bounding flower structures. In addition, left-lateral movement along the Melinda fault during post-Waterberg but pre-Karoo times (Brandl and Reimold, 1990) fits well into this model/scenario.

However, the many EW orientated anticlines and synclines, and thrust faults along the southern margin of the Waterberg basin are not accommodated by stress ellipse A (Table 7.3). These folds show strong evidence for NS directed compression during post-Waterberg times (Jansen, 1982). Stress ellipse B (Table 7.3) illustrates the possible stress fields and the related structures. This stress field could have caused left-lateral reactivation along the TML as observed by Du Plessis (1990).

The final post-Waterberg deformation is marked by NE directed tension, exemplified by the Vaalwater and Boschpoort normal faults (Jansen, 1982). Stress ellipse C (Table 7.3) accounts for the structures formed due to these stress directions. The NW trending post-Waterberg lineaments are also reconcilable with these tensional conditions.

It is noteworthy that the previously constantly NE and NW directed stresses prevailing since pre-Transvaal times, change to NS and EW during post-Waterberg times. However, the regional tectonic event responsible for this NS compression remains enigmatic. The approximately 1000Ma Kibaran orogeny, marking collision along the SW and SE margins of the Kaapvaal Craton, can be a possible cause.

7.6 Pilanesberg

The intrusion of alkaline complexes is a characteristical feature during 1400Ma to 1300Ma. These complexes might have been structurally controlled by a NNE trending lineament (Figure 4.9) (Verwoerd, 1993). However, active post-Karoo structures, such as the Melinda fault and Zebediela fault, cut across this supposed lineament. Therefore, due to offsets caused by younger structures, the lineament observed today might not have been a lineament during Pilanesberg times.

The stress directions for the Pilanesberg times are solely derived from the Bos2 area, in which syenite dykes trend NW and the circular Pilanesberg Complex intruded along the western margin of the Rustenburg Layered Suite.

Syenite dykes indicate a NE orientated extensional stress field. This stress field would be similar to the stress ellipse C (Table 7.3) of late post-Waterberg times, and therefore it is possible that post-Waterberg stress conditions prevailed during the intrusion of syenite dykes.

The intrusion of the Pilanesberg Complex resulted in a localized circular stress field (stress ellipse D Table 7.3). However, σ_1 remains vertical during the intrusion, similar to stress ellipse C, and therefore the regional stress field could have been similar as during syenite dyke intrusion.

7.7 Post-Karoo

Reactivated post-Karoo normal faults, such as the Zebediela and Melinda faults, are probably responsible for Karoo rocks being preserved on the northern Kaapvaal Craton. The NE trending Olifants River dyke swarm (Uken and Watkeys, 1997a) is also a prominent extensional feature of this time period.

A single stress ellipse (ellipse A Table 7.4) can accommodate the orientation of the dyke swarm as well as the post-Karoo normal faults. The noticeable deflection in the orientation of the Olifants River dyke swarm in the Transvaal rocks versus the adjacent Archaean rocks (Figure 6.5 B and C) should not change the orientation of the proposed stress field. If the dykes in the adjacent Archaean granites are planes of pre-existing weaknesses of Archaean age (see 7.1) then they too would have been reutilized under this stress field. However, they might not be Archaean in age

but simply have a slightly different orientation to dykes in the Transvaal rocks due to competency differences of the host rock.

A different set of dolerite dykes, trending NW, occur in the western Bushveld Complex area (Figure 6.3). The age of these dykes are unknown and they might be related to the post-Bushveld extensional period (stress ellipse H, Table 7.2). However, if these dykes are post-Karoo in age, they do not conform to stress ellipse A (Table 7.4), and therefore probably reflect a another opposing extensional stress field existing during post-Karoo times.

Table 7.1. The Randian and Swazian periods (for discussion of stress ellipse see text)

Erathem	Age	Regional Events	Specific events	Intrusions	Formation	Stress ellipse
Randian	2.6			Various Granites	Amalia Kraaipan - greenstone belt	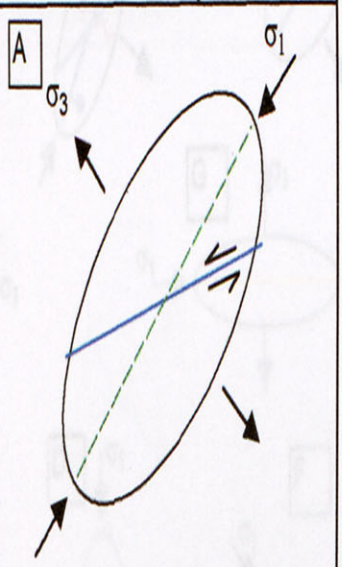
	2.65	Limpopo orogeny	Intra-cratonic tectonics - development of basins with ENE strike, continental growth along western and northern margin		Ventersdorp basin	
	2.687					
	2.7					
	2.8	Development of the Kaapvaal Craton - mosaic of crustal blocks accreted along large-scale ENE-striking shear zones.		Various Granites- Northern and western Kaapvaal Craton	Pietersburg greenstone belt	
Swazian	2.9				Witwatersrand basin	
	3				Murchison greenstone belt	
	3.1		Southern and central parts coherent unit - start of TML	Various Granites - eastern and southern Kaapvaal Craton	Dominion basin Pongola basin	
	3.2		Intra-oceanic tectonics - greenstones and granitization		Barberton greenstone belt	
	3.3					
	3.4			Johannesburg dome		

Table 7.2. The Vaalian period (for discussion of stress ellipses, see text)

Erathem	Age	Regional events	Specific events	Intrusions	Formation	Stress ellipse
V A A L I A N			Thermal collapse			
	2.02	Vredefort Dome				
	2.05	Left-lateral movement along TML	Intrusion of the Bushveld Complex	Lebowa Granite Suite		
	2.06			Rustenbug Layered Suite		
			Pre-Bushveld diabase intrusions - updoming	sills/dykes		
	2	Eburnian orogeny, plate-collision at the SW margin of Kaapvaal Craton	Folding of Transvaal rocks, D_1 (NW trending folds) D_2 (NE trending folds)			
	2.15		Volcanic activity		Rooiberg (felsite)	
	2.25	Half-graben - controlled by TML	Fluvial sedimentation. Rifting/Thermal subsidence		Pretoria	
	2.3	Regional NNW-SSE compresional tectonics	Uplift of Chuniespoort basin - sedimentary hiatus		Unconformity	
	2.4	Widespread Transvaal basin development - thermal subsidence, initially WNW axial trend	Minor periodical regional compression – Shallow eperic sea		Chuniespoort	
	2.6		Shallow sea		Black Reef	
	2.67	Transvaal proto-basin,	Strike-slip along TML, NNW-SSE extensional tectonics, active growth faults		Wolkberg	

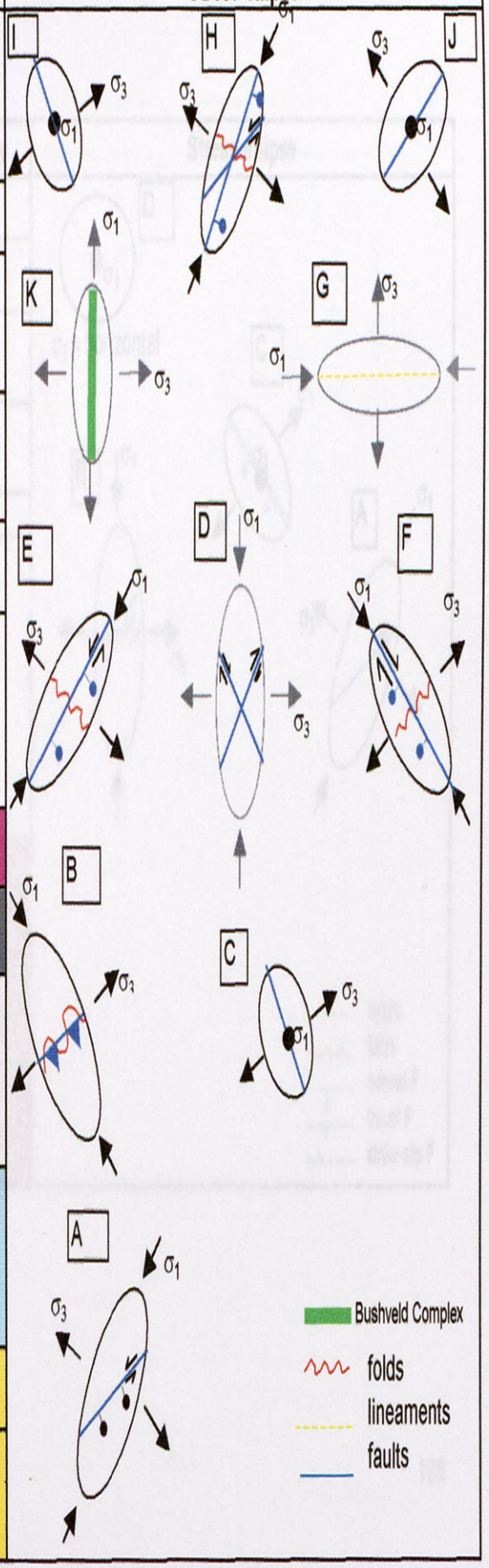

Table 7.3. The Mogolian period (for discussion of stress ellipses, see text)

Erathem	Age	Regional Events	Specific events	Intrusions	Stratigraphy	Stress ellipse
Mogolian	1	Kibaran orogeny - Natal-Namaqua structural and metamorphic province				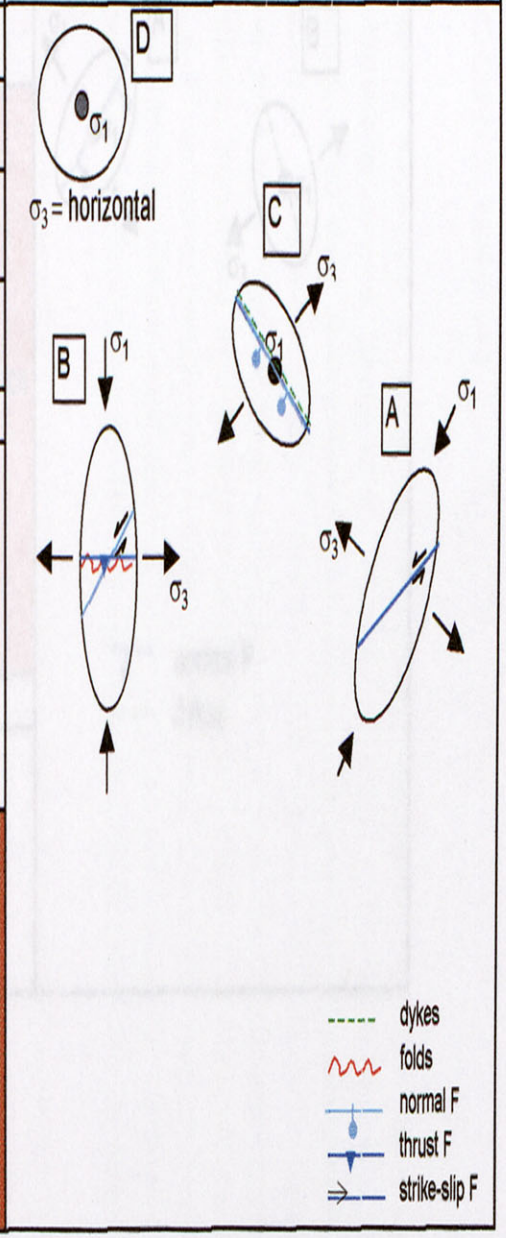
	1.2					
	1.3	Intrusion of alkaline complexes		Pilanesberg		
	1.4			Spitskop		
			Tensional faulting	Diabase		
			Large scale NS compression			
	1.5	Deposition of Waterberg Group	Fluvial enviornment (alluvial fans, lakes, local deserts)		Waterberg	
	1.6					
	1.7		Block faulting			
	1.8	Nylstroom proto-basin and Alma trough, developed along TML				

Table 7.4. Karoo period (for discussion of stress ellipses, see text).

Erathem	Age	Regional Events	Specific events	Intrusions	Formation	Stress ellipse
Cenozoic	65	Epeirogenetic - Sea-level fluctuations				
Mesozoic	135	separation of west Gondwana (South America)	tension in Limpopo belt	Mesozoic dyke swarm	Karoo Sequnce	
	150	separation of east Gondwana (Antartica)		Karoo dolerites		
	190					
	200			Mesozoic dyke swarm		
	245	Cape orogeny				
Palaeozoic	280	Gondwana super continent	Formation of Karoo basin - rifting			
	300					
	400					
	500	Pan African orogeny - continental rifting				
	600					
	700					
	800					
	900					

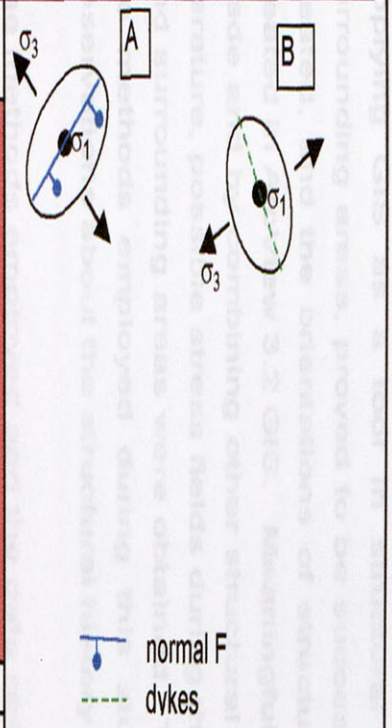

8. CONCLUSION

Applying GIS as a tool in structural analysis of the Bushveld Complex and surrounding areas, proved to be successful. A functional structural database was created, and the orientations of structures can be represented by rose diagrams created in ArcView 3.2 GIS. Meaningful stress analyses of the rose diagrams were made and by combining other structural and tectonic information obtained from the literature, possible stress fields during the tectonic history of the Bushveld Complex and surrounding areas were obtained. This chapter evaluates the effectiveness of the methods employed during this study as well as discuss some conclusive observations about the structural history of the Bushveld Complex.

The methods employed and the data obtained during this study proved that GIS can be used as an effective means of evaluating large amounts of geological data. Therefore, any regional-scale structural study can benefit from the use of GIS techniques. In addition, this new technique provides a fast method for determining the orientations of lines and representing these orientations by means of rose diagrams. By merely clicking consecutively on the various customized icons in the ArcView program the desired results are produced. By using the structural database in conjunction with analytical techniques of ArcView, different criteria (type, age, displacement type etc.) can be specified by which structures are considered.

The main shortcoming of applying an automated technique such as this, is the computer assigned ages for the structures. Ages are assigned based on cross-cutting relationships which provide a maximum age for a structure. The possibility remains that a structure could have been a pre-existing plane of weakness, or could have reactivated during later stages. The GIS assigned ages might not always be correct and it is therefore important to incorporate ages obtained form geological field evidence, as well as consider reactivation ages.

The main shortcomings of the analytical techniques used during this study, result from considering the map exposure of a structure as its true orientation. This might result in erroneous interpretations of stress directions especially for low-angle structures in areas of high relief. Also, most stress directions are interpreted assuming the structures are primary and not the result of reactivation of planes of pre-existing weaknesses. Again, erroneous interpretations of stress directions might

result, since oblique stresses can cause reactivation of a plane of pre-existing weakness.

For a study such as this, the quality of the data is of utmost importance. The structural database for the Bushveld Complex and surrounding areas is far form complete. Much more detailed structural field work is necessary especially on the large faults of the eastern Bushveld Complex (Wonderkop, Steelpoort, Laersdrif faults). Without knowing the timing, reactivation histories, type, and sense of displacement of these faults, the deformational history of the Bushveld Complex will remain enigmatic. However, this study allowed for the consideration of various possibilities regarding the timing, displacement and possible tectonic causes for the structures. Detailed structural data will place more constraints on the interpretation of the data and, will further result in better tectonic models. Nevertheless, despite of the deficiencies in structural information the following conclusive observations are made:

- Structures, such as dykes, lineaments, faults and folds, in and around the Bushveld Complex reflect a definite NE and NW structural trend. It is possible that these directions were established early in the tectonic evolution of the Kaapvaal Craton, and served as planes of pre-existing weakness during later deformation of the Craton.

- It is evident that NE and NW stress directions were constantly reutilized, and the identities of the principal stress directions alternated between these NE and NW orientations during the structural history of the area. However, the only variation to this occurs during post-Waterberg times when prominent NS stress directions prevailed. However, during post-Karoo times the characteristically NE and NW directions reoccurred.

- Most of the stress fields obtained for the various time periods are consistent with constant reactivation of the TML. Left-lateral, right-lateral, thrust and normal movements are known to have occurred at various times along the TML during the history of the Bushveld Complex and surrounding areas.

- On a regional scale, the Transvaal basin and Bushveld Complex seem to have been subjected to the same deformation. However, the Transvaal Basin appears to have been deformed mildly to intensely in localized areas before the intrusion of the Bushveld Complex.

9: ACKNOWLEDGEMENTS

I wish to thank the following people:

Prof. S.A. de Waal for arranging funding of the project.

Magdel Combrinck for help with software and programming.

Dr. Louis van Rooy – just for everything.

Dr. H.J. Brynard for sacrificing his valuable time to help supervising this project, and for all the insightful contributions.

Dr. Roelof van der Merwe for his guidance and patience, and especially for help during crises times.

10. REFERENCES

Allsopp, H.L. 1961: Rb-Sr age measurements on total rock and separated-mineral fractions from the Old Granite of the central Transvaal. Journal of Geophysical Research 66, 1499-1408.

Anderson E.M. 1951: The dynamics of faulting. Oliver and Boyd, Edinburgh.

Anhaeusser, C.R. 1973: The geology and geochemistry of the Archeaen granites and gneisses of the Johannesburg-Pretoria dome. Special Publication Geological Society South Africa 3, 361-385.

Anhaeusser, C.R. and Wilson, J.F. 1981: The Granitic Gneiss-Greenstone Shield. In: Precambrian of the southern Hemisphere, (ed.) Hunter, D.R. Elsevier, Amsterdam, 423-492.

Armstrong, R.A, Compstone, W., Retief, E.A., Williams, I.S. and Welke, H.J. 1990: Zircon ion microprobe studies bearing on the age and evolution of the Witwatersrand Triad. Precambrian Research 53, 243-266.

Barton, J.M., Fripp, R.E.P., Horrocks, P., and McLean, N. 1979: The geology, age and tectonic setting of the Messina layered Intrusion, Limpopo Mobile Belt, southern Africa. American Journal of Science 279, 1108-1134.

Barton, E.S., Altermann, W., Williams, I.S., and Smith, C.B. 1994: U-Pb zircon age for a tuff in the Campbell Group, Griqualand West Sequence, South Africa: Implications for Early Proterozoic rock accumulation rates. Geology 22, 343-346.

Beukes, N.J. 1983: Paleoenvironmental setting of iron-formations in the depositional basin of the Transvaal Supergroup, South Africa, In: Iron-formation: Facts and problems, (eds.) Trendall, A.F., and Morris, R.C. Elsevier, Amsterdam, 131-209.

Beukes, N.J. and Cairncross, B. 1991: A lithostratigraphic-sedimentological reference profile for the Late Archaean Mozaan Group, Pongola sequence: application to sequence stratigraphy and correlation with the Witwatersrand Supergroup. South African Journal of Geology 94, 44-69.

Bickle, M.J., and Eriksson, K.A. 1982: Evolution and subsidence of early Precambrian sedimentary basins. Phil. Trans. Royal Society of London, A, 305, 225-247.

Biesheuvel, K. 1970: An interpretation of a gravimetric survey in the area west of the Pilanesberg, in the Western Transvaal, In: Symposium on the Bushveld Igneous Complex and other layered intrusions, (eds.): Visser, D.J.L. and von Gruenewaldt, G.. Special Publication, Geological Society of South Africa 1, 1-18.

Bloy, P.D. 1986: The Rustenburg Fault. Unpublished B.Sc. Honours dissertation, University of Natal.

Brandl, G. 1987: The Geology of the Tzaneen area. Explanation, Sheet 2330, Geological Survey, Pretoria.

Brandl, G. and de Wit, M.J. 1997: The Kaapvaal Craton. In: Greenstone belts, (eds.) de Wit, M.J. and Ashwal, L.D. Claredon Press, New York, 581-607.

Brandl, G. and Reimold, W.U. 1990: The structural setting and deformation associated with pseudotachylite occurrences in the Palala Shear Belt and Sand River Gneiss, Northern Transvaal, Tectonophysics 171, 201-220.

Broekhuizen A. 1998: The geology of the Koedoesrand Formation, northwestern Transvaal, and its relationship to the Palala Shear Zone. Unpublished M.Sc. thesis, University of Pretoria.

Brynard, J.H. 1996: BOSGIS – 'n Geografiese inligtingstelsel vir die Bosveldkompleks, Handleiding. Unpublished, University of Pretoria, Department of Earth Sciences.

Bumby, A.J. 1997: The geology of the Rustenburg fault. Unpublished M.Sc. thesis, University of Pretoria.

Bumby A.J., Eriksson P.G., van der Merwe R. 1998: Compressive deformation in the floor rocks to the Bushveld Complex (South Africa): evidence from the Rustenburg Fault Zone. Journal of African Earth Sciences 27, 307-330.

Bumby, A.J. 2000: The geology of the Blouberg Formation, Waterberg and Soutpansberg Group in the area of Blouberg mountain, Northern Province, South Africa. Unpublished Ph.D. thesis, University of Pretoria.

Burke, K., Kidd, W.S.F. and Kusky, T., 1985: Is the Ventersdorp Rift System of southern Africa related to a continental collision between the Kaapvaal and Zimbabwe cratons at 2.64 Ga ago? Tectonophysics 115, 1-24.

Burke, K., Kidd, W.S.F. and Kusky, T. 1986: Archaean foreland basin tectonics in the Witwatersrand, South Africa. Tectonics 5, 439-456.

Button, A., 1973: A regional study of the stratigraphy and development of the Transvaal basin in the eastern and north-eastern Transvaal. Unpublished Ph.D. thesis, University of the Witwatersrand.

Button, A., 1981: The Ventersdorp Supergroup. In: Precambrian of the southern hemisphere, (ed.) D.R. Hunter. Elsevier, Amsterdam, 520-527.

Callaghan, C.C., Eriksson, P.G., and Snyman, C.P. 1991: The sedimentology of the Waterberg Group in the Transvaal, South Africa: an overview. Journal of African Earth Sciences 13, 121-139.

Cawthorn R.G. 1998: Geometrical relations between the Transvaal Supergroup, the Rooiberg Group, and the mafic rocks of the Bushveld Complex. South African Journal of Geology 101, 275-279.

Cawthorn R.G., Davies G., Clubley-Armstrong A. and McCarthey T.S. 1981: Sills associated with the Bushveld Complex, South Africa: an estimate of the parental magma composition. Lithos 14, 1-15.

Charlesworth E.G., McCarthy, T.S., Stanistreet, I.G. and Cadle, A.B. 1986: Structural geology of the Rietfontein fault system on the Cenral Rand. Geogongress 1986, Extended abstracts. Geological Society of South Africa, Johannesburg, 23-26.

Clendenin, C.W. 1989: Tectonic influence on the evolution of the early proterozoic Transvaal Sea, southern Africa. Unpublished Ph.D. thesis, University of Witwatersrand.

Clubley-Armstrong, A.R. and Sharpe, M.R., 1979: The structural evolution of the Dennilton Dome and its relationships to the intrusion of the Bushveld Complex: Transactions Geological Society of South Africa 82, 23-26.

Coertze, F.J. 1962: The Rustenburg Fault as a controlling factor of ore-deposition southwest of Pilanesberg. Transactions Geological Society of South Africa 62, 179-201.

Coertze, F.J., 1970: The geology of the western part of the Bushveld Igneous Complex. In: Symposium on the Bushveld Igneous Complex and other layered intrusions, (eds.) D.J.L. Visser and G. von Gruenewaldt, Special Publication 1, Geological Society of South Africa, 5-22.

Coertze, F.J. 1974: The geology of the basic portion of the western part of the Bushveld Igneous Complex. Geological Survey South Africa, Memoir 66.

Cole, D.I. 1992: Evolution and development of the Karoo Basin. In: Inversion Tectonics of the Cape Fold Belt, Karoo and Cretaceous Basins of Southern Africa, (eds.) de Wit, M.J. and Ransome, I.G.D. Balkema, Rotterdam, 87-100.

Corner, B., Durrheim, R.J. and Nicolaysen, L.O., 1990: Relationship between the Vredefort structure and the Witwatersrand basin within the tectonic framework of the Kaapvaal craton as interpreted from regional gravity and aeromagnetic data: Tectonophysics 171, 49-61.

Courtnage, P.M. 1995: Post-Transvaal deformation between the Johannesburg Dome and the Bushveld Complex. Unpublished M.Sc. thesis, University of the Witwatersrand.

Cousins, C.A., 1959: The structure of the mafic portion of the Bushveld Igneous Complex: Transactions Geological Society of South Africa 62, 179-201.

Coward, M.P. and Fairhead, J.D., 1980: Gravity and structural evidence for the deep structure of the Limpopo Belt, southern Africa. Tectonophysics 68, 31-43.

Coward, M.P. Spencer, R.M. and Spencer, C.E. 1995: Development of the Witwatersrand Basin, South Africa. In: Early Precambrian Processes, (eds.) Coward, M.P. and Ries, A.C. Geological Society Special Publication 95, 243-269.

Cox, K.G., 1970: Tectonics and volcanism of the Karoo Period and their bearing on the postulated fragmentation of Gondwanaland in African magmatism and tectonics, (eds.) T.N. Clifford and I.G. Gass. Oliver and Boyd, Edinburgh, 211-235.

Crocker, I.T. 1976: Fluorite mineralisation in the Bushveld Granites southeast of Rooiberg, Transvaal. Unpublished M.Sc. thesis, University of Stellenbosch.

Crockett, R.N., 1969: Geological significance of the margin of the Bushveld basin in Botswana: Unpublished Ph.D. thesis, University of London.

Crockett, R.N., 1971: Some aspects of post-Transvaal tectogenesis in southeastern Botswana, with particular reference to the Lobatse-Ramotswa areas. Transactions Geological Society of South Africa 74, 211-235.

Daly, 1928: The Bushveld Igneous Complex of the Transvaal. Geological Society America Bulletin 55,125-145.

DeMers, M.N. 1997: Fundamentals of Geographic Information Systems. John Wiley and Sons, New York.

De Waal, S.A. 1963: Die plooikompleks van die Sisteem Transvaal noord van Marble Hall en die meegaande metamorfe en intrusiegesteentes. Unpublished M.Sc. thesis, University of Pretoria.

De Waal, S.A. 1970: Interference-folding of Bushveld Igneous Complex age in the Transvaal System north of Marble Hall, Transvaal. In: Symposium on the Bushveld Igneous Complex and other layered intrusions, (eds.) Visser, D.J.L., and Von Gruenewaldt, G. Special Publication of the Geological Society of South Africa 1, 283-298

De Wit, M.J. 1992: The geology and tectonic evolution of the Pietersburg Greenstone Belt, South Africa. Precambrian Research 55, 123-153.

De Wit, M.J., and Hart, R.A. 1993: Earth's earliest continental lithosphere, hydrothermal flux and crustal recycling. Lithos 30, 309-335.

De Wit, M.J. and Roering, C., 1990: Episodes of formation and stabilization of the Kaapvaal craton in the Archaean: an overview based on some selected recent data, In: The Limpopo Belt: a field workshop on granulites and deep crustal tectonics, (ed.): J.M. Barton. Extended abstracts, Johannesburg, 42-52.

De Wit, M.J., Jeffery, M., Bergh, H. and Nicolayson L.O. 1988: The Geological map of Gondwana, with explanatory notes. American Association of Petroleum Geologists, Tulsa.

De Wit, M.J., Roering, C., Hart, R. J., Armstrong, R.A., De Ronde, C.E.J., Green, R.W.E., Tredoux, M., Peberdy E., and Hart R.A. 1992: Formation of an Archean continent. Nature 357, 553-562.

De Wit, M.J., Armstrong, R.A., Kamo, S.L. and Erlank, A.J., 1993: Gold-bearing sediments in the Pietersburg greenstone belt: age equivalents of the Witwatersrand Supergroup sediments. South Africa. Economic Geology 88, 1242-1252.

Dingle, R.V., Siesser, W.G. and Newton, A.R. 1983: Mesozoic and Tertiary geology of southern Africa: Balkema, Rotterdam.

Du Plessis, M.D. 1978: Geological Map of Nylstroom 1:250 000 sheet (2428), explanatory notes. Geological Survey of South Africa.

Du Plessis, C.P. 1991: Tectonism along the Thabazimbi-Murchison Lineament. Unpublished Ph.D. thesis, University of the Witwatersrand.

Du Plessis, A. and Levitt, J.G., 1987: On the structure of the Rustenburg Layered Suite – insight from seismic data. Abstracts, Indaba on the Tectonic Setting of Layered Intrusives, Pretoria, South Africa.

Du Plessis C.P. and Walraven F. 1990: The tectonic setting of the Bushveld Complex in Southern Africa, Part 1. Structural deformation and distribution. Tectonophysics 179, 305-319.

Du Toit, A.L., 1929: The Volcanic belt of the Lebombo: a region of tension: Transactions, Royal Society of South Africa, XVIII (111), 189-218.

Eales, H.V., Botha, W.J., Hattingh, P.J., De Klerk, W.J., Maier, W.D. and Odgers, A.T.R., 1993: The mafic rocks of the Bushveld Complex: a review of emplacement and crystallization history, and mineralization, in the light of recent data: Journal of African Earth Sciences 16, 121-142.

Engelbrecht, J.P., 1986: Die Bosveld Kompleks en sy vloergesteentes in die omgewing van Nietverdiend, Wes-Transvaal: Unpublished Ph.D. thesis, University of Pretoria.

Eriksson, K.A., Turner, B.R., and Vos, R.G. 1981: Evidence of tidal processes from the lower part of the Witwatersrand Supergroup, South Africa. Sedimentary Geology 29, 309-325.

Eriksson, P.G., Meyer, R., and Botha, W.J. 1988: A hypothesis on the nature of the Pretoria Group Basin. South African Journal of Geology 91, 490-497.

Eriksson P.G., Schreiber U.M., and Van der Neut M. 1991: A review of the sedimentology of the Early Proterozoic Pretoria Group, Transvaal Sequence, South Africa: implications for tectonic setting. Journal of African Earth Sciences 13, 107-119.

Eriksson, P.G. and Reczko, B.F.F. 1995: The sedimentary and tectonic setting of the Transvaal Supergroup floor rocks to the Bushveld complex. Journal of African Earth Sciences 21, 487-504.

Eriksson P.G, Reczko B.F.F., Corner B. and Jenkins S.L. 1996: The Kanye axis, Kaapvaal craton, southern Africa: a postulated Archaean crustal architectural element inferred from three-dimensional basin modeling of the lower Transvaal Supergroup. Journal of African Earth Sciences 22, 223-233.

Eriksson P.G, van der Merwe R., and Bumby A.J. 1998: The Palaeoproterozoic Woodlands Formation of eastern Botswana-northwestern South Africa: lithostratigraphy and relationship with Transvaal Basin inversion structures. Journal of African Earth Sciences 27, 349-358.

Fourie, E.T. 1984: Die stratigrafie en sedimentologie van die Chuniespoort-Groep in noordwes-Transvaal. Unpublished M.Sc. thesis, Rand Afrikaans University.

Friese, A.E.W., Charlesworth, E.G. and McCarthy, T.S. 1995: Tectonic processes within the Kaapvaal craton during the Kibaran (Grenville) orogeny: Structural, geophysical and isotopic constraints from the Witwatersrand basin and environs. Economic Geology Research Unit, Information Circular 292. University of Witwatersrand, Johannesburg.

Fripp, R.E.P., 1981: The ancient Sand River Gneisses, Limpopo mobile belt, South Africa. Special Publication of Geological Society of Australia 7, 329-335.

Fripp, R.E.P., Van Nierop, D.A., Callow, M.J., Lilly, P.A. and du Plessis, L.U. 1980: Deformation in part of the Archaean Kaapvaal Craton, South Africa: Precambrian Research 13, 241-251.

Gibson, R.L., Courtnage, P.M., and Charlesworth, E.G. 1999: Bedding-parallel shearing and related deformation in the lower Transvaal Supergroup north of the Johannesburg Dome, South Africa. South African Journal of Geology 102, 99-108.

Gold, D. 1983: The geological evolution of a part of the Pongola Sequence, southern Kaapvaal Craton. Unpublished Ph.D. thesis, University of Natal, Pietermaritzburg.

Good, N., and de Wit, M.J. 1997: The Thabazimbi-Murchison Lineament of the Kaapvaal Craton, South Africa: 2700 Ma of episodic deformation. Journal Geological Society, London 154, 93-97.

Grobler, N.J., 1972: The geology of the Pietersburg greenstone belt. Unpublished D.Sc. thesis, University of the Orange Free State.

Groenewald, P.B., Grantham, G.H. and Watkeys, M.K. 1991: Geologic evidence for a Proterozoic to Mesozoic link between southeastern Africa and Dronning Maud Land, Antarctica. Journal Geological Society, London 148, 1115-1123.

Hall, A.L. 1932: The Bushveld Igneous Complex of the central Transvaal: Memoir, Geological Survey of South Africa 28.

Hamilton, W.B. 1977: Bushveld Complex – Product of impacts. In: Symposium on the Bushveld Igneous Complex and other layered intrusions, (eds) Visser, D.J.L., and Von Gruenewaldt, G. Special Publication Geological Society South Africa 1, 367-379.

Harmer, R.E., and Von Gruenewaldt, G. 1991: Magmatism associated with the Transvaal Basin – Implications for its tectonic setting. Research Report 91, Institute Geological Research Bushveld Complex, University of Pretoria, 53.

Hartzer, F.J. 1987: Die geologie van die Krokodilrivierfragment, Transvaal: Unpublished M.Sc. Thesis, Rand Afrikaans University.

Hartzer F.J. 1994: Geology of Transvaal inliers in the Bushveld Complex. Unpublished Ph.D. thesis, Rand Afrikaans University.

Hartzer, F.J. 1995: Transvaal Supergroup inliers: The geology, tectonic development and relationship with the Bushveld complex, South Africa. Journal of African Earth Sciences 21, 521-547.

Hatton C.J. 1995: Mantle plume origin for the Bushveld and Ventersdorp magmatic provinces. Journal of African Earth Sciences 21, 571-577.

Hofmann, C. 1997: Strukturele studie van die Nebo Graniete. Unpublished Honours dissertation, University of Pretoria.

Holzer, L., Frei, R., Barton, J.M., Jr. and Kramers, J.D. 1998: Unravelling the record of successive high grade events in the Central Zone of the Limpopo belt using Pb single phase dating of metamorphic minerals. Precambrian Research 87, 87-115.

Hunter, D.R. 1974: Crustal development in the Kaapvaal Craton, I: The Archaean: Precambrian Research 1, 295-326.

Hunter, D.R. 1975: The regional geological setting of the Bushveld Complex. (An adjunct to the provisional tectonic map of the Bushveld Complex): Economic Geology Research Unit, University of the Witwatersrand.

Hunter, D.R. 1976: Some enigmas of the Bushveld Complex: Economic Geology 71, 229-248.

Hunter, D.R. 1981: Plutonic events in the cratonic areas - Granitic events in Precambrian of the Southern hemisphere, (eds.) D.R. Hunter: Elsevier, Amsterdam, 562-569.

Hunter, D.R. and Hamilton, P.J. 1978: The Bushveld Complex. In: Evolution of the earth's crust, (ed.): D.H. Tarling. Elsevier, Amsterdam, 397-422.

Jansen H. 1982: The Geology of the Waterberg Basin. Geological Survey of South Africa Memoir 71.

Keyser, 1997: Geological map of the Republic of South Africa and the Kingdoms of Lesotho and Swaziland, scale 1:1000 000. Council for Geoscience, Pretoria.

Lapidus, D.F. 1990: Collins Dictionary of Geology. Caledonian, Glasgow.

Lee C.A, and Sharpe M.R. 1986: The structural setting of the Bushveld Complex - an assessment aided by Landsat imagery. In: Mineral Deposits of Southern Africa I&II, (eds.) Anhaeusser, C.R. and Maske, S. Geological Society of South Africa, Johannesburg,1031-1038.

Lenthall, D.H. 1975: Aspects of the geochemistry of the acid phase of the central and Bushveld complex. Information Circular 99, Economic Geology Research Unit, University of the Witwatersrand.

Leube, A., and Strumpfl, E.F. 1963: The Rooiberg and Leeupoort Tin Mines, Transvaal, South Africa. Economic Geology 58, 391-418.

Light, M.P.R. 1982: The Limpopo Mobile Belt: A result of continental collision. Tectonics 1, 325-342.

MacCaskie, D.R. 1983: Differentiation of the Nebo granite (Main Bushveld granite), South Africa. Unpublished M.Sc. thesis, University of Oregon.

Martin, K.K. and Hartnady, C.J. 1986: Plate tectonic development of the southwest Indian Ocean: a revised reconstruction of East Antarctica and Africa. Journal of Geophysical Research 91, 4767-4786.

Matthews, P.E. 1990: A plate tectonic model for the Late Archaean Pongola Supergroup in southeastern Africa. In: Crustal evolution and orogeny, (eds.) Sychanthavong, S.P.H. Oxford, New Delhi, 41-73.

McCourt, S. 1995: The crustal architecture of the Kaapvaal crustal block South Africa, between 3.5 and 2.0 Ga. Mineral Deposita 30, 89-97.

McCourt, S. and Vearncombe, J.R. 1987: Shear zones bounding the Central Zone of the Limpopo Mobile Belt, southern Africa: Journal of Structural Geology 9, 127-137.

McCourt, S. and Vearncombe, R. 1992: Shear zones of the Limpopo Belt and adjacent granitoid-greenstone terranes: implications for late Archaean collision tectonics in southern Africa Precambrian Research 55, 553-570.

McCourt, S. and Wilson, J.F. 1992: Late Archaean and Early Proterozoic tectonics of the Limpopo and Zimbabwe provinces, southern Africa. In: The Archaean: Terrains, processes and Metallogeny, (eds.) Glover, J.E. and Ho, S.E., 237-246.

Molyneux, T.G., 1970: A geological investigation of the Bushveld Complex in Sekhukhuneland and part of the Steelpoort valley, eastern Transvaal with particular reference to the oxide minerals. Unpublished Ph.D. thesis, University of Pretoria.

Molyneux, T.G. and Klinker P.S, 1978: A structural interpretation of part of the eastern mafic lobe of the Bushveld Complex and its surrounds. Geological Society of South Africa Transactions 81, 359-368.

Nicolaysen, L.O. 1985: Renewed ferment in the earth sciences - Especially about power supplies for the core, for the mantle and for crises in the faunal record: South African Journal of Science 81, 120-132.

Nicolaysen, L.O. and Ferguson, C., 1980: Diapirs driven by high pore fluid pressure: Abstract, Tectonic Studies Group, Symposium on diapirism and gravity tectonics, Leeds.

Park R.G, 1997. Foundations of Structural Geologly, 3rd edition. Chapman and Hall, London.

Potgieter G.J. 1992: Tektonisme langs die noordoostelike rand van die Bosveld kompleks. Unpublished Ph.D. thesis, University of Pretoria.

Pringle, I.C. 1986: Zwartkloof fluorite deposits, Warmbaths district. Mineral deposits of Southern Africa. In: Mineral deposits of southern Africa, (eds.) Anhaeusser, C.R. and Maske, S. Geological Society of South Africa, Johannesburg, 1343-1349.

Ramsay, J.G. 1963: Structural investigation in the Barberton Mountain Land, Eastern Transvaal: Transactions Geological Society of South Africa 66, 355-401.

Reimold, W.U. and Gibson, R.L. 1996: Geology and evolution of the Vredefort Impact Structure. Journal of African Earth Sciences 23, 125-162.

Robb, L.R, Davies, D.W and Kamo, S.L. 1991: Chronological framework for the Witwatersrand Basin and environs: towards a time-constrained depositional model. South African Journal of Geology 94, 86-95.

Roering, C. 1984: The Witwatersrand Supergroup at Swartkops: A re-examination of the structural geology. Transactions Geological Society of South Africa 87, 87-99.

Roering, C. 1986: Aspects of thrust faulting on the northern margin of the Witwatersrand basin. Geocongress 1986, extended abstracts. The Geological Society of South Africa, Johannesburg, 59-62.

Roering, C. and Smit , C.A. 1987: Bedding-parallel shear, thrusting and quartz vein formation in Witwatersrand quartzites. Journal of Structural Geology 9, 419-427.

Roering, C., Barton, J.M. and Winter, H. de la R. 1990: The Vredefort Structure; A perspective with regard to new tectonic data from adjoining terranes: Tectonophysics 171, 7-22.

Roering, C. van Reenen, D.D., Smit, C.A., Barton Jr., C.A., de Beer, J.H., de Wit, M.J., Stettler, E.H., van Schalkwyk, J.F., Stevens, G. and Pretorius, S. 1992: Tectonic model for the evolution of the Limpopo Belt. Precambrian Research 55, 539-552.

S.A.C.S. (South African Committee for Stratigraphy). 1980: Stratigraphy of South Africa. Part 1, (ed). Kent, L.E. Lithostratigraphy of the Republic of South Africa, South West Africa/Namibia, and the Republics of Boputhatswana, Transkei and Venda. Handbook of the Geological Survey of South Africa 8.

Schreiber, U.M., Eriksson, P.G., van der Neut, M. and Snyman, C.P. 1992; Sedimentary petrography of the early proterozoic Pretoria Group, Transvaal Sequence, South Africa: implications for tectonic setting. Sedimentary Geology 80, 89-103.

Schwellnus, J.S.I, Engelbrecht, L.N.J., Coertzee, F.J., Russel, H.D., Malherbe, S.J., Van Rooyen, D.P., Crooke, R. 1962: The Geology of the Olifants River area, Transvaal. An explanation of sheet 2429B (Chuniespoort) and 2430A (Wolkberg), Department of Mines, Geological Survey.

Sharpe, M.R. and Snyman, J.A. 1980: A model for the emplacement of the eastern compartment of the Bushveld Complex: Tectonophysics 65, 85 –110.

Sharpe, M.R., Bahat, D. and Von Gruenewaldt, G. 1981: The concentric elliptical structure of feeder sites to the Bushveld Complex and possible economic implications: Transactions, Geological Society of South Africa 84, 239-244.

Sharpe, M.R. and Chadwick, B. 1982: Structures in Transvaal Sequence rocks within and adjacent to the eastern Bushveld Complex. Transactions Geological Society of South Africa 85, 29-41.

Smit, P.J., Hales, A.L. and Gough, D.I. 1962: The Gravity survey of the Republic of South Africa, I. Gravimeter observations: Handbook, Geological Survey of South Africa 3.

Snyman, C.P. 1956. 'n Koepelstruktuur en die metamorfose van die Sisteem Transvaal suid van Marble Hall, Transvaal. Unpublished M.Sc. thesis, University of Pretoria.

Snyman, C.P. 1996: Die geologie van Suid-Afrika, Volume1. Department of Geology, University of Pretoria.

Stanistreet, I.G. and McCarthy, T.S. 1991: Changing tectono-sedimentary scenarios relevant to the development of the late Archaean Witwatersrand Basin. Journal of African Earth Sciences 13, 65-81.

Stear, W.M. 1976: The geology and ore controls of the Northern Rooiberg Tin-field, Transvaal. Unpublished M.Sc. thesis, Stellenbosch University.

Stesky, R.M. 1998: SpheriStat™ 2 for Windows 3.1 Version 2.2. User's Manual. Pangaea Scientific.

Strauss, C.A. 1954: The geology and mineral deposits of the Potgietersrus Tin Fields. Memoir Geological Survey of South Africa, 46.

Tankard, A.J., Jackson, M.P.A., Eriksson, K.A., Hobday, D.K., Hunter D.R., Minter, W.E.L. 1982: Crustal evolution of southern Africa. 3.8 Billion Years of Earth History. Springer- Verlag, Berlin.

Teigler, B. 1990: Platinum group element distribution in the lower and middle group chromitites in the western Bushveld Complex: Mineralogy and Petrology 42, 165 –179.

Thomas R.J., von Veh M.W., and McCourt, S. 1993: The tectonic evolution of southern Africa: an overview Journal of African Earth Sciences 16, 5-24.

Treloar, P.J., Coward, M.P. and Harris, N.B.W. 1992: Himalayan-Tibetan analogies for the evolution of the Zimbabwe Craton and Limpopo Belt. Precambrian Research 55, 571-587.

Twiss, R.J. and Moores, E.M. 1992: Structural Geology. W.H. Freeman and Company, New York.

Tyler, R. and Tyler, N. 1996: Stratigraphic and structural controls on gold mineralization in the Pilgrim's Rest goldfield, eastern Transvaal, South Africa. Precambrian Research 79, 141-169.

Uken R. and Watkeys M.K. 1997a: An interpretation of mafic dyke swarms and their relationship with major mafic magmatic events on the Kaapvaal Craton and Limpopo Belt. South African Journal of Geology 100, 341-348.

Uken R. and Watkeys M.K. 1997b: Diapirism initiated by the Bushveld Complex, South Africa. Geology 25, 732-726.

Van Biljon, W.J. 1976: Goud is nie waar dit gevind word nie. Transactions Geological Society of South Africa 79, 155-167.

Van Breemen, O. and Dodson, M.H. 1972: Metamorphic chronology of the Limpopo Belt, South Africa: Geological Society of America Bulletin 83, 2005-2018.

Van der Merwe, M.J. 1976: The layered sequence of the Potgietersrus limb of the Bushveld Complex: Economic Geology 71, 1337-1351.

Van der Merwe, R. 1994. The nature of the western margin of the Witwatersrand basin. Unpublished PhD. Thesis, Rand Afrikaans University.

Van der Neut, M., and van der Merwe, R. 2000: The nature of the northern margin of the (Middelburg) Waterberg Basin. Geocongress 2000: 27th Earth Science Congress of the GSSA (abstracts). Journal of African Earth Sciences 31, 82-83.

Van Reenen, D.D., Roering, C., Ashwal, L.D. and de Wit, M.J. 1992: Regional geological setting of the Limpopo Belt. Precambrian Research 55, 1-5.

Van Reenen, D.D., Roering, C., Smit, C.A., Van Schalkwyk, J.F. and Barton, J.M., Jr., 1988: Evolution of the northern high-grade margin of the Kaapvaal Craton, South Africa. Journal of Geology 96, 549-560.

Vermaak, C.F., 1970: The geology of the lower portion of the Bushveld complex and its relationship to the floor rocks. In the area west of the Pilanesberg, Western Transvaal. In: symposium on the Bushveld Igneous complex and other layered intrusions, (eds.) Visser, D.J.L. and von Gruenewaldt, G. Special Publication Geological Society of South Africa 1, Johannesburg, 242-262.

Vermaak, C.F. 1976: The Merensky Reef - thoughts on its environment and genesis: Economic Geology 71, 1270-1298.

Vermaak, C.F., and Lee, C.A. 1981: The Bushveld and Kindred Complexes in Precambrian of the Southern hemisphere, (ed.) D.R. Hunter. Elsevier, Amsterdam, 599-618.

Vearncombe, J.R. 1988: Structure and metamorphism of the Archaean Murchison Belt, Kaapvaal Craton, South Africa: Tectonics 7, 761-774.

Vearncombe, J.R., Barton, J.M., Cheshire, P.E., De Beer, E.H., Stettler, E.H. and Brandl, G., 1992: Geology, geophysics and mineralisation of the Murchison schist belt, Rooiwater Complex and surrounding granitoids: Memoir 81. Geological Survey of South Africa, Pretoria.

Verwoerd, W.J. 1993: Update on carbonatites of South Africa and Namibia: South African Journal of Geology 96, 75-95.

Visser, D.J.L. 1998: The geotectonic evolution of South Africa and offshore areas. Explanation of Structure Map. Scale 1:1 000 000. Council for Geoscience (Geological Survey of South Africa), Pretoria.

Von Gruenewaldt, G. 1979: The Rooiberg felsite north of Middelburg and its relation to the layered sequence of the Bushveld Complex: Transactions Geological Society of South Africa 71, 153-172.

Von Gruenewaldt G., and Harmer R.E. 1993: Tectonic setting of Proterozoic layered intrusions with special reference to the Bushveld Complex. In: Proterozoic Crustal Evolution, (ed.) Condie, K.C. Elsevier, Amsterdam, 181-213.

Walraven, F. 1974: Tectonism during the emplacement of the Bushveld Complex and the resulting fold structures: Transactions Geological Society of South Africa 77, 323-328.

Walraven, F. 1986: Stratigraphy and structure of the Nebo granite, Bushveld Complex, South Africa: Abstracts Geocongress 1986. Geological Society of South Africa, Johannesburg, 637-642.

Walraven, F. 1990: A chronostratigraphic framework for the north-central Kaapvaal craton, the Bushveld Complex and the Vredefort structure. In: Crytoexplosios and Catastrophes in the Geological Record, with a Special Focus on the Vredefort Structure, (eds.) L.O. Nicolaysen and W.U. Reimold and W.U. Reimold. Tectonophysics 171, 23-48.

Walraven, F., and Darracott, B.W. 1976: Quantitative interpretation of a gravity profile across the western Bushveld complex. Transactions Geological Society of South Africa 79, 22-26.

Watkeys, M.K. 1984: The Precambrian geology of the Limpopo Belt north and west of Messina: Unpublished Ph.D. thesis, University of the Witwatersrand.

Watkeys, M.K. and Sweeney, R.J. 1988: Tuli-Lebombo volcanism and Gondwana rifting. Extended abstracts, Geocongress '88. Geological Society South Africa, Durban, 725-728.

Weijermars, R. 1997: Principles of Rock Mechanics. Alboran, Amsterdam.

Willemse, J. 1959: The geology of the Bushveld Igneous Complex, the largest repository of magmatic ore-deposits in the world: Economic Geology Monograph 4, 1-22.

Winter, H. de la R. 1987: A cratonic foreland model for Witwatersrand development in a continental back-arc, plate-tectonic setting: South African Journal of Geology 90, 409-42.

11. APPENDICES

Appendix 1

Look-up tables for the fault database

Bos2

FAULT_NAME	NAME_ID
	0
Belt of Hills/Gatkop	1
Bobbejaanwater splay	2
Boschpoort	3
Brits	4
Brits Graben	5
Buffelshoek/Belt of Hill	6
Bultfontein	7
Bushveld	8
Crocodile Bridge/Bobbeja	9
Crocodile River	10
Crocodile River fragment	11
Derdepoort	12
Donkerpoort	13
Droogekloof/Sandrivier	14
Elandsberg	15
Dwarsberg	16
Gevonden	17
Groot Marico	18
Johannesburg dome	19
Kwarriehoek	20
Liliput	21
Magaliesberge	22
Mahobieskraal	23
Mankwe	24
Mannyelanong	25
Nieuwpoort	26
Pilaansberg	27
Rietfontein fault system	28
Rooiberg	29
Rooiberg fragment	30
Rosseauspoort Range	31
Ruighoek	32
Rustenburg	33
Sandrivier	34
South parallel/Nieuwpoor	35
Springbok flats	36
Swartruggens	37
Syferfontein	38
Vaalwater	39
Vaalwater fault zone	40
Vlakfontein fault	41
Zeerust	42

Bos3

STRUCTURE	USER_ID
Northern Transvaal	11
Zebediela fault	23
Swaershoek	17
Northern Bushveld	9
Warmbaths	19
Nederland	8
De Hoop	4
Northern Melinda	10
Sunnyside	16
Blouberg	2
Makgabeng	6
Zoetfonein/Melinda	24
Uitkomst	18
Abbotspoort	1
Southern Melinda	15
Melinda	7
Potgietersrus	13
Pruizen	14
Grootvlei	5
Welgevonden	20
Northern Waterberg	12
Zebediela	22
Ysterberg	21

Bos5

NAME	USER_ID
unknown	0
Acre	1
Archaean	2
Barberton Greenstonebelt	3
Eastern Transvaal	4
Penge-Sabie Gravity	5
Groblersdal	6
Jarrabad	7
Laersdrift	8
Loskopdam	9
Magnet Heights	10
Malta	11
Marble Hall	12
Mhlapitsi	13
Murchison Greenstonebelt	14
Northeastern Transvaal	15
Pietersburg Greenstonebelt	16
Sekhukhune	17
Sekhukhuneberge	18
Serala	19
Stavoren	20
Steelpoort	21
Steelpoort extension	22
Strydpoort	23
Welkommyn	24
Wilgerrivier	25
Wolkberg	26
Wonderkop	27
Zebediela	28

USER_ID	DISPLACEMENT
dn	down north
de	down east
ds	down south
dw	down west
dnw	down northwest
dse	down southeast
dsw	down southwest
dnw	down northwest
un	up north
ue	up east
us	up south
uw	up west
une	up northeast
use	up southeast
usw	up southwest
unw	up northwest
ll	left-lateral
rl	right-lateral

USER_ID	FAULT_TYPE
1	normal
2	thrust
3	strike-slip
4	reverse
5	dip-slip
10	fault observed
15	fault inferred
16	inferred normal
17	inferred reverse
18	inferred thrust
19	inferred strike-slip

USER_ID	AGE
500	Pre-Transvaal
400	Post-Tvl/Pre-Bush
300	Post-Bush/Pre-Waterberg
200	Post-Water/Pre-Karoo
150	Post-Pilanesberg/Pre-Karoo
100	Post-Karoo

Look-up Tables for fold database

Bos2

NAME_ID	FOLD_NAME
1	Blaaubank
2	Crocodile River dome
3	Elandsberg
4	Johannesburg dome
5	Kalkfontein - Piet Zyn Kop
6	Kwa-Lobatleng - Ruitjesvlakte
7	Kwarriehoek
8	Loubad
9	Magaliesberg
10	Makoppa dome
11	Marico River
12	Nebo
13	Nylstroom
14	Pilanesberg
15	Rooiberg
16	Rooiberg fragment
17	Rustenburg
18	Swaershoek
19	Waterberg
20	Witkleigat
21	Zwartkloof

Bos3

STRUCTURE	USER_ID
	0
Loubad	1
Swaershoek	7
Nylstroom	3
Pruizen	4
Zebediela	9
Spanje	5
Makapans	2
de Hoop	10
Tweefontein	8
Sterkrivierdam	6

Bos4

NAME	USER_ID
Moltke	11
Malta	8
The Downs	18
Mhlapitsi	10
Serala	15
Wolkberg	20
Acre	1
Welkommyn	19
Schwerin	14
Adriaanskop	2
Katkloof	6
Fortdraai	5
Steelpoort Pericline	17
Magnet Heights	7
Paradys Structure	13
Marble Hall	9
Nebo	12
Dennilton	3
Dwars River	4
Stavoren	16

USER_ID	AXIAL_PLANE
N	north
E	east
S	south
W	west
NE	northeast
SE	southeast
SW	southwest
NW	northwest
u	upright
c	curved

USER_ID	FOLD_TYPE
0	undifferentiate
1	anticline
2	syncline
3	pericline

USER_ID	FOLD_AXIS_
N	north
E	east
S	south
W	west
NE	northeast
SE	southeast
SW	southwest
NW	northwest
NS	doubly plunging NS
EW	doubly plunging EW
NE-SW	doubly plunging NE-SW
NW-SE	doubly plunging NW-SE

Appendix 2

Scripts used in rose diagram production

```
' Name:  View.ShapeToGenerate
'
' Title:  Exports active theme to ARC/INFO export format
'
' Topics:  GeoData
'
' Description:  Exports the active themes to ARC/INFO Export (Generate)
' format files.  Each active theme will require the user to specify an
' output file name.  The format of the export file with be either POINT,
' LINE, or POLYGON depending upon the type of Shape Field found in the
' Theme FTab (the Enum Type FieldEnum).
'
' The user will be prompted for the field from which to create IDs in
' the generate file.  If <None> is selected the ID for the feature will
' be set to the current FTab record number.
'
' In the case of overlapping polygons, the data should be further
' converted into an ARC/INFO region coverage with the REGIONCLASS
' command.  ArcView polygon shapes may need to be modeled in ARC/INFO as
' regions to handle the case of polygons with multiple parts.
'
' Following conversion of the generate file to an ARC/INFO coverage
' the Theme's FTab can be exported to an INFO file that can be joined to
' the coverage Feature Attribute Table (FAT) to restore all attributes as
' found in the original Theme.  Consult ARC/INFO command documentation for
' JOINITEM and related commands.
'
' When creating polygon format Generate files the AUTO keyword is used
' along with the feature ID to indicate that labels will be automatically
' created when coverages are imported using ARC/INFO Generate.  Consult
' the ARC/INFO Generate documentation for additional options and discussion.
'
' Requires:  A View must be the active document.
'
' Self:
'
' Returns:
'


' View should be the Active Document
'
theView = av.GetActiveDoc

' Establish output precision...
'
Script.The.SetNumberFormat( "d.dddddd" )

for each t in theView.GetActiveThemes
  defaultName    = FN.Make("$HOME").MakeTmp(t.GetName.LCase,"gen")
  ungenFileName  = FileDialog.Put( defaultName,"*.gen","Export"++t.GetName )
  if (ungenFileName = nil) then
    exit
  else
    exportFile = LineFile.Make(ungenFileName, #FILE_PERM_WRITE)
```

```
end

' The ARC/INFO generate format uses the ID number of the feature
' in the export file to provide a means for joining attributes.
' When the generate file is converted to an ARC/INFO coverage the ID
' as found in the generate file will be used as the ID in the coverage
' feature attribute table (the .AAT or .PAT).  Allow the user to specify
' the ID field to use or default to the record number....
'
fieldList = t.GetFTab.GetFields.Clone
fieldList.Insert( "<None>" )
idField = MsgBox.ChoiceAsString( fieldList,
  "Select ID field for export file:","Choose ID Field" )
if ( idField = nil ) then
  exit
elseif ( idField = "<None>" ) then
  useID = false
else
  useID = true
end

theFTab     = t.GetFTab
shapeField  = theFTab.FindField( "Shape" )
shapeType   = shapeField.GetType
numRecs     = theFTab.GetNumRecords

av.ShowStopButton
av.ShowMsg( "Exporting"++t.GetName+"..." )

for each recNum in theFTab
  currentShape = theFTab.ReturnValue( shapeField, recNum )

  if ( useID ) then
    id =theFTab.ReturnValueString( idField, recNum )
  else
    id = (recNum + 1).SetFormat("d").AsString
  end

  if (shapeType = #FIELD_SHAPEPOINT) then
    ' ARC/INFO POINT format export file...
    '
    Xvalue = currentShape.GetX.AsString
    Yvalue = currentShape.GetY.AsString
    outputLine = id+", "+Xvalue+", "+Yvalue
    exportFile.WriteElt( outputLine )

  elseif (shapeType = #FIELD_SHAPEMULTIPOINT) then
    ' ARC/INFO POINT format export file...
    '
    pointList = currentShape.AsList
    for each pt in pointList
      Xvalue = pt.GetX.AsString
      Yvalue = pt.GetY.AsString
      outputLine = id+", "+Xvalue+", "+Yvalue
      exportFile.WriteElt( outputLine )
    end

  elseif (shapeType = #FIELD_SHAPELINE) then

    ' ARC/INFO LINE format export file...
    '
```

```
      ' exportFile.WriteElt( id )
      shapeList = currentShape.AsList
      for each shapePart in shapeList
        for each xyPoint in shapePart
          outputLine = id+", "
            +xyPoint.GetY.AsString+", "+xyPoint.GetX.AsString
          exportFile.WriteElt( outputLine )
        end
        exportFile.WriteElt( "END" )
      end

    elseif (shapeType = #FIELD_SHAPEPOLY) then

      ' ARC/INFO POLYGON format export file...
      '
      ' exportFile.WriteElt( id++"AUTO" )  'automatic label generation flag...
      shapeList = currentShape.AsList
      for each shapePart in shapeList
        for each xyPoint in shapePart
          outputLine = id++"AUTO"+", "
            +xyPoint.GetY.AsString+", "+xyPoint.GetX.AsString
          exportFile.WriteElt( outputLine )
        end
        'exportFile.WriteElt( "END" )
      end
    end

    progress = (recNum / numRecs) * 100
    proceed = av.SetStatus( progress )
    if ( proceed.Not ) then
      av.ClearStatus
      av.ShowMsg( "Stopped" )
      exit
    end

  end

  'exportFile.WriteElt( "END" )
  exportFile.Close

  av.ClearStatus
  av.ClearMsg
end
```

Linears.exe

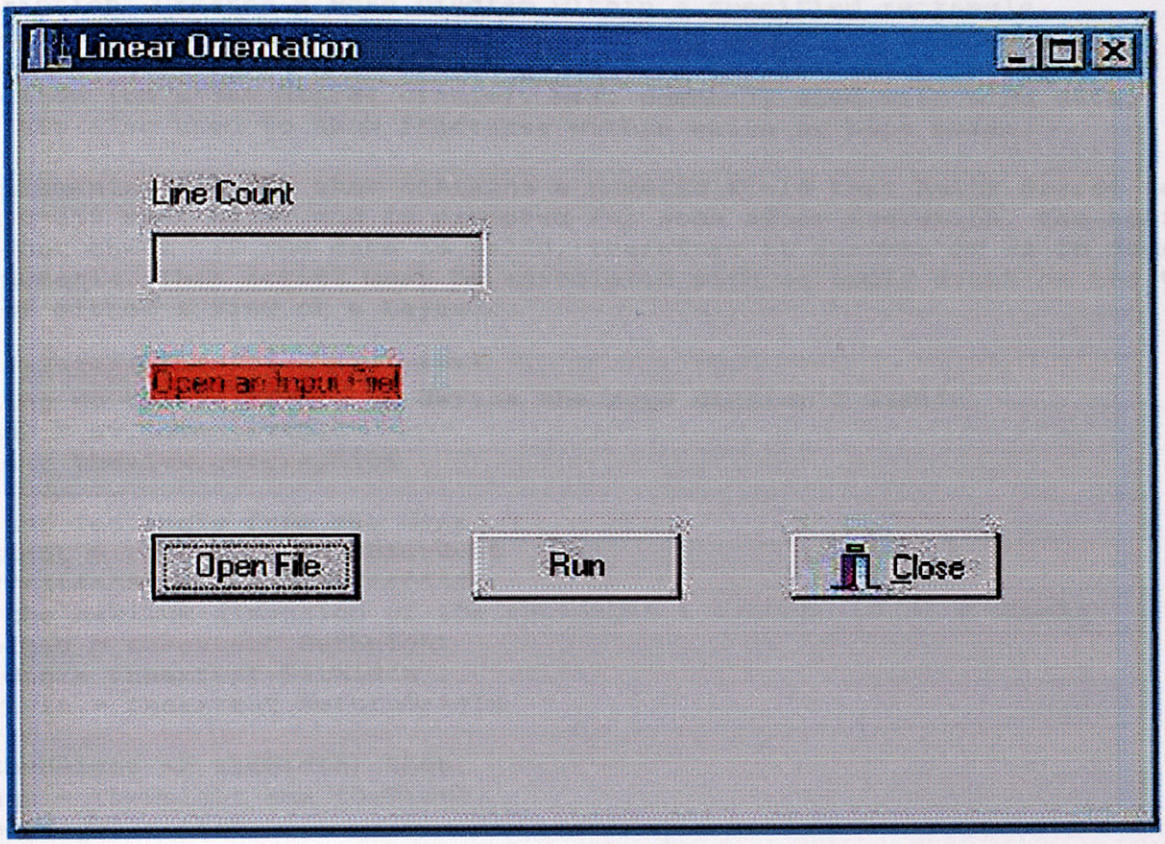

```
'Name: rose.ave
'
'Description: Creates a Rose Diagram within a specified rectangle.
'The diagram is based on the percentage of the number of degrees within
'a specified interval. Rose diagrams are used to show major trends of
'direction (on a 360 degree circle). Most commonly used with wind data,
'they are also used to show fractures within wells or bore holes.
'
'Requirements: A table that contains a numeric field that holds degree values
'from 0-359 must exist and is prompted for soon after execution. The script
'does not check  if the data is valid, therefore it assumes it is in degrees
'and numeric. This script must be associated with an apply event on the tool
'bar of either a View or a Layout.
'
'*********************************
'Setting up the rectangle to define the rose diagram's limits
theView = av.GetActiveDoc
thegra = theview.getgraphics

'get the rectangle from the user
theextent = theView.ReturnUserRect
'*********************************
'Get the maximum dimension of the rectangle & convert it to a square
theHeight = theextent.GetHeight
theWidth = theextent.GetWidth
theOrigin = theextent.ReturnOrigin
'
 if(theHeight <> theWidth) then
   test = theHeight Max theWidth
   newHeight = test
   newOffSet = Point.Make(newHeight,newHeight)
 end
aBox = Rect.Make(theOrigin, newOffSet)
theExtent = aBox
'*********************************
'Rose Programme starts here
'*********************************
' get user stuff
thefn = filedialog.show ("*.*","*.*","Please Select a table.")
if (thefn = NIL) then
exit
else
thevtab = vtab.make (thefn,FALSE,FALSE)
end

thefld = msgbox.choice (thevtab.getfields,"Please Select a trend field.","Trend
Selection")
if (thefld = NIL) then
exit
end
' ***********************************
'Optional routine to use cumulative length instead of frequency to draw rose
petals
'This program section reads the "Length" field in the table

huh = msgbox.yesnocancel ("Use cumulative length?","Length",TRUE)
if (huh = NIL) then
exit
end
 if (huh = TRUE) then
   cum_length = TRUE
```

```
  thelength = msgbox.choice (thevtab.getfields,"Please Select a Length
field.","Length Selection")
 else
  cum_length = FALSE
 end
if (thefld = NIL) then
exit
end
' **********************************
shrink = 0.005
'
huh = msgbox.input ("Enter number of intervals. Max: 30","Intervals","5")
if (huh = NIL) then
exit
end
if (huh.isnumber.not) then
exit
else
deg = huh.asnumber
end
'
' **********************************
'Optional routine to draw break lines within rose
'huh = msgbox.yesnocancel ("Show interval break lines within rose?","Interval
Lines",TRUE)
'if (huh = NIL) then
'exit
'end
'if (huh = TRUE) then
 interval_lines = TRUE
'end
'if (huh = FALSE) then
 'interval_lines = FALSE
 'end
' **********************************
'Optional routine to show diagram labels within rose
'************************************************
'huh = msgbox.yesnocancel ("Show diagram labels?","Circle labels",TRUE)
'if (huh = NIL) then
'exit
'end
'if (huh = TRUE) then
 labels = TRUE
'end
'if (huh = FALSE) then
' labels = FALSE
'end
' ********************************
' some constants (change if nessesary)
txtspc = 0.01  ' text mover to place on the line (for single digits)
txtspc2 = 0.019 ' same as above for double digits
thefont = font.make ("Helvetica","Normal")
textsize = 5
rings = 5
sumdeg = 360 / deg
' ********************************
' initalize dict to all zeros 0..359
dict = {}
for each num in 0..(sumdeg - 1)
dict.add (0.0)
end
```

```
' ***********************************
' break up values in intervals from user
' if a value falls within a interval, it adds to a certain bit in the list
for each rec in thevtab
val = thevtab.returnvaluenumber (thefld,rec)
 if (cum_length = TRUE) then
  len = thevtab.returnvaluenumber (thelength,rec)
 end
mover = deg
tester1 = 0
tester2 = (deg - 0.001).abs
for each num in 0..dict.count
 if ((val >= tester1) AND (val <= (tester2))) then
' ** change this line to add cumulative length **
  if (cum_length = TRUE) then
   dict.set (num,(dict.get(num) + len))
  else
   dict.set (num,(dict.get(num) + 1))
  end
 end
 mover = mover + deg
tester1 = tester2 + 0.001
tester2 = (mover - 0.001)
end
end
'***********************************
' get percentages of values in the list dict (was a dictionary, but lists are
sometimes easier)
newdict = {}
for each num in dict
newdict.add (((num / thevtab.getnumrecords)))
end
' ***********************************
' determine largest value in list
count = 0
for each val in newdict
if (count = 0) then
 val2 = val
 themax = 0
 else
  test = val Max val2
   if (test > themax) then
    themax = test
    end
  end
count = count = 1
val2 = val
end
mulval =  (1 / themax)
fmax = mulval * themax
' ********************************
' multipy all values by milval to scale (largest % becomes the largest line )
testdict = {}
for each val in newdict
testdict.add (mulval * val)
end
newdict = testdict
' ***********************************
' determine user rect characteristics for drawing
theheight =  theextent.getheight
cntr = theextent.returncenter
```

```
inc = ((theheight / 2) / rings) ' - shrink)
' ************************************
' determine scale labels
lablst = {}
'lab_end = themax * 100
lab_end = fmax * 100
lab_range = lab_end / rings
hold = lab_range.asstring.left (3)
lab_range = hold.asnumber
count = lab_range
for each num in 1..rings
if (count.asstring.count > 3) then
hold = count.asstring.left (3)
count = (hold.asnumber + 0.5).round
end
lablst.add (count)
count = count + lab_range
end
' ************************************
' create a white shaded box around the rose diagram for use in a layout or view
etc..
gra = graphicshape.make (theextent)
gra.getsymbol.setstyle (#RASTERFILL_STYLE_SOLID)
gra.getsymbol.setcolor (color.getwhite)
gra.setselected (TRUE)
theview.getgraphics.add (gra)
theview.getgraphics.moveselectedtoback
' ************************************
'circles and labels
cnt = 0
i = inc
for each num in 0..(rings - 1)
if (cnt = 0) then
cir = circle.make (cntr, (inc))
gra = graphicshape.make (cir)
gra.setselected (TRUE)
theview.getgraphics.add (gra)
if (labels = TRUE) then
gratxt = graphictext.make (lablst.get(num).asstring, (cntr.getx -
txtspc)@((cntr.gety + inc - txtspc)))
gratxt.setselected (TRUE)
gratxt.getsymbol.setfont (thefont)
gratxt.getsymbol.setsize (textsize)
theview.getgraphics.add (gratxt)
gratxt = graphictext.make (lablst.get(num).asstring, (cntr.getx -
txtspc)@((cntr.gety - inc - txtspc)))
gratxt.setselected (TRUE)
gratxt.getsymbol.setfont (thefont)
gratxt.getsymbol.setsize (textsize)
theview.getgraphics.add (gratxt)
gratxt = graphictext.make (lablst.get(num).asstring, (cntr.getx + inc -
txtspc)@((cntr.gety - txtspc)))
gratxt.setselected (TRUE)
gratxt.getsymbol.setfont (thefont)
gratxt.getsymbol.setsize (textsize)
theview.getgraphics.add (gratxt)
gratxt = graphictext.make (lablst.get(num).asstring, (cntr.getx - inc -
txtspc)@((cntr.gety - txtspc)))
gratxt.setselected (TRUE)
```

```
gratxt.getsymbol.setfont (thefont)
gratxt.getsymbol.setsize (textsize)
theview.getgraphics.add (gratxt)
end
else
cir = circle.make (cntr, (inc + i))
gra = graphicshape.make (cir)
gra.setselected (TRUE)
theview.getgraphics.add (gra)
if ((lablst.get(num)).asstring.trim.count < 2) then
if (labels = TRUE) then
gratxt = graphictext.make (lablst.get(num).asstring, (cntr.getx -
txtspc)@((cntr.gety + inc + i - txtspc)))
gratxt.setselected (TRUE)
gratxt.getsymbol.setfont (thefont)
gratxt.getsymbol.setsize (textsize)
theview.getgraphics.add (gratxt)
gratxt = graphictext.make (lablst.get(num).asstring, (cntr.getx -
txtspc)@((cntr.gety - inc - i - txtspc)))
gratxt.setselected (TRUE)
gratxt.getsymbol.setfont (thefont)
gratxt.getsymbol.setsize (textsize)
theview.getgraphics.add (gratxt)
gratxt = graphictext.make (lablst.get(num).asstring, (cntr.getx + inc + i -
txtspc)@((cntr.gety - txtspc)))
gratxt.setselected (TRUE)
gratxt.getsymbol.setfont (thefont)
gratxt.getsymbol.setsize (textsize)
theview.getgraphics.add (gratxt)
gratxt = graphictext.make (lablst.get(num).asstring, (cntr.getx - inc - i -
txtspc)@((cntr.gety - txtspc)))
gratxt.setselected (TRUE)
gratxt.getsymbol.setfont (thefont)
gratxt.getsymbol.setsize (textsize)
theview.getgraphics.add (gratxt)
end
else
if (labels = TRUE) then
gratxt = graphictext.make (lablst.get(num).asstring, (cntr.getx -
txtspc2)@((cntr.gety + inc + i - txtspc)))
gratxt.setselected (TRUE)
gratxt.getsymbol.setfont (thefont)
gratxt.getsymbol.setsize (textsize)
theview.getgraphics.add (gratxt)
gratxt = graphictext.make (lablst.get(num).asstring, (cntr.getx -
txtspc2)@((cntr.gety - inc - i - txtspc)))
gratxt.setselected (TRUE)
gratxt.getsymbol.setfont (thefont)
gratxt.getsymbol.setsize (textsize)
theview.getgraphics.add (gratxt)
gratxt = graphictext.make (lablst.get(num).asstring, (cntr.getx + inc + i -
txtspc2)@((cntr.gety - txtspc)))
gratxt.setselected (TRUE)
gratxt.getsymbol.setfont (thefont)
gratxt.getsymbol.setsize (textsize)
theview.getgraphics.add (gratxt)
gratxt = graphictext.make (lablst.get(num).asstring, (cntr.getx - inc - i -
txtspc2)@((cntr.gety - txtspc)))
gratxt.setselected (TRUE)
gratxt.getsymbol.setfont (thefont)
gratxt.getsymbol.setsize (textsize)
```

```
theview.getgraphics.add (gratxt)
end
end
inc = inc + i
end
cnt = cnt + 1
end
lastcir = cir
pntlst = lastcir.asmultipoint.aslist
' ***************************
' adjust the point list from the largest circle to make 0 start at the top
' get different results on ???
count = 0
deglst = {}
for each pnt in pntlst
if (count >= 270) then
deglst.add (pnt)
end
count = count + 1
end
count = 0
for each pnt in pntlst
if (count < 270) then
deglst.add (pnt)
end
count = count + 1
end
newlst = {}
count = 0
for each rec in deglst
newlst.add (count)
count = count + 1
end
'*****************************
' reverse list so 90 is on the right side
count = (deglst.count - 1)
for each pnt in deglst
newlst.set (count,pnt)
count = count - 1
end
deglst = newlst
' ***********************************
' interval lines
count = 0
cnt = deg
linelst = {}
for each pnt in deglst
if (cnt = deg) then
aline = line.make (cntr,pnt)
if (interval_lines = TRUE) then
gra = graphicshape.make (aline)
'gra.getsymbol.setpattern ({5,5})
gra.setselected (TRUE)
theview.getgraphics.add (gra)
end
count = count + 1
cnt = 0
linelst.add (aline)
end
cnt = cnt + 1
```

```
end
thedist = aline.returnlength
' ********************************************
' create petal polygons
count = 0
for each val in newdict
if (val <> 0) then
line1 = linelst.get (count)
if (count >= (linelst.count - 1)) then
line2 = linelst.get(0)
else
line2 = linelst.get (count + 1)
end
center1 = line1.returncenter
center2 = line2.returncenter
diffx1 = ((line1.returnstart.getx - center1.getx)  * 2) * (val)
diffy1 = ((line1.returnstart.gety - center1.gety)  * 2) * (val)
diffx2 = ((line2.returnstart.getx - center2.getx)  * 2) * (val)
diffy2 = ((line2.returnstart.gety - center2.gety)  * 2) * (val)
newx1 = (diffx1 + line1.returnstart.getx )
newy1 = (diffy1 + line1.returnstart.gety )
newx2 = (diffx2 + line2.returnstart.getx )
newy2 = (diffy2 + line2.returnstart.gety )
pntlst = {cntr,newx1@newy1,newx2@newy2,cntr}
apoly = polygon.make ({pntlst})
if (apoly.returnlength >= thedist) then
end
gra = graphicshape.make (apoly)
gra.getsymbol.setstyle (#RASTERFILL_STYLE_SOLID)
if (val = fmax) then
gra.getsymbol.setcolor (color.getred)
else
gra.getsymbol.setcolor (color.getblue)
end
gra.setselected (TRUE)
theview.getgraphics.add (gra)
av.showmsg ("Building petals...")
'av.setstatus ((count / newdict.count) * 100)
end
count = count + 1
end
' ******************************
' places the file name at the origin
'gratxt = graphictext.make (thefn.getbasename,(gra.getorigin.getx +
0.01)@(gra.getorigin.gety + 0.01))
'gratxt.setselected (TRUE)
'gratxt.getsymbol.setfont (thefont)
'gratxt.getsymbol.setsize (textsize + 1)
'theview.getgraphics.add (gratxt)

' ******************************
'Select graphic text and move to front

theview.getgraphics.unselectall
count = thegra.count-1

for each rec in 0..count by 1
theshape = thegra.Get(rec)
if(theshape.Is(GraphicText) = TRUE) then
theshape.SetSelected(TRUE)
end
```

```
end
thegra.MoveSelectedToFront
'thegra.unselectall
' ******************************
theview.getgraphics.selectall
theview.getgraphics.groupselected
theview.getgraphics.unselectall
theview.getgraphics.endbatch
av.clearmsg
av.clearstatus
```